



HAL
open science

Non conventional synthetic strategies of stapled peptides : modulation of secondary structures to optimise biological recognition

Chiara Testa

► **To cite this version:**

Chiara Testa. Non conventional synthetic strategies of stapled peptides : modulation of secondary structures to optimise biological recognition. Other. Université de Cergy Pontoise; dipartimento di chimica Ugo Schiff, Università di Firenze, 2012. English. NNT : 2012CERG0588 . tel-00799790

HAL Id: tel-00799790

<https://theses.hal.science/tel-00799790>

Submitted on 27 Nov 2014

HAL is a multi-disciplinary open access archive for the deposit and dissemination of scientific research documents, whether they are published or not. The documents may come from teaching and research institutions in France or abroad, or from public or private research centers.

L'archive ouverte pluridisciplinaire **HAL**, est destinée au dépôt et à la diffusion de documents scientifiques de niveau recherche, publiés ou non, émanant des établissements d'enseignement et de recherche français ou étrangers, des laboratoires publics ou privés.



PhD THESIS OF
THE UNIVERSITY OF CERGY-PONTOISE
CO-TUTORED WITH
THE UNIVERSITY OF FLORENCE

**Non conventional synthetic strategies of stapled peptides:
modulation of secondary structures to optimise
biological recognition**

presented by :
Chiara TESTA

PhD discussed on March 26th 2012,
Composition of the evaluation committee:

Pr. Solange LAVIELLE	Rapporteur
Pr. Luis MORODER	Rapporteur
Pr. Anna Maria PAPINI	Directrice de thèse
Pr. Nadège GERMAIN	Directrice de thèse
Pr. Paolo ROVERO	Directeur de thèse
Pr. Michael CHOREV	Examineur
Pr. Jacques AUGE	Examineur
Pr Andrea GOTI	Examineur

Table of contents

INTRODUCTION.....	1
1 Difficult peptide synthesis optimized by microwave-assisted approach: a case study of PTHrP(1–34)NH₂.....	18
1.1 The Parathyroid hormone (PTH) and the Parathyroid hormone-related protein (PTHrP)	18
1.2 Microwave assisted peptide synthesis	20
1.2.1 Thermal effects	21
1.2.2 Specific non-thermal effects	22
1.2.3 Modes.....	22
1.3 Synthetic strategies for difficult peptide sequences.....	23
1.4 Synthesis of PTHrP(1-34).....	25
1.5 MW-assisted mini-cleavage of PTHrP(1-34)NH ₂ fragments	26
1.5.1 MW-assisted mini-cleavage protocol of 19-34 fragment of.....	27
PTHrP(1-34)NH ₂ : a case study of multi-arginine containing peptides.	27
1.5.2 Characterization of PTHrP(1-34)NH ₂ fragments by UPLC-ESI-MS analysis.....	29
1.5.3 Characterization of the 12-34 fragment of PTHrP(1-34)NH ₂ by UPLS-ESI-MS/MS analysis.....	32
1.6 RP-HPLC Semi-preparative of PTHrP(1–34)NH ₂	33
1.7 Results.....	33
1.8 Advantages of MW irradiation in SPPS	34
2 Intramolecular i-to-(i+5) Side-Chain-to-Side Chain Cyclization to stabilize β-turn Secondary Structures: the melanocortin peptides hormones.....	38
2.1 The Endocrine System	38
2.1.1 Peptide hormones.....	41
2.1.2 The Nervous and Endocrine Systems	43
2.2 Melanocortin peptide hormones	44
2.2.1 G Protein-coupled Melanocortin receptors: MCRs	47
2.2.2 Development of Agonist for MCRs.....	51
2.3 Stabilization of β -turn conformation in melanocortin like peptide by Click Chemistry	54

2.4	Click Chemistry	56
2.5	Synthetic Strategy	60
2.6	Synthesis of non-coded amino acids.....	61
2.6.1	Synthesis of N ^α -Fmoc-ω-azido-α-amino acids	61
2.6.2	Synthesis of N ^α -Fmoc-ω-alkynyl-α-amino acids.....	63
2.6.3	Collection of linear peptide precursor	65
2.6.4	Collection of triazole containing cyclo-peptides	67
2.6.5	Solid Phase Synthesis of lactam bridge-containing cyclopeptide	69
2.7	Biological study	70
2.8	Conformational study.	72
2.9	NMR analysis	73
2.10	NMR Structure Calculations.....	75
2.11	Conclusion	78
3	PART B: Impact of Endocrine disruptor Chemicals on human health	84
3.1	Phthalates	85
3.1.1	Metabolism of DEHP in humans	87
3.2	Health effect.....	90
3.2.1	Endocrine disruptor (EDs)	90
3.2.2	PPAR-mediated activity of phthalates	91
3.2.3	Alteration of Thyroid Hormone Levels	93
3.2.4	Exposure to DEHP in fetuses and infants.....	94
3.3	Detection of DEHP metabolites in urine	95
3.4	Synthesis of DEHP metabolites.....	96
3.5	Quantitative analysis.....	97
3.6	Relationships between urinary concentrations of DEHP metabolites, obesity and insulin sensitivity in obese children	101
3.6.1	Obesity	101
3.6.2	Causes	102
3.6.3	Mechanism of action.....	103
3.7	Detection of DEHP metabolites in obese children	104
3.8	Results.....	106
3.9	Association between urinary excretion of di(2-ethylhexyl)phthalate secondary metabolites and Autism Spectrum Disorders in children ..	109

3.9.1	Autism Spectrum Disorders.....	109
3.9.2	Etiology of ASDs.....	110
3.9.3	Subjects' population	111
3.9.4	Statistical analysis.....	112
3.9.5	Results.....	112
4	EXPERIMENTAL PART	122
4.1	Materials and methods	122
5	Solid Phase Peptide Synthesis (SPPS).	124
5.1	General procedure for in batch SPPS on a manual synthesizer	124
5.1.1	Conventional and MW-assisted synthesis of PTHrP(1–34)NH ₂	125
5.2	Amino Terminal Acetylation. General Procedure	126
5.3	Deprotection, Cleavage and Purification of Free Peptide. General Procedure	126
5.4	General procedure for solid-phase extraction SPE.....	127
5.5	MW-assisted Mini-cleavage. General Procedure	127
5.6	HPLC Analysis of PTHrP(1–34)NH ₂	128
5.7	UPLC-ESI-MS Analysis of intermediate fragments of PTHrP(1–34)NH ₂	128
6	Synthesis of N^α-Fmoc-ω-azido-α-amino acids and N^α-Fmoc-ω-alkynyl-α-amino acids.....	129
6.1	Deprotection of Boc-protecting group. General procedure	129
6.2	Fmoc Protection of the Free Amino Acid. General Procedure.....	129
6.3	Diazotransfert on ω-aminic group of N ^α -Boc or N ^α -Fmoc-amin acids with triflic anhydride. General procedure.....	129
6.4	Synthesis of imidazole-1-sulfonyl azide hydrochloride as diazotransfer reagent.....	130
6.5	Diazotransfert on ω-aminic group of N ^α -Fmoc- amino acids with Imidazole-1-sulfonyl azide hydrochloride. General Procedure	130
6.5.1	6-Azido-2S-[[[(9H-fluoren-9-ylmethoxy)carbonyl] amino]hexanoic acid (6-Azido-Fmoc-L-norleucine) (m=4)	131
6.5.2	5-Azido-2S-[[[(9H-fluoren-9-ylmethoxy)carbonyl]amino] pentanoic acid (5-azido-Fmoc-1-Norvaline) (m=3).....	131

6.5.3	4-Azido-2S-[[<i>(9H-fluoren-9-ylmethoxy) carbonyl</i>]amino] butanoic acid (Fmoc-Abu(γ -N ₃)-OH) (m=2)	132
6.5.4	3-Azido-2S-[[<i>(9H-fluoren-9-ylmethoxy)carbonyl</i>]amino] propanoic acid (3-Aziodo-Fmoc-L-Alanine) (m=1)	133
6.6	General procedure for the synthesis of <i>p</i> -toluenesulfonate derivatives	133
6.6.1	5-Hexyn-1-ol 1-(4-methylbenzene sulfonate)	133
6.6.2	4-Pentyn-1-ol 1-(4-methylbenzene sulfonate)	134
6.7	Synthesis of ω -alkynyl bromo derivatives. General procedure	134
6.7.1	6-Bromohex-1-yne	134
6.7.2	5-Bromopent-1-yne	134
6.8	Synthesis of chiral inducer	135
6.8.1	Synthesis of (S)-N-benzylproline (BP)	135
6.8.2	Synthesis of (S)-2-(N-Benzylpropyl)aminobenzophenone (BPB)	135
6.8.3	Synthesis of [Gly-Ni-BPB]	136
6.9	Alkylation of the Gly-Ni-BPB complex with bromoalkynes. General procedure	137
6.9.1	Alkylation of the Gly-Ni-BPB complex with 6-bromohex-1-yne (n=4) ..	137
6.9.2	Alkylation of the Gly-Ni-BPB complex with 5-Bromopent-1-yne (n=3) ..	138
6.9.3	Alkylation of the Gly-Ni-BPB complex with 4-bromo-1-butyne (n=2) ...	138
6.10	Hydrolysis of the Alkylated Complexes. General Procedure	139
6.10.1	2S-[[<i>(9H-Fluoren-9-ylmethoxy) carbonyl</i>]amino]-7-octynoic acid (n=4) ..	139
6.10.2	2S-[[<i>(9H-Fluoren-9-ylmethoxy)carbonyl</i>] amino]-6-heptynoic Acid (n=3) ..	140
6.10.3	2S-[[<i>(9H-Fluoren-9-thoxy) carbonyl</i>]amino]-5-hexynoic acid (n=2). ..	140
6.11	General procedure for click chemistry	141
6.12	Lactam bridge formation. General procedure	141
6.13	cAMP Based Functional Bioassay	143
6.14	NMR conformational analysis	144

6.14.1	NMR structure calculation.....	144
7	EXPERIMENTAL PART B.....	145
7.1	Synthesis of 1-Hydroxy-2-ethylhex-5-ene.....	145
7.1.1	2-ethylhex-5-enoic acid	145
7.1.2	2-ethylhex-5-en-1-ol	145
7.1.3	Mono(2-ethylhexenyl) 1,2-benzenedicarboxylate (MEHP)	146
7.1.4	Mono(2-ethyl-6-hydroxyhexyl) 1,2-benzenedicarboxylate (6-OH-MEHP).....	146
7.1.5	Mono(2-ethyl-5-oxohexyl)1,2-benzenedicarboxylate(5-oxo-MEHP).....	147
7.1.6	Mono(5-carboxy-2-ethylpentyl)1,2-benzenedicarboxylate (5-cx-MEHP)	148
7.1.7	Mono(2-ethyl-5-hydroxyhexyl)1,2-benzenedicarboxylate (5-OH-MEHP).....	148
8	Detection of DEHP metabolites in urines.....	149
8.1.1	Calibration curves	149
8.2	Samples pre-treatment	150
8.2.1	Sample Preparation: Solid-Phase Extraction (SPE).....	150
8.2.2	Daily protocol	151
9	Abbreviations.....	153

Supplementary Material

INTRODUCTION

Bioactive conformations in proteins

Peptides play an important role in many biologically relevant processes and are of outstanding interest in pharmaceutical research. However their use as drugs is limited by their conformational flexibility, instability to proteases, poor oral bioavailability, and pharmacodynamics. A central role in peptide and protein research is the development of rational approaches for the design of peptide and protein ligands, with specific physical, chemical and biological properties. Moreover the determination of the relationship between the conformation and the activity of biologically relevant peptides, e.g. hormones, is of great interest to design potent and very selective agonist/antagonist that could be used in pharmacology.

Information about these interactions improves our understanding of disease conditions and can provide the basis for new therapeutic approaches.

In nature, protein functions, including enzyme activities, are often regulated through conformational change, triggered by ligand-binding or by post-translational modifications at specific sites^{1,2}. The conformational state of receptor-protein complexes determines the functional state of a receptor.

Peptides are flexible molecules, which tend to adopt myriad of conformations in solution but can assume a single specific conformation only when bound to their receptors. When peptides interact with their receptors, these ligand assume a specific conformation and this folding is crucial for triggering the biological activity.

For example, the interaction of linear and flexible peptides with their macromolecular target, such as G protein-coupled receptors (GPCRs), involves a limited number of closely related conformations that are recognized and after binding either activate or block the biological activity of these targets. The so called bioactive conformation represents only a small subset of the larger ensemble of accessible conformations, which are in a dynamic equilibrium. Identifying the bioactive conformation of the ligand and the structure of the receptor–ligand complex is crucial to design more potent and selective ligands.

Two of the basic secondary structural elements that occur locally in protein structures are β -sheets and α -helices. Mimics of these structure can be useful in performing structure/activity relationship studies. In particular, β -turns (Figure 1)³ are the most common type of non-repetitive structure recognized in proteins and comprise, on average, 25% of the residues⁴. β -turns play an important role in proteins providing a direction change for the polypeptide chain and have been implicated in molecular recognition⁵ and in protein folding.

Turn type	ϕ_2	ψ_2	ϕ_3	ψ_3
I	-60°	-30°	-90°	0°
I'	60°	-30°	90°	0°
II	-60°	120°	80°	0°
II'	60°	120°	-80°	0°
III	-60°	-30°	-60°	-30°
III'	60°	-30°	60°	-30°
IV	Other			

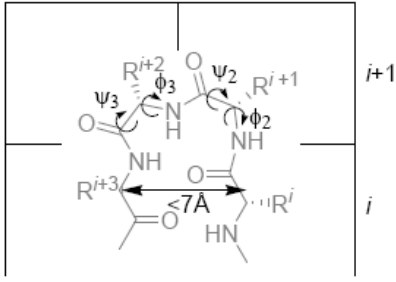


Figure 1. β -Turn types

Stabilization of secondary structures

Conformation of peptide fragments is fundamental to express the biological activity in proteins and it is related to the amino acid sequence. Peptides or proteins that do not have the correct conformation do not display their biological role.

The receptor-bound conformation may be poorly populated in solution but this structure may be promoted by incorporating conformational constraints into the peptide. Moreover, in the development of a peptidomimetic the identification of the key residues, and portions of the backbone in the peptide that are responsible for the biological effect, is crucial. A peptidomimetic embodies the conformational and molecular characteristics thought to be important for biological activity of the native sequence. Mimetics might exhibit enhanced potency and might be more selective for various receptor sub-types than their parent sequence, but several generations of variants may need to be prepared before a drug candidate emerges.

Characterization of possible relationship between peptide structure and biological activity is often aided by reduction in diversity of the possible conformational states that a linear peptide can adopt by generating cyclic analogues⁶.

The primary approach to design peptide ligands with high potency and specific biological and conformational properties, involves the introduction of conformational constraints. Accessible peptide conformation can be limited through cyclization and further by incorporation of constraints into the cycle. Locking the active conformation in cyclic peptides can give superpotent analogues in matched cases⁷. In addition, conformational constraints provide the basis for receptor selectivity. In fact, different receptors often bind the same flexible substrate in different conformations. If the conformation stabilized by the constraint closely resembles the structure responsible for the bioactivity, this modification can increase potency and selectivity of the resulting peptide.

Cyclic peptides offer the possibility of conveniently varying both scaffold geometry and R-group functionality. For example, parameters such as ring size can have a dramatic effect on the conformations of cyclic peptides, allowing access to structurally diverse species based on simple modifications in their linear sequences. Cyclization affects the degrees of freedom of all residues within the ring and thus a macrocycle should adopt a more defined conformation than the equivalent linear sequence (Figure 2).

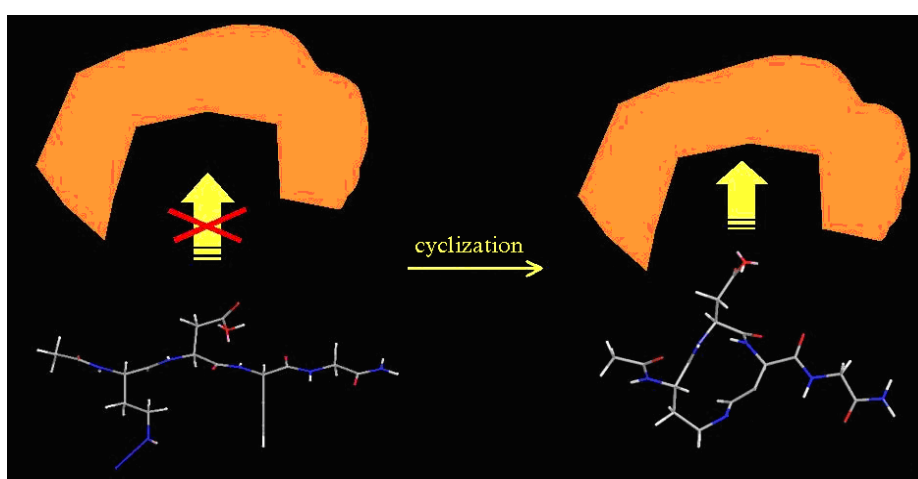


Figure 2. Differences concerning the interactions ligand-receptor between a linear peptide and cyclic peptide (Kessler H. *Angew. Chem. Int. Ed. Engl.* **1982**, *21*, 512).

Biologically active cyclic peptides specifically designed and prepared from the corresponding linear peptides, have been developed and demonstrated to possess several additional attributes including: (i) increased agonist or antagonist potency; (ii) prolonged biological activity and extended pharmacokinetics; (iii) increased stability to enzymatic degradation; and (iv) increased specificity for a particular receptor^{8,9,10,11,12,13}. The conformation of a peptide can be stabilized by introduction of bridges of various lengths between different parts of the molecule. The bridge can either be local and occurring within a single amino acid residue or being global and linking distant parts of the sequence. Intramolecular side-chain-to-side-chain cyclization is an established approach to achieve stabilization of specific conformations, and has been employed to achieve rigidification that results in restricting the conformational freedom. Therefore a larger conformational constraint can be introduced.

Types of cyclic peptides

Cyclic peptides are polypeptide chains whose amino and carboxyl *termini*, or two amino acids side chains, are themselves linked together by an amide (CO-NH), disulfide (S-S), carbon-carbon (CH₂-CH₂ or CH=CH), reduced amide (CH₂-NH), methylene thioether (CH₂-S), methylene sulfoxide (CH₂-SO), methylene ether (CH₂-O), thioamide (CS-NH), keto methylene (CO-CH₂), aza (NH-NR-CO) bond or recently 1,4-[1,2,3]triazolyl bridge (Figure 3)^{14,15,16}.

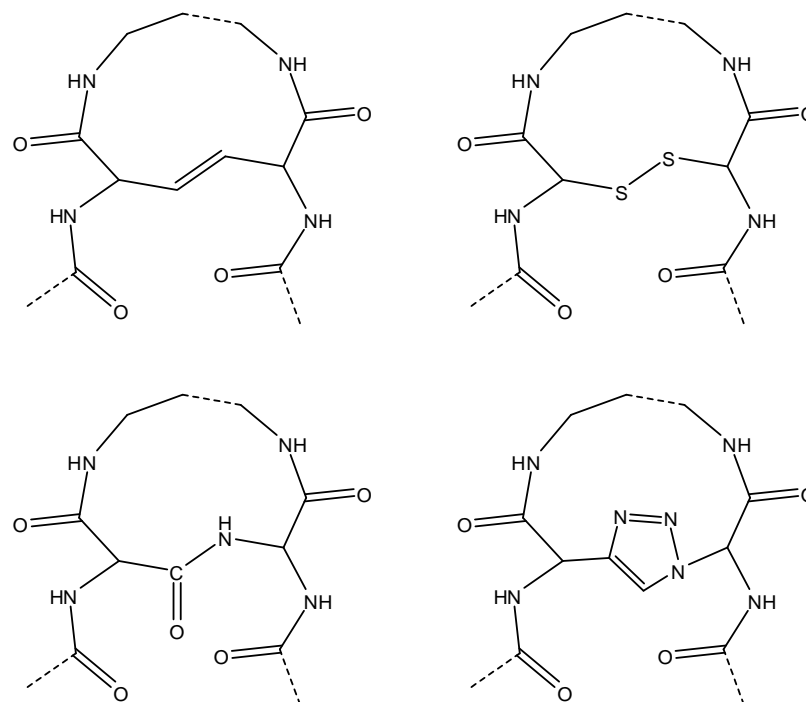


Figure 3. The most common types of cyclopeptides

In a number of studies, side-chain-to-side-chain cyclization has been performed by lactam bridge formation between *N*- and *C-termini*, side-chain and the *N*- or *C-terminus*, or two side-chains, to generate highly active peptides characterized by α -helix or β turn structures^{17,18,19}. Moreover the introduction of the amide isosteres also results in local and global changes of dipole moments and in the pattern of intramolecular and peptide-receptor hydrogen-bond formation. Thus, incorporation of amide bond isosteres cannot only improve *in vivo* stability as the mimetic is no longer a substrate for peptidases, but can improve selectivity towards receptor subtypes, can change pharmacological functions and can enhance pharmacokinetic properties.

On the other hand, cyclization in the form of a disulfide bridge between two cysteines, or other thiol-containing amino acids, is the most abundant post-translational modification resulting in side-chain-to-side-chain cyclization. However, under certain redox potentials, the disulfide bridge will behave as a relatively transient modification yielding either the reduced linear form or generate a variety of intermolecular disulfide containing products.

Moreover, the disulfide bridge can be reduced by specific enzymes such as glutathione reductase, or by nucleophilic agents. An alternative could be the ring

closing metathesis (RCM). This reaction allows the obtainment of cycles, starting from dienic substrates²⁰. The substrate scope includes rings of 6 to 20 members. In addressing macrocyclic peptides, a class of tetrapeptide disulfides inspired the synthesis of the carbon-carbon bond analogs. For example, replacement of cysteine residues by allylglycines resulted in the acyclic precursors, which were subjected to RCM to afford the corresponding macrocycles. Ruthenium complexes have been applied to RCM²¹. Moreover the carba replacement (CH₂-CH₂) is non-polar and does not allow the possibility of intramolecular or peptide-receptor hydrogen bonding, while the reduced amide (CH₂-NH) unit is conformationally different from the amide bond because it does not have any double-bond character.

All of these types of cyclization require orthogonal protection of side chains to afford a peptide cyclization. While side-chain to side-chain cyclization of peptide sequences has been successful in many instances, a number of factors are known to significantly influence the efficiency of the cyclization reaction and the yield of the desired cyclic peptide product.

Therefore cyclizations, which do not require complicated orthogonal protection schemes, are of great interest.

Cyclopeptides containing disulfide bridge: the case of somatostatine

In eukaryotic cells, nature has used disulfide bonds as its major covalent bond for conformational control and stabilization. Disulfide bonds constitute an abundant and important structural element in the folding of proteins and peptides. Disulfide bonds stabilize the properly folded conformation of proteins and/or destabilize denatured conformations by decreasing conformational entropy. While disulphide-containing peptide rings have reduced conformational properties relative to their linear counterparts, many cyclic disulphide-containing peptides still can be flexible. In many proteins and peptides, disulfide bridges are prerequisite for their proper biological function

The somatostatin hormones, or somatotropin release-inhibiting factor (SRIFs) are side-chain to side-chain disulfide-bridged cyclic peptides. The highly potent cyclic peptide somatostatin, SRIF^a H-Ala¹-Gly²-c[Cys³-Lys⁴-Asn⁵-Phe⁶-Phe⁷-Trp⁸-Lys⁹-

Thr¹⁰-Phe¹¹-Thr¹²-Ser¹³-Cys¹⁴]-OH (SRIF-14) (Figure 4), was isolated from mammalian hypothalamus and first synthesized by J. Rivier²².

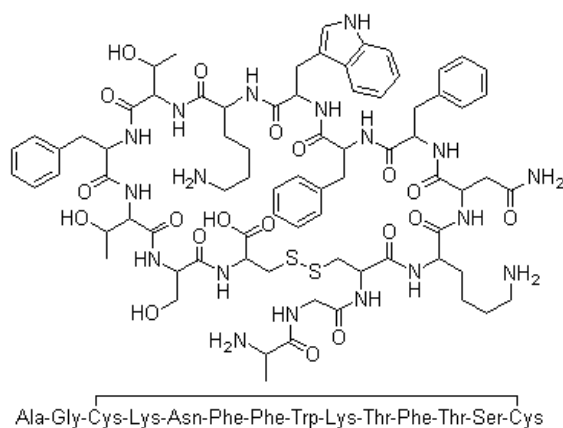


Figure 4. Somatostatin structure

Later on, it was found that native SRIF occurs in two biologically active forms, SRIF-14 and a 28-residue peptide. The natural hormone is widely distributed in the endocrine and central nervous systems and it has many modulating actions in the body, such as growth hormone (GH) inhibition, and glucagon, insulin, and gastrin release suppression.

A family of five G-protein-coupled somatostatin receptors (sst1–5), located in the cell membrane, mediates the biological effects of SRIF.

It is known that some of these receptors, mainly the sst2 and sst5 subtypes, mediate the antiproliferative effects of SRIF on cellular growth of many sort of tumors.

SRIF receptors are strongly expressed in various types of malignant cells, particularly in some neuroendocrine or neuroendocrine-like tumors. A lot of somatostatin analogues radiolabeled, were designed mainly for the targeting of malignant cells with γ - or β -emitting radionuclides, for tumor imaging and for therapy. The clinical use of native SRIF has been precluded by its short half-life in vivo (1–2 min) but the broad spectrum of physiological activity of this hormone has prompted many researchers to investigate the structural requirements necessary to elicit the biological activity. As a consequence, in the past decades, hundreds of peptide and nonpeptide analogues were synthesized and tested for their structure–activity relationships²³. Among them, Octreotide (trade name Sandostatin[®], provided

by Novartis Pharmaceutical), (Figure 5) a cyclic octapeptide SRIF agonist, was synthesized by Sandoz researchers¹⁵.

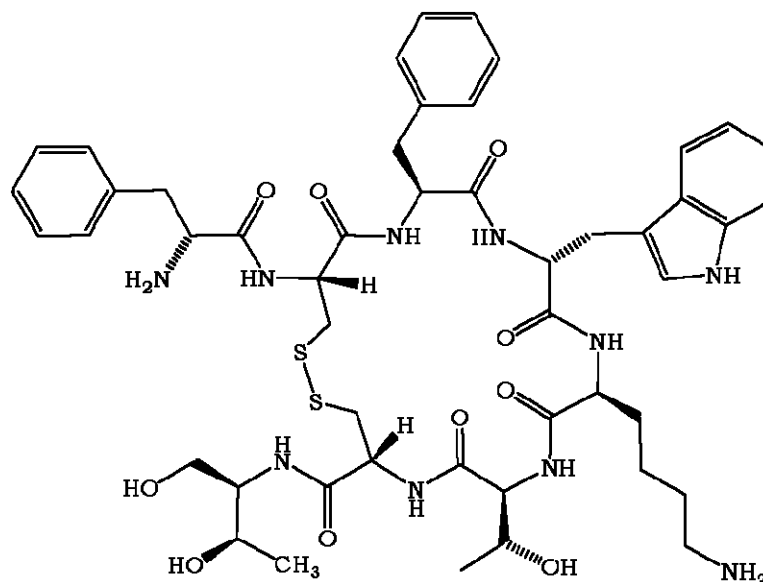


Figure 5. Structure of octreotide

Octreotide contains the disulfide bridging of the parent peptide and shows high affinity and specificity toward *sst2* receptor subtype²⁴. It was the first analogue to be used in clinical protocols. However, the administration of octreotide itself as a cell growth inhibitor, was successful only in a few cancer types as acromegaly and metastatic carcinoid diseases²⁵. It is used in clinical protocols mainly as a carrier of radionuclides for diagnostic or therapeutic purposes^{24,26,27}. Octreotide incorporates D-Trp in place of Trp⁸ of SRIF and exhibits the so-called pharmacophore sequence, Phe⁷-D-Trp⁸-Lys⁹-Thr¹⁰. The disulfide tether of octreotide stabilizes a β -turn type II' structure spanning the D-Trp⁸-Lys⁹ residues, supposed to be mandatory for the binding to the *ssTs*²⁸. Nevertheless, Octreotide presents side effects and low affinity toward the same receptors, prompting many researchers to look for more stable bridging regions and peptide sequences to produce more selective and long acting analogues. Interestingly, the action mode of *sst*-related compounds is mediated by a massive endocytosis of the *sst*-analogue/*sstr* complex²⁹, thus enabling the accumulation of compound within the targeted cell. This property has been thoroughly exploited for imaging cancer cells using radiolabeled analogues of

octreotide, in which the cyclopeptide is conjugated to a metal chelating moiety, generally a polynitrogen molecule either linear (e.g. diethylene triamine pentaacetic acid, DTPA) or cyclic (tetraazacyclododecane tetraacetic acid, DOTA)³⁰.

On the other hand, it is well-known that the disulfide bridge is prone to be attacked by endogenous reducing enzymes, such as glutathione reductase and thioredoxin reductase, or by nucleophilic and basic agents³¹. Disulfide isomerases, as well as reducing agents and thiols, can affect this covalent bond and can lead to structural rearrangement with a complete loss of activity. For this reason, octreotide and its analogues demonstrated side effects as limited bioavailability and selectivity, as well as chemical instability of the S-S bridge. Furthermore, the labeling of the octreotide derivatives with isotopes such as ^{99m}Tc and ¹⁸⁸Re need a step in reducing medium that can afford ring cleavage, especially at the level of the disulfide linkage. The replacement of this essential structural element by bioisosteric, hydrolytically, and reductively stable substitutes is therefore of great interest.

Several approaches to substitution of the disulfide bridge by more stable covalent connections such as amides, thioether, diselenides, or carbon-based bridges, have been reported^{14,32,33,34,35,36,37}. For example, the effect was studied of the replacement of the disulfide bridge with a dicarba-bond, obtained by RCM reactions, catalyzed by ruthenium, on two allylglycines substituting the Cys^{3,14} residues in the linear peptide²⁰. Moreover, very recently Meldal and co-workers studied the potential of [1,2,3]triazoles as functional mimetics of multiple naturally occurring disulfide bonds in biologically active peptides³⁸. By replacing of cysteines involved in the disulfide bridge of the peptide sequence with unnatural synthetic amino acids able to generate, via copper catalyzed 1,3-dipolar Huisgen reaction, more stable tethers bridging the bioactive site are produced. Moreover, this strategy allows the possibility to investigate the cycle dimension and orientation of triazolyl moiety that can induce the best bioactivity.

Triazoles exhibit chemical orthogonality and provide excellent stability against isomerases and proteases^{39,40}. Moreover, triazoles can be formed in a two-component approach, which is comparable to that of disulfide bond formation from two cysteine residues. This strategy allows directional formation of disulfide bond mimetics by the substitution of two or more cysteine residues in a peptide with alkynyl- and azido-functionalized amino acids (Figure 6).

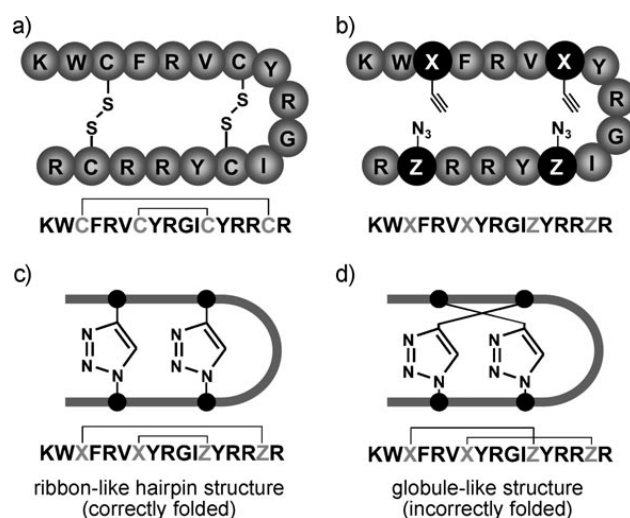


Figure 6. Mimicking of disulfide bridges by triazoles in tachyplesin-I by the replacement of cysteine residues by alkyne (X) and azido amino acids (Z), which form triazoles upon the copper-catalyzed cycloaddition of the azides and alkynes (“click” reaction): a) tachyplesin-I and b) linear analogues. Cyclization leads to c) the correctly folded hairpin structure or d) incorrectly folded globule-like structure (Holland-Nell K., Meldal M., *Angew. Chem. Int. Ed.* **2011**, *50*, 5204-06).

Moreover, when four cysteine residues are involved in disulfide bridging, their replacement with functionalized amino acids able to perform the “click” reaction, can lead to the correct folding in the case of the correct positioning of the reactive groups.

Triazole-containing cyclopeptides

The recently introduced Cu^I-catalyzed azido-to-alkyne 1,3-dipolar cycloaddition (CuAAC), or 1,3-dipolar Huisgen’s cycloaddition^{41,42,43}, as a prototypic “Click chemistry reaction”⁴⁴ presents a promising opportunity to develop a new paradigm for intramolecular side-chain-to-side-chain cyclization in peptides. In fact, the 1,4-1,2,3-triazolyl bridge offers interesting mode to generate structural constraint.

The inherent low reactivity of the azide and alkynyl functions toward an expansive range of functional groups and reagents eliminates the need for elaborate protection schemes. In addition, the 1,4-disubstituted 1,2,3-triazolyl bridging moiety is also inert toward a vast variety of synthetic conditions and its proteolytic stability is of great importance for applications in biological and material sciences. Therefore, the 1,2,3-triazolyl bridge offers interesting mode to generate structural constraint.

The 1,2,3-triazole is isosteric to the peptide bond and offers an appealing structural motif in peptidomimetics thanks to its structural and electronic features that are similar to those of a peptide bond. In particular, the 1,4-disubstituted-[1,2,3]-triazole represents a trans-amide peptide bond mimicking moiety⁴⁵, positioning the substituents in positions 1 and 4 at 5.1 Å apart, which is only slightly longer than the distance between two carbons separated by a trans-amide bond (3.9 Å). Triazole moiety is planar and possesses a large dipole moment of ~5 Debye, which bisects the ring plane near atoms N3 and C5, and has the capacity of the N2 and N3 electron lone pairs to serve as hydrogen bond acceptors (Figure 7). However, unlike peptide bonds, triazoles are both proteolytically and metabolically stable. In addition, the azide and alkyne precursors required for their synthesis are relatively inert, making the Huisgen cycloaddition bio-orthogonal.

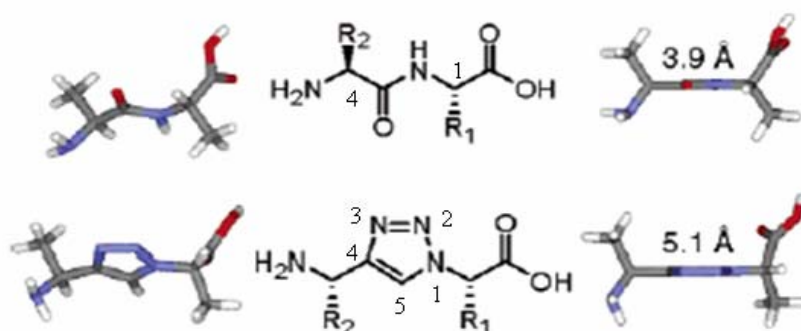


Figure 7. Topological similarities of amide and [1,2,3] triazole (Bock V.D., Perciaccante R., Jansen T.P., Hiemstra H., van Maarseveen J.H., *Org. Lett.*, 2006, 8, 919-922).

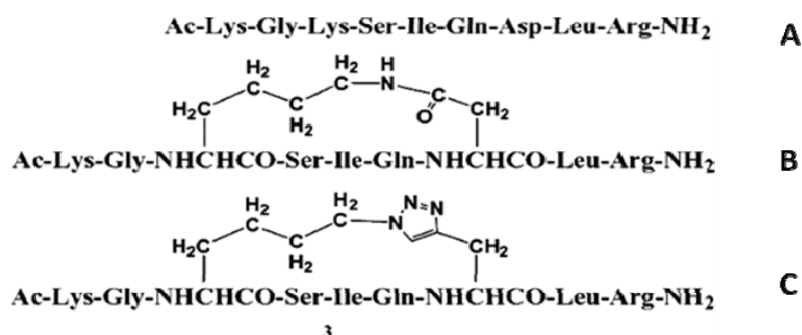
Intramolecular *i*-to-(*i*+4) side-chain-to-side chain cyclization stabilize the formation of helix-like secondary structures: the case of parathyroid hormone and Parathyroid hormone – related protein

Previous studies⁴⁶ performed in our Laboratory of Peptide & Protein Chemistry & Biology (PeptLab) were focused on the bioactive conformation of parathyroid hormone (PTH) and PTH-related protein (PTHrP). PTHrP is an autocrine, paracrine and intracrine regulator of processes such as endochondrial bone formation and epithelial-mesenchymal interactions during the development of mammary glands. The *N*-terminal fragments (1-34) of both PTH and PTHrP, regulate calcium in the blood, by interaction with the receptor PTH1-Rc. Moreover they have in common

only 8 amino acids in the first 13 residues. Chorev *et al.*^{47,48,49,50} hypothesized that both hormones assume the same conformation when they bind to the receptor. In particular, in biomimetic medium, like H₂O/TFE (2,2,2-trifluoroethanol), PTH and PTHrP share the *N*-terminal part, as α -helical structure. Therefore, this particular conformation can be important for their biological activity because interaction with the receptor is higher. Moreover, stabilization of the α -helical structure by lactam ring between Lysine¹³ and Aspartic acid¹⁷ (*i*-*i*+4) increased antagonist activity⁴⁷. Starting from the observation that 1,4-disubstituted [1,2,3]triazolyl serves as a rigid linking unit mimicking a trans-amide bond, in previous work we reported the synthesis and conformational analysis of a series of *i*-to-*i*+4 side chain-to-side chain 1,4-disubstituted-[1,2,3]triazolyl-bridged cyclo-nonapeptides, analogous of the model *i*-to-*i*+4 lactam-bridged cyclo-nonapeptide *N* ^{α} -Ac-PTHrP(11-19)NH₂, that is a truncated version of the α -helical and potent parathyroid hormone receptor 1 (PTHr1) agonist, [Lys¹³(&¹),Asp¹⁷(&²)]PTHrP(1-34)NH₂^{18,50}, (Scheme 1). In this context, a synthetic strategy was set up to obtain a series of *N* ^{α} -Fmoc- ω -azido- α -amino- and *N* ^{α} -Fmoc- ω -ynoic- α -amino acids^{51,16} needed for CuAAC.

These previous studies explored the relationship between the size of the bridge containing the 1,2,3-triazolyl moiety, the location of this moiety within the bridge, its orientation relative to the peptide backbone, and the predominant conformations displayed by these heterodetic cyclic peptides⁴⁶.

The CD and NMR conformational analysis allowed to identify the permutations that mimic at the best the cyclo[Lys¹³,Asp¹⁴]PTH(11-19).



Scheme 1. Amino acid sequence of a modified fragment of *N* ^{α} -Ac-hPTHrP(11-19)NH₂ (A), lactam cyclopeptide [Ac-Lys-Gly-Lys(&¹)-Ser-Ile-Gln-Asp(&²)-Leu-Arg-NH₂] (B), *i*-to-*i*+4 side-chain to side-chain 1,4-disubstituted [1,2,3]triazolyl-bridged peptide (C).

It was demonstrated that the optimal conformational organization may be related to the right size of the methylen bridge and to the favourable location of triazolyl ring, which supports non-distorting intramolecular interactions and stabilizes ordered regular conformations⁵². The *i*-to-*i*+4 side chain-to-side chain 1,4-disubstituted-[1,2,3]triazolyl-bridged cyclo-nonapeptide (Scheme 1C) share conformational properties with its structurally related helical *i*-to-*i*+4 lactam-bridged cyclo-nonapeptide (Scheme 1B). Therefore the CuAAC reaction can be used to generate a 1,4-substituted 1,2,3-triazole between side chain azido and alkynyl moieties at the *i* and *i*+4 positions of a peptide chain that effectively mimics the use of the analogous lactam bridge.

Optimized synthesis of PTHrP(1–34)NH₂

PTHrP(1-34)NH₂ sequence is: H-Ala¹-Val-Ser-Glu-His-Gln-Leu-Leu-His-Asp¹⁰-Lys-Gly-Lys-Ser-Ile-Gln-Asp-Leu-Arg-Arg²⁰-Arg-Phe-Phe-Leu-His-His-Leu-Ile-Ala-Glu³⁰-Ile-His-Thr-Ala-NH₂. Considering the presence of clusters of arginines, sterically hindered and hydrophobic amino acid residues in the 19-28 sequence of PTHrP and the considerable length of the peptide, the synthesis of PTHrP(1-34)NH₂ is quite challenging. Therefore we focused our effort in the optimization of a synthesis protocol for this peptide. In particular, we showed the advantages that the use of microwaves have, in obtaining the best results in terms of yield and purity of the final peptide. The application of microwave irradiation in peptide chemistry has been reported in several publications, most of which describe case studies of successful syntheses of difficult peptides. Microwaves have also been used to monitor the synthesis of the peptide PTHrP(1-34)NH₂. In fact, during the elongation of the peptide chain, we analyzed by UPLC-ESI-MS intermediate fragments obtained through micro-cleavages assisted by microwaves. This strategy has allowed us, through the characterization of sequences of deletion, to understand what are the critical points of the synthesis that may require the use of microwaves.

Intramolecular *i*-to-(*i*+5) side-chain-to-side chain cyclization stabilize the formation of β -turn secondary structures: melanocortin peptides hormones.

Following the previous studies performed on PTH and PTHrP, we decided to apply the triazole strategy to another peptide hormone, involved in a lot of different biological process in human: the melanocortin peptide hormones.

Melanocortins are a family of hormones secreted by pituitary gland and also expressed in the brain and peripheral tissues. Melanocortins include adrenocorticotropin (ACTH) and α -, β -, and γ - melanocyte stimulating hormones (MSHs). These hormones are involved in many biological functions by interacting with five receptors hMC1R-hMC5R. Consequently they are considered a potential target for drugs to treat diseases such as obesity and sexual dysfunction.

MTII, Ac-Nle⁴-c[Asp⁵-D-Phe⁷-Lys¹⁰] α MSH₄₋₁₀-NH₂,^{53,54,55} is a potent long acting non-selective super-agonist of MC1R, MC3R, MC4s⁵⁶. This homodetic Asp⁵ to Lys¹⁰ side chain-to-side chain bridged lactam stabilizes the pharmacophore containing sequence His⁶-D-Phe⁷-Arg⁸-Trp⁹ in a type-II β -turn. The particular importance of melanocortin system, underscores the unmet need for highly selective, pharmacokinetically diverse, and bioavailable agonists and antagonists analogs.

The introduction of [1,2,3]triazole was aimed to stabilize a β -turn conformation replacing the lactam bridge of MTII with an *i*-to-*i*+5 side chain-to-side chain cyclization via Cu^I-catalyzed azido-to-alkyne 1,3-dipolar cycloaddition (CuAAC) generating 1,4- or 4,1-disubstituted [1,2,3]triazolyl-containing ring structures.

A series of heterodetic MTII related cyclo-heptapeptides, that varied in the size, location and in the orientation of the disubstituted [1,2,3]-triazolyl bridge, was synthesized for a fine-tuning of the best conformation needed for bioactivity. Studying this modification in the context of the MTII scaffold provides the opportunity to evaluate its potential as a modulator of receptor sub-type selectivity. Conformational and biological studies were performed on the peptides synthesized to identify the location and direction of the 1,2,3-triazolyl in the bridge that best reproduce the β -turn conformation leading to highly potent and selective MT-II agonists.

Reference

- ¹ Kiessling L.L., Gestwicki J.E., Strong L.E., *Curr. Opin. Chem. Biol.* **2000**, *4*, 696.
- ² Pearl L.H., Barford D. *Curr. Opin. Struct. Biol.* **2002**, *12*, 761.
- ³ Venkatachalam C.M., *Biopolymers*, **1968**, *6*, 1425–1436.
- ⁴ Kabsch W., Sander C., *Biopolymers*, **1983**, *22*, 2577-2637.
- ⁵ Rose G.D., Gierasch L.M., Smith J.A., *Adv Protein Chem*, **1985**, *37*, 1-109.
- ⁶ Felix A.M., Wang C.T., Heimer E.P., Fournier A., *Int. J. Peptide Protein Res.*, **1988**, *31*, 231–238.
- ⁷ Kessler H., *Angew. Chem. Int. Ed. Engl.* **1982**, *21*, 512.
- ⁸ Hruby V.J., *Life Sci*, **1982**, *31*, 189–199.
- ⁹ Schmidt B., Ho L., Hogg P.J., *Biochemistry*, **2006**, *45*, 7429.
- ¹⁰ Li P., Roller P.P., Xu J., *Curr. Org. Chem*, **2002**, *6*, 411 – 440.
- ¹¹ Lambert J.N., Mitchell J.P., Roberts K.D., *J. Chem. Soc. Perkin Trans. 1* **2001**, 471 – 484.
- ¹² Walensky L.D., Kung A.L., Escher I., Malia T.J., Barbuto S., Wright R.D., Wagner G., Verdine G.L., Korsmeyer S.J., *Science*, **2004**, *305*, 1466.
- ¹³ Moellering R.E., Cornejo M., Davis T.N., Del Bianco C., Aster J.C., Blacklow S.C., Kung A.L., Gilliland D.G., Verdine G.L., Bradner J.E., *Nature*, **2009**, *462*, 182.
- ¹⁴ Stymiest J.L., Mitchell B.F., Wong S., Vederas J.C., *J. Org. Chem.*, **2005**, *70*, 7799-7809.
- ¹⁵ Bauer W., Briner U., Doepfner W., et al., *Life Sci.*, **1982**, *31*, 1133-1140.
- ¹⁶ Le Chevalier Isaad A., Barbetti F., Rovero P., D’Ursi A.M., Chelli M., Chorev M., Papini A.M., *Eur. J. Org. Chem.*, **2008**, *31*, 5308–5314
- ¹⁷ Felix A.M., Heimer E.P., Wang C.T., Lambros T.J., Fournier A., Mowles T.F., Maines S., Campbell R.M., Wegrzynski B.B., Toome V., Fry D., Madison V.S., *J. Pept. Protein Res.* **1988**, *32*, 441.5.
- ¹⁸ Chorev M., Roubini E., McKee R.L., Gibbons S.W., Goldman M.E., Caufield M.P., Rosenblatt M., *Biochemistry* **1991**, *30*, 5968.
- ¹⁹ Kapurniotu A., Taylor J.W., *J. Med. Chem.*, **1995**, *38*, 836.
- ²⁰ D’Addona D., Carotenuto A., Novellino E., Piccand V., Reubi J.C., Di Cianni A., Gori F., Papini A.M., Ginanneschi M., *J. Med. Chem.*, **2008**, *51(3)*, 512-520.
- ²¹ Miller S.J., Blackwell H.E., Grubbs R.H., *J. Am. Chem. Soc.*, **1996**, *118*, 9606-9614.
- ²² Rivier J., *J. Am. Chem. Soc.*, **1974**, *96*, 2986–2992.
- ²³ Janecka A., Zubzycka M., Janecki T., *J. Pept. Res.*, **2001**, *58*, 91–107.
- ²⁴ Weckbecker G., Lewis I., Albert R., Schmid H.A., Hoyer D., Bruns C, *Nat. Rev. Drug Discov*, **2003**, *2*, 999–1018.

-
- ²⁵ Lamberts S.W., Van der Lely A.J., Hofland L., *J. New Eur. J. Endocrinol.*, **2002**, *146*, 701–705.
- ²⁶ Deshmukh M.V., Voll G., Kühlewein A., Schmitt J., Kessler H., Gemmecker G., *J. Med. Chem.*, **2005**, *48*, 1506–1514.
- ²⁷ Fichna J., Janecka A, *Bioconjug. Chem.*, **2003**, *14*, 3–17.
- ²⁸ Mattern R.H., Moore S.B., Tran T.A., Rueter J.K., Goodmann M., *Tetrahedron* **2000**, *56*, 9819
- ²⁹ Reubi J.C., Waser B., Cescato R., Gloor B., Stettler C., Christ E., *J. Clin. Endocrinol. Metab.*, **2010**, *95*, 2343.
- ³⁰ Parker D., Dikins R.S, Puschmann H., Crossland C., Howard J.A.K., *Chem. Rev.*, **2002**, *102*, 1977.
- ³¹ Williams R.M., Liu J., *J. Org. Chem.*, **1998**, *63*, 2130–2132.
- ³² Buchman G.W, Banerjee S., Hansen J.N., *J. Biol. Chem.*, **1988**, *263(16)*, 260.
- ³³ Hargittai B., Sole N.A., Groebe D.R., Abramson S.N., Barany G., *J. Med. Chem.*, **2000**, *43*, 4787. .
- ³⁴ Bondebjerg J., Grunnet M., Jespersen T., Meldal M., *Chem Bio Chem*, **2003**, *4*, 186.
- ³⁵ Armishaw C.J., Daly N.L., Nevin S.T., Adams D.J., Craik D.J., Alewood P.F., *J. Biol. Chem.*, **2006**, *281*, 14136.
- ³⁶ Moroder L., *J. Pept. Sci.*, **2005**, *11*, 187.
- ³⁷ Robinson A.J., van Lierop B.J., Garland R.D., Teoh E., Elaridi J., Illesinghe J.P., Jackson W.R., *Chem. Commun.* **2009**, 4293
- ³⁸ Holland-Nell K., Meldal M., *Angew. Chem. Int. Ed.*, **2011**, *50*, 1–4.
- ³⁹ Henchey L.K., Jochim A.L., Arora P.S., *Current Opinion in Chemical Biology*, **2008**, *12*, 692.
- ⁴⁰ Kim Y.W., Verdine G.L., *Bioorganic and Medicinal Chemistry Letters*, **2009**, *19*, 2533.
- ⁴¹ Huisgen R., in *1,3-Dipolar Cycloaddition Chemistry* (Ed: A. Padwa), Wiley, New York, **1984**, 1-176.
- ⁴² Rostovtsev V.V., Green L.G., Fokin V.V., Sharpless K.B., *Angew. Chem. Int. Ed. Engl.* **2002**, *41(14)*, 2596-2599.
- ⁴³ Tornøe C.W., Christensen C., Meldal M., *J. Org. Chem.* **2002**, *67(9)*, 3057-3064.
- ⁴⁴ Kolb H.C., Finn M.G., Sharpless K.B., *Angew. Chem. Int. Ed. Engl.* **2001**, *40(11)*, 2004-2021.
- ⁴⁵ Bock V.D., Perciaccante R., Jansen T.P., Hiemstra H., van Maarseveen J.H., *Org. Lett.*, **2006**, *8*, 919-922.

-
- ⁴⁶ Cantel S., Le Chavelier Isaad A., Scrima M., Levy J.J., Di Marchi R.D., Rovero P., Halperin J.A., D'Ursi A.M., Papini A.M., Chorev M., *J.Org.Chem.*, **2008**, *73*,5663-5674.
- ⁴⁷ Schievano E., Mammi S., Bisello A., Rosenblatt M., Chorev M., Peggion E., *J. Peptide Sci.*, **1999**, *5*, 330-337.
- ⁴⁸ Bisello A., Nakamoto C., Roseblatt M., Chorev M., *J. Am. Chem. Soc.* **1997**, *36*, 3293-3299.
- ⁴⁹ Mierke D.F., Maretto S., Schievano E., De Luca D., Bisello A., Mammi S., Rosenblatt M., Peggion E., Chorev M., *J. Am. Chem. Soc.* **1997**, *36*, 10372-10383.
- ⁵⁰ Maretto S., Mammi S., Bisacco E., Peggion E., Bisello A., Rosenblatt M., Chorev M., Mierke D.F., *J. Am. Chem. Soc.* **1997**, *36*, 3300-3307.
- ⁵¹ Le Chevalier Isaad A., Papini A.M., Chorev M., Rovero P., *J. Pept. Sci.*, **2009**, *15*, 451–454.
- ⁵² Scrima M., Le Chevalier Isaad A., Rovero P., Papini A.M., Chorev M., D'Ursi A.M. *Eur.J. Org. Chem*, **2010**, 446-457.
- ⁵³ Haskell-Luevano C., Nichiforovich G., Sharma S.D., Yang Y.K., Dickinson C., Hraby V.J., Gantz, I., *J. Med Chem* **1997**, *40*, 1738-1748.
- ⁵⁴ Al-Obeidi F.A., Hadley M.E., Pettitt M.B., Hraby V.J., *J. Am Chem Soc.*, **1989**, *111*, 3413-3416.
- ⁵⁵ Al-Obeidi F.A., Castrucci A.L., Hadley M.E., Hraby V.J., *J. Med Chem.*, **1989**, *32*, 2555-2561.
- ⁵⁶ Ying J., Kövér K.E., Gu X., Han G., Trivedi D.B., Kavarana M.J., Hraby V.J., *Biopolymers*, **2003**, *71*, 696-716.

1

Difficult peptide synthesis optimized by microwave-assisted approach: a case study of PTHrP(1–34)NH₂

1.1 The parathyroid hormone (PTH) and the parathyroid hormone-related protein (PTHrP)

Parathyroid hormone (PTH), the most important hormonal regulator of mineral ion homeostasis in mammals, is secreted by the parathyroid glands as a protein containing 84 amino acids. Parathyroid hormone-related protein (PTHrP) was first identified and cloned from malignant tumor cells and tissues from patients with the syndrome of humoral hypercalcemia of malignancy^{57,58}. PTHrP is an autocrine, paracrine and intracrine hormone, produced by most tissues in the body. It regulates different processes such as endochondrial bone formation and epithelial–mesenchymal interactions during the development of mammary glands, produced by most tissues in the body. PTH regulates mineral metabolism and bone turnover by activating specific receptors located on osteoblastic and renal tubular cells, while PTHrP which has partial sequence homology to PTH, is associated with the syndrome of humoral hypercalcemia of malignancy⁵⁹. PTH acts to increase the concentration of calcium in the blood by acting upon PTH receptor in three parts of the body. Increasing calcium concentration in the blood acts (*via* feedback inhibition) to decrease PTH secretion by the parathyroid glands (Figure 8).

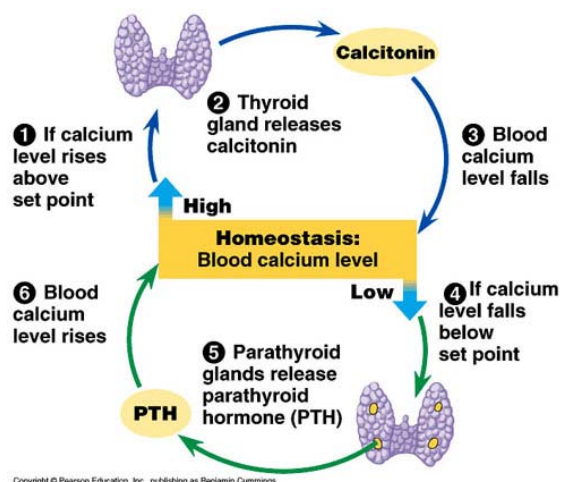


Figure 8. Process for the activation of PTH.

transepithelial fluxes of calcium, but many of its actions have nothing to do with calcium homeostasis. Most prominently, PTHrP peptides exert significant control over proliferation, differentiation and death of many cell types. They also play a major role in development of several tissues and organs.

1.2 Microwave assisted peptide synthesis

Microwave (MW) is a form of electromagnetic energy located between infrared radiation and radiowave with frequencies in the range of 0.3-300 GHz, which corresponds to wavelengths of 1 mm - 1 m, but only the frequency of 2.45 GHz, corresponding to a wavelength of 12.24 cm, is utilized by industrial and domestic microwave apparatus, in order to avoid interferences with radar and telecommunication activities operating within this region.

The energy of the microwave photon in this frequency region (0.0016 eV) is too low to break chemical bonds and is also lower than the energy of Brownian motion. It is therefore clear that microwaves cannot induce chemical reactions^{66,67,68}. Microwave heating works quite differently than conventional heating that transfers energy to reaction via conduction or convection. Conventional heating is a comparatively slow and inefficient method for transferring energy into the system because it depends on the thermal conductivity of the reaction vessel materials. On the contrary microwave approach is based on temperature increase by dielectric heating, which operates through two mechanisms: dipolar polarization and ionic conduction (Figure 10).

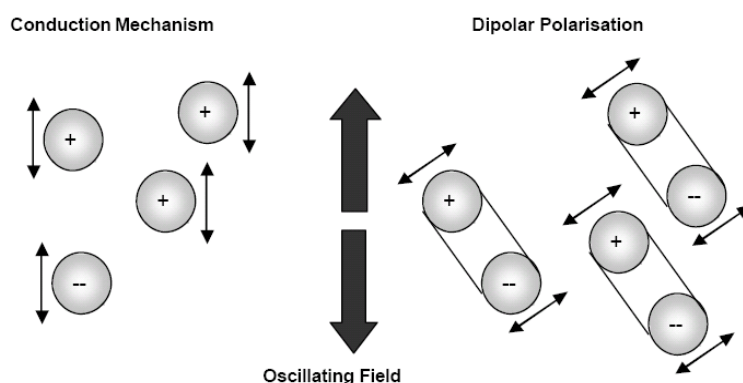


Figure 10. Methods of heating by microwave irradiation.

Since only the electric field transfers energy to heat a substance, this component of microwave irradiation causes dipoles and ions to align, and as the applied electric field oscillates, the dipole-ion field is forced to realign itself. In both events, since alignment doesn't occur completely, a part of this energy is lost as heat and cause a sudden rise of molecular temperature and, thereby, of the entire reaction mixture. Thus microwave energy enhances reaction rates and increases yields by limiting side reactions. While some believe that these results can be explained through thermal/kinetic effects, others argue that additional specific non-thermal microwave effects are at work.

1.2.1 Thermal effects

Thermal effects are strictly connected to the different characteristics between microwave and conventional heating. Microwave heating uses the ability of some compounds (liquids or solids) to transform electromagnetic energy into heat. The attitude of a substance to convert electromagnetic radiation into heat depends on its dielectric properties⁶⁷ and is calculated by the loss angle, $\tan\delta$, which is expressed as $\tan\delta = \varepsilon'' / \varepsilon'$. The loss factor ε'' quantifies the efficiency through which the absorbed energy is converted into heat, while the dielectric constant ε' , describes the ability of the molecules to be polarized by an electric field. A reaction medium with a high $\tan\delta$ value efficiently absorbs electromagnetic radiation and converts it into heat, whereas substances with low $\tan\delta$ values are not affected by microwaves⁶⁹. Therefore, energy transmission is produced by dielectric losses, which is in contrast to conduction and convection processes observed in conventional heating and the amount of heating is directly dependent on the dielectric properties of the molecules. These characteristics mean that absorption of the radiation and heating may be performed selectively. Moreover microwave irradiation is rapid and volumetric, with the whole material heated simultaneously, in contrast with conventional heating that is a process starting from the surface of a sample and slowly is transferred inside. The thermal effects observed under microwave irradiation conditions are a consequence of the inverted heat transfer (overheating)^{70,71}, the non-homogeneities of the microwave field within the sample, known as "hot spots"⁷², and the selective absorption of the radiation by polar compounds. These effects can be used efficiently

to improve processes, modify selectivities or even to perform reactions that do not occur under conventional conditions.

1.2.2 Specific non-thermal effects

Some authors have also justified the enhancement obtained in microwave applications, by the existence of specific non-thermal microwave effects that essentially result from a direct interaction of the electric field with specific molecules in the reaction medium. These effects can be rationalized considering the Arrhenius law:

$$k = Ae^{(-E_a/RT)}$$

It has been affirmed that the presence of an electric field leads to orientation effects of dipolar molecules and consequently changes the pre-exponential factor A or the activation energy (entropy term) in the Arrhenius equation^{73,74}. A similar effect should be observed for polar reaction mechanisms, where the polarity is increased going from the ground state to the transition state, thus resulting in an enhancement of reactivity by lowering the activation energy.

1.2.3 Modes

When the microwaves enter a cavity, they are reflected by the walls. The reflections of the waves eventually generate a three dimensional stationary pattern of standing waves within the cavity, called modes. Most early microwave-enhanced synthesis works were done in multi-mode systems. Multi-mode reactors present larger cavities with a microwave field that contains multiple modes of energy of different intensity, so called hot and cold spots. As a consequence, this non uniform microwave irradiation inside the reactor is compensated, if possible, by rotation of samples through the field. While multi-mode strategy is particularly suitable for parallel synthesis, the small individual samples characteristic of drug discovery are problematic in multi-mode systems, due to the hot and cold spots intrinsic in the cavity design. Moreover, the power density in the cavity is low, making it difficult to heat small individual samples. Recently, in order to obtain a well-defined heating pattern for small loads, single-mode cavities with good uniform energy distribution

and the ability to couple with small samples more efficiently have become available. These cavities are better suited for drug discovery work, because the higher power density allows the energy to be more focused. Because of this type of cavity allows only one single mode to be present. Much higher field strengths can be obtained, giving rise to more rapid heating. A suitably designed cavity also prevents the formation of ‘hot and cold spots’ within the sample, resulting in a uniform heating pattern. This is very important when microwave technology is used in organic chemistry, since the heating pattern for small samples can be well controlled. This allows for higher reproducibility and predictability of results as well as optimization of yields, which are usually more difficult when using a domestic microwave oven.

1.3 Synthetic strategies for difficult peptide sequences

Peptide synthesis by solid-phase methods is often hampered by partial unmasking of the N^α -protection and the occurrence of incomplete coupling. These problems generally depend on structuration and/or poor solvation of the growing peptide chain and are especially severe in the presence of the so-called “difficult sequences”.

Kinetic problems due to intermolecular aggregation or steric hindrance of protecting groups can generate premature termination of the sequence during the different steps of the solid-phase pathway. As a consequence, the desired products are contaminated by a series of structurally and chemically very similar compounds such as diastereoisomers formed after epimerization, or mismatch and incomplete sequences. Although conventional SPPS remains the principal strategy for peptide synthesis, we were attracted by the possibility to improve peptide reactions, by using microwave energy, decreasing chain aggregation during the syntheses, improving the coupling rates and preventing side reactions in particularly difficult peptide sequences.

The introduction in 1992 of MW irradiation in peptide chemistry stimulated a lot of interest followed by numerous efforts to use it to overcome synthetic difficulties resulting in sluggish reactions, low yields, and complex reaction crude products that were hard to purify⁷⁵.

Several different groups have reported the synthesis of peptides using microwave strategy, dramatically reducing reaction times and improving the yield of final product. During the last decade the growing interest in MW field has been marked by

the progress in developing scientific MW equipment to embrace specific research needs⁷⁶. In general, introduction of MW technology led to the shortening of reaction time that resulted in higher purity of crudes and increased yields of the pure final product. The application of MW irradiation in peptide chemistry has been reported in several publications, most of which describe case studies of successful syntheses of difficult peptide sequences⁷⁷.

However, a definitive comparison of conventional RT and MW-assisted-SPPS protocols must be performed on identical instruments. In fact, comparing conventional RT and MW-assisted SPPS carried out on different instruments that apply protocols that differ in the equivalent excess of reagents and their molar ratios, stirring techniques and the nature and number of washing steps, may be misleading. In addition, the automated synthesizers are generally developed to produce peptides without monitoring of the progress of the synthesis. Therefore by-products caused by side reactions such as aspartimide and diketopiperazine formation, incomplete couplings and deprotections may be detected only after the final cleavage of the deprotected peptide from the resin.

In this part of my PhD we focused the attention on the comparison between the Fmoc/tBu RT-SPPS with the MW-assisted synthesis of the 1–34 *N*-terminal fragment of PTHrP using the same instrument (LibertyTM, CEM, Matthews, NC, USA), and monitoring the progress of the synthesis by UPLC-ESI-MS of MW-assisted mini-cleaved fragments of the growing peptide chain.

1.4 Synthesis of PTHrP(1-34)

The sequence of PTHrP(1–34)NH₂ is shown in Figure 11.



Figure 11. Characteristics of the PTHrP(1–34)NH₂ sequence are a cluster of arginine residues in the positions 19–21, sterically hindered and hydrophobic amino acid sequences

Importantly, the presence in the sequence of clusters of arginine [Arg¹⁹-Arg-Arg²¹], of sterically hindered (underlined in yellow) and hydrophobic (underlined in red) amino acid residues, represents a synthetic challenge that was the subject of this comparative study. The comparison of conventional RT and MW-assisted-SPPS protocols was performed on identical instruments, LibertyTM automated peptide synthesizer, using the some excess of reagents and molar ratios.

The synthesis was initially carried out following the conventional RT protocol, using the LibertyTM automated peptide synthesizer, excluding MW irradiations. The synthesis was performed on Rink-amide NovaSyn[®] TGR resin (0.2 mmol/g, 500 mg), following Fmoc/tBu chemistry. After deprotection of the *N*-terminal Fmoc group with a 20% solution of piperidine in DMF, Fmoc-protected amino acids (5 equiv), TBTU (5 equiv) and DIEA (10 equiv) in DMF were used in the coupling steps. The RT-SPPS protocol consists of two consecutive deprotection steps of 5 and 10 min employing deprotecting reagent, and 20 min for the coupling steps (Table 1)⁷⁸. In MW-assisted SPPS protocol, the deprotection steps were performed at 75 °C using 35 W for 30 sec for the first one and 60 W for 180 sec for the second one, while the coupling steps were performed at 75 °C using 30 W for 300 sec for all amino acids except Arg and His, for which the protocols reported in Table 1 were applied. Specifically, we have decreased the power of MW irradiation and lowered the temperature in order to avoid side reactions such as δ -lactam formation for Arg and racemization for His⁷⁹.

Table 1. RT and MW-assisted SPPS deprotection and coupling protocols used for the PTHrP(1-34)NH₂ synthesis.

Protocol	1 st Deprotection			2 nd Deprotection			Coupling		
	Time (sec)	Power (W)	Temperature (°C)	Time (sec)	Power (W)	Temperature (°C)	Time (sec)	Power (W)	Temperature (°C)
RT-SPPS	300	-	20	600	-	20	1200	-	20
General MW-assisted-SPPS	30	35	75	180	60	75	300	30	75
Arg ^a	step 1						1500	-	20
	step 2						300	25	75
His	step 1						120	-	20
	step 2						240	30	50

^a Arg residues were coupled twice.

1.5 MW-assisted mini-cleavage of PTHrP(1-34)NH₂ fragments

As modern automated SPPS protocols allow the assembly of larger and increasingly complex peptides, a precise control of the coupling reactions is a crucial prerequisite in peptide synthesis. In fact monitoring the progress of synthesis allows the detection of undesirable products caused by side reactions, incomplete couplings or deprotections. Although different methods have been developed for monitoring of SPPS, we observed that the use of colorimetric monitoring or continuous-flow UV absorbance of the reaction column effluent was not informative enough to identify difficult steps in the synthesis.

Therefore, we decided to monitor the progress of PTHrP(1–34)NH₂ synthesis by UPLC-ESI-MS analyses of small aliquots of cleaved peptide fragments obtained by MW-assisted mini-cleavages. The application of MW-assisted mini-cleavages of resin-bound peptides has been proposed as a fast, reliable method to monitor SPPS⁸⁰. Consequently, after specific coupling cycles, suspected to be difficult, we stopped the synthesizer and withdrew a small aliquot for analysis by UPLC-ESI-MS. A small sample of Fmoc-protected peptide-resin beads was removed from the reactor vessel, weighted into a fritted polypropylene tube and treated with a 20% solution of piperidine in DMF (2 × 1 mL) for 5 min. The sample was then washed with DMF (2 × 1 mL) and DCM (3 × 1 mL), and dried under vacuum. Mini-cleavages were performed in a 10 mL glass tube containing 2 mL of cleavage mixture consisting of TFA/TIS/water solution (95:2.5:2.5 v/v/v). Tubes were inserted into the microwave cavity of Discover™ S Class (CEM) and the cleavage was carried out at 45 °C, using 15 W for 15 min assisted by external cooling of the reactor vessel.

The crude fragments obtained from the MW-assisted mini-cleavages were analyzed by UPLC-ESI-MS on an ACQUITY™ UPLC system (Waters) coupled with a Micromass® Q-ToF MICRO™ mass spectrometer (Waters) equipped with an ESI source.

1.5.1 MW-assisted mini-cleavage protocol of 19-34 fragment of PTHrP(1-34)NH₂: a case study of multi-arginine containing peptides.

The use of microwave-assisted mini-cleavage protocol to monitor the growing peptide chains was useful to optimize in time the crucial reactions, i.e. multi-arginine containing peptides, with side-chains protected by Pbf group.

The 19-34 fragment of PTHrP(1-34)NH₂ H-Arg¹⁹-Arg-Arg-Phe-Phe-Leu-His-His-Leu-Ile-Ala-Glu-Ile-His-Thr-Ala³⁴-NH₂ is characterized by a cluster of arginine residues in the region 19-21.

In order to validate the use of microwave irradiation during the mini-cleavage step, we compared the RT and MW-assisted mini-cleavage protocols. A sample of beads carrying Fmoc-protected resin-bound peptide (10 mg) was weighted into a fritted polypropylene tube and treated twice with a 20% solution of piperidine in DMF (1 mL) each time for 5 min. The beads were then washed with DMF (2 × 1 mL) and DCM (3 × 1 mL), dried under vacuum and transferred into a 10 mL glass tube containing 2 mL of TFA/TIS/water cleavage solution (95:2.5:2.5 v/v/v). RT mini-cleavage reactions was performed by magnetic stirring in 15min as well as MW-assisted mini-cleavages. The reaction mixture was then filtered and the crude peptide was precipitated from the cleavage mixture by addition of ice-cold diethyl ether followed by cooling for 5 min at -20 °C. The product was collected by centrifugation and directly subjected to UPLC-ESI-MS analysis. Based on the results obtained by UPLC-ESI-MS reported in (Figure 12A), we can assume that 15 min at RT were not adequate to completely remove the Pbf groups from the arginine side-chain residues.

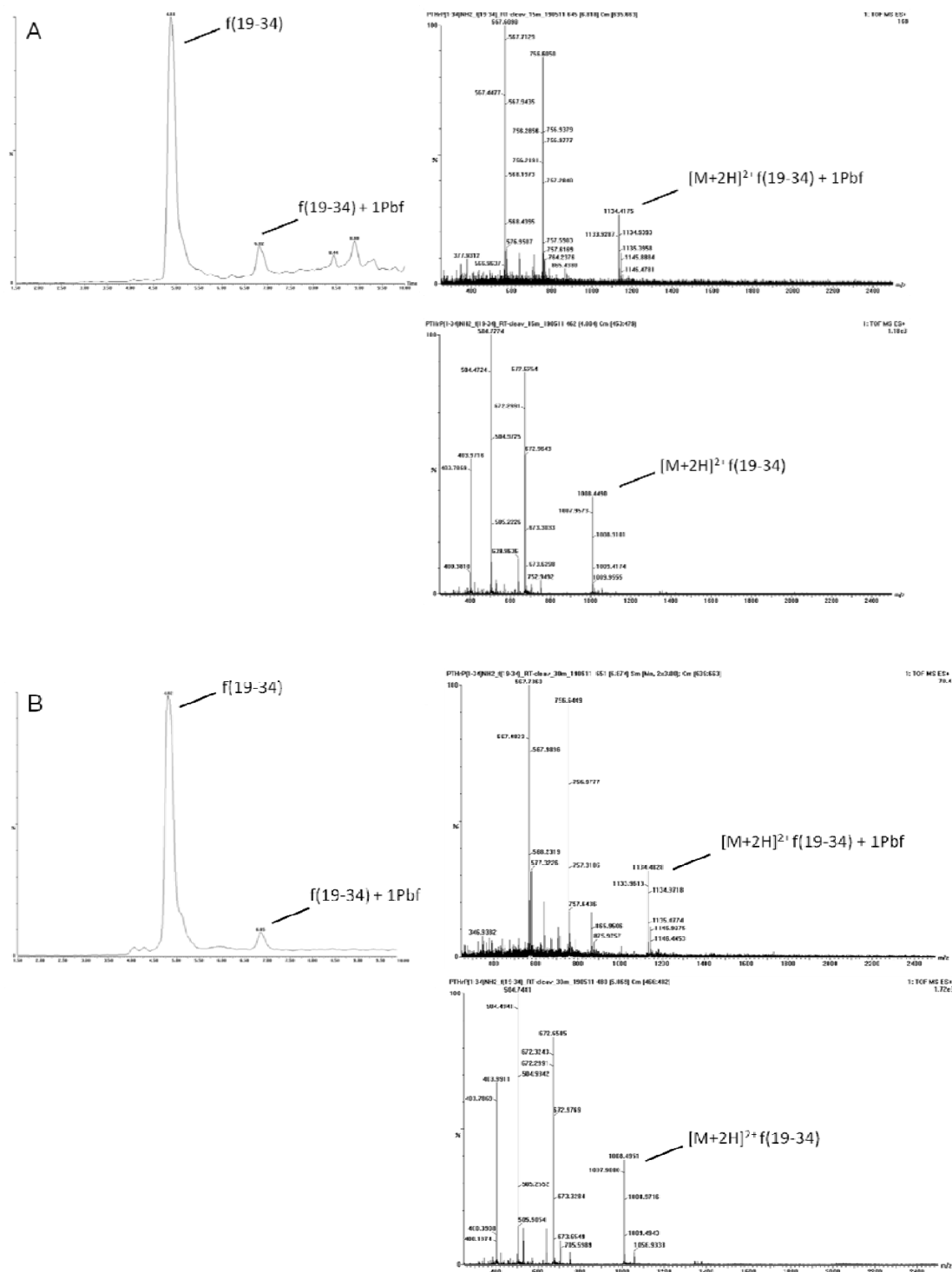


Figure 12. (A-C) TIC chromatograms and ESI-MS analyses to monitor the 19-34 fragment of PTHrP(1-34)NH₂ (RT-Fmoc/tBu SPPS, Liberty™, CEM) after RT mini-cleavage performed at 15 min (A), 30 min (B), 1 h (C).

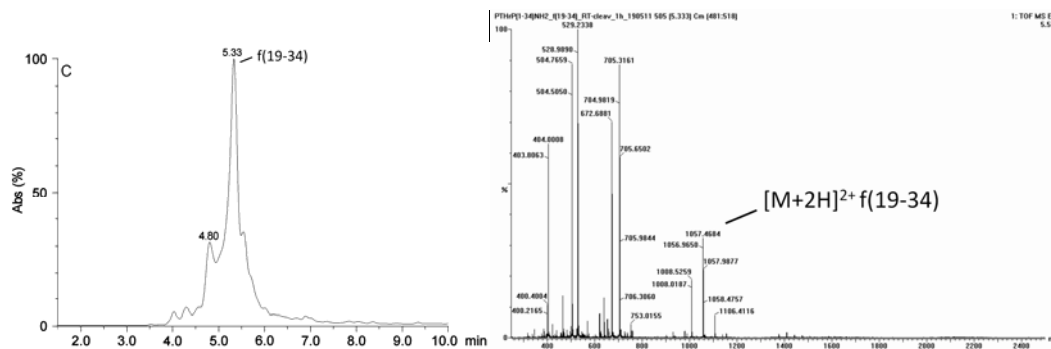


Figure 12. Continued.

Therefore the RT mini-cleavage time was extended to 30 min and the related analyses still confirm the presence of one arginine side-chain bearing the Pbf group as in Figure 12(B). Finally after 1 h of cleavage treatment, the 19-34 fragment of PTHrP(1-34)NH₂ was completely cleaved by protecting groups as reported in Figure 12(C). On the other hand, the MW-assisted mini-cleavage reaction let us to obtain final result just in 15 min, confirming that the use of MW-assisted mini-cleavages is an efficient strategy to monitor also difficult peptide couplings, such as multi-arginine peptides (Figure 13).

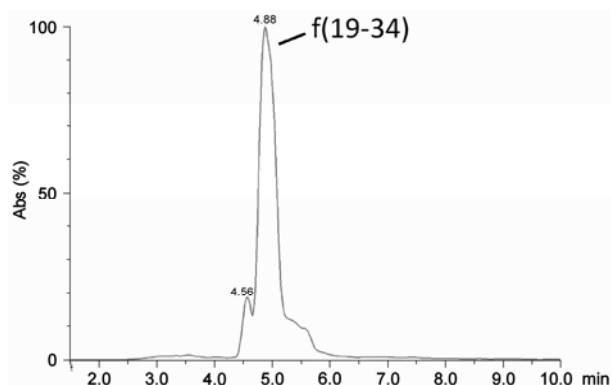


Figure 13. TIC chromatogram of the 19-34 fragment of PTHrP(1-34)NH₂ (RT-Fmoc/tBu SPPS, Liberty™, CEM) obtained after MW-assisted mini-cleavage procedure performed at 15 min.

1.5.2 Characterization of PTHrP(1-34)NH₂ fragments by UPLC-ESI-MS analysis

Thanks to the analysis of minicleavages intermediate fragments of the PTHrP(1-34)NH₂ by UPLC-ESI-MS, we were able to detect the presence of the desired peptide as well as of some by-products (Figure 14). In particular, we focused our

attention on the PTHrP fragments related to the 19–34 sequence, characterized by clusters of Arg residues and highly hydrophobic residues.

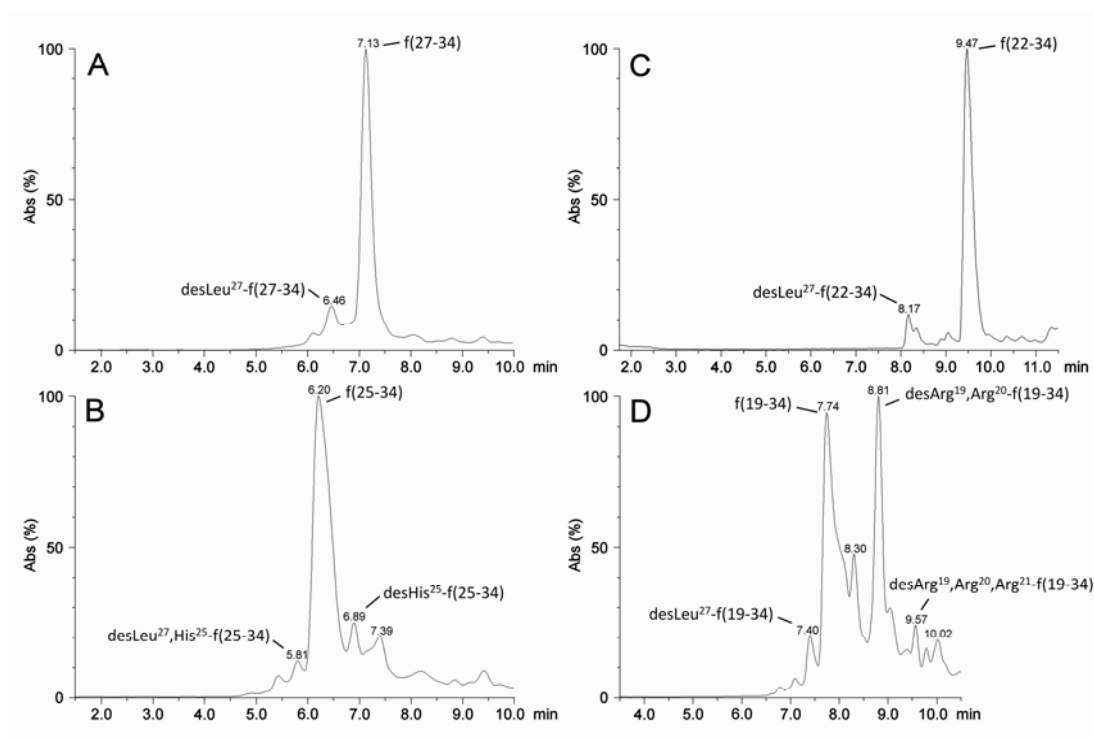


Figure 14. (A–D) TIC chromatogram of selected crude mixtures of intermediate resin-bound sequences obtained during the synthesis of PTHrP(1–34)NH₂ (Fmoc/tBu RT-SPPS) generated by the MW-assisted mini-cleavages.

The fragmentation patterns of these by-products in ESI-MS/MS allowed us to confirm the formation of deletion sequences. The UPLC-ESI-MS/MS analyses of the intermediate resin-bound fragments obtained from the RT-SPPS of PTHrP(1–34)NH₂ confirm that it is a difficult sequence for SPPS. The desired peptide was usually present as the major component in the cleavage mixture, but it was accompanied by some deletion peptides mainly lacking Arg, Leu and His residues (Table 2). It is well known that Arg-containing peptides are difficult to synthesize due to the sterically hindered Pbf group as side-chain protection and the tendency to form δ -lactam leading to low yield couplings⁸¹.

Table 2. RT Fmoc/tBu SPPS: list of PTHrP(1-34)NH₂ fragments produced by MW-assisted minicleavages of intermediate resin-bound peptides. The relative amounts of the deletion sequences are calculated in percentage of area under the peak from the total area under the curve obtained from the TIC chromatogram.

Analyzed sequences	Calcd mass	Intact sequences (m/z) found	Deletion sequences (m/z) found	Missing aa residues from deletion sequences	Deletion sequences (%)
27-34	865.51	866.39 [M+H] ⁺	753.41 [M+H] ⁺	Leu ²⁷	7
25-34	1139.62	1140.90 [M+H] ⁺	1003.95 [M+H] ⁺	His ²⁵	2
			890.93 [M+H] ⁺	Leu ²⁷ His ²⁵	5
22-34	1546.84	1547.41 [M+H] ⁺	1434.44 [M+H] ⁺	Leu ²⁷	8
			952.19 [M+2H] ²⁺	Leu ²⁷	6
19-34	2015.15	1008.69 [M+2H] ²⁺	852.72 [M+2H] ²⁺	Arg ¹⁹ Arg ²⁰	39
			774.73 [M+2H] ²⁺	Arg ¹⁹ Arg ²⁰ Arg ²¹	51
			1322.29 [M+2H] ²⁺	Leu ²⁷	5
12-34	2756.55	1379.24 [M+2H] ²⁺	1315.26 [M+2H] ²⁺	Gln ¹⁶ /Lys ¹³	55
			1258.81 [M+2H] ²⁺	Leu ²⁷ Gln ¹⁶ /Lys ¹³	3
			1065.43 [M+2H] ²⁺	Gly ¹² -Lys-Ser-Ile-Gln-Asp ¹⁷	12

As the length of the resin-bound peptide increases, the related UPLC-ESI-MS analyses become much more complex (Figure 15).

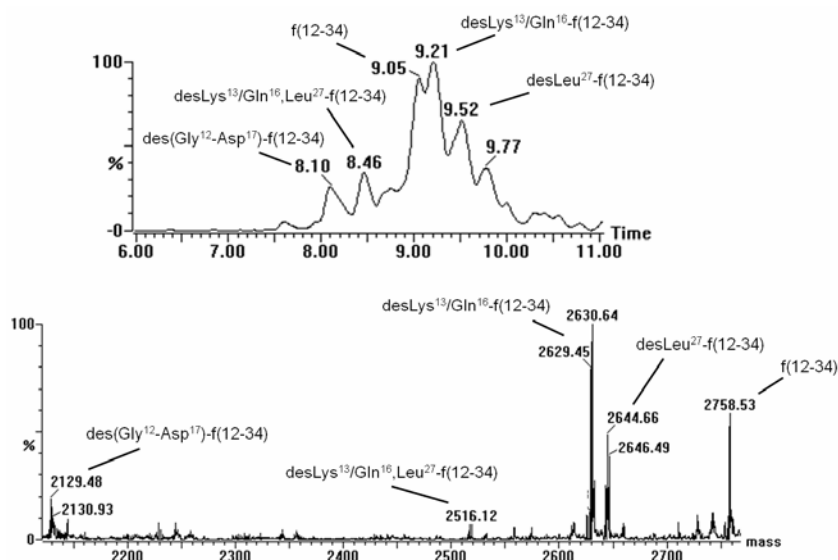


Figure 15. TIC chromatogram and deconvoluted spectrum of the cleaved mixture of the intermediate resin-bound sequence PTHrP(12–34)NH₂ (Fmoc/tBu RT-SPPS) generated by the MW-assisted minicleavages.

1.5.3 Characterization of the 12-34 fragment of PTHrP(1-34)NH₂ by UPLS-ESI-MS/MS analysis

The characterization of the 12-34 fragment of PTHrP(1-34)NH₂ synthesized by RT-Fmoc/tBu SPPS (Liberty™, CEM) was obtained by deconvolution with the attribution of the deletion sequences, where the fragments desLys¹³/Gln¹⁶-f(12-34) and desLys¹³/Gln¹⁶,Leu²⁷-f(12-34) were identified as two isobaric peptide sequences lacking either Lys¹³ or Gln¹⁶ residues. Since it is tricky to discriminate among the different combinations of deletion sequences in case of isobaric peptides affecting the SPPS, we suggest to plan rationally stops during the synthesis accurately monitoring the missing amino acid residues.

Thus, we report the UPLC-ESI-MS/MS data of the fragment 16-34 of PTHrP(1-34)NH₂ focusing the attention on the presence of the desGln¹⁶-f(16-34) consisting of a 40% of deletion sequence. The deconvoluted spectrum obtained for the cleaved mixture of this sample resulted in several deletion sequences (Figure 16).

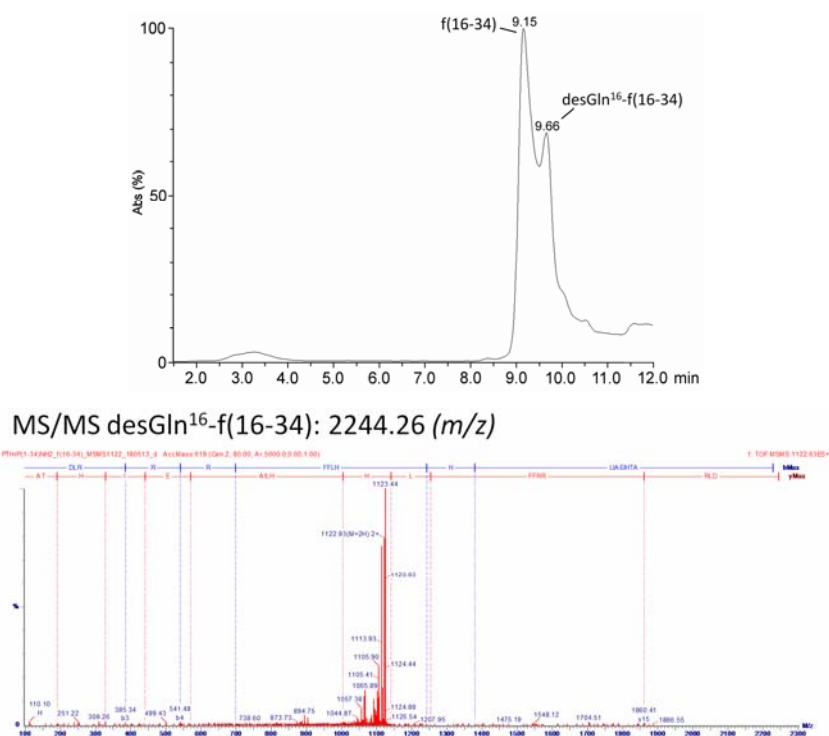


Figure 16. TIC chromatogram and MS/MS analysis of the fragment 16-34 of PTHrP(1-34)NH₂ (RT-Fmoc/tBu SPPS, Liberty™, CEM) obtained after MW-assisted mini-cleavages monitoring.

1.6 RP-HPLC Semi-preparative of PTHrP(1–34)NH₂

Lyophilized crude peptide was pre-purified by solid-phase extraction with an RP-18 LiChroprep silica column from Merck (Darmstadt, Germany) using H₂O/ACN as eluents. The purification of the peptide was performed by semi-preparative RP-HPLC on a Supelco C18 180 Å (250 × 10 mm, 5 μm) column (Sigma Aldrich, St. Louis, MO, USA); eluents: A 0.1% TFA in H₂O; B 0.1% TFA in ACN; flow 4ml/min; gradient 30–60% of B in 30min.

1.7 Results

After semi-preparative purification the MW-assisted SPPS of PTHrP(1–34)NH₂ yielded 27 mg of >95% pure peptide, whereas RT-SPPS gave only 18 mg of >95% of pure peptide. This improvement is attributed to the higher purity of the crude cleaved peptide mixture (Figure 17).

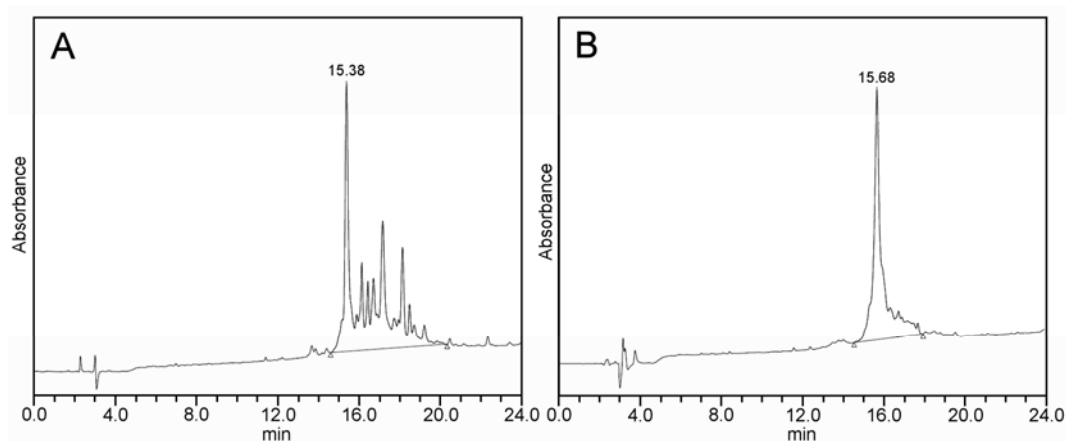


Figure 17. Analytical RP-HPLC of crude PTHrP(1–34)NH₂. Fmoc/tBu RT-SPPS (A) and Fmoc/tBu MW-assisted SPPS (B). HPLC: 10–60% B (0.1% TFA in ACN) in A (0.1% TFA in H₂O) over 20 min

On the basis of the results of the analytical RP-HPLC of the crude PTHrP(1–34)NH₂, we can conclude that the use of MW irradiations in SPPS has enhanced the efficiency of crucial coupling cycles improving the final yield and purity of crude peptide and speeding up the remaining coupling cycles. This improvement can be attributed to the prevention of peptide backbone aggregation and acceleration of deprotection and coupling steps.

Although the application of MW-assisted SPPS to the synthesis of PTHrP(1–34)NH₂ led only to a moderate improvement in final yield (6.3% vs 4.4%), it allowed us to obtain a crude product of higher quality (77% vs 35%) and in a shorter time (20 h vs 34 h used for the RT and MW-assisted SPPS strategies). Moreover, we demonstrated the usefulness of the combination of an MW-assisted mini-cleavage protocol and the UPLC-ESI-MS analysis for monitoring the quality of the reaction step. Compared to the ninhydrine colorimetric monitoring, our strategy is faster and the UPLC-ESIMS/MS analysis is more accurate and more informative.

1.8 Advantages of MW irradiation in SPPS

The monitoring of traditional RT-SPPS by MW-assisted mini-cleavages combined with fast, efficient and sensitive UPLC-ESI-MS analysis (15 min/analysis vs 30–45 min/analysis for traditional mini-cleavage) is helpful to identify the presence of difficult coupling steps that result in truncated and deletion sequences.

Moreover we can tune MW-assisted SPPS using modified cycles targeting difficult couplings. In these couplings the first step is carried out at RT (without applying MW power, 20 °C) and for variable duration (25 or 2 min) and the second step is carried out in the presence of MW power (75 or 50 °C) for shorter time intervals (5 or 4 min). In the synthesis of PTHrP(1-34)NH₂ we applied such type of couplings for the three arginine residues (R¹⁹-R-R²¹) and for the two histidine residues (H²⁵-H²⁶). Evidently, carrying out the RT and MW-assisted SPPSs on the same instrument allowed unbiased side-by-side comparison and the conclusion that the latter procedure is superior to the RT-SPPS. Although the modification of the coupling steps for Arg and His in the MW-assisted SPPS seems to be empirical in nature, it was guided by strong rationale that took into account the distinct capacity of this methodology to overcome putative hydrophobic interactions and aggregation. The impact of these phenomena increases with the progression of the coupling reactions. We therefore decided to take advantage of the MW radiation only for a short duration after the bulk of the reaction has been already taken place. In this manner, the completion of the coupling reaction was facilitated without causing undesired side reactions. We propose this MW-based protocol as a general strategy for overcoming difficult coupling reactions. Admittedly, applying this strategy to

different peptides will require fine tuning that will include the adjustment of parameters such as duration of coupling and recoupling steps as well as the level of MW energy employed in the recoupling step.

References

- ⁵⁷ Strewler G.J., Stern P.H., Jacobs J.W., Eveloff J., Klein R.F., Leung S.C., Rosenblatt M., Nissenson R.A., *J. Clin. Invest.* **1987**, *80*, 1803–1807.
- ⁵⁸ Moseley J.M., Kubota M., Diefenbach-Jagger H., Wettenhall R.E.H., Kemp B.E., Suva L.J., Rodda C.P., Ebeling P.R., Hudson P.J., Zajac J.D., Martin T.J., *Proc. Natl. Acad. Sci. USA*, **1987**, *84*, 5048–5052.
- ⁵⁹ (a) Suva L.J., Winslow G.A., Wettenhall R.E., Hammonds R.G., Moseley J.M., Diefenbach-Jagger H., Rodda C.P., Kemp B.E., Rodriguez H., Chen E.Y., Hudson P.J., Martin T.J., Wood W.I., *Science*, **1987**, *237*, 893–896. (b) Mangin M., Webb A.C., Dreyer B. E., Posillico J.T., Ikeda K., Weir E.C., Stewart A.F., Bander N.H., Milstone L., Barton D.E., Francke U., Broadus A.E., *Proc. Natl. Acad. Sci. U.S.A.*, **1988**, *85*, 597–601. (c) Strewler G. J., Stern P.H., Jacobs J.W., Eveloff J., Klein R.F., Leung S.C., Rosenblatt M., Nissenson R. A., *J. Clin. Invest.*, **1987**, *80*, 1803–1807.
- ⁶⁰ Segre G.V. *Principles of Bone Biology*, (Bilezikian J.P., Raisz L.G., Rodan G.A., Eds.), **1996**, 377–403, Academic Press. San Diego.
- ⁶¹ (a) Jüppner H., *Curr. Opin. Nephrol. Hypertens.*, **1994**, *3*, 371–378. (b) Serge G.V., Goldring S.R., *Trends Endocrinol. Metab.* **1993**, *4*, 309–314.
- ⁶² Stewart A.F. *N. Engl. J. Med.*, **2005**, *352*, 373–379.
- ⁶³ Mannstadt M, Jüppner H., Gardella T.J., *Am. J. Physiol.* **1999**, *277*, 665–675.
- ⁶⁴ Tregear, G. W.; Van Rietschoten, J.; Greene, E.; Keutmann, H. T.; Niall, H. D.; Reit, B.; Parsons, J. A.; Potts, J. T.; Jr. *Endocrinology*, **1973**, *93*, 1349–1353
- ⁶⁵ Takasu, H., Gardella, T. J., Luck, M. D., Potts, J. T., Jr., Bringham, F. R.; *Biochemistry*, **1999**, *38*, 13453–13460
- ⁶⁶ Baghurst D.R., Mingos D.M.P., *Chem. Soc. Rev.* **1991**, *20*, 1–47.
- ⁶⁷ Gabriel C., Gabriel S., Grant E.H., Halstead B.S., Mingos D.M.P., *Chem. Soc. Rev.* **1998**, *27*, 213–223.
- ⁶⁸ Stuerger D., Delmotte M., in *Microwaves in Organic Synthesis* (Ed.: A. Loupy), Wiley-VCH, Weinheim, **2002**, 1–34.
- ⁶⁹ Kappe C.O., *Angew. Chem. Int. Ed.* **2004**, *43*, 6250–6284.
- ⁷⁰ Baghurst D.R. Mingos D.M.P., *J. Chem. Soc. Chem. Commun.* **1992**, 674–677
- ⁷¹ Klán P., Literák J. Relich S., *J. Photochem. Photobiol. A*, **2001**, *143*, 49–57.
- ⁷² Zhang X., Hayward D.O. Mingos D.M.P., *Catal. Lett.*, **2003**, *88*, 33.
- ⁷³ Westaway K.C., Gedye R., *J. Microwave Power* **1995**, *30*, 219–230.
- ⁷⁴ Perreux L., Loupy A., *Tetrahedron*, **2001**, *57*, 9199–9223.

⁷⁵ Yu H-M, Chen S-T, Wang K-T., *J. Org. Chem.*, **1992**, *57*, 4781–4784.

⁷⁶ (a) Collins J.M., Leadbeater N.E., *Org. Biomol. Chem.*, **2007**, *5*, 1141–1150; (b) Malik L., Tofteng A.P., Pedersen S.L., Sørensen K.K., Jensen K.J., *J. Pept. Sci.*, **2010**, *16*, 506–512; (c) Sabatino G., Papini A.M., *Curr. Opin. Drug Discov. Dev.*, **2008**, *11*, 762–770.

⁷⁷ (a) Bacsa B., Bosze S., Kappe C.O., *J. Org. Chem.*, **2010**, *75*, 2103–2106; (b) Rizzolo F., Sabatino G., Chelli M., Rovero P., Papini A.M., *Int. J. Pept. Res. Ther.*, **2007**, *13*, 203–208.

⁷⁸ Rizzolo F., Testa C., Lambardi D., Chorev M., Chelli M., Rovero P., Papini A.M., *Journal of Peptide Science*, **2011**, *17*, 708-714.

⁷⁹ Loffredo C., Assuncao N.A., Gerhardt J., Miranda M.T.M., *J. Pept. Sci.*, **2009**, *15*, 808–817.

⁸⁰ Kluczyk A., Rudowska M., Stefanowicz P., Szewczuk Z., *J. Pept. Sci.*, **2010**, *16*, 31–39.

⁸¹ White P, Collins J, Cox Z. In Poster Presentation at the 19th American Peptide Symposium, San Diego, CA, **2005**.

2

Intramolecular *i*-to-(*i*+5) side-chain-to-side chain cyclization to stabilize β -turn secondary structures: the melanocortin peptides hormones

2.1 The Endocrine System

The endocrine system is a complex group of glands, including the pituitary gland and hypothalamus in the brain, adrenal glands in the kidneys, and thyroid in the neck, as well as the pancreas, ovaries and testes. Hormones are chemical messengers, released by a cells or a glands, that transfer a signal from one cell (or group of cells) to another. Endocrine system, through the secretion of hormones, regulates the control of reproduction, metabolism, growth, development, tissue function, mood, and energy balance, in response to external stimulations.

The typical pathway for hormones signal transduction is endocrine signaling. However, there are also other modes, i.e., paracrine, autocrine, and neuroendocrine signaling (Figure 18).

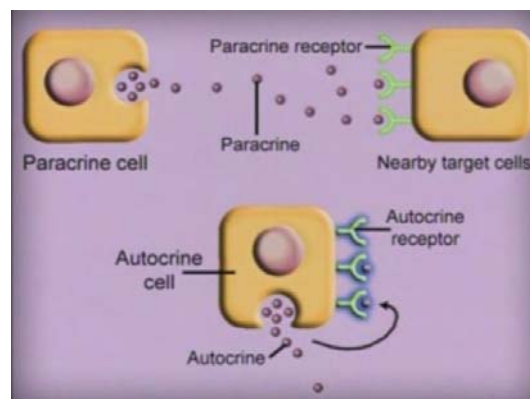


Figure 18. Endocrine, paracrine and autocrine secretion

Endocrine hormone molecules are released directly into the bloodstream, where they are addressed to target cells in remote tissue. In fact, endocrine glands are vascularized, and present intracellular vacuoles or granules, to store their hormones. On the contrary, exocrine glands secrete hormones directly into a duct. Sweat glands, salivary glands, and digestive glands are examples of exocrine glands. Paracrine signaling is a form of cell signaling in which the target cell is near the signal-

releasing cell. Autocrine signaling is a form of signal transduction in which a cell secretes a hormone or chemical messenger (called the autocrine agent) that binds to autocrine receptors on the same cell. This signaling is finely regulated by *feedback* mechanism. In fact, the reaction of the target cells may then be recognized by the original hormone-producing cells, leading to a down regulation in hormone production. The endocrine system uses cycles and *negative feedback* to regulate physiological functions. *Negative feedback* regulates the secretion of almost every hormone. Cycles of secretion maintain physiological and homeostatic control. These cycles can range from hours to months in duration (Figure 19).

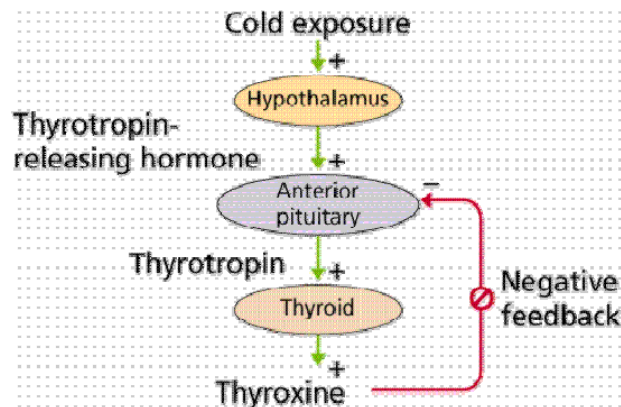


Figure 19. *Negative feedback* in the thyroxine release reflex.

Hormones may enter the cells without interaction with a receptor and activation of second messenger, or may interact with their specific receptor (with the same aim) triggering DNA to produce new messenger ribonucleic acid (mRNA) that generates a new protein (Figure 20). The hormone binds to the receptor protein, resulting in the activation of a signal transduction mechanism that ultimately leads to cell type-specific responses. The recognition of the hormone by an associated cell membrane or intracellular receptor protein, results in amplification of the received hormonal signal *via* a signal transduction process.

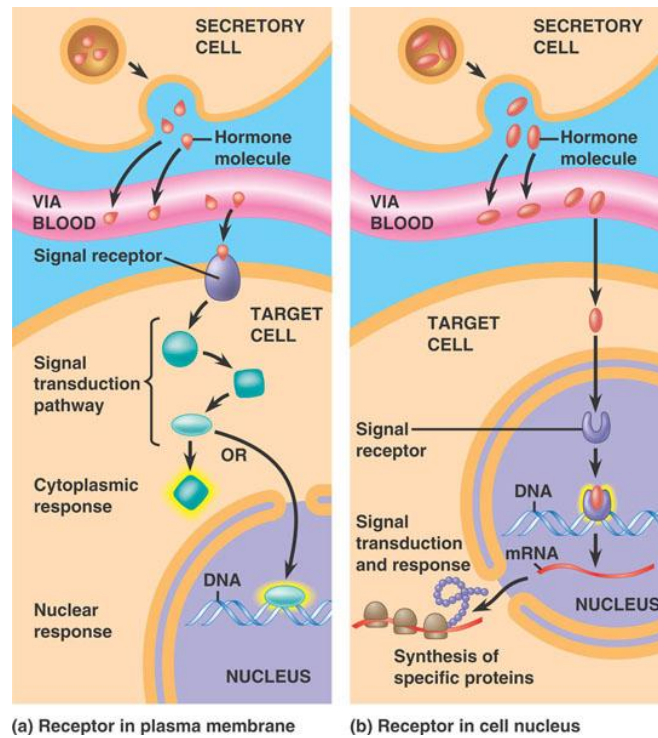


Figure 20. The two pathways of hormonal action in cells.

Hormones can be classified in three class:

- **Monoamines** derived from aromatic amino acids like phenylalanine, tyrosine, tryptophan by the action of aromatic amino acid decarboxylase enzymes. They are secreted from the thyroid and the adrenal medulla and their solubility is different from a hormone to another one. Example of amine hormones are adrenaline, melatonin and serotonin.
- **Lipid and phospholipid-derived hormones** derive from lipids such as linoleic acid and arachidonic acid and phospholipids. The main classes are the steroid hormones that derive from cholesterol and the eicosanoids. Examples of steroid hormones are testosterone and cortisol.
- **Peptide and protein hormones** consist of chains of amino acids of different length. They are secreted by the pituitary, parathyroid, heart, stomach, liver, and kidneys. Examples of protein hormones include insulin, growth hormone, and melanocortins. Peptides composed of scores or hundreds of amino acids are referred to as proteins. More complex protein hormones bear carbohydrate side-chains and are called glycoprotein hormones.

2.1.1 Peptide hormones

Peptide hormones exert their endocrine function to control and regulate the activity of certain cells or organs. Like other proteins, peptide hormones are synthesized by amino acids according to an mRNA template, which is itself synthesized by a DNA template inside the nucleus. Peptide hormone precursors (pre-prohormones) are then processed in several stages, typically in the endoplasmic reticulum, including removal of the *N*-terminal signal sequence and sometimes glycosylation, resulting in prohormones. The prohormones are then packaged into membrane-bound secretory vesicles, which can be secreted by exocytosis in response to specific stimuli. In fact, specific endopeptidases in the cell, cleave the prohormones just before its releasing into the blood stream, generating the mature hormone. Mature peptide hormones then diffuse through the blood to all cells, where they interact with specific receptors on the surface of their target cells. These protein hormones often contain amino acid residues necessary to direct folding of the hormone molecule into its active configuration, but with no function once the hormone folds. In the inactive state, hormones do not have a fixed conformation, but after interaction with their receptor, they assume a specific bioactive conformation that is crucial for the triggering of biological response. The binding of hormones, to hormone-receptors triggers the start of a biochemical signal that can lead to further signal transduction pathways, or triggers activation or inhibition of genes. Steroid hormones, for example, pass through the plasma membrane and, once inside the cell, bind to the nuclear membrane receptors, producing an activated hormone-receptor complex. The activated hormone-receptor complex binds to DNA and activates specific genes, increasing production of proteins. Non-steroid hormones, such as peptide and protein hormones are sufficiently hydro soluble to arrive up to their target cells, in all the organisms by blood circulation. However, they do not penetrate the double plasma membrane, strictly impermeable, but bind to plasma membrane receptors, generating a chemical signal (second messenger) inside the target cell. Peptide hormone receptors are often transmembrane proteins, such as G-protein-coupled receptors (GPCRs), sensory receptors or ionotropic receptors. These receptors generally function *via* intracellular second messenger, including cyclic adenosine monophosphate (cAMP), inositol 1,4,5-trisphosphate (IP3), and calcium (Ca^{2+})-calmodulin system (Figure 21). Second messengers activate the mechanism of

“transduction of signals”, in which, in addition to the receptors, other molecules take part.

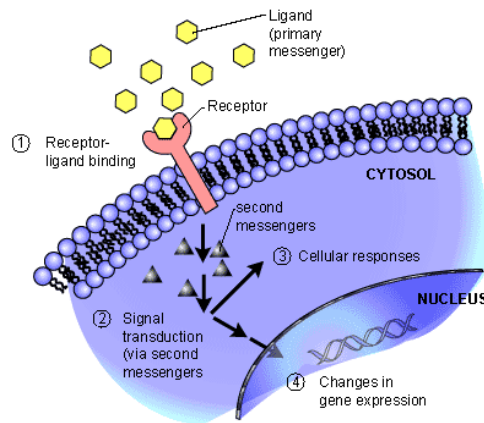


Figure 21. Signal Transduction

Another major class of receptors is intracellular proteins such as those for steroid and intracrine peptide hormone receptors. These receptors can often enter the cell nucleus and modulate gene expression in response to activation by the ligand.

A ligand is a molecule able to bind and to form a complex with a biomolecule to serve a biological purpose. Ligands can be small molecules, such as GABA (γ -aminobutyric acid) having neurotransmitter function, or large ones with molecular weight around ten of thousands daltons like proteins, nucleic acids, polysaccharides or lipids. The tendency or strength of binding is termed affinity. High affinity ligand binding implies that a relatively low concentration of a ligand is adequate to maximally occupy a ligand binding site and trigger a physiological response.

For example it is possible that two different ligands bind to the same receptor binding site, but only one of the agonists can maximally stimulate the receptor and thus can be defined as a "full agonist". An agonist that bind and activate a given receptor, but have only partial efficacy at the receptor relative to a full agonist, is called a "partial agonist". Ligands that bind to a receptor but fail to activate the physiological response are receptor antagonists^{82 83}.

2.1.2 The Nervous and endocrine systems

In neurocrine signaling, neurons synthesize neuro-hormones, that are released at the synaptic cleft into a gap between the terminals and the dendrites of the next neuron. Hypothalamus is a portion of the brain that contains a number of small nuclei with a variety of functions. The hypothalamus is responsible for a lot of metabolic processes and other activities of the autonomic nervous system. One of the most important functions of the hypothalamus is to link the nervous system to the endocrine system via the pituitary gland (hypophysis) (Figure 22).

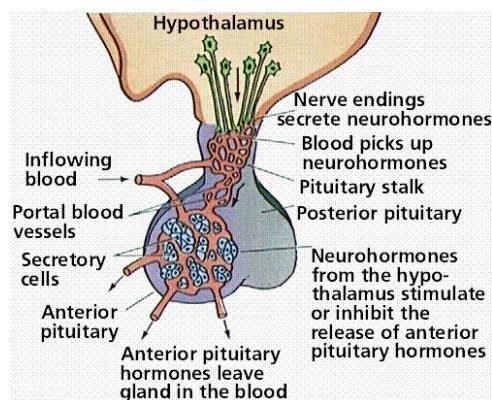


Figure 22. The roles of the hypothalamus and pituitary glands.

The pituitary gland, often called the “master gland”, is located in a small bony cavity at the base of the brain. A stalk links the pituitary to the hypothalamus, which controls release of pituitary hormones. The pituitary gland has two lobes: the anterior and posterior lobes. The posterior pituitary stores and secretes oxytocin and the antidiuretic hormones. Oxytocin is one of the few hormones to create a *positive feedback loop*. For example, uterine contractions stimulate the release of oxytocin from the posterior pituitary, which, in turn, increases uterine contractions. This *positive feedback loop* continues throughout labor. The anterior pituitary is glandular and secretes the majority of the hormones that regulate the bulk of the endocrine glands. This includes the thyroid-stimulating hormone (TSH), which regulates the thyroid, the adrenocorticotrophic hormone (ACTH), which regulates the adrenal cortex, the gonadotrophic hormone, which is responsible for regulating the gonads, melanotrophins, prolactin, secreted near the end of pregnancy and prepares the breasts for milk production, and somatotropins (Growth Hormone) (Figure 23).

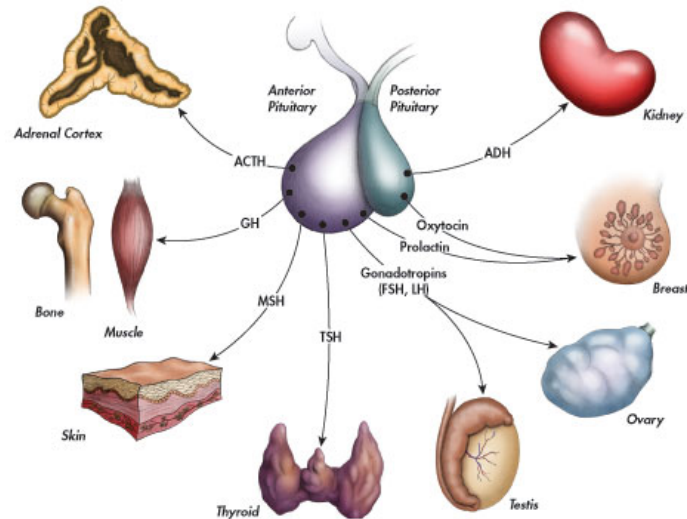


Figure 23. The role of pituitary gland

These hormones are released from the anterior pituitary under the influence of the hypothalamus. Hypothalamic hormones are secreted to the anterior lobe by way of a special capillary system, called the hypothalamic-hypophysial portal system (HPA or HTPA axis).

2.2 Melanocortin peptide hormones

Melanocortin peptides are endogenous neuropeptides hormones, including adrenocorticotropin (ACTH) and α -, β -, and γ - melanocyte stimulating hormones (α -MSH, β -MSH, γ -MSH). They are involved in many biological pathways, including sexual function⁸⁴, energy homeostasis^{85,86}, modulation of fever and inflammation, control of food intake, feeding behavior^{87,88}, endocrine secretion, pain modulation⁸⁹, thermoregulation, cardiac frequency, blood pressure and skin pigmentation^{90,91,92,93}. Genetic mutations in melanocortin system have been associated with early onset of obesity, adrenal insufficiency, red hair pigmentation, and hyperphagy^{94,95,96}. For these reasons, melanocortins peptides are considered *leads* for drugs to treat diseases such as obesity, pigmentation diseases and sexual dysfunction.

Melanocortin peptides derived from post-translational modification of the pro-opiomelanocortin prohormone (POMC), a 241 amino acids polypeptide precursor. The POMC gene, located on chromosome 2p23, is expressed in both the anterior and intermediate lobes of the pituitary gland. In addition to the pituitary POMC

expression and peptide processing occur normally in the nervous system and in widespread peripheral tissues. The POMC gene encodes a 285-amino acid polypeptide hormone precursor, the pre-pro-opiomelanocortin (pre-POMC), that undergoes extensive, tissue-specific, post-translational processing via cleavage by subtilisin-like enzymes, known as prohormone convertases⁹⁷.

There are eight potential cleavage sites within the polypeptide precursor, consisting of the sequences, Arg-Lys, Lys-Arg or Lys-Lys. Depending on tissue type, the stimulus and the available convertases, processing may yield as many as ten biologically active peptides involved in diverse cellular functions (Figure 24).

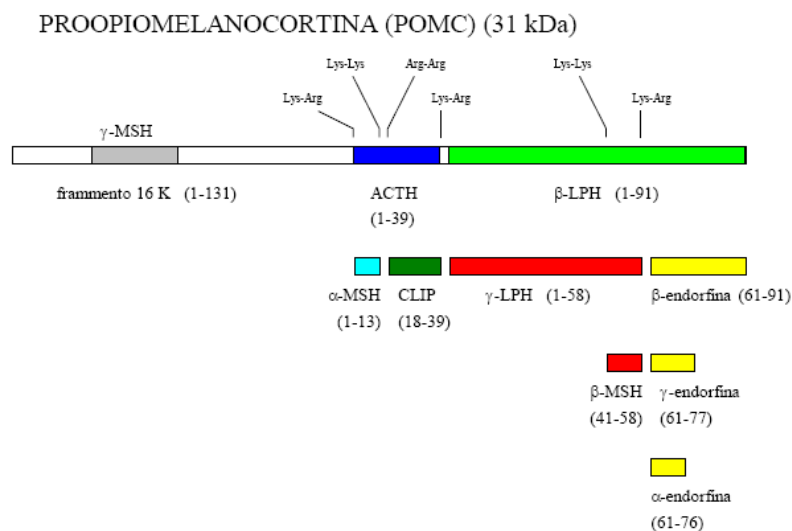


Figure 24. Melanocortin peptides, ACTH and α -, β -, and γ -MSH, derive from post-translational processing of POMC, which is also the precursor for opioid peptides and CLIP (corticotropin-like intermediate lobe peptide)⁹⁵

In particular, enzymes responsible for processing of POMC peptides include prohormone convertase 1 and 2 (PC1/2), carboxypeptidase E (CPE), peptidyl α -amidating monooxygenase (PAM), N-acetyltransferase (N-AT), and prolylcarboxypeptidase (PRCP). Data showed that PC1 generated ACTH and β -lipotropin (β -LPH), whereas PC2 was required for production of α -MSH and β -endorphin⁹⁸. This was the first evidence that tissue-specific processing of POMC could be explained by the relative expression of its convertases.

Thus, in the corticotrophs where PC1 predominates, ACTH and β -LPH, are the final POMC-processing products. In contrast, expression of PC2 in the pituitary gland results in production of α -MSH and β -endorphin. In other tissues, including the

hypothalamus, placenta, and epithelium, all cleavage sites may be used, giving rise to peptides with roles in pain and energy homeostasis, melanocyte stimulation, and immune modulation. These include several distinct melanotropins, lipotropins, and endorphins that are contained within the adrenocorticotrophin and beta-lipotropin peptides. ACTH is an important component of the HPA axis and is often produced in response to biological stress. Its principal effect is to increase the production and release of corticosteroids. Therefore it is essential for normal steroidogenesis and the maintenance of normal adrenal weight. ACTH consists of 39 amino acids and in the melanotrophs of the intermediate lobe of the pituitary, is the precursor of α -MSH. α -MSH was found to share the sequence of ACTH (1–13), although α -MSH is acetylated at the *N* terminus and *C*-terminally amidated. The primary roles of α -MSH is the regulation of pigmentation. α -MSH is a tridecapeptide, Ac-Ser-Tyr-Ser-Met-Glu-His-Phe-Arg-Trp-Gly-Lys-Pro-Val-NH₂, and is one of the first peptide hormones isolated from the pituitary gland. Extensive studies of this hormone have confirmed its role in skin pigmentation as well as in various central nervous system (CNS)⁹⁹. Although adrenal stimulatory effects of ACTH and pigmentary influences of α -MSH have been known for over 50 years, the discovery that melanocortin peptides have multiple effects on the host is much more recent.

β -LPH is a 90-amino acid polypeptide deriving from the carboxy-terminal fragment of POMC. It stimulates melanocytes to produce melanin, and can also be cleaved into smaller peptides such as γ -lipotropin, β -MSH, γ -MSH, α -endorphin, β -endorphin, γ -endorphin, and met-enkephalin. β -LPH also performs lipid-mobilizing functions such as lipolysis and steroidogenesis.

2.2.1 G protein-coupled melanocortin receptors: MCRs

Human melanocortin peptide hormones share the common tetrapeptide core [His-Phe-Arg-Trp]¹⁰⁰⁻¹⁰¹ (Figure 25).

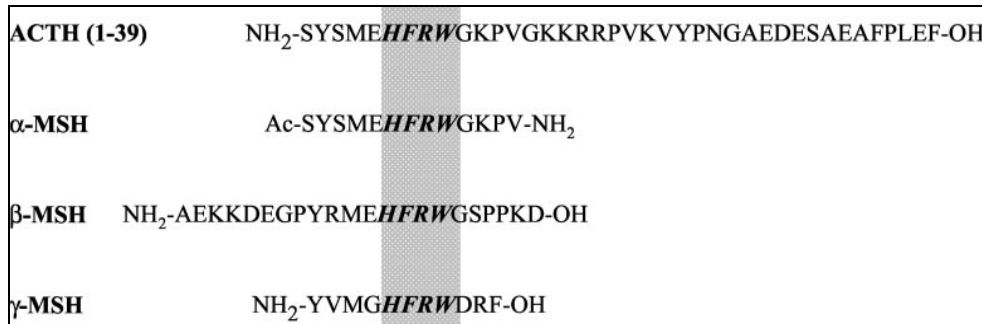


Figure 25. Amino acid sequence of melanocortin peptides. All the melanocortins share the invariant sequence HFRW

The physiological activity of the melanocortins is modulated via five human melanocortin receptors (MC1R-MC5R). Melanocortin receptors belong to the class A of G protein-coupled receptors (GPCR), the rhodopsin/ β_2 -adrenergic-like family, which also includes biogenic amine, cannabinoid, melatonin, chemokine, and several other receptors. MCRs are the smallest GPCRs known, with short amino- and carboxyl-terminal ends and a very small second extracellular loop (Figure 26) MCRs consist of a single polypeptide featuring seven α -helical trans membrane domains, an extracellular *N*-terminus, and an intracellular *C*-terminus. MCRs share many features with other GPCRs: they have several potential *N*-glycosylation sites in their amino-terminal domains, consensus recognition sites for protein kinases C and/or A (PKC/A), which indicate that they may undergo regulation by phosphorylation, and conserved cysteines in their carboxyl termini¹⁰², potential sites for fatty acid acylation, anchoring the *C*-terminal end to plasma membrane.

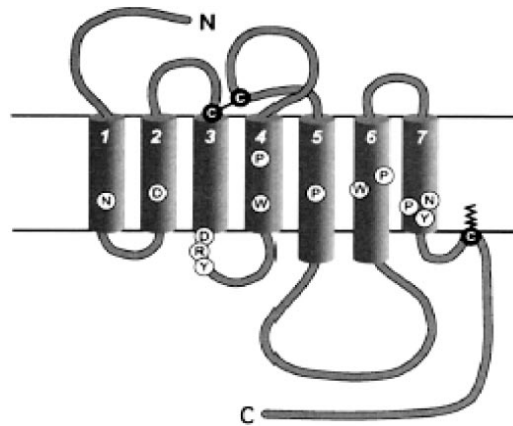


Figure 26. The MCRs belong to the family of G protein-coupled.

All the MCRs intracellularly mediate their effects by activating pathways that are cyclic adenosine monophosphate (cAMP) dependent (Figure 27).

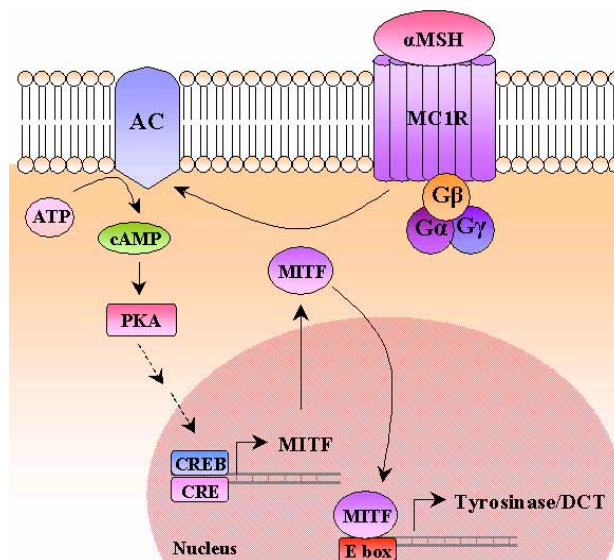


Figure 27. Melanocortin-receptor signaling pathway

All the melanocortin receptors possess unique tissues distributions, and are involved in different physiological effects (Figure 28). The cloning of the human melanocortin receptor genes led to great progress in understanding the biological effects of the melanocortin peptides at the melanocortin receptors^{91,103,104}.

MC1 receptor is mainly expressed in cutaneous melanocytes, where plays a key role in determining skin and hair pigmentation. Binding of α -MSH to its MC1R in melanocytes starts a signal cascade that activates adenylate cyclase, increases intracellular cAMP, and induces activity of tyrosinase, the rate-limiting enzyme in

the eumelanin synthetic pathway. The relative affinity of the human MC1R for the natural melanocortins is $\alpha\text{-MSH} \geq \text{ACTH} > \beta\text{-MSH} \gg \gamma\text{-MSH}$ ¹⁰⁵. These differences in affinity reproduce the relative potency of the melanocortin peptides in stimulation of melanogenesis and explain the lack of melanogenic activity of $\gamma\text{-MSH}$.

MC1R functions extend well beyond regulation of melanogenesis MC1 receptor is also expressed at leukocytes, where it mediates the anti-inflammatory property^{106,107}.

MC2R, also known as ACTH receptor, is selectively activated by adrenocorticotrophic hormone¹⁰⁸. MC2R is expressed only in adrenal cortex zona reticularis and zona fasciculata, where it mediates production and release of steroid hormones. Binding of ACTH to its receptor stimulates adenylyl cyclase and induces increases in cell cAMP; this leads to activation of PKA, which promotes expression of steroidogenic enzymes

The MC3 receptor is identified in many areas of the nervous system and peripheral tissues, in brain, placenta and is involved in energy homeostasis, feeding behavior, and inflammation. The MC3R is the only MCR activated by $\gamma\text{-MSH}$ with potency similar to that of other melanocortins ($\gamma\text{-MSH} = \text{ACTH} \geq \alpha\text{-MSH}$). Recent data suggest that MC3R activation mediates protective influences of melanocortins in myocardial ischemia/ reperfusion-induced arrhythmias in rats¹⁰⁹.

Melanocortin MC4 receptor is expressed predominantly in the central nervous system, including the cortex, the thalamus, the hypothalamus, the brainstem, and the spinal cord. The order of potency for activation of MC4R is $\alpha\text{-MSH} = \text{ACTH} > \beta\text{-MSH} \gg \gamma\text{-MSH}$ Distribution of MC4R is consistent with its involvement in autonomic and neuroendocrine functions. It regulates both food intake and sexual function. MC4R deficiency is related to maturity-onset obesity, hyperphagia, hyperinsulinemia, and hyperglycemia.

Finally, the MC5 receptor is ubiquitously expressed in peripheral tissues. It occurs in the adrenal glands, fat cells, kidney, liver, lung, lymph nodes, bone marrow, thymus, mammary glands, testis, ovary, pituitary testis, uterus, esophagus, stomach, duodenum, skin, lung, skeletal muscle, and exocrine glands. It plays a role in regulating exocrine gland function¹¹⁰, particularly sebaceous gland secretion

discovered by targeted deletion of the receptor^{111,112}. Presence of MC5R in B- and T-lymphocytes suggests also a function in immune regulation.

MCR Subtype	Ligand Affinity	Prevalent Tissue Expression	Functions
MC1R	α -MSH \geq ACTH \gg γ -MSH	Melanocytes Immune/inflammatory cells; keratinocytes; Endothelial cells; glial cells	Pigmentary effects Antipyretic/anti-inflammatory
MC2R	ACTH	Adrenal cortex	Steroiogenesis
MC3R	γ -MSH=ACTH \geq α -MSH	CNS Macrophages	Autonomic functions Anti-inflammatory
MC4R	α -MSH=ACTH \gg γ -MSH	CNS	Control of feeding and energy homeostasis; Erectile activity
MC5R	α -MSH \geq ACTH \gg γ -MSH	Exocrine glands, lymphocytes	Regulation of exocrine sections, immunoregulatory functions

Figure 28. Affinity, distribution, and functions of MCR subtypes

The primary native ligand for MC1R, MC3R, MC4R and MC5R is α -MSH or possibly γ -MSH. These native ligand, presenting the minimum sequence necessary for the activation [His-Phe-Arg-Trp], are rather non-selective for these receptors.

Two melanocortin-receptor antagonists, the agouti (also termed agouti signaling protein) and the agouti-related protein (AgRP), participate in control of melanocortin signaling¹¹³. Agouti is a competitive antagonist at melanocortin receptors with high affinity at MC1R, although it also shows antagonistic activity for the human MC4R. This receptor antagonist may be important in inflammatory responses. In mice, the agouti gene encodes a paracrine signaling molecule that induces hair follicle melanocytes to synthesize pheomelanin, a yellow pigment, instead of the black or brown pigment, eumelanin. The human agouti is a protein closely homologous to the rodent agouti, but it shows a much wider distribution as it is expressed in adipose tissue, testis, ovary, heart, and, at lower levels, in foreskin, kidney, and liver¹¹⁴. Pleiotropic effects of constitutive expression of the mouse gene include adult-onset obesity, increased tumor susceptibility, and premature infertility. The AgRP shows a very distinct expression in the central nervous system, as it is expressed in neural cell bodies of posterior hypothalamus in close vicinity to the POMC-expressing neurons. The POMC and AgRP systems may function as physiologically opposing systems,

where the former decreases the drive for feeding and the latter increases it. Both agouti and AgRP contain cysteine-rich C-terminal domains that form disulfide bridges leading to similar folded structures¹¹⁵. The entire antagonistic activity for MCRs resides in the Cys-rich end of the molecule¹¹⁶.

2.2.2 Development of agonists for MCRs

Melanocortins hormones are involved in a lot of biological processes. For this reason the development of selective, potent and long-acting agonist for MCRs, is of great interest for medical applications. The physiological significance of the melanocortin receptor family has promoted considerable research activity over the past decade^{117, 118, 119}.

α , β -MSH (Figure 29) are rather non-selective for their receptors in human (hMC1R-hMC5R), and, like other peptide hormones, are biologically unstable, being easily hydrolyzed by proteases. In addition the Met⁴ residue in the α -MSH sequence is easily oxidized leading to a modified ligand with decreased biological activity.

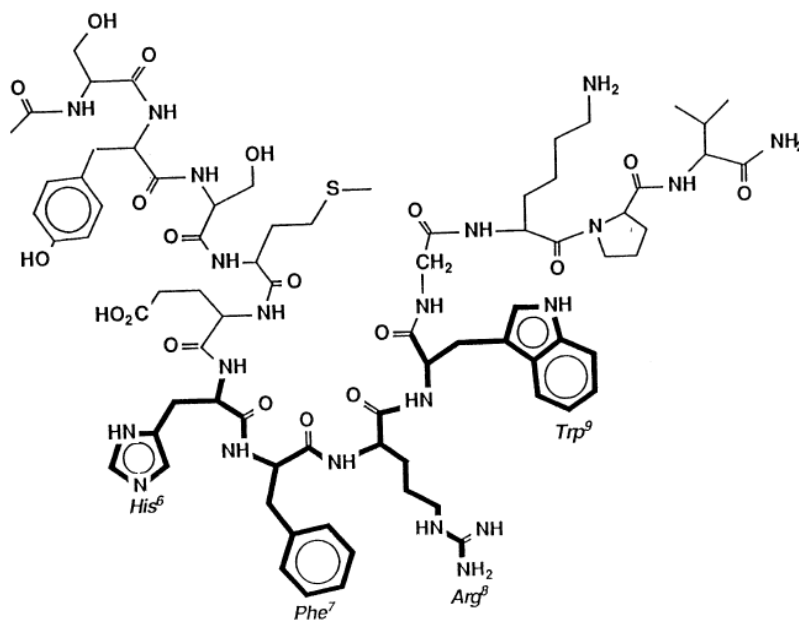


Figure 29. α -MSH (Ac-Ser¹-Try²-Ser³-Met⁴-Glu⁵-His⁶-Phe⁷-Arg⁸-Trp⁹-Gly¹⁰-Lys¹¹-Pro¹²-Val¹³-NH₂), and the pharmacophore core [His⁶-Phe⁷-Arg⁸-Trp⁹]⁹³

Thus a primary need of the research is to obtain melanotropin analogues which are: 1) biologically stable to proteolysis and oxidation; 2) agonists or antagonists; 3) selective for one of the melanocortin receptors; 4) able to cross the blood-brain-barrier (or not); and 5) orthosteric or allosteric ligands. Development of selective ligands has been critical not only to establish structure–activity relationships but equally important, to establish the biological functions of the various melanocortin receptors and melanocortin systems.

Several peptides were designed and studied in the effort to develop potent, long acting and selective agonists for different subtypes of MCRs receptors. In particular research focused on the importance of the tetrapeptide [His-Phe-Arg-Trp], that is present in all the melanocortins peptides, in receptor binding and in agonistic activity¹²¹. Researchers observed that exchanges Glu⁵ with Asp, Phe⁷ with D-Phe, Gly¹⁰ with Lys, and performing amidation of the C-terminal carboxyl function and acetylation of the N-terminal, lead to agonists equipotent with native melanocortins hormones¹²⁰. Moreover it was observed that exchange Met⁴ with norleucine (Nle), having a side chain group pseudoisosteric of Met, the bioactivity of the analogs was increased. This could be due to the side chain of methionine that is rather easily oxidized to the sulfoxide form, which increases the hydrophilicity dramatically and thus decreases the bioactivity of the peptide^{121,122}.

This finding, led to the discovery of the first generation superpotent α -MSH agonist: Ac-Ser-Tyr-Ser-Nle-Glu-His-D-Phe-Arg-Trp-Gly-Lys-Pro-Val-NH₂ or [Nle⁴, D-Phe⁷]- α -MSH (NDP-MSH)^{90,93}, known as MTI or Afamelanotide, that was approximately 1,000 times more potent than natural α -MSH.

MTI, is a linear peptide approved on May 5, 2010 by the Italian Medicines Agency (AIFA-Agenzia Italiana del Farmaco) as drug for treatment of erythropoietic protoporphyria (EPP) disease¹²³. Afamelanotide, is designed as “*orphan drug*” from FDA (*US Food and Drug Administration*), for treatment of EPP, and it is also being tested and clinically trialed by the Australian company Clinuvel Pharmaceuticals, in an implant delivery formulation,¹²⁴ for polymorphous light eruption (PMLE), solar urticaria (SU), phototoxicity associated with systemic photodynamic therapy and actinic keratosis (AK) and squamous cell carcinoma skin cancer in patients who have received organ transplants.

The discovery of the enhanced potency for D-Phe⁷ containing analogues, suggested the importance of β -turn conformation for the biological activity. In fact, the known effects of D- amino acids on peptide turn structure¹²⁵, led to speculate on occurrence of a turn within the tetrapeptide core, and led to the development of a new library of cyclic peptides⁵⁵.

The first cyclopeptide synthesized, Ac-[Cys⁴,Cys¹⁰]- α -MSH, was found to possess superpotent bioactivity in the frog skin bioassay, but lacked significant prolonged activity, because of the sensibility of the Cys-Cys bridges to the cellular redox conditions^{126,127}.

Subsequently, it was developed a cyclic lactam containing analog, Ac-Nle⁴-c[Asp⁵-D-Phe⁷-Lys¹⁰] α MSH₄₋₁₀-NH₂, called "Melanotan II" or MTII (Figure 30)^{53,54,55}.

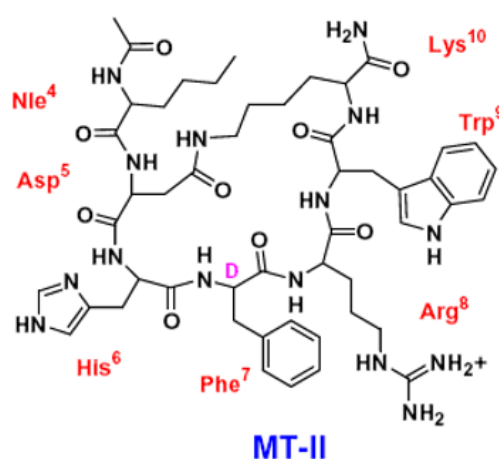


Figure 30. MT-II Sequence (Ac-Nle-c[Asp-His-D-Phe-Arg-Trp-Lys]-NH₂)

MTII is characterized by lactam bridge between residues Asp⁵ and Lys¹⁰ stabilizing a type-II β -turn structure, that is critical for its bioactivity. The minimal active sequence [His⁶-D-Phe⁷-Arg⁸-Trp⁹]⁵⁶, is included in the cyclic portion formed by lactam ring. MT-II, resulted to be 90-100 time more potent than native agonists, but nonselective agonist at the four melanocortin receptors MC1R, MC3R, MC4R, MC5R. MT-II showed during phase I *trials* side effects including nausea and a "stretching and yawning complex" that correlated with spontaneous penile erections¹²⁸. Therefore the therapeutics for skin disease was interrupted. Nevertheless, MTII can be considered a *lead* molecule for the development of new specific and selective analogues, although problems need to be solved. One is that

synthetic agonists or antagonists may encounter difficulties in reaching their target(s). For example, MC4R is located within the brain and, therefore, ligands must penetrate the blood-brain barrier to exert their effects. This important issue must be addressed before any new MC4R-targeted molecule could be considered for clinical use. The ultimate goal for the development of any new therapeutic agent for melanocortin receptors is to identify a drug that produces the desired effect with minimal side effects. To this end, the concept of directed signaling and functional selectivity has generated significant interest, as a means to develop compounds that can selectively activate or block receptor-signaling pathways that lead only to the desired therapeutic effect. This is of particular importance for the melanocortin receptors as a potential target for the treatment of skin cancer, food intake, and exocrine disorders.

2.3 Stabilization of β -turn conformation in melanocortin like peptide by click chemistry

The biological function of peptides and proteins is defined by their ability to adopt well-defined conformations, that complement those of their corresponding binding partner or receptor. Introduction of 1,2,3-triazole into an amino acid backbone is an established approach to achieve stabilization of specific conformations, such as α -helices and β -turns, and a recognized strategy to improve resistance toward proteolytic degradation, thus increasing the metabolic stability *in vitro* and *in vivo*^{39,40}.

Side chain-to-side chain cyclizations represents a strategy to select for a family of bioactive conformations, by reducing the entropy and locking them into receptor binding conformations. This structural manipulation contributes to increased target specificity, enhanced biological potency, improved pharmacokinetic properties, higher binding affinity and lower metabolic susceptibility.

This approach can provide a convenient and versatile access to cyclic peptidomimetics, by incorporation of the building blocks N^{α} -Fmoc-Xaa(ω -N₃)-OH and N^{α} -Fmoc-Yaa(ω -yl)-OH and the subsequent solution phase Cu^I-catalyzed intramolecular azide-alkyne cycloaddition. In this way is possible to develop a new paradigm for an orthogonal bio-organic and intramolecular side chain-to-side chain

cyclization. In fact, the proteolytic stable side chain-to-side chain connecting 1,4- or 4,1-disubstituted [1,2,3]triazolyl moiety, is isosteric with the peptide bond and can function as a surrogate of the classical side chain-to-side chain lactam forming bridge. Moreover is it possible to obtain cycle head to tail, side chain to side chain or head/tail to side chain (Figure 31)¹²⁹.

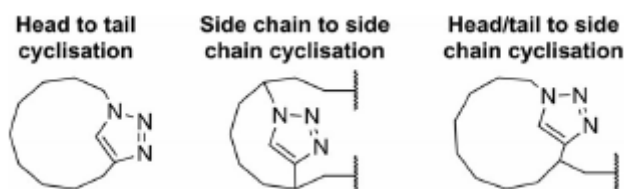


Figure 31. Possible cyclisation approaches utilising triazoles

In this PhD work, the 1,2,3-triazolyl-bridging strategy was applied to stabilize the β -turn conformation of melanocortin analogues peptides. In fact, MCRs mediate a plethora of biological functions that include sexual function, feeding behavior, pain modulation, thermoregulation, energy homeostasis, cardiovascular effects, and skin pigmentation, making them potential drug targets for treating pain, food intake and body weight as well as erectile dysfunction. Therefore, development of an expansive toolbox of structural modifications that can be used to fine tune the predominant conformations, to achieve modulation of specificity toward receptor subtypes, physicochemical and pharmacological properties, continues to be of great interest in the development of peptide-based drugs in general, and melanocortinergic drugs in particular. Evidently, the plethora of melanocortins-mediated activities, the multitude of melanocortin receptor subtypes, and the high profile of potential therapeutic targets associated with the melanocortin system, underscores the unmet need for highly selective, pharmacokinetically diverse, and bioavailable agonists and antagonists. Understanding the bioactive conformation of the ligand and the structure of the receptor–ligand complex is crucial to design more potent and MCR-subtype selective ligands. Our studies explored the relationship between the size of bridge containing the 1,2,3-triazolyl moiety, the location of this moiety within the bridge, its orientation relative to the peptide backbone, and the predominant conformations displayed by these heterodetic cyclic peptides (Figure 32). Therefore, we synthesize a series of heterodetic cyclo-heptapeptides, based on the scaffold MT-II, varied in the

size of the bisubstituted [1,2,3]-triazolyl-containing bridge connecting C $^{\alpha}$ s of residues 4 and 10, in the location and in the orientation of the [1,2,3]-triazolyl moiety within the bridge. The 1,2,3-triazolyl moiety was flanked on each side by 1 to 4 methylenes totaling in 4 or 5 methylenes.

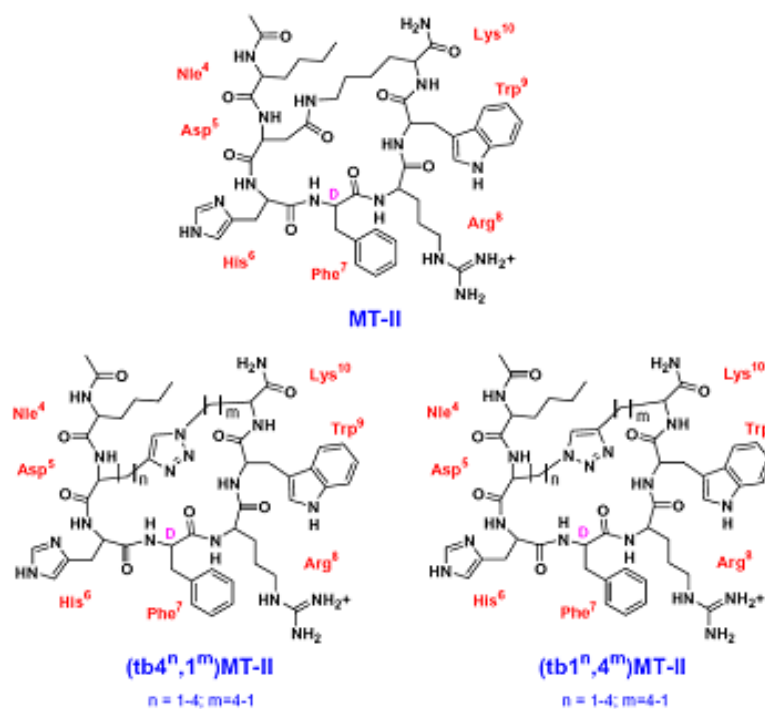


Figure 32. Ac[Yaa⁵(&¹),Xaa¹⁰(&²)] α MSH₄₋₁₀ [{&¹(CH₂)_n-1,4-[1,2,3]triazolyl-(CH₂)_m&²}] and Ac[Xaa⁵(&¹),Yaa¹⁰(&²)] α MSH₄₋₁₀ [{&¹(CH₂)_m-1,4-[1,2,3] triazolyl-(CH₂)_n&²}] .

This study was in collaboration with Professor Michael Chorev, of the Laboratory for Translational Research, Harvard Medical School, with Professor Carrie Haskell-Luevano, Departments of Pharmacodynamics, University of Florida, USA, and Medicinal Chemistry, University of Minnesota, Minneapolis and with professor Anna Maria D'Ursi of Department of Pharmaceutical Science, University of Salerno.

2.4 Click chemistry

Click chemistry is an entire reaction group in which new substances are generated by joining small units together⁴⁴. A set of stringent criteria that a process should meet to be useful in this context are defined as follows:

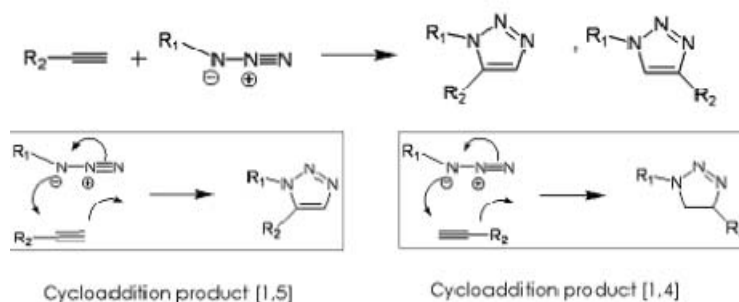
- simple reaction conditions;

- ideally, the process should be insensitive to oxygen and water;
- very high yields;
- only inoffensive by-products that can be removed without using chromatographic methods;
- to be stereospecific (but not necessarily enantioselective);
- high thermodynamic driving force, usually greater than 20 kcal.mol⁻¹.

One of the most interesting reactions that can enter in the click chemistry definition are the cycloaddition reactions involving heteroatoms, such as Diels-Alder and, especially, 1,3-dipolar cycloaddition, that provide fast access to a variety of five- and six-membered heterocycles. In particular, Huisgen 1,3-dipolar cycloaddition of azides and alkynes⁴¹ can ideally meet all prerequisites for an efficient “click chemistry”. The chemistry of alkynyl and azido group is completely orthogonal to the chemistry of all endogenous functional groups in proteins.

Azides and alkynes are crucial functional group for click chemistry. In fact they are easy to install and, being among the most energetic species known, they are also among the least reactive functional groups in organic chemistry. This stability, being purely kinetic in origin, is responsible for the slow nature of the cycloaddition reaction and the inertness of these functional groups towards biological molecules and towards the reaction conditions inside living systems (i.e. aqueous, and mild reducing environments).

Classically the cycloaddition between azides and alkynes is carried out in refluxing toluene leading to mixture of the 1,4- and 1,5- regioisomers (Scheme 2), but modified proteins and peptides may not survive in this strong condition.



Scheme 2. [1,2,3]-Triazole formation by [3+2] cycloaddition of an alkyne and an azide.

Moreover, the obtainment of mixture of products is not useful in synthesis of peptidomimetics. Meldal⁴³ and co-workers and Sharpless⁴⁴ and co-workers developed a mild and efficient method to generate 1,4-disubstituted [1,2,3]-triazoles by metal-catalyzed reaction using Cu(I) salts as catalyst even in the presence of H₂O. This copper catalyzed azide-alkyne cycloaddition (CuAAC), or Huisgen copper catalyzed cycloaddition, represent a new generic application for linking fragments under mild condition, so called bio-orthogonal conditions. The CuAAC was later described by Sharpless as a key example of the click chemistry concept⁴⁴. Meldal and co-workers described the use of Cu(I) salts in the solid phase, while Sharpless⁴² reported solution phase by in situ reduction of Cu(II) salts. It is also possible to envisage the formation of Cu(I) from the oxidation of copper metallic.

The copper (I) alkyne-azide “click” cycloaddition mediated mechanism follows presumably the pathway outlined in Figure 33. The catalytic cycle shows that a source of Cu(I) is fundamental for the regioselectivity. A dimeric copper species (**8**) may be responsible for the catalytic cycle. This may explain the greatly enhanced reactivity of a second azide in diazide-containing species. A pre-organized catalyst the eventually gives rise to the formation of ditriazoles over statistically expected mixtures, even when a 10-fold excess of azide is used.

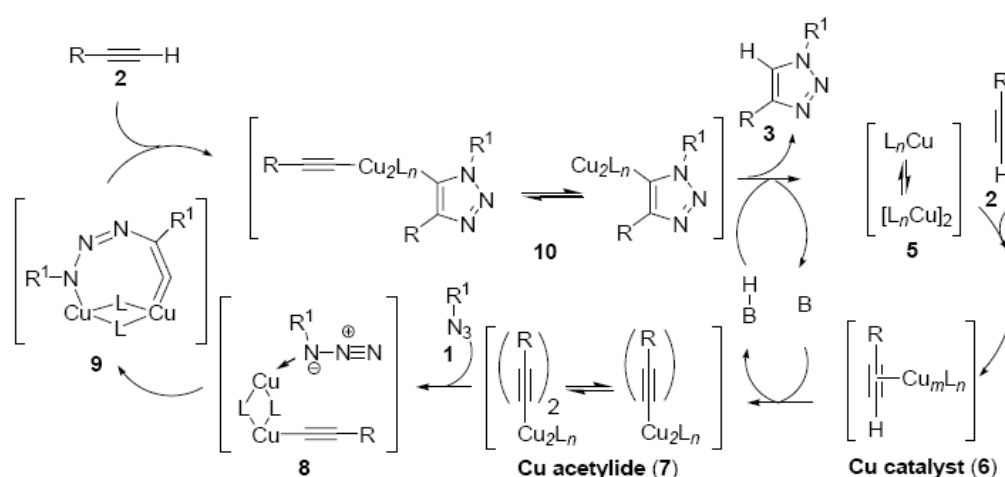


Figure 33. Proposed mechanism of the click-reaction

First, the copper(I)-catalyst forms a π -complex with the acetylene (**6**) and subsequently replaces the acidic proton of the acetylene. The azide coordinates to the

copper via negatively charged nitrogen atom (**8**), followed by attack and subsequent formation of a new intermediate (**9**). This slightly bent allene-like structure then rearranges to form the copper-triazoles species (**10**). Finally, copper (I) exchange with an acidic proton delivers the triazole (**3**) and the copper (I) species that can enter the next cycle. However, in aqueous solution the formation of copper species (**7**) is exothermic, a result consistent with experimental findings of a rate acceleration in water. Moreover, the copper coordination lowers the pKa of the alkyne CH, thus making deprotonation in aqueous systems possible without the addition of a base; DIPEA and 2,6-lutidine minimize the side-product formation. Therefore, the choice of the condition reaction (solvent, base) is crucial for cycloaddition.

Subsequently, Sharpless and co-workers, set up a Ruthenium catalysed azide alkyne cycloaddition (RuAAC), generating selectively 1,5-disubstituted [1,2,3]-triazoles, but the reaction conditions doesn't respect the criteria for click chemistry^{130, 131,132,133}. Nevertheless, this reaction represents an innovate strategy because it allows further control of the conformations of a peptide sequence and provide access to the alternative 1,5-substituted triazoles. More recently, Rademann and co-workers reported a metal-free cycloaddition of phosphoranes and azides for the obtainment, on solid phase, of 1,5-disubstituted [1,2,3]-triazoles containing-peptides, both linear and cyclic^{134,135}.

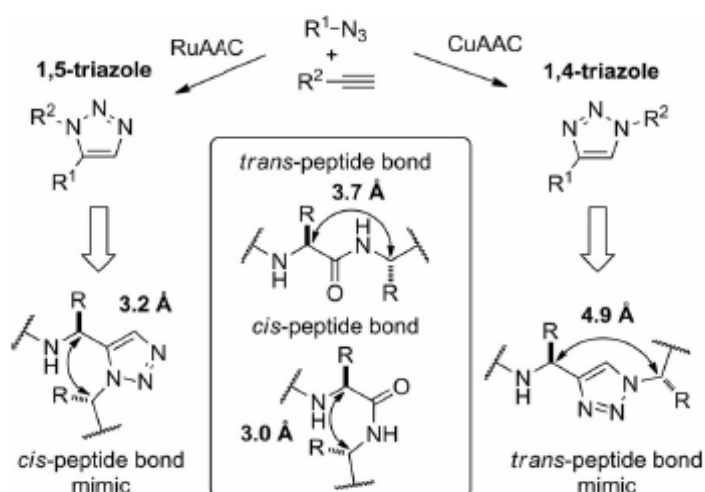


Figure 34. CuAAC and RuAAC synthesis of triazoles. Comparison of 1,4- and 1,5-substituted triazoles with *trans*- and *cis*-peptide bonds.

2.5 Synthetic strategy

In the current study we explored the potential of the *i*-to-*i*+5 side chain-to-side chain 1,4- and 4,1-disubstituted [1,2,3]triazolyl-containing bridges to stabilize β -turn conformations. Studying this modification in the context of the MTII scaffold provides the opportunity to evaluate its potential as a modulator of receptor sub-type selectivity. To this end, we designed a series of 1,4-disubstituted-1,2,3-triazolyl containing cyclo heptapeptides, derived from the model cyclic peptide lactam MTII, Ac-Nle⁴-c[Asp⁵-D-Phe⁷-Lys¹⁰] α MSH₄₋₁₀.NH₂, varied in the size, the location, and the orientation of the [1,2,3]-triazolyl moiety within the bridge.

In this context, a series of N ^{α} -Fmoc- ω -azido- α -amino- and N ^{α} -Fmoc- ω -ynoic- α -amino acids with different length of the side chain, was synthesized and introduced in position *i*-*i*+5 or *i*+5-*i*, to replace Asp⁵ and Lys¹⁰ residues in the sequence of MTII. Solution phase intramolecular CuAAC converted linear precursor I'-X' in to the 1,4- and 4,1-disubstituted-[1,2,3]triazolyl-containing cyclopeptides, I-X.

2.6 Synthesis of non-coded amino acids

The non-coded amino with different lengths of the side chains, were synthesized following the procedure previously described^{16,51} (Figure 35).

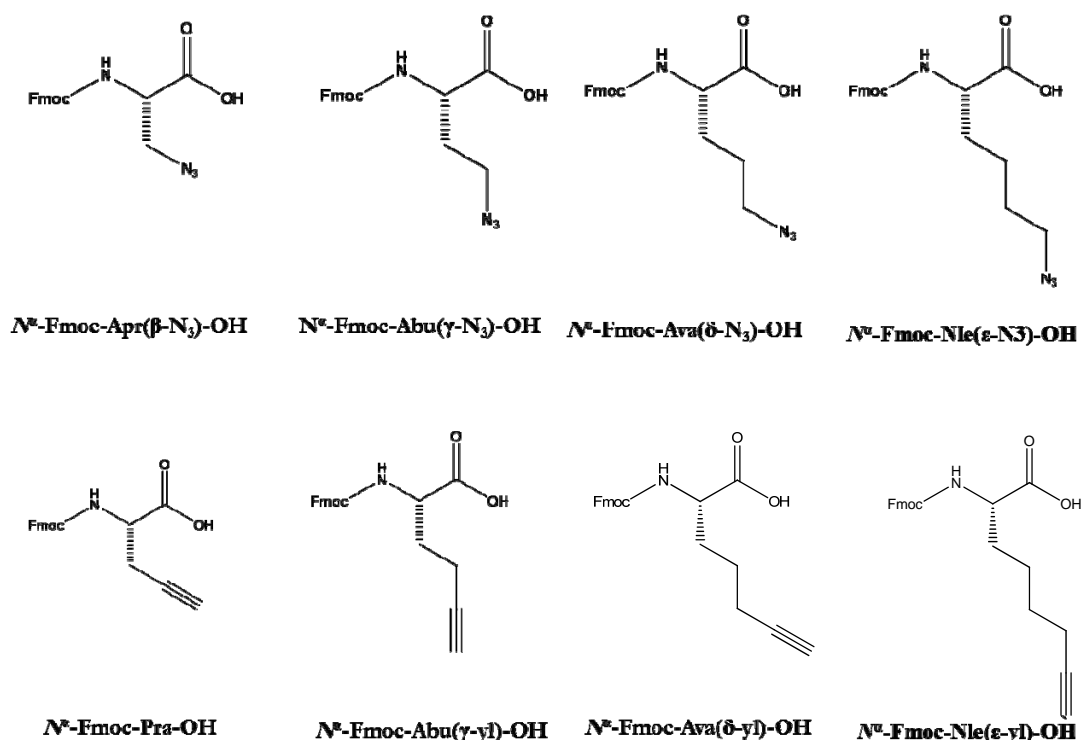
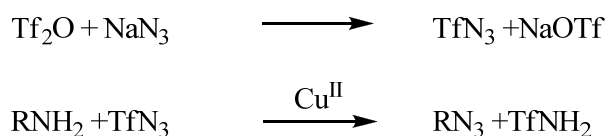


Figure 35. N^{α} -Fmoc- ω -azido- α -amino- and N^{α} -Fmoc- ω -ynoic- α -amino acids

2.6.1 Synthesis of N^{α} -Fmoc- ω -azido- α -amino acids

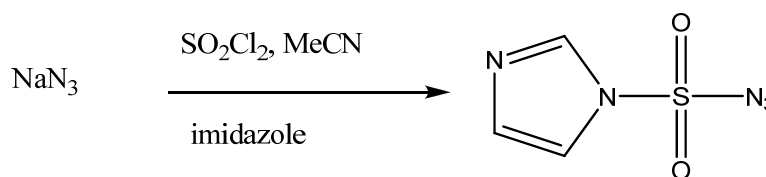
N^{α} -Fmoc- ω -azido- α -amino acids were synthesized by *diazo-transfer* reaction starting from the correspondent N^{α} -protected ω -amino- α -amino acids^{51,16}.

This process utilizes trifluoromethanesulfonyl azide (TfN₃) as a “diazo donor” in the Cu(II)-catalyzed conversion of a primary amine, into an azide^{136,137,138,139} (Scheme 3).



Scheme 3. TfN₃ in the diazotransfer reaction

The process is amenable to scale-up, employ commercially available reagents and does not require anhydrous conditions. Moreover, since the transformation does not involve the C^α, it is accomplished with a complete retention of the original configuration of the α -amino acid residues. However, this reaction is not without problems. The explosive nature of neat TfN₃ and its relatively poor shelf life necessitate its preparation in solution prior to use. Furthermore, inconsistent yields in the preparation of TfN₃ mean that the solution must either be standardized or used in a liberal excess. The removal of trifluoromethanesulfonamide from polar products has in the past also required specialized workup procedures. Finally, perhaps most significantly, the expense of trifluoromethanesulfonic anhydride, used in the preparation of TfN₃, prohibits the deployment of this reaction on a large scale. To circumvent these problems a cheap, robust, and safe alternative to TfN₃ is required. A possible alternative to TfN₃ is represented by imidazole-1-sulfonate-azide-hydrochloride. Imidazole-1-sulfonyl azide exhibit very similar reactivity to TfN₃, miming its ability to act as a diazotransfer reagent, but it also might be less costly to prepare, more stable (hopefully crystalline), and produce more easily removed by-products. The synthesis of imidazole-1-sulfonate-azide-hydrochloride is easily accomplished by the addition of two mole equivalents of imidazole to chlorosulfonyl azide, preformed in situ by the reaction of equimolar quantities of sodium azide and sulfuryl chloride in acetonitrile. Subsequent aqueous workup and flash chromatography afforded the desired product as a colorless liquid in good yield (72%), (Scheme 4).



Scheme 4. Synthesis of imidazole-1-sulfonyl-azide

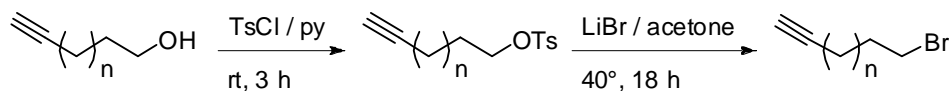
To obtain a crystalline diazotransfer reagent, desired for reasons of stability ability and easy purification, we treated the imidazole-1-sulfonyl-azide with HCl in EtOH¹⁴⁰. We obtained in a one-pot reaction, the imidazole-1-sulfonyl-azide hydrochloride as crystalline solid, in good yield and high purity without the need for

chromatography. The imidazole-1-sulfonyl-azide hydrochloride was used as “diazo donor” in a reaction Cu^{II}-catalyzed, starting from the N^α-Fmoc amino acids, obtaining the correspondent N^α-Fmoc- ω -azido- α -amino acids in good yields and with high purity.

2.6.2 Synthesis of N^α-Fmoc- ω -alkynyl- α -amino acids

Inside the series of N^α-Fmoc- ω -alkynyl- α -amino acids, only propargylglycine (n=1, Pra) is commercially available. The higher N^α-Fmoc- ω -alkynyl- α -amino acids homologs containing (CH₂)_n (n=2, 3 and 4), were synthesized by alkylation of a Ni(II) complex of the Schiff base formed between glycine and (S)-2-(N-benzylpropyl)aminobenzophenone, [Ni^{II}-(S)BPB-Gly] as chiral inducer, with alk- ω -ynyl bromides respectively^{141, 142, 143, 144, 145}.

The ω -bromoalkynes used for the alkylation of the nickel complex were prepared from the corresponding alcohol by treatment with TsCl followed by LiBr, with the exception for 4-bromo-1-butyne, commercially available (Table 3).

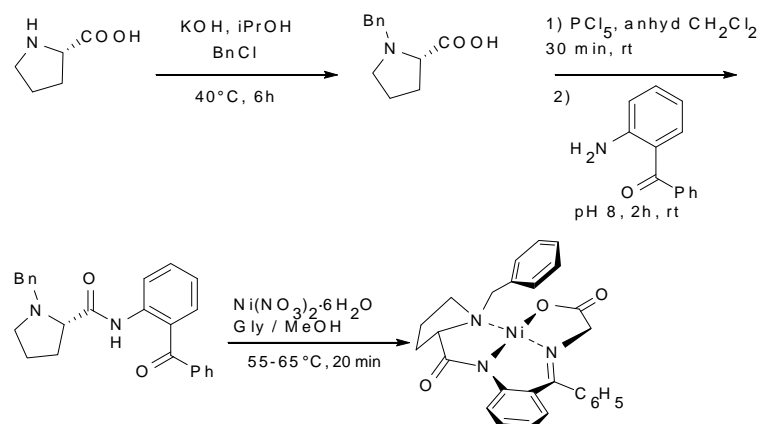


n	OTs (yield %)	Br (yield %)
1	82	65
2	69	82

Table 3. Synthesis of ω -alkynyl-bromide and ω -alkynyl-bromide yields

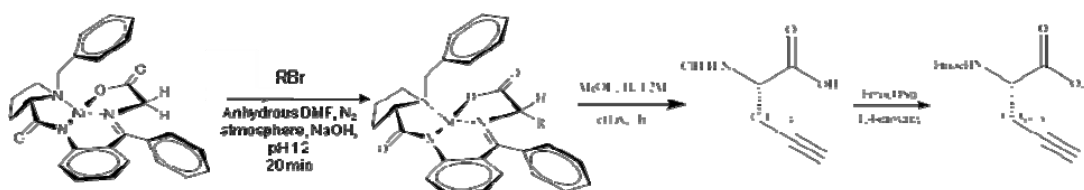
The (S)-N-Benzylproline (BP) was obtained by the reaction of (S)-proline and benzylchloride. The coupling step between N-benzyl-(S)-proline (BP) and 2-aminobenzophenone was accomplished in situ by PCl₅-mediated transformation of the carboxyl function into the acyl chloride, which was used to acylate the 2-aminobenzophenone at pH 8, affording the chiral inducer, BPB. In the following step, the yield of formation of the nickel complex, [Gly-Ni(II)-(S)BPB], we improved

from 80 to 95%, increasing the molar excess of BPB, although a multistep work up was needed (Scheme 5).



Scheme 5. Synthesis of the chiral inducer [Gly-Ni(II)-(S)BPB]

The [Gly-Ni(II)-(S)BPB-] was used for the asymmetric synthesis of the non-coded amino acid by reaction with alkynyl bromides (Scheme 6). The alkylation reaction was performed under heterogeneous conditions employing minimum amount of an aprotic solvent, DMF.



Scheme 6. Chiral synthesis of L- ω -alkynyl- α -amino acids employing the chirality inducer [Ni^{II}-(S)BPB-Gly].

The complexes provide easy generation of intermediate carbanion due to high acidity of α -hydrogen of an amino acid fragment ($pK_a \geq 19$). The alkylations through the si-face of the glycine enolate are largely favored to lead to (S)- ω -alkynyl amino acids. That is depending by the repulsion between ortho-protons of the benzyl group and equatorial substituents of C α of glycine¹⁴⁶. The diastereoisomeric excess can be evaluated by UPLC (Table 4). The separation of the diastereoisomers was successfully achieved by flash column chromatography, FCC. Alkylation of glycine by alkynyl bromides in the presence of the chirality inducer [Ni^{II}-(S)BPB-Gly],

yielded the corresponding α -alkynyl- ω -amino acids in good diastereoisomeric excess.

Table 4. Diastereoisomeric excess of the alkynylated complexes.

Products of alkylation of the Gly-Ni-BPB complex with	<i>S,S</i> -diastereoisomeric excess (%)	Alkylation yield (%)
5-Bromopent-1-yne	71	58
6-Bromohex-1-yne	88	68

The free l' - ω -alkynyl-(*S*)- α -amino acid was obtained by hydrolysis of the resultant alkylated complex in 2M HCl in MeOH. Workup afforded a pale green solid containing the free alkynylated amino acids in the presence of Ni⁰ and BPB. This strategy presents the advantage that the chiral auxiliary, BPB, is regenerated in good yield (90%) at the end of the process and can be re-used in a new reaction, although the excess nickel in the waste water is a potential environmental problem. The traces of Ni⁰, which interfere in the following N ^{α} -Fmoc-protection reaction, were removed from the free and crude α -alkynylated ω -amino acids, by overnight solid phase extraction of its MeOH/H₂O (15:20) solution with Na⁺ Chelex resin. Finally, the free ω -alkynyl- α -amino acids were N ^{α} -protected with Fmoc employing Fmoc-O-Su, to yield the *building blocks* in adequate for the Fmoc/tBu solid phase peptide synthesis¹⁶.

2.6.3 Collection of linear peptide precursor

Ac[Yaa⁵(ω -N₃),Xaa¹⁰(ω -yl)] α MSH₄₋₁₀ (V', VI', VII', VIII', X'), and Ac[Xaa⁵(ω -yl),Yaa¹⁰(ω -N₃)] α MSH₄₋₁₀ (I', II', III', IV', IX')

Peptides I'–X' were synthesized on Rink-amide NovaSyn TGR resin (0.14 mmol/g, 300 mg), on a manual batch synthesizer (PLS 4X4, Advanced ChemTech), following the Fmoc/tBu chemistry. The Fmoc-Rink-amide resin was swelled with DMF (1 mL/100 mg of resin) for 20 min before use. Stepwise peptide assembly was performed by repeating for each added amino acid the standard procedure, using TBTU/HOBt/NMM (2 eq./2 eq./3 eq.) as the coupling system and 2 eq. of the Fmoc protected amino acids, except for N ^{α} -Fmoc-Xaa(ω -N₃)-OH and N ^{α} -Fmoc-Yaa(ω -yl)-

OH for which 1.5 eq. were used. The coupling was carried out in DMF (1mL/100 mg of resin) for 50 min. The solid phase assembly of the linear precursors I'-X', was performed by incorporation of the N^α-Fmoc-ω-azido-α-amino- and N^α-Fmoc-ω-ynoic-α-amino acids in positions i-i+5 and i+5-i, replacing Lys¹⁰ and Asp⁵ of MTII, during the stepwise build-up of the resin bond peptide. This strategy was found to be the most convenient approach to introduce the functions essential for the subsequent CuAAC. Moreover, thanks to the relative ease introduction of the azido and alkynyl functions, and their inertness toward a wide range of reaction condition and nucleophiles and electrophiles^{44,147} orthogonal protection scheme is not required. Each coupling was monitored by Kaiser test¹⁴⁸ and was negative, therefore recouplings were not needed. Once the peptide sequences were completed, the free N-terminal α-amino of the resin-bound peptides was acetylated following the protocol described in Experimental Part. The reaction was monitored by Kaiser test. All the linear peptides were purified by semi-preparative RP-HPLC, employing a linear gradient 20-to-60% of B in 30min (A - 0.1% TFA in H₂O; B - 0.1% TFA in ACN) flow 4 ml/min., and characterized by ESI-MS. Analytical data are reported in Table 3.

Table 5. Chemical data of linear precursors I'-X'.

Linear precursor	Rt (*) UPLC	MS ⁺ (ESI) m/z	
		found	calculated
I'	4.91 min	[M+H] ⁺ =1048.61 [M+2H] ²⁺ =525.30	[M+H] ⁺ =1048.24
II'	4.74 min	[M+H] ⁺ =1048.61 [M+2H] ²⁺ =525.30	[M+H] ⁺ =1048.24
III'	4.51 min	[M+H] ⁺ =1048.61 [M+2H] ²⁺ =525.30	[M+H] ⁺ =1048.24
IV'	4.46 min	[M+H] ⁺ =1048.91 [M+2H] ²⁺ =525.45	[M+H] ⁺ =1048.24
V'	4.97 min	[M+H] ⁺ =1048.61 [M+2H] ²⁺ =525.30	[M+H] ⁺ =1048.24
VI'	4.47 min	[M+H] ⁺ =1048.71 [M+2H] ²⁺ =525.35	[M+H] ⁺ =1048.24
VII'	4.46 min	[M+H] ⁺ =1048.61 [M+2H] ²⁺ =525.30	[M+H] ⁺ =1048.24
VIII'	4.77 min	[M+H] ⁺ =1048.71 [M+2H] ²⁺ =525.35	[M+H] ⁺ =1048.24
IX'	4.41 min	[M+H] ⁺ =1034.62 [M+2H] ²⁺ =518.31	[M+H] ⁺ =1034.24
X'	4.77 min	[M+H] ⁺ =1034.91 [M+2H] ²⁺ =518.46	[M+H] ⁺ =1034.24

(*) solvent system: A 0,1 % TFA in H₂O; B 0,1% TFA in ACN; gradient 10-60% B in 5 min. Flow 0.6 ml/min

2.6.4 Collection of triazole containing cyclo-peptides

Ac[Yaa⁵(&¹),Xaa¹⁰(&²)] α MSH(4-10) [{{&¹(CH₂)_n-1,4-(1,2,3)triazolyl-(CH₂)_m&²}] (V', VI', VII', VIII', X'), and Ac[Xaa⁵(&¹),Yaa¹⁰(&²)] α MSH(4-10) [{{&¹(CH₂)_m-1,4-(1,2,3)triazolyl-(CH₂)_n&²}] (I', II', III', IV', IX)

Intramolecular Cu^I-catalyzed side-chain-to-side-chain azide-alkyne 1,3-dipolar Huisgen cycloaddition (CuAAC), converted the purified (>95% purity) linear precursors I'-X' in to the 1,4-disubstituted-[1,2,3]triazolyl-containing cyclopeptides I-X, presenting different permutations in terms of size, orientation and position of the triazolyl bridges. Depending on the respective position (i-i+5 or i+5-i) of the azido and alkynyl amino acids in the peptide sequence, we generated two classes of cyclopeptides (Figure 36 and Figure 37).

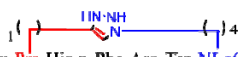
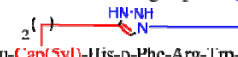
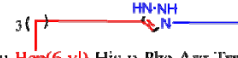
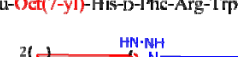
Linear Precursor	4,1-disubstituted 1,2,3-triazolyl cyclopeptide
I' Ac-NLeu-Pra-His-D-Phe-Arg-Trp-NLe(N ₃)-NH ₂	I 
II' Ac-NLeu-Cap(5yl)-His-D-Phe-Arg-Trp-Nva(δN ₃)-NH ₂	II 
III' Ac-NLeu-Hep(6-yl)-His-D-Phe-Arg-Trp-hAla(γ-N ₃)-NH ₂	III 
IV' Ac-NLeu-Oct(7-yl)-His-D-Phe-Arg-Trp-Ala(β-N ₃)-NH ₂	IV 
IX' Ac-NLeu-Cap(5-yl)-His-D-Phe-Arg-Trp-hAla(γ-N ₃)-NH ₂	IX 

Figure 36. Ac[Xaa⁵(&¹),Yaa¹⁰(&²)] α MSH(4-10) [{{&¹(CH₂)_m-1,4-(1,2,3)triazolyl-(CH₂)_n&²}]

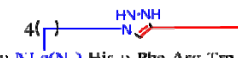
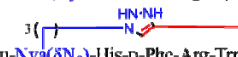
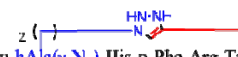
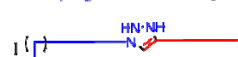
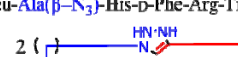
Linear Precursor	1,4-disubstituted 1,2,3-triazolyl cyclopeptide
V' Ac-NLeu-NLe(N ₃)-His-D-Phe-Arg-Trp-Pra-NH ₂	V 
VI' Ac-NLeu-Nva(δN ₃)-His-D-Phe-Arg-Trp-Cap(5yl)-NH ₂	VI 
VII' Ac-NLeu-hAla(γ-N ₃)-His-D-Phe-Arg-Trp-Hep(6-yl)-NH ₂	VII 
VIII' Ac-NLeu-Ala(β-N ₃)-His-D-Phe-Arg-Trp-Oct(7-yl)-NH ₂	VIII 
X' Ac-NLeu-hAla(γ-N ₃)-His-D-Phe-Arg-Trp-Cap(5-yl)-NH ₂	X 

Figure 37. Ac[Yaa⁵(&¹),Xaa¹⁰(&²)] α MSH(4-10) [{{&¹(CH₂)_n-1,4-(1,2,3)triazolyl-(CH₂)_m&²}]

The click reaction conditions were identical to those reported by us previously⁵¹. In particular, the complete conversion of the linear precursors I'-X' to the desired cyclic [1,2,3]triazolyl-containing peptide, was achieved after ON incubation at RT in tBuOH/H₂O (1:2 v/v), in the presence of 4.4-fold molar excess of CuSO₄•5H₂O and ascorbic acid, obtaining Cu(I) by in-situ formation from Cu(II) salts.

Under these conditions there is no formation of oligomeric products resulting from intermolecular click reactions, thus suggesting formation of a Cu^I/acetylide/azide complex with high preference for intramolecular cyclizations. Moreover following this protocol we didn't observe side products formed by dimerizations and macrocyclizations, which are often observed in on-resin CuAAC, thus generating easy to purify crude products. All copper salts were eliminated by solid phase extraction from the crude material by eluting with water, and cyclopeptides were afforded by elution from 10% to 30% of acetonitrile in water. The clicked peptides were further purified by RP-HPLC, using the same conditions reported before, and characterized by ESI-MS (Table 4).

For the yields of the pure cyclopeptides, we did not observe a large difference between the cyclopeptides containing triazolyl ring with alkyl chains of different lengths: from 40% (for the longer alkyl chains) to 55%.

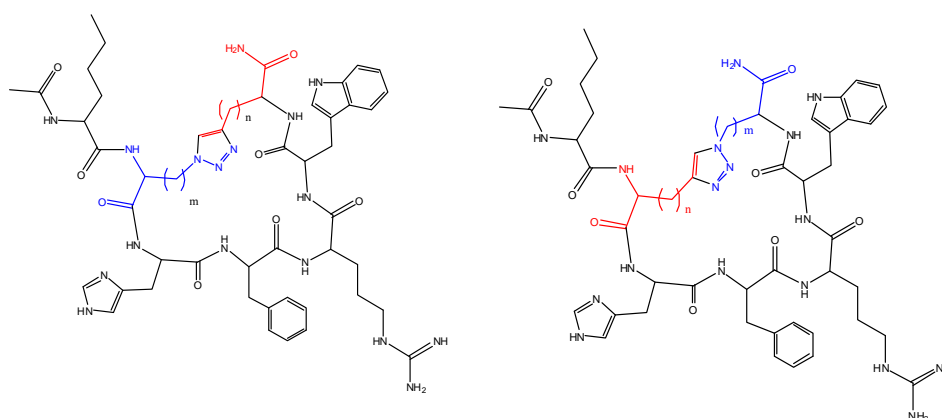


Table 6. Chemical data of clicked peptides I-X.

Clicked peptide	Xaa	Yaa	Rt (*) UPLC	MS ⁺ (ESI) m/z	
				found	calculated
I	n = 1	m = 4	3.66 min	[M+H] ⁺ =1048.61 [M+2H] ²⁺ =525.30	[M+H] ⁺ =1048.24
II	m = 2	n = 3	3.67 min	[M+H] ⁺ =1048.61 [M+2H] ²⁺ =525.30	[M+H] ⁺ =1048.24
III	n = 3	m = 2	3.81 min	[M+H] ⁺ =1048.61 [M+2H] ²⁺ =525.30	[M+H] ⁺ =1048.24
IV	n = 4	m = 1	3.47 min	[M+H] ⁺ =1048.91 [M+2H] ²⁺ =525.40	[M+H] ⁺ =1048.24
V	m = 4	n = 1	3.68 min	[M+H] ⁺ =1048.61 [M+2H] ²⁺ =525.30	[M+H] ⁺ =1048.24
VI	m = 3	n = 2	3.62 min	[M+H] ⁺ =1048.71 [M+2H] ²⁺ =525.31	[M+H] ⁺ =1048.24
VII	m = 2	n = 3	3.99 min	[M+H] ⁺ =1048.61 [M+2H] ²⁺ =525.30	[M+H] ⁺ =1048.24
VIII	m = 1	n = 4	3.79 min	[M+H] ⁺ =1048.71 [M+2H] ²⁺ =525.31	[M+H] ⁺ =1048.24
IX	n = 2	m = 2	3.51 min	[M+H] ⁺ =1034.62 [M+2H] ²⁺ =518.71	[M+H] ⁺ =1034.24
X	m = 2	n = 2	3.73 min	[M+H] ⁺ =1034.91 [M+2H] ²⁺ =518.61	[M+H] ⁺ =1034.24

(*) solvent system: A 0,1 % TFA in H₂O; B 0,1% TFA in ACN; gradient 10-60% B in 5 min. Flow 0.6 ml/min.

2.6.5 Solid Phase Synthesis of lactam bridge-containing cyclopeptide

MTII Ac-Nle⁴-c[Asp⁵-D-Phe⁷-Lys¹⁰]αMSH₄₋₁₀-NH₂.

MTII, Ac-Nle⁴-c[Asp⁵-D-Phe⁷-Lys¹⁰]αMSH₄₋₁₀-NH₂, was synthesized using a Rink-amide NovaSyn TGR resin on a manual batch synthesizer (PLS 4X4, Advanced ChemTech) applying the same Fmoc/tBu solid procedure reported for the MTII linear analogs I'-X'. The formation of the lactam bridges between side chain groups of Lys¹⁰ and Asp⁵ was performed in solid phase, following an orthogonal protocol of deprotection. In particular we used Lys¹⁰ protected in side chain with 1-[(4,4 - dimethyl-2,6-dioxocyclohex -1-ylidene)ethyl] group (Dde), that is stable in the condition of elongation of the peptide. After acetylation of the N-terminus, Dde was removed using hydrazine 20% in DMF (1mL). After deprotection of Lys¹⁰, the formation of intramolecular lactam bound was performed using TBTU/HOBt/NMM (2.5:2.5:3.5 equiv.) as coupling system, for 40 minutes. The reaction of cyclization was monitored by UPLC-ESI-MS analysis of MW-assisted mini-cleavage resin bond fragment. The peptide was purified by RP-HPLC, using the same conditions reported before, and characterized by ESI-MS (Table 5).

Table 7. Chemical data of MTII an MTII linear precursor.

Peptide	Rt (*)UPLC	MS ⁺ (ESI)m/z	
		found	calculated
MTII Linear precursor	2.88	[M+H] ⁺ =1043,55 [M+H] ⁺ =522.11	[M+H] ⁺ =1043,22
MTII	1.79	[M+H] ⁺ =1025,71 [M+2H] ²⁺ =513.83	[M+H] ⁺ =1025,32

(*) solvent system: A 0,1 % TFA in H₂O; B 0,1% TFA in ACN; gradient 10-60% B in 5 min. Flow 0.6 ml/min.

2.7 Biological activities

The biological studies were performed in collaboration with prof. Carrie Haskell-Luevano, Department of Pharmacodynamics, University of Florida, USA, and Medicinal Chemistry, University of Minnesota, Minneapolis.

The biological activity of all the 1,4- and 4,1-disubstituted-[1,2,3]triazolyl-containing cyclopeptides I ÷ X (Table 7), are compared to the lactam-containing peptide MTII, as well as the linear control precursors I' ÷ X' (Table 6).

The potency of MTII, analogues I ÷ X and I' ÷ X', was pharmacologically evaluated for functional potency (EC₅₀) and efficacy using a reporter gene based bioassay for cAMP in HEK cells stably expressing the murine (mouse) melanocortin receptor subtypes mMC1R, mMC3R, mMC4R, and mMC5R^{149,150}.

Table 8. Adenylate cyclase activity (EC_{50}) of linear precursor (I' ÷ X') compared with MTII.

Peptide		mMC1R	mMC3R	mMC4R	mMC5R
		EC_{50} (nM)	EC_{50} (nM)	EC_{50} (nM)	EC_{50} (nM)
MTII		0.03 ±0.005	0.18 ±0.04	0.06 ± 0.02	0.19 ± 0.05
I'	1yl+4az	0.46 ±0.11	2.19 ±0.45	1.50 ±0.69	3.22 ±0.92
V'	4az+1yl	0.24 ±0.08	1.92 ±0.45	0.81 ±0.32	1.90 ±0.51
II'	2yl+3az	0.72 ±0.15	3.27 ±0.88	2.22 ±1.06	5.33 ±1.65
VI'	3az+2yl	0.83 ±0.26	3.66 ±1.16	2.15 ±0.81	5.04 ±1.59
III'	3yl+2az	0.82 ±0.12	0.91 ±0.22	0.13 ±0.01	0.13 ±0.009
VII'	2az+3yl	0.36 ±0.09	0.86 ±0.2	0.098 ±0.017	0.086 ±0.013
IV'	4yl+1az	1.24 ±0.027	1.58 ±0.2	0.19 ±0.04	0.18 ±0.049
VIII'	1az+4yl	0.53 ±0.13	1.32 ±0.16	0.14 ±0.009	0.13 ±0.006
IX'	2yl+2az	1.98 ±0.50	2.33 ±0.31	0.29 ±0.009	0.23 ±0.002
X'	2az+2yl	0.25 ±0.09	0.44 ±0.06	0.058 ±0.006	0.051 ±0.007

Table 9. Adenylate cyclase activity (EC_{50}) cyclic analogs (I-X) compared with MTII

Peptide		mMC1R	mMC3R	mMC4R	mMC5R
		EC_{50} (nM)	EC_{50} (nM)	EC_{50} (nM)	EC_{50} (nM)
MTII		0.03 ±0.005	0.18 ±0.04	0.06 ± 0.02	0.19 ± 0.05
I	tb4 ¹ ,1 ⁴	5.18 ±0.54	3.14 ±0.25	1.62 ±0.57	1.93 ±0.07
V	tb1 ⁴ ,4 ¹	0.85 ±0.07	3.70 ±0.36	0.58 ±0.14	1.76 ±0.37
II	tb4 ² ,1 ³	0.11 ±0.029	0.29 ±0.1	0.22 ±0.06	0.34 ±0.09
VI	tb1 ³ ,4 ²	0.71 ± 0.11	1.91 ±0.73	0.85 ±0.36	1.88 ±0.70
III	tb4 ³ ,1 ²	0.1 ±0.009	0.21 ±0.038	0.051 ±0.006	0.042 ±0.005
VII	tb1 ² ,4 ³	0.074 ±0.02	0.20 ±0.006	0.048 ±0.007	0.045 ±0.004
IV	tb4 ⁴ ,1 ¹	0.087 ±0.029	0.2 ±0.002	0.041 ±0.001	0.035 ±0.007
VIII	tb1 ¹ ,4 ⁴	0.53 ±0.14	0.60 ±0.04	0.14 ±0.02	0.13 ±0.015
IX	tb4 ² ,1 ²	0.32 ±0.097	0.63 ±0.13	0.14 ±0.029	0.15 ±0.02
X	tb1 ² ,4 ²	0.20 ±0.023	0.29 ±0.07	0.067 ±0.004	0.07 ±0.004

The results show that the cyclic peptides are more potent than their linear precursors, confirming that conformational stabilization in the form of side chain-to-side chain cyclization enhances *in vitro* potency. Moreover, the clicked cyclic peptides have similar potency compared to the parent lactam-containing MTII analogs, indicating that these types of side chain modifications are a feasible alternative to the lactam types of cyclizations to enhance desired *in vivo* chemotype biophysical properties. Of interest is the emergence of mMC5R selectivity. While the prototypic MTII is 3- and

5-fold more potent toward mMC1R and mMC4R, respectively, than toward mMC3R and mMC5R (cf. $EC_{50} = 0.03$ and 0.06 nM with 0.18 and 0.19 nM, respectively). Analogs III, IV, and VII display higher mMC1R-mediated activities as compared with MTII.

In summary, our study supports our idea that the i-to-i+5 side chain-to-side chain bridged [1,2,3]triazolyl containing- cyclopeptides can successfully replace the classical β -turn stabilizing i-to-i+5 side chain-to-side chain bridged lactam containing cyclopeptides and generate equipotent analogs. This enhancement of their *in vitro* potency relative to the linear precursors suggests that the imposed structural rigidification achieves the conformational stabilization of biological relevant conformation. In the future it could be interesting to fine-tune this modification to improve receptor-subtype selectivity.

2.8 Conformational analysis

NMR conformational studies of cyclopeptides I, IV, V were performed in collaboration with prof. Anna Maria D'Ursi, Dr. Mario Scrima and Manuela Grimaldi, of University of Salerno.

In solution, most of the peptides assume multiple flexible conformations. Determination of the dominant conformers and evaluation of their populations is the aim of peptide conformational studies, in which theoretical and experimental methods play complementary roles¹⁵¹. Cyclic peptides typically assume multiple conformations; these conformations are rather flexible, with torsional angles of the backbone (φ , ψ) as well as of the side chain groups (χ_i) fluctuating within large intervals (Figure 38).

In addition, coupling constants between NH and $C^\alpha H$ can give information about the average values of the peptide backbone torsional φ angles.

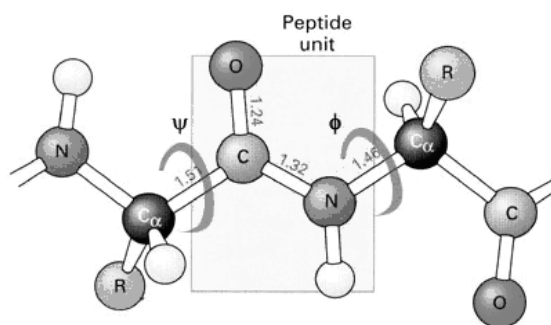


Figure 38. ϕ and ψ Dihedral angles.

Moreover, another goal of conformational investigations is to determine the relationship between conformation and activity of biologically important peptides, e.g. Structure Activity Relationship, SAR. Numerous biological results are strongly supported by conformational investigations, clearly indicating that biological peptide activity is determined not only by the presence of specific functions binding to a target protein, but dramatically depends on the conformational properties of the whole peptide structure, too. The collected [1,2,3]triazolyl-ring containing peptides (I-X) and the lactam ring containing peptide MTII, were analysed by NMR, in order to understand the influence of the alkyl ring size containing the triazolyl moiety, the spatial orientation of triazole ring and the spatial arrangement of all the side chains that is fundamental for the interactions with the receptor.

2.9 NMR analysis

NMR spectra of MTII analogues peptides were acquired in DMSO- d_6 . To exclude potential aggregation, we recorded the 1D proton spectra of the cyclopeptides at a concentration range spanning 1–0.1 mM. At a peptide concentration of 0.1 mM, the peptides did not display any noticeable effects of aggregation. Chemical shift assignments of the proton spectra were achieved via the standard systematic application of DQF-COSY¹⁵², TOCSY¹⁵³, and NOESY¹⁵⁴ experiments, using the SPARKY¹⁵⁵ software package according to the procedure of Wüthrich¹⁵⁶.

Analysis of NOESY spectra evidences a high number of well resolved cross-peaks suggestive of significant presence of ordered conformers.

Figure 39 and 40 show the diagnostic sequential and medium-range connectivities observed in the NOESY spectra of cyclopeptides I, V, II, IV and X.

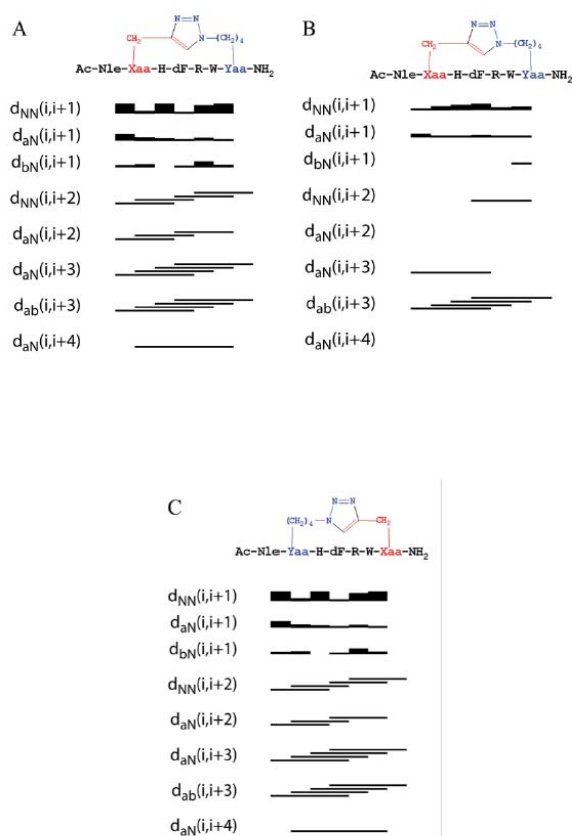


Figure 39. Sequential and medium-range NOEs for [1,2,3]triazolyl-containing cyclopeptides MTII-I (A-B) and MTII-V (C). Panels A and B are relative to the NOE connectivities of the most (A) and the less (B) abundant MTII-I conformers. Data were obtained from a 600 MHz NOESY experiments with a mixing time of 200 ms and collected in DMSO-d₆ at 300 K.

The NOEs bar diagrams relative to cyclopeptides I and V show $d_{NN}(i, i+1)$ sequential connectivities and numerous $d_{aN}(i, i+3)$, $d_{a\beta}(i, i+3)$, and $d_{aN}(i, i+4)$ medium range connectivities typical of a well structured cyclopeptide molecules.

Interestingly analysis of cyclopeptides I NOESY spectra in DMSO-d₆ evidence the presence of double signal patterns, indicating the presence of a slow conformational equilibrium among the different populations of analog I energetically stable conformers.

According to the observation of a double signal pattern in the NOESY spectrum, two different bar diagrams (Figure 39A and Figure 39B) are reported for analog I, there

of the most abundant evidences a higher number of medium range NOEs, whereas the less abundant evidences less intense and less numerous NOE effects. Interestingly the less abundant conformational population is characterized by the presence along the whole sequence, of a systematic $\alpha\beta(i, i+3)$ NOE correlations.

NOESY spectra of cyclopeptides II and X, shows a drastic reduction of diagnostic cross peaks indicating a minor presence of ordered conformers.

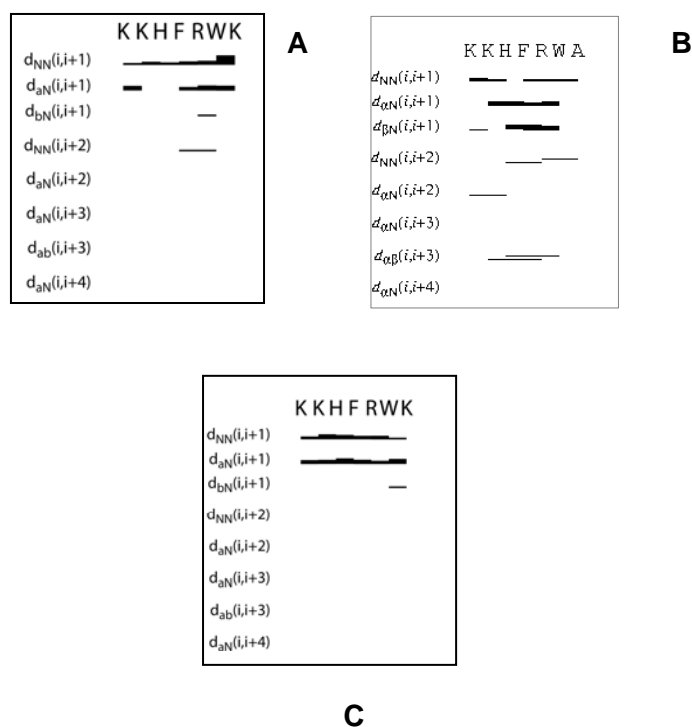


Figure 40. Sequential and medium-range NOEs for [1,2,3]triazolyl-containing cyclopeptides MTII-II (A), MTII-IV (B) and MTII-X (C). Data were obtained from a 600 MHz NOESY experiments with a mixing time of 200 ms and collected in DMSO-d₆ at 300 K

2.10 NMR Structure Calculations

Three-dimensional structures of MTII analogues peptides were calculated by simulated annealing procedures based on sequential and medium-range NOE-derived restraints. To avoid overestimation of NOE effects, NOESY spectra were collected using 100, 200, 300, and 450 ms mixing times. Interprotonic distances were derived from 300 ms mixing time NOESY spectrum. The best 20 structures out of 50 calculated were chosen according to the lowest values of the penalty (f) for the target

function. These structures were energy minimized using the distance restraints with a progressively smaller force constant. The minimization procedure yielded an improved helical geometry and a lower total energy of the structures. To validate the resulting structures the PDB files were submitted to online PROCHECK software.

Figure 41 shows an overlap of the 20 best structures of cyclopeptides I and V conformers, calculated by DYANA and then minimized with the SANDER module of the AMBER 5 software package. In all the sets of structures a good overlap is observed in residues within the cyclic regions of the peptides. The structure bundle relative to the cyclopeptide I shows that the conformational preferences of the most populated conformer (Figure 41A) are consistent with the presence of type I β -turn including the residues His⁶-Trp⁹, whereas the less populated conformer (Figure 41B) show the presence of α -helical structure including all residues. The cluster of NMR structures relative to the cyclopeptide V (Figure 41C) shows the presence of type I β -turn including the residues His⁶-Trp⁹.

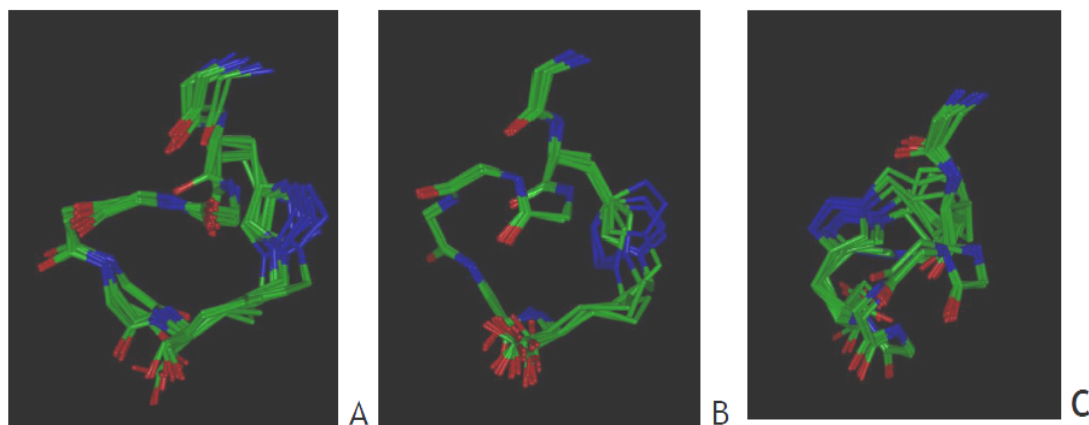


Figure 41. NMR structure bundles of MTII-I (A- B) and MTII-V (C) Best 20 calculated structures are shown. Panels A and B show the most (A) and the less (B) abundant MTII-I conformers respectively

Figure 42 shows the comparison of the analog I conformers representative of the most (Figure 42A) and the less (Figure 42B) abundant conformer populations. As shown in figure, in spite of the difference in the structure of the backbone, which in the most abundant conformation is a type I β -turn and in the less abundant is an α -helix, in both the conformers a common orientation of Phe, His, and Arg side chains is observable. Trp side chain is oriented toward different directions.

The comparison between cyclopeptides I and V low energy conformers shows that in spite of the different position of the triazolyl ring, both the cyclopeptides assume type I β -turn conformation in the cyclic region. Even in this case the conformers have a common orientation of Phe, His and Arg side chains, while exhibit a different orientation of the Trp ring.

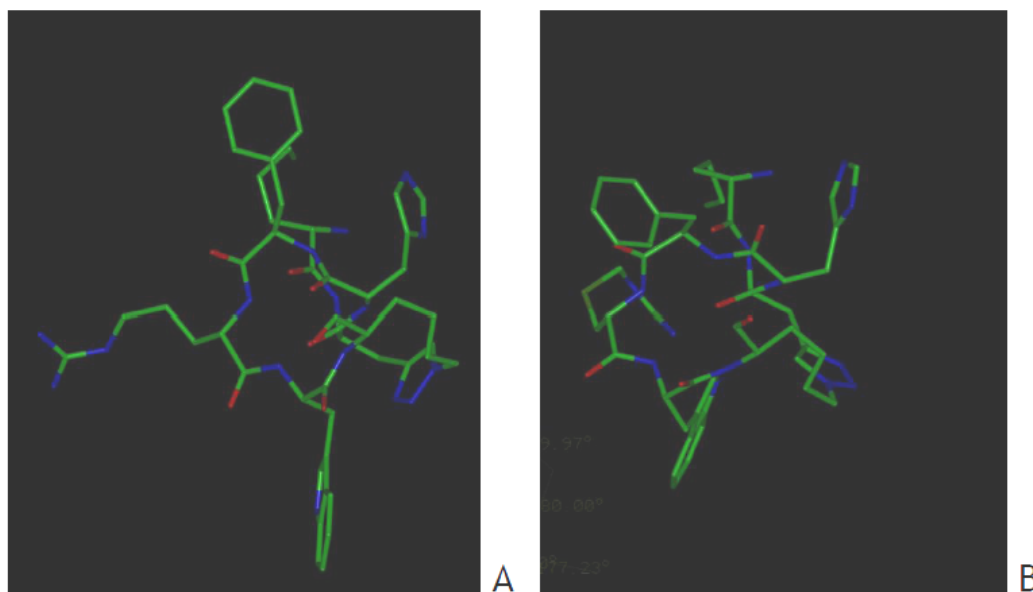


Figure 42. Comparison of MTII-I conformers representative of the most (A) and the less (B) abundant MTII-I conformer populations

Figure 43 shows the structure bundles relative to analogs IV, II and X. Comparing these structure with those of analogs I and V, it is evident in peptides II (cycle 2-3) and III (cycle 3-2) cyclopeptides, the presence of more disordered conformers. However a quantitative estimation of the backbone arrangement of the structures presented in the bundle points to the presence of a consistent population of conformers exhibiting γ -turn structures in correspondence of hAla(γ -N₃)⁵/Cap(5yl)⁵-Arg⁸ residues of cyclopeptides II and X. Additionally analysis of the NMR structure bundle of peptide IV evidences the preponderance of type I β -turn including the residues His⁶-Trp⁹ together with a minor amount of γ -turn conformations including the residues NLe⁴-D-Phe⁷.

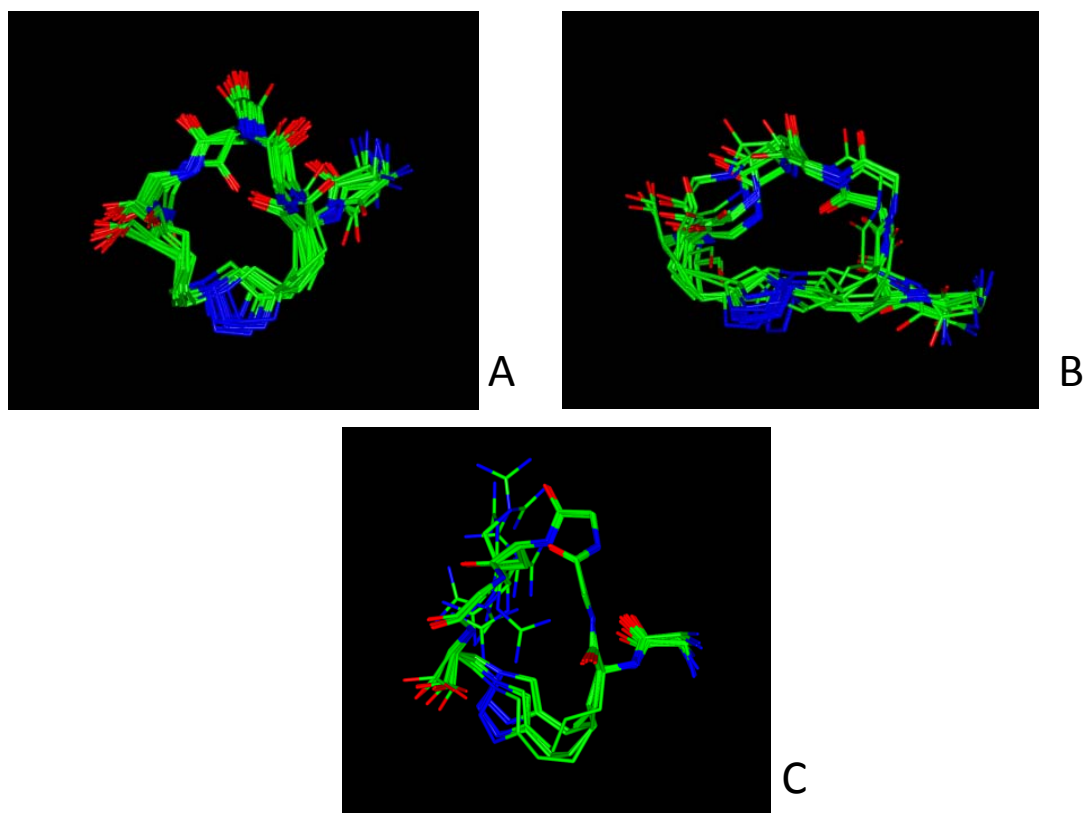


Figure 43. NMR structure bundles of MTII-II(A), MTII-X (B), and MTII-IV (C). Best 20 calculated structures are shown.

Taken together these conformational data indicate that the size of the cycle and the position of the triazolyl ring have a key role in regulating the conformational preferences of the triazolyl bridged cyclopeptides and the orientation of the side orientation strategic for the preservation of the biological activity.

2.11 Conclusion

A collection of N^{α} -Fmoc protected unnatural amino acids bearing on the side chain azide or alkynyl functions was synthesized and introduced by SPPS in the MTII peptide sequences to afford by Cu(I) catalyzed Huisgen reaction, a new collection of cyclopeptides containing the triazolyl moiety.

The side-chain-to-side chain cyclization of linear peptides generated via click chemistry lead to cyclopeptides containing the triazolyl moiety linked to the α -carbon of the amino acids by alkyl chains of different lengths.

A conformational study of these pure cyclopeptides was performed to understand, by comparison to the parent lactam model, the structural analogies fundamental for the receptor recognition. As preliminary results, we can assume that cyclopeptides containing residues involved in the intramolecular cyclization, bearing the longer side chain, assume more canonical structure than those containing residues with a shorter side chain.

The NMR conformational study of cyclopeptides analogs containing triazolyl moiety that could mimic at the best the orientation of side chains and the secondary structure of the lactam MTII cyclopeptide, are in progress at the University of Salerno.

References

-
- ⁸² Nussey S., Whitehead S., *Endocrinology: An Integrated Approach* **2001**, BIOS Scientific Publishers Ltd.
- ⁸³ Alberts B., Bray D., Lewis J., Raff M., Roberts K., Watson J.D., *Molecular Biology of The Cell*, **1994**, 3rd edition, Garland Publishing, New York.
- ⁸⁴ Wessells H., Hrubby V.J., Hackett J., Han G., Balse-Srinivasan P., Vanderah T.W., *Neuroscience*, **2003**, *118*, 755-762.
- ⁸⁵ Chen A.S., Marsh D.J., Trumbauer M.E., Frazier E.G., Guan X.M., Yu H., Rosenblum C.I., Vongs A., Feng Y., Cao L., Metzger J.M., Strack A.M., Camacho R.E., Mellin T.N., Nunes C.N., Min W., Fisher J., Gopal-Truter S., MacIntyre D.E., Chen H.Y., Van der Ploeg L.H.T., *Nat. Genet.*, **2000**, *26*, 97-102.
- ⁸⁶ Butler A.A., Kesterson R.A., Khong K., Cullen M.J., Pellemounter M.A., Dekoning J., Baetscher M., Cone R.D., *Endocrinology*, **2000**, *141*, 3518-3521.
- ⁸⁷ Fan W., Boston B.A., Kesterson R.A., Hrubby V.J., Cone R.D., *Nature*, **1997**, *385*, 165-168.
- ⁸⁸ Huszar D., Lynch C.A., Fairchild-Huntress V., Dunmore J.H., Fang Q., Berkemeir L.R., Gu W., Kesterson R.A., Boston B.A., Cone R.D., Smith F.J., Campfield L.A., Burn P., Lee F., *Cell*, **1997**, *88*, 131-141.
- ⁸⁹ Mogil J.S., Wilson S.G., Chesler E.J., Rankin A.L., Nemmani V.S., Lariviere W.R., Groce M.K., Wallace M.R., Kaplan L., Staud R., Ness T.J., Glover T.L., Stankova M., Mayorov A.V., Hrubby V.J., Grisel J.E., Fillingim R.B., *Proc. Natl. Acad. Sci. U.S.A.*, **2003**, *100*, 4867-4872.
- ⁹⁰ Hrubby V.J., Wilkes B.C., Cody W.L., Sawyer T.K., Hadley M.E., *Pept. Protein Rev.* **1984**, *3*, 1-64.
- ⁹¹ Mountjoy K.G., Robbins L.S., Mortrud M.T., Cone R.D., *Science*, **1992**, *257*, 1248-1251.
- ⁹² FitzGerald L.M., Fryer J.L., Dwyer T., Humphrey S.M., *Peptides*, **2006**, *27*, 388-394.
- ⁹³ Hadley M.E., Dorr R.T., *Peptides*, **2006**, *27*, 921-930.
- ⁹⁴ Kask A., Rago L., Korrovits P., Wikberg J.E.S, Shioth H.B., *Biochemical and Biophysical Research Communications*, **1998**, *248*, 245-249.
- ⁹⁵ Lam D.D., Farooqi I.S., Heisler L.K., *Current Topics in Medicinal Chemistry*, **2007**, *7*, 1098-1110.
- ⁹⁶ Voisey J., Imbeault P., Hutley L., Prins J.B., Van Daal A., *Obesity Research*, **2002**, *10* (6), 447-452.
- ⁹⁷ Seidah N.G. and Chretien M., *Methods Enzymol*, **1994**, *244*, 175-188

-
- ⁹⁸ Benjannet S., Rondeau N., Day R., Chretien M., and Seidah N.G., *Proc Natl Acad Sci USA* **1991**, *88*, 3564–3568.
- ⁹⁹ Eberle A., *The Melanotropins*, Karger, Basel, Switzerland, **1988**.
- ¹⁰⁰ Castrucci A.M.L., Hadley M.E., Sawyer T.K., Wilkes B.C., Al-Obeidi F., Staples D.J., DeVaux A.E., Dym O., Hintz M.F., Riehm J., Rao K.R., Hruby V.J., *Gen Comp Endocrinol*, **1989**, *73*, 157-163.
- ¹⁰¹ Hruby V.J., Wilkes B.C., Hadley M.E., Al-Obeidi F., Sawyer T.K., Staples D.J., DeVaux A., Dym O., Castrucci A.M., Hintz M.F., Riehm J.P., Rao K.R., *J Med Chem*, **1987**, *30*, 2126-2130.
- ¹⁰² Wikberg J.E., Muceniece R., Mandrika I., Prusis P., Lindblom J., Post C., and Skottner A., *Pharmacol Res*, **2000**, *42*, 393–420.
- ¹⁰³ Gantz I., Muraoka A., Yang Y.K., Samuelson L.C., Zimmerman E.M., Cook H., Yamada T., *Genomics*, **1997**, *42*, 462–466.
- ¹⁰⁴ Gantz I., Miwa H., Konda Y., Shimoto Y., Tashiro T., Watson S.J., Del Valle J., Yamada T., *J Biol Chem*, **1993**, *268*, 15174–15179.
- ¹⁰⁵ Chhajlani V., Wikberg J.E., *Febs Lett*, **1992**, *309*, 417–420.
- ¹⁰⁶ Vaudry H., Eberle A.N., *Ann. N.Y. Acad. Sci*, **1993**, *680*, 1-687.
- ¹⁰⁷ Hadley M.E., Ed. *The Melanotropic Peptides*; CRC Press: Boca Raton, FL, **1988**; Vol. I-III.
- ¹⁰⁸ Kavarana M.J., Trivedi D., Cai M., Ying J., Hammer M., Cabello C., Grieco P., Han G., Hruby V.J., *J Med Chem*, **2002**, *45*, 2644-2650.
- ¹⁰⁹ Guarini S., Schioth H.B., Mioni C., Cainazzo M., Ferrazza G., Giuliani D., Wikberg J.E., Bertolini A., and Bazzani C., *Arch Pharmacol*, **2002**, *366*, 177–182.
- ¹¹⁰ Chen W.B., Kelly M.A., Opitz Araya X., Thomas R.E., Low M.J., Cone R.D., *Cell*, **1997**, *91*, 789-798.
- ¹¹¹ Adan R.A., Oosterom J., Toonen R.F., Kraan M.V., Burbach J.P., Gispen W.H., *Recept Channels*, **1997**, *5*, 215–223.
- ¹¹² Cone R.D., *Trends Endocrinol. Metab.*, **1999**, *10*, 211–216.
- ¹¹³ Ollmann M.M., Lamoreux M.L., Wilson B.D., Barsh G.S. *Genes Dev*, **1998**, *12*, 316–330.
- ¹¹⁴ Wilson B.D., Ollmann M.M., Kang L., Stoffel M., Bell G.I., Barsh G.S., *Hum Mol Genet*, **1995**, *4*, 223–230.
- ¹¹⁵ Cone RD *The Melanocortin Receptors*, Humana Press, **2000** Totowa, NJ.
- ¹¹⁶ Willard D.H., Bodnar W., Harris C., Kiefer L., Nichols J.S., Blanchard S., Hoffman C., Moyer M., Burkhart W., Weiel J., et al., *Biochemistry*, **1995**, *34*, 12341–12346.

-
- ¹¹⁷ Adan, R.A., Vink, T., *Eur. Neuropsychopharmacol*, **2001**, 11, 483–490.
- ¹¹⁸ Chen C., Jiang W., Tucci F., Tran J.A., Fleck B.A., Hoare S.R., Joppa M., Markison S., Wen J., Sai Y., Johns M., Madan A., Chen T., Chen C.W., Marinkovic D., Arellano M., Saunders J., Foster A.C., *J. Med. Chem*, **2007**, 50, 5249–5252.
- ¹¹⁹ Hwa J.J., Ghibaudi L., Gao J., Parker E.M., *Am. J. Physiol. Regul. Integr. Comp. Physiol* **2001**, 281, 444–451.
- ¹²⁰ Al-Obeidi F., Hruby V.J., Castrucci A.M.L, Hadley M.E., *J. Med. Chem.*, **1989**, 32, 174–179.
- ¹²¹ Grieco P., Balse-Srinivasan P., Han G., Weinberg D., MacNeil T., Van der Ploeg L.H., and Hruby V.J., *J Pept Res.*, **2002**, 59, 203–210.
- ¹²² Haskell-Luevano C., Sawyer T.K., Trumpp-Kallmeyer S., Bikker J.A., Humblet C., Gantz I., Hruby V.J., *Drug Des Discov*, **1996**, 14, 197–211.
- ¹²³ <http://www.melanoma.org>
- ¹²⁴ <http://www.clinuvel.com/scenese/clinuvels-program/regulatory-process>
- ¹²⁵ Chandrasekaran R., Lakshminarayanan A.V., Pandya U.V., Ramachandran G.N., *Biochim Biophys Acta*, **1973**, 303, 14–27.
- ¹²⁶ Knittel J.J., Sawyer T.K., Hruby V.J., Hadley M.E., *J. Med. Chem.*, **1983**, 26, 125.
- ¹²⁷ Sawyer T.K., Hruby V.J., Darman P.S., Hadley M.E., *Proc. Natl. Acad. Sci. U.S.A.*, **1982**, 79, 1751.
- ¹²⁸ Dorr R.T., Lines R., Levine N., Brooks C., Xiang L., Hruby V.J., Hadley M.E., *Life Sci.*, **1996**, 58(20), 1777–84.
- ¹²⁹ Pedersen D.S., Abell A., *Eur. J. Org. Chem.*, **2011**, 2399–2411.
- ¹³⁰ Majireck M.M., Weinreb S.M., *J. Org. Chem.*, **2006**, 71, 8680–8683.
- ¹³¹ Rasmussen L.K., Boren B.C., Fokin V.V., *Org. Lett.*, **2007**, 9, 5337–5339.
- ¹³² Boren B.C., Narayan L.K., Rasmussen L.K., Zhang L., Zhao H., Lin Z., Jia G., Fokin V.V., *J. Am. Chem. Soc.*, **2008**, 130, 8923–8930.
- ¹³³ Zhang L., Chen X.J., Xue P., Sun H.H.Y., Williams I.D. Sharpless K.B. Fokin V.V., Jia G.C., *J. Am. Chem. Soc.*, **2005**, 127, 15998–15999.
- ¹³⁴ Ahnsanullah, Shmieder P., Kuhne R., Rademann J., *Angew. Chem.*, **2009**, 121, 5143; *Angew. Chem. Int. Ed.*, **2009**, 48, 5042–5045.
- ¹³⁵ Ahnsanullah, Rademann J., *Angew. Chem. Int. Ed.*, **2010**, 49, 5378–5382.
- ¹³⁶ Cavender C.J., Shiner V.J., *J. Org. Chem.*, **1972**, 37, 3567–3569.
- ¹³⁷ Vasella A., Witzig C., Chiara J.L., Martin-Lomas M., *Helv. Chim. Acta*, **1991**, 74, 2073–2077.
- ¹³⁸ Alper P.B., Hung S.C., Wong C.H., *Tetrahedon Lett.*, **1996**, 37, 6029–6032.

-
- ¹³⁹ Nyffeler P.T., Liang C.H., Koeller K.M., Wong C.H., *J. Am. Chem. Soc.*, **2002**, *124*, 10773–10778.
- ¹⁴⁰ Goddard-Borger E.D., Stick R.V., *Organic letters*, **2007**, *9(19)*, 3797-3800.
- ¹⁴¹ Popkov A., Cisarova I., Sopkova J., Jirman J., Lycka A., Kochetkov K.A., *Collect. Czech. Chem. Commun.*, **2005**, *70*, 1397-1410.
- ¹⁴² Belokon. Y.N., Bulychev A.G., Vitt S.V., Struchkov Y.T., Batsanov A.S., Timofeeva T.V., Tsyryapkin V.A., Ryzhov M.G., Lysova L.A., Bakhmutov V.I., Belikov V.M., *J. Am. Chem. Soc.*, **1985**, *107*, 4252.
- ¹⁴³ Belokon Y.N., Tararov V.I., Maleev V.I., Savel'eva T.F., Ryzhov M.G., *Tetrahedron Asymmetry* **1998**, *9*, 4249–4252.
- ¹⁴⁴ Collet S., Bauchat P., Danion-Bougot R., Danion D. *Tetrahedron: Asymmetry* **1998**, *9*, 2121–2131
- ¹⁴⁵ Ueki H., Ellis T.K., Martin C.H., Boettiger T.U., Bolene S.B., Soloshonok V.A., *J. Org. Chem.* **2003**, *68*, 7104-7107.
- ¹⁴⁶ Popkov, A.; Cisarova, I.; Sopkova, J.; Jirman, J.; Lycka, A.; Kochetkov, K. A.; *Collect. Czech. Chem. Commun.* **2005**, *70*, 1397-1410
- ¹⁴⁷ Bodine K.D., Gin D.Y., Gin M.S., *J. Am. Chem. Soc.*, **2004**, *126*, 1638–9.
- ¹⁴⁸ Kaiser E., Colescott R., Bossinger C., Cook P., *Anal. Biochem*, **1970**, *34*, 595-598.
- ¹⁴⁹ Haskell-Luevano C., Cone R.D., Monck E.K., Wan Y.P., *Biochemistry* **2001**, *40*, 6164-6179.
- ¹⁵⁰ Chen W., Shields T. S., Stork P.J.S., Cone R.D., *Anal. Biochem.*, **1995**, *226*, 349-354.
- ¹⁵¹ Bierzyński A., *Acta Biochimica Polonica* **2001**, *48 (4)*, 1091–1099.
- ¹⁵² Piantini U., Sorensen O.W., Ernst R.R., *J. Am. Chem. Soc.* **1982**, *104*, 6800-6801.
- ¹⁵³ Bax A., Davis D.G., *J. Magn. Res.* **1985**, *63*, 207-213.
- ¹⁵⁴ Jeener J., Meyer B.H., Bachman P., Ernst R.R., *J. Chem. Phys.* **1979**, *71*, 4546-4553.
- ¹⁵⁵ Goddard T.D., Kneller D.G., SPARKY 3 NMR software. *University of California, San Francisco* **2001**.
- ¹⁵⁶ Wüthrich K., *NMR of Proteins and Nucleic Acids*. John Wiley & Sons: New York, **1986**.

PART B

3

Impact of endocrine disruptor chemicals on human health

Endocrine disorders are commonly related to improper functioning of the endocrine system, for example malfunctions in pancreas, pituitary, thyroid and adrenal glands. The hormone imbalance (or endocrine disease/condition) can affect human health inducing a lot of conditions such as diabetes mellitus, thyroid disease, and obesity. A number of factors are believed to cause endocrine disorders. Genetic factors, seems to play a relevant role in the etiology of endocrine diseases. For example mutations at the level of thyroid can determin congenital hypothyroidism, while mutations of pituitary glands can induce a lot of disease, because pituitary gland secretes a series of hormones that regulate different biological function.

Nevertheless, in many cases, the exact cause of a particular endocrine disorder is not known. In the last years, it took importance the hypothesis that also environmental or nutritional factors could be involved in etiology of endocrine disorders. In fact, the increased rate of metabolic and neurodevelopmental diseases seems to correlate with severe changes in the chemical environment, affected by new industrial and agricultural procedures over the past 40 years. Environmental chemicals with hormone-like activity can disrupt programming of endocrine signaling pathways during development, and result in adverse effects, some of which may not be apparent until much later in life. Recent studies linked the exposure to environmental endocrine disrupting chemicals during development with obesity, diabetes and neurodevelopmental disorders. These particular diseases are quickly becoming significant public health problems and are fast reaching epidemic proportions worldwide. Therefore, understand the role of endocrine disrupting chemicals, such as phthalates, in the etiology of different pathologies is crucial¹⁵⁷. The detection in human fluid, such as urine, of metabolites of specific compounds, supposed to be endocrine disruptors, could be a valid method to explore the potential causes for endocrine disorders. Phthalates are used in a variety of consumer products, therefore they are considered ubiquitous contaminants. In particular di-(2-ethylhexyl) phthalate (DEHP) was the most used plasticizer for PVC in a lot of products and in particular

in medical devices. Very recently, phthalates were suspected to be correlated to two relevant disorders of childhood: early obesity and Autism Spectrum Disorders (ASDs). In fact, children are known to be exposed to DEHP twice as high as compared to adult subjects. In particular, fetuses and neonates are highly sensitive to physiologically active agents because they are exposed during critical periods of human development. Furthermore, in the case of intensive therapy procedures, neonates can have higher exposure to phthalates and to their toxic monoesters supposed to be endocrine disruptors.

Therefore, in this part of PhD, we focused on the investigation of the presence of urinary concentrations of DEHP metabolites by HPLC-ESI-MS, in two populations of obese and autistic patients in comparison with healthy controls.

3.1 Phthalates

Polyvinylchloride (PVC) is one of the most widely produced plastic in the world. PVC is used extensively for a lot of different purposes, ranging from a lining for landfill waste disposal sites to a food wrapper for foods. One of the key attributes of PVC that led to its widespread use, is its stability and flexibility, which is achieved by the incorporation of plasticizers. A plasticizer is a substance which when added to a material, usually a polymer, makes it flexible, resilient and easier to handle. There are more than 300 different types of plasticizers described. The most commonly plasticizers used in PVC are phthalates.

Phthalates, the diesters of phthalic acid, are a family of industrial compounds with a common chemical structure (Figure 44). They are widely used, since their introduction in 1930s, as plasticizers to soften PVC, in solvent, and as additives in many consumer products such as vinyl flooring, wall coverings, food containers, cosmetics^{158,159}. End-applications include adhesives and glues, electronics, agricultural adjuvants, building materials, personal-care products, medical devices, detergents and surfactants, packaging, children's toys, modeling clay, waxes, paints, printing inks and coatings, pharmaceuticals, food products, and textiles.

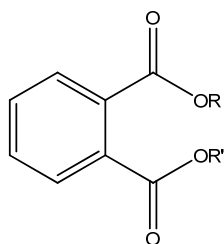


Figure 44. General chemical structure of phthalates

Phthalates are easily released into the environment because they are not chemically bond to the polymer, and leach from PVC items with time and use. As plastics age and break down, the release of phthalates accelerates. These compounds are released in the environment and persist for a long time, because of their stability, both in water as in air. For these reasons they are now considered ubiquitous contaminants and uptake of phthalates is possible for everyone.

Di-(2-ethylhexyl) phthalate (DEHP) was the most abundant phthalate among phthalate esters (Figure 45). It is a colorless viscous liquid, soluble in oil.

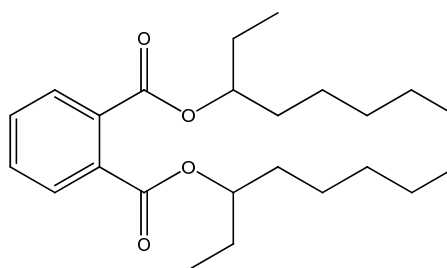


Figure 45. DEHP structure.

Thanks to its good plasticizing properties, DEHP-plasticized PVC have been used for a wide variety of applications including building products (insulation of cables and wires, tubes and profiles, flooring, wallpapers, out-door wall and roof covering, pastes vinyl flooring, wall coverings, food containers, cosmetics, medical products, and infant toys), clothing (footwear, outwear and rainwear), car products (e.g. car under-coating, car seats made of imitation leather). DEHP is also used in non-polymer materials such as lacquers and paints, adhesives, fillers and printing inks, etc

Importantly, DEHP has been used in medical devices since 1955. In fact, DEHP-plasticized PVC has specific properties that make it attractive, particularly in the health care setting including flexibility, strength, suitability for steam sterilization, resistance to kinking, optical clarity, weld ability, surface finish, and low cost.

DEHP softens PVC making tubes and catheters softer and more flexible. This can make medical devices easier to use, less likely to cause damage to tissue and more comfortable for the patient. Also, DEHP-plasticized PVC presents a good resistance to high temperatures, which are used for sterilization. Medical devices that may contain DEHP-plasticized PVC include: intravenous tubing and bags, catheters, nasogastric tubes, dialysis bags and tubing, blood bags and transfusion tubing, and air tubes.

In addition there are no safety data on most of the alternatives to DEHP-plasticized PVC. Unfortunately, in the last 20 years, a lot of concerns have grown over the safety of these nearly ubiquitous compounds, especially for developing fetuses and young children. For these reasons DEHP is no longer used in toys for children under the age of three in Europe (EU decision 1999/815/EG, renewed December 2005), as well as in US and Canada regarding toys intended for mouthing (nipples, teething rings, pacifiers, rattles). Very recently, the French National Assembly has required the ban of phthalates and parabens (Bill of law adopted by French National Assembly on May 3, 2011).

3.1.1 Metabolism of DEHP in humans

Phthalates can be inhaled, usually on dust particles from vinyl flooring or other surfaces containing phthalates, absorbed through the skin, usually through use of cosmetics and other body care products containing phthalates, swallowed, usually from plastic food containers or cling wraps that have leached phthalates into food or drink, or injected intravenously, usually through medical equipment. DEHP is extensively metabolized after all routes of uptake. Normally phthalate follow a metabolic pathway in at least two steps. In a first and fast step DEHP is hydrolyzed into the primary metabolite monoester, mono(2-ethylhexenyl) 1,2-benzenedicarboxylate, MEHP, in a process catalyzed by lipase¹⁶⁰ and esterase in the intestine and parenchyma^{161,162}. Pancreatic lipase is the most effective enzyme

hydrolyzing DEHP to MEHP in the gut, after oral ingestion. Normally this first step in the metabolism would be a detoxification, but *in vitro* and *in vivo* studies have shown that diesters phthalates become more bioactive when they are hydrolyzed to monoester phthalates and oxidized metabolites¹⁶³.

MEHP subsequently undergo several biotransformation in the liver and it is metabolized to produce a large number of oxidative metabolites^{164,165} (Figure 46).

Oxidative metabolism of MEHP starts with hydroxylation of the alkyl chain at various positions and the formation of primary (ω -oxidation) and secondary (ω -1 oxidation) alcohols. These hydroxylated products can undergo further oxidative reactions to the respective ketones and carboxylic acids. After that, the carboxylated alkyl chain can be subject to α - or β -oxidation to yield shorter carboxylated alkyl chains.

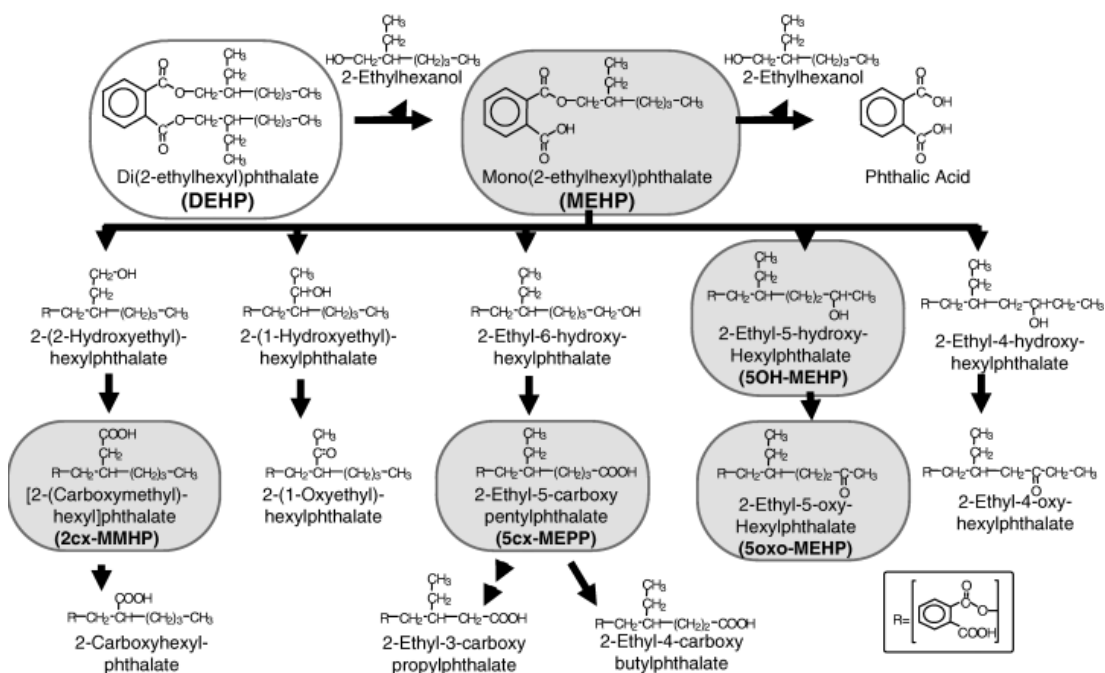


Figure 46. Metabolism of DEHP (Koch et al., *Int J Androl*, 2006, 29,155–165)

Finally the secondary metabolites are conjugated to glucuronic acid in a reaction catalyzed by 5'-diphosphoglucuronyl transferase, forming the glucuronide conjugates, that are easily excreted in urine and feces (Figure 47). The glucuronidation increases the solubility in water facilitating the excretion.

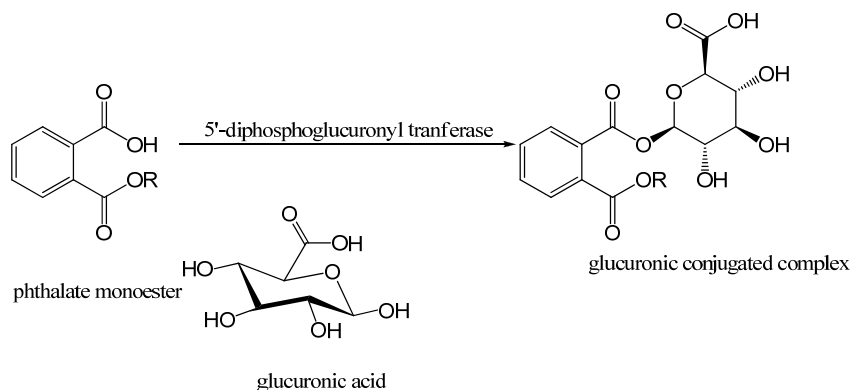


Figure 47. Glucuronidation of phthalate monoester

Urine contains the major concentrations of the oxidized secondary metabolites of DEHP: mono(2-ethyl-6-hydroxyhexyl) 1,2-benzenedicarboxylate (6-OH-MEHP), mono(2-ethyl-5-carboxypentyl) 1,2-benzenedicarboxylate (5-cx-MEHP), mono(2-ethyl-5-oxohexyl) 1,2-benzenedicarboxylate (5-oxo-MEHP), mono(2-ethyl-5-hydroxyhexyl) 1,2-benzenedicarboxylate (5-OH-MEHP). On the contrary, the primary metabolite MEHP is the minor metabolite detected in urine.

The long half-life of elimination makes secondary metabolites excellent parameters to reflect the DEHP exposure, and can reflect a chronic exposure to DEHP. Hypothetically, a different set of enzymes might lead to different elimination pattern of metabolites in some individuals and in some cases can be lead taking to bioaccumulation of metabolites in organism. In fact, phthalates are lipophilic compounds, and can survive in organism interfering with the endocrine system. The secondary metabolites have been recognized as much more reliable biomarkers for an assessment of the DEHP exposure. They are excreted to a higher extent than MEHP, and are more specific as they are not susceptible to contamination. By contrast, MEHP can be formed by hydrolysis of DEHP during sample handling and processing. It is also important to underline that about 60% of DEHP is excreted in humans as the metabolite-glucuronide conjugates. A reduced glucuronidation capacity could result in delayed excretion of DEHP metabolites. Polymorphisms have been also detected in several human UDP-glucuronyltransferase (UGT) genes resulting in variability in UGT activity and therefore also in the conjugation of DEHP metabolites, in the human population. As glucuronidation is a major process for the metabolism and removal of lipophilic chemicals, polymorphic variations in

genes encoding the UGT, may have a significant impact on our capacity to detoxify and eliminate these toxins¹⁶⁶.

3.2 Health effect

DEHP is only physically dispersed in PVC and can therefore easily migrate from PVC articles. Therefore DEHP can be present in air, dust, water, soils, sediments, and food and has become a ubiquitous environmental contaminant. Dietary DEHP exposure can result from bioaccumulation in foods, as well as from leaching during processing, packaging and storing. DEHP concentrations in a variety of foods have been detected because DEHP is highly lipophilic, thus fatty foods including dairy products, fish, meat and oils, contain great concentration of DEHP¹⁶⁷. For these reasons, the biological properties of the DEHP, have been the subject of a very substantial amount of research.

3.2.1 Endocrine disruptor (EDs)

Endocrine disruptors (EDs) are exogenous substances that can interfere with the normal function of the endocrine system by affecting the balanced system of glands and hormones that regulate vital body functions including growth, stress response, sex development, gender behavior, ability to reproduce, production and utilization of insulin, and metabolic rate. This effect could determine a dysregulation in normal development, behavior, fertility, and in the maintenance of normal homeostasis¹⁶⁸.

EDs can mimic hormones, or enhance or block the binding of hormones to their receptors, or otherwise lead to activating or inhibiting the endocrine signaling pathways and hormone metabolism. Research advances, based on experiments in animals, confirm that EDs can disrupt the gene-controlled, normal signaling systems that determine every aspect of fetal development.

Several studies suggested that prenatal exposure to certain phthalate, specially dibutyl phthalate (DBP) and DEHP resulted in altered sexual differentiation in male rats. DEHP, and its toxic metabolites, exert an adverse effect on the function of Leydig cells in the testis, decreasing androgen production and thus, increasing luteinizing hormone (LH) secretion from the pituitary, as it is released from the

negative feedback mechanism of testosterone¹⁶⁹. Animal exposed in utero to DEHP show reduced anogenital distance and nipple retention. Additionally effects observed include cryptorchidism, decreased testosterone levels, testicular atrophy, Sertoli cell (a testicular cell type specialized in providing nutrients to sperm-producing structures) abnormalities, decreased weight of the androgen-dependent organs, reduction in sperm production, and lower epididymal sperm counts^{170,171, 172,173}. In female offspring in utero and lactational exposure to high dose of DEHP results in delay of the time of puberty onset and ovarian polycystic¹⁷⁴.

3.2.2 PPAR-mediated activity of phthalates

A privileged mechanism for EDs interference with metabolic pathways is their direct or indirect activity on nuclear receptors. These receptors regulate the gene expression program according to the signals that they receive in the form of specific ligands, for example hormones or molecules that belong to metabolic pathways as substrates, intermediates or end-products. In particular, peroxisome-proliferator activated receptor (PPAR) has been shown to act as xenobiotic sensor, triggering adaptive transcriptional responses linked to xenobiotic metabolism that may also interfere with their response to endogenous metabolites.

PPARs are a group of nuclear receptor proteins that function as transcription factors regulating the expression of genes. Phthalate metabolites, and in particular MEHP, activate three different PPAR isotypes (PPAR α , β/δ , γ), (Figure 48)¹⁷⁵.

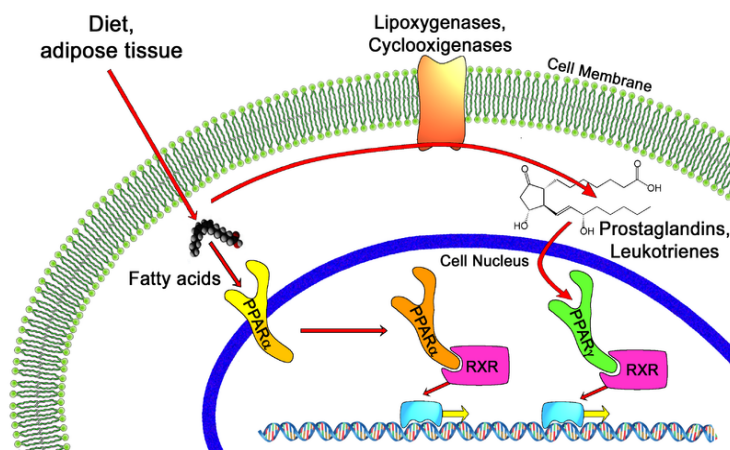


Figure 48. PPAR -alpha and -gamma pathways.

Most of the identified PPAR target genes are involved in various aspects of lipid metabolism and energy homeostasis, reflecting the importance of these receptors in vertebrate physiology. The best characterized functions of PPARs include the roles of PPAR α and PPAR β/δ in hepatic and muscle fatty acid catabolism, and the opposite but complementary role of PPAR γ in adipogenesis and lipid storage. These functions are crucial for the maintenance of the energy balance in adult animals. In particular, PPAR γ is crucial for white adipose tissue development and adipogenesis in general. Therefore, its ability to bind some EDs might contribute to fat accumulation in mature adipocytes upon exposure to the compounds and metabolic consequences of human phthalate exposure result from the possible activation of the three PPARs.

In the recent years questions and concerns have focused on metabolic disorders caused by EDs. Strikingly, the increased rate of metabolic diseases correlates with severe changes in the chemical environment. This has led to the hypothesis that some of the numerous environmental pollutants could interfere with various aspects of metabolism. Urinary concentrations of phthalate metabolites were correlated with abdominal obesity, waist size and with the cellular resistance to insulin, a precursor to Type II diabetes. Moreover prenatal phthalate exposure was related to low birth weight in infants¹⁷⁶. Low birth weight is the leading cause of death in children under 5 years of age and increases the risk of cardiovascular and metabolic disease in adulthood.

Recently signal transduction pathway of α -PPAR was also correlated to progression of neurodegenerative and psychiatric diseases. In fact, the activation of α -PPAR, by phthalates interferes with cellular proliferation and lipid metabolism, also in the brain¹⁷⁷. Moreover, the peroxisome proliferation, mediated by PPAR, leads to oxidative stress and generation of electrophilic free radicals. A link between oxidative brain damage and neurodevelopmental disorders, such as Autism in children, was observed in the last years^{178, 179}. In 2009, South Korean scientists reported findings of a statistically-significant correlation between urine phthalate concentrations in children and symptoms of attention-deficit/hyperactivity disorder (ADHD)¹⁸⁰. Although more research is needed in order to conclusively determine the

relationship between phthalate and ADHD, the article suggests that consumers should be aware of its potential effects on behavior and neurological disorders.

3.2.3 Alteration of Thyroid Hormone Levels

A normal thyroid function is essential for fetal development of the brain, neurons, heart and other organs during critical points of gestation¹⁸¹. Some environmental toxicants, such as perchlorate, polychlorinated biphenyls (PCBs), inorganic mercury, and phthalates potentially alter human thyroid function during pregnancy by inhibiting iodide transport, thyroglobulin iodination, or competitively inhibiting thyroid hormone binding receptors¹⁸². Beside being essential for normal brain development, thyroid hormones play an important role in many physiologic system, and alterations in thyroid hormone levels can lead to a myriad of adverse clinical conditions. The prevalence of subclinical hypothyroidism is 2–5% in pregnant women. Maternal hypothyroidism during pregnancy causes preterm birth and low birth weight, and it impairs post-natal mental development in infants^{183,184}.

Phthalates have thyroid-disrupting properties interfering with the thyroid hormone system inducing altered thyroid activity. Although much is still unknown about mechanism and consequences involved with the relationship between environmental exposures and change in thyroid hormone levels, phthalates and other environmental chemicals may bind to thyroid receptors and influence the thyroid hormone signaling. In particular phthalates are associated to a decreases in serum total thyroxine (T4) and triiodothyronine (T3) concentrations, leading to hypothyroidism¹⁸⁵. Deficiency of thyroid hormones during critical periods of brain development, both in utero and in early postpartum period is a well-recognized cause of brain damage. Recent studies correlated hypothyroxinemia to permanent alteration of the cerebral cortical architecture, decreased intellectual capacity, mental retardation, and neurological diseases. Transient intrauterine deficits of thyroid hormones (THs) have been shown to result in permanent alterations of cerebral cortex similar to those found in brains of children with autism¹⁸⁶. As a consequence, the current surge of this disease could be related to transient maternal hypothyroxinemia resulting from exposure to antithyroid environmental contaminants.

3.2.4 Exposure to DEHP in fetuses and infants

Exposure of the developing fetus or infant to endocrine-disrupting chemicals is of particular concern¹⁸⁷. Infants are believed to be the most sensitive population, as they are exposed since early in life to several different sources, including breast milk, infant formula, baby food, indoor air, and by dermal and oral exposure via indoor dust containing DEHP. The developing fetus and neonate are particularly sensitive to perturbation by endocrine disrupting chemicals because they are exposed during critical periods of human development^{188,189,190}. EDs may also be transferred from mother to developing fetus crossing the placenta, or as neonates incorporating them through breastfeeding^{191,192}. Moreover, the placenta does not completely protect the unborn fetus from its external environment and the organism undergoes periods of extremely rapid cell division and differentiation thus resulting in cells that can differentiate abnormally and pass altered programming to subsequent generations. In many cases, the damage that occurs prenatally is irreversible, while adult exposure is usually reversible. The developing organism lacks the protective mechanisms that are available to the adult such as DNA repair mechanisms, a fully competent immune system, detoxifying enzymes, liver metabolism, and has an immature blood/ brain barrier¹⁹³. Also, the developing fetus and neonate have increased rates of lipase activity and/or decreased rates of glucuronidation activity as compared to adults, which in some cases may make them more vulnerable to chemical toxicity, resulting in a possible bioaccumulation of DEHP metabolites in their body.

Exposure to environmental chemicals during development can interfere with complex differentiating endocrine signaling pathways and cause adverse consequences later in life. In general, neonates receive higher doses, in terms of body / weight, of DEHP than the general population and their daily dose to DEHP may increase up to 20 folds the tolerable daily intake.

Moreover, in cases of intensive therapy procedures, neonates can have higher exposure to phthalates and to their toxic monoesters supposed to be EDs. Medical devices and tubing may contain 20-40% DEHP by weight, which easily leach out of tubing when heated (as with warm saline/blood).

The combination of prenatal and postnatal exposures may exacerbate the reproductive hazard. Therefore a concern was raised about potential health effects of DEHP. Specifically, EDs are known to cause learning disabilities, severe attention

deficit disorder, cognitive and brain development problems, deformations of the body (including limbs); sexual development problems, feminizing of males or masculine effects on females, metabolic diseases etc. In fact, any system in the body controlled by hormones, can be derailed by hormone disruptors. These disruptions can cause different diseases such as cancerous tumors, birth defects, and other developmental disorders.

3.3 Detection of DEHP metabolites in urine

Aim of this part of PhD study was to evaluate the levels of the primary and secondary metabolites of DEHP in two different populations. To one side we studied the urinary concentration of DEHP metabolites in children obese and/or affected by metabolic syndrome. This study was in collaboration with professor Bernasconi “Centro Turbe dell’Accrescimento, Clinica Pediatrica Azienda Ospedaliero-Universitaria di Parma”, and with professor M. Street, Department of Pediatrics University Hospital of Parma. The study was aimed to evaluate a possible correlation between urinary concentrations of phthalates, obesity and insulin sensitivity in obese children.

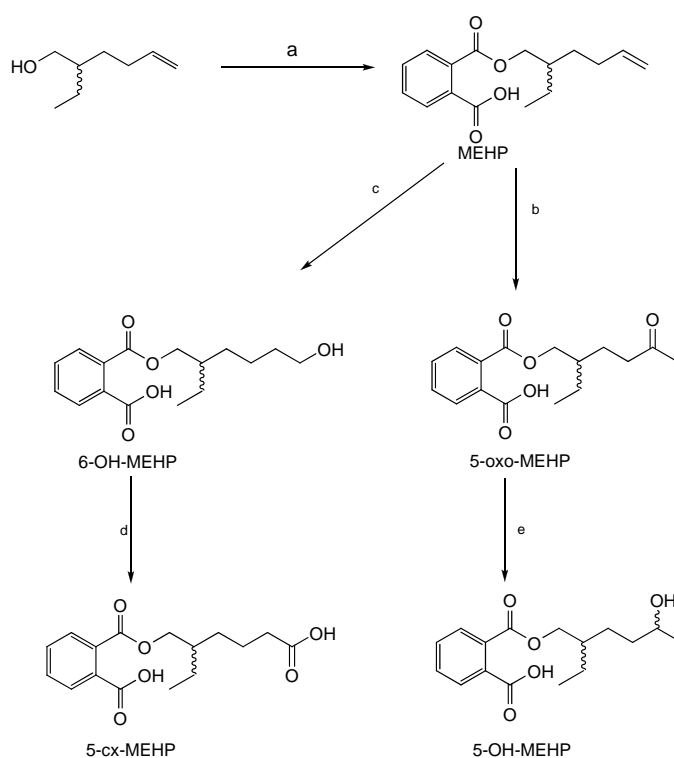
On the other hand, we evaluate the levels of the primary and secondary metabolites of DEHP in autistic children. This work was in collaboration with professor J. Hayek, Child Neuropsychiatry Unit, University Hospital AOUS of Siena, and C. de Felice, Neonatal Intensive Care Unit, University Hospital AOUS of Siena.

Urine concentrations of secondary metabolites derived from DEHP were measured in triplicate applying an HPLC-ESI-MS method. The metabolites measured included: MEHP, 6-OHMEHP, 5-oxo-MEHP, 5-OH-MEHP and 5-cx-MEHP. The unequivocally characterized synthetic metabolites were used as pure analytical standards (>98% purity) for quantitative determination in urines from obese or autistic children and healthy controls.

3.4 Synthesis of DEHP metabolites

Five DEHP metabolites, MEHP, 6-OHMEHP, 5-oxo-MEHP, 5-OH-MEHP and 5-cx-MEHP, were synthesized in the Laboratory of Peptide & Protein Chemistry & Biology (PeptLab) following the procedure previously described¹⁹⁴.

The primary metabolite MEHP was used as starting material to achieve four oxidative metabolites of DEHP (Scheme 5).



Scheme 7. Reagents and conditions: (a) phthalic anhydride, pyridine (Py), under N₂; (b) PdCl₂, quinone in DMF/H₂O (7:1); (c) 1 M B₂H₆ in THF, then H₂O₂, OH⁻ in THF; (d) CrO₃, H₂SO₄ in acetone; (e) NaBH₄ in EtOH.

All the products were purified by Flash Column Chromatography, and were obtained in good yield, with chemical purity >98%. DEHP metabolites were characterized by ¹H, ¹³C NMR and RP-UPLC (Table 8).

Table 10. characterized of DEHP metabolites by RP-UPLC.

metabolites	Rt (min)*	[M+H] ⁺
MEHP	3.54	277.3
5-oxo-MEHP	2.86	291.3
5-cx-MEPP	2.81	309.3
5-OH-MEHP	2.82	295.3
6-OH-MEHP	2.84	295.3

*solvent system: A 0,1% TFA in H₂O; B 0,1% TFA in CH₃CN.
Gradient 50 to 100 % of CH₃CN in 5 min, flow 0,6 ml/min.

3.5 Quantitative analysis

Before analysis all the materials used during the entire process were pre-screened by HPLC-ESI-MS to verify the absence of external contamination. In particular, all the solvents (e.g., acetonitrile, water, buffers, etc.), laboratory equipments (polypropylene vials containing urines, solvent bottles, SPE cartridge, teflon capped-glass bottles, pipettes), and instrumentation used during the entire validated, sensitive, and selective HPLC-ESI-MS analytical process, were verified to be DEHP-metabolites free. To this end, we applied the same HPLC-ESI-MS method reported for phthalates detection in urines, to solutions that have been contained in the equipments used. No DEHP- metabolites could be detected in any of the above mentioned material even after two week storage. The internal standards were prepared in ACN and were used as reported in literature^{195,196}.

Calibration curves

The unequivocally characterized synthetic metabolites, MEHP, 6-OH-MEHP, 5-cx-MEPP, 5-oxo-MEHP, 5-OH-MEHP, were used as pure analytical standards (>98%) for quantitative determination in human urines. The standard calibration curves were constructed using working standards solutions of DEHP metabolites, ranging from 0.00025 to 2.5µg/mL. A linear regression analysis was carried out by plotting the peak area (y) against the concentration (x) for each analyte. The linearity of the calibration curve was expressed by the correlation coefficients (r^2). The lower limit of detection (LLOD) is defined as the lowest concentration of analyte in a sample

that can be detected, but not necessarily quantified, under the stated experimental conditions. It can be calculated from the standard deviation (SD) of the response and the slope associated with the calibration curve¹⁹⁷, according to the equation:

$$\text{LLOD} = \frac{\text{SD} \times 3.3}{\text{slope}}$$

The lower limit of quantification (LLOQ), similarly defined, quantifies the lowest concentration of analyte that can be determined with acceptable precision and accuracy under the stated experimental conditions. It can be calculated from the standard deviation of the response and the slope associated with the calibration curve, according to the following equation:

$$\text{LLOQ} = \frac{\text{SD} \times 10}{\text{slope}}$$

In urines, LLOQs were 0.042 µg/L [MEHP], 0.048 µg/L [5-OH-MEHP], 0.049 µg/L [5-oxo-MEHP], 0.047 µg/L [5-cx-MEHP], and 0.008 µg/L [6-OH-MEHP]. In urine, LLODs were 0.014 µg/L [MEHP], 0.016 µg/L [5-OH-MEHP], 0.016 µg/L [5-oxo-MEHP], 0.018 µg/L [5-cx-MEHP], and 0.002 µg/L [6-OH-MEHP].

Instrumental and chromatographic conditions

The HPLC-ESI-MS analysis was carried out using an high-performance liquid chromatography tandem mass spectrometry RP-HPLC-ESI-MS (Waters, Alliance 2695, Waters, Micromass ZQ) equipped with phenyl column (Betasil, 5 µm, 50 mm x 3 mm, Keystone Scientific, Bellefonte, PA) and with a Waters 2996 Photodiode Array Detector. An aliquot of each sample (20 µL) was injected into the apparatus. All standards were injected three times in the same day. Curves with correlation coefficients (R^2) greater than 0.998 were generated (MEHP, 5-OH-MEHP, 5-oxo-MEHP 0.999; 6-OH-MEHP, 5-cx-MEHP 0.998). The chromatographic separations of metabolites were resolved using a linear gradient from 3% to 60 % B in 10 min (solvent system A: 0.1% acetic acid in water; B: 0.1% acetic acid in ACN). The flow rate was 0.6 mL/min. The column temperature was 32 °C. A guard column (XBridgeTm Phenyl 3.5µm, 3.0x20 mm) was used to prevent column degradation.

Column eluates were monitored at 215, 230 and 254 nm. The mass specific detection was achieved using a Waters, Micromass ZQ Electrospray ionization (ESI) in positive ion mode. The product ion with higher signal intensity was selected for the quantitative analysis for each of the four phthalates. The optimal MS parameters were as follows: the source and desolvation temperature were 120 °C and 400 °C respectively; the capillary voltage was 3.24 kV; cone voltage 30 kV, nitrogen gas was used as desolvation gas and as cone gas as well; the cone gas and the desolvation flow was 60 L/h and 800 L/h respectively; The collision gas was argon with a flow of 0.60 ml/min. Data were acquired and processed using MassLynx™ software (Waters). The analytical methodology adapted for measuring MEHP and secondary oxidative metabolites in urine was already described in the literature^{196,198 199}.

One water reagent blank and one quality-control (QC) sample, were processed through the entire process along with unknown urine sample, and were included in each batch of samples to monitor for contamination. The QC sample was spiked with pooled urine and DEHP metabolites standards in known concentration (200 ng/mL). When urine analysis resulted in values of metabolites concentration exceeding from linear range of the analytical method, we subjected a new aliquot of the same sample to the entire process (deconjugation and SPE) and we analysed again.

A known standard was also injected into the entire sample set in order to confirm chromatographic resolution. The identification of the peak was confirmed by matching retention times of the unknown sample, with the standard.

Sample pre-treatment

First morning urine specimens were collected. All the samples were subjected to two steps of Solid Phase Extraction (SPE) before RP-HPLC-ESI-MS analysis, in order to remove components from biological matrix that could interfere with the analysis. For SPE treatment of urine, we prepared the following buffers: buffer ammonium acetate 1 M pH 6.5; acid buffer pH 2.0 by preparing a solution of NaH₂PO₄ (0.14 M) and 1% of 85% H₃PO₄; basic buffer was prepared by adding concentrated ammonium hydroxide (1 mL 30% NH₃ solution) to a 50:50 acetonitrile/water (200 mL). All buffers were stored in sealed bottles at room temperature: basic buffer was discarded after one week, acid buffer after one month.

Human urines (1 mL) were defrosted, sonicated, mixed, and dispensed in glass tubes. Then buffer ammonium acetate (250 μ L, pH 6.5) was added. Incubation with β -glucuronidase (5 μ L, 200units/mL, Roche Biochemical, Mannheim, Germany) was performed at 37 °C for 90 min, resulting in quantitative glucuronide hydrolysis of phthalates metabolites. *Escherichia coli* K12 β -glucuronidase has excellent glucuronidase activity and no measurable lipase activity on phthalate diesters^{195,196}. After deconjugation, samples were treated with two steps of solid phase extraction (SPE), in order to remove contamination of biological matrix (Figure 49). A first cartridge was used to retain hydrophobic compounds while the phthalate metabolites were eluted. A second cartridge was helpful to remove residual salts. Analytes were finally eluted with acetonitrile and ethyl acetate, concentrated, re-suspended in water and transferred into vials. All the samples were analysed by RP-HPLC-ESI-MS.

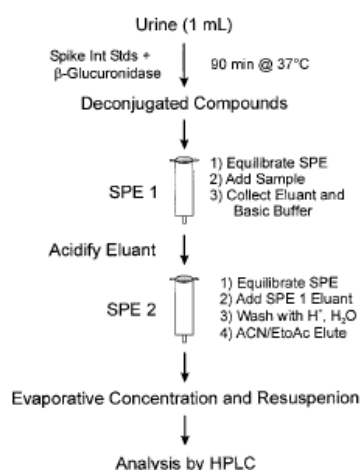


Figure 49. SPE procedure

The recovery of the extraction procedure was determined by comparing the peak-area of the DEHP metabolites after extraction of spiked urine, with the response of respective standard solutions. The extraction efficiencies were evaluated by averaging the results of three replicate measures at three concentration levels (0.25, 1.0 and 2.5 μ g/mL). These data together with the corresponding precision, as quantified by the percentage relative standard deviation (%RSD), are reported in Table 9. These data demonstrate that the solid phase extraction protocol provides the

almost quantitative recovery of all the analytes from urine sample. Moreover, this method exhibits a quite good repeatability (%RSD less than 7%).

Table 11. Efficiency of the solid phase extraction procedure of 5-OH-MEHP, 6-OH-MEHP, MEHP, 5-cx-MEHP, 5-oxo MEHP from human urine spiked samples.

concentration added $\mu\text{g/mL}$	5-OH-MEHP % Recovery mean \pm RSD	6-OH-MEHP %Recovery mean \pm RSD	MEHP %Recovery mean \pm RSD	5-cx-MEHP %Recovery mean \pm RSD	5-oxo-MEHP %Recovery mean \pm RSD
2,50	95.2 \pm 4.5	96.6 \pm 5.2	96.1 \pm 6.2	96.0 \pm 5.3	94.9 \pm 4.3
1,00	97.4 \pm 3.9	97.8 \pm 6.4	98.8 \pm 6.3	96.8 \pm 7.1	97.8 \pm 6.6
0,25	97.6 \pm 3.8	98.1 \pm 5.8	94.1 \pm 6.1	98.1 \pm 4.1	97.1 \pm 4.8

n = 3; RSD = relative standard deviation (%).

The data were corrected for creatinine. All specimens displayed urinary creatinine in the children reference value range, dependent on age and lean body mass (0.5-4.0 mg/Kg/24 h). For creatinine measurement, we used a Beckman Synchron AS/ASTRA clinical analyzer (Beckman Instruments, Inc., Brea, CA). We used value (micrograms per liter)/creatinine (grams per liter) for dilution correction in the analyses.

3.6 Relationships between urinary concentrations of DEHP metabolites, obesity and insulin sensitivity in obese children

3.6.1 Obesity

Obesity is a medical condition characterized by a pathological excess of body fat, that it may have an adverse effect on health, leading to reduced life expectancy and/or increased health problems. Obesity is a complex disease, affecting virtually all ages, races, sexes, and socioeconomic groups, with serious social and psychological repercussions. Further, obesity and overweight are major contributors to the global burden of chronic diseases and are associated with Type 2 diabetes, hyperinsulinemia, insulin resistance, coronary heart disease, high blood pressure, stroke, gout, liver disease, asthma and pulmonary problems, gall bladder disease, kidney disease, reproductive problems, osteoarthritis, and some forms of cancer. Frequently,

many of these illnesses are being reported in children who are overweight or obese, whereas in the past these diseases were only seen in older individuals.

Body mass index (BMI), a measurement which compares weight and height, defines people as overweight (pre-obese) if their BMI is between 25 and 30 kg/m², and obese when it is greater than 30 kg/m².

Obesity is a leading preventable cause of death worldwide, with increasing prevalence in adults and children, and authorities view it as one of the most serious public health problems of the 21st century. In fact, over the last 2 to 3 decades, the prevalence of obesity has risen dramatically in wealthy industrialized countries, and also in poorer underdeveloped nations where it often coexists with under-nutrition²⁰⁰. In the United States, the Center for Disease Control (CDC) reported in 2008 that obesity has reached epidemic proportions with more than 60% of U.S. adults being either obese or overweight²⁰¹. Similar statistics have been reported for many European countries, the Middle East, Australia, and China.

The reasons for this sharp increase in overweight/obesity are not well understood but factors such as diets, genetics/epigenetics, higher maternal age, use of certain pharmaceuticals, pollution, and the exposition to endocrine disruptors have all been proposed as playing a role.

3.6.2 Causes

Obesity is most likely caused by a complicated interaction between genetic, behavioral, and environmental factors. However, the most common causes are thought to be overeating high calorie fatty diets combined with a sedentary lifestyle, which is imposed on a background of genetic predisposition for the disease. Although much interest has centered on these factors, the exact etiology of obesity is unknown. Some studies report a link between some persistent organic pollutants, such as phthalates, bisphenol A, heavy metals and polychlorobiphenyl, and increased body weight and diabetes²⁰². In a cross-sectional study, concentrations of urinary phthalates metabolites were associated with increased waist circumference and insulin resistance in adult males in the United States¹⁷⁶. This epidemiological study suggest that environmental exposures to various endocrine disrupting chemicals, plays a role in overweight /obesity and in the complications associated with these

diseases, such as diabetes. Recently, the adipocytes were proposed as a new target of EDs²⁰³. Environmental chemicals, such as DEHP, have a disrupting activity on normal adipocyte development as well as on homeostatic control of adipogenesis and early energy balance. These chemicals have been termed “obesogens” based on the idea that they desregulate the lipid metabolism and adipogenesis, promoting obesity. Transgeneration effects may also be seen following exposure to endocrine disrupting chemicals during development, not only to the exposed individual but also to subsequent generations. This would imply that the mechanisms of transmission occur through the germ line and they may involve genetic and/or epigenetic events. In the case of epigenetic changes, effects are not due to a genetic impairment but to a modification of factors that regulate gene expression, such as DNA methylation and histone acetylation²⁰⁴.

3.6.3 Mechanism of action

The exact mechanisms that may induce phthalates to cause obesity are not known, but it may involve a great variety of pathways.

For example, EDs exert their effects altering thyroid function metabolism and/or energy homeostasis. However, the most commonly proposed mechanism involves direct binding to α/γ PPAR. EDs could also act indirectly inhibiting enzymatic activity of P450 family members, CYP19 and CYP3A1, which convert testosterone to estradiol, or by activating expression of the P450 enzymes, thus altering hormone levels. Finally, another mechanism that has been proposed is altering the neuronal synapse formation,²⁰⁵ which could affect release of brain-produced substances that bind to nuclear receptors and may affect energy regulation. An additional complexity is that these proposed mechanisms may be interacting with each other. The altered signal or tissue may involve adipocytes, brain, liver, stomach, pancreas, etc. Identifying the mechanisms whereby EDs influence weight homeostasis and energy balance is an important area of future research.

3.7 Detection of DEHP metabolites in obese children

Data suggest that endocrine-disrupting chemicals, as phthalates, found in a variety of household products, may influence mechanisms related to obesity. In vitro studies have shown that these chemicals may interact with PPARs and play a key role in the differentiation of adipocytes and deposition of triglycerides in adipose tissue.

Therefore, in this study we focused on the evaluation of a possible association between urinary phthalate metabolites and age, gender, pubertal development, age at onset of obesity, BMI, waist circumference, indexes of insulin sensitivity, and metabolic syndrome in obese children.

For the study, 42 obese patients and 39 healthy controls were recruited from the staff of “*Centro Turbe dell’Accrescimento della Clinica Pediatrica*” Azienda Ospedaliero-Universitaria di Parma. Urine was collected early in the morning. All the subject enrolled for the study were classified according to sex, age, BMI, chronological age onset of obesity, birth weight, etc. The auxological parameters were reported in Table 10.

Table 12. Auxological parameters of obese patients and controls

Parameter	Obese (mean ± SEM)	Controls (mean± SEM)
Number	42	39
Males/Females	20/19	23/16
Prepubertal/Pubertal	9/30	10/29
Chronological age	12,23 ± 0,45	12,52± 0,63
Height SDS	0,94 ± 0,17	-0,78± 0,26
Genetic target SDS	-0,17 ± 0,16	
BMI SDS Cole	3,34 ± 0,06	1,74± 0,21
Waist circumference	106,8 ± 2,72	
Waist circumference/ height ratio	0,68 ± 0,01	
Chronological age onset of obesity	4,7 ± 0,5	NO
Birth weight	3,4 ± 0,09	3,09± 0,11

All the patients and healthy controls were subjected to the oral glucose tolerance test (OGTT). Before the test glycemia, insulin, triglycerides, total cholesterol and High-

density lipoprotein (HDL) were measured. The following insulin indices were evaluated for all the subjects: fasting glucose/ insulin ratio (FGIR), insulinogenic index²⁰⁶, homeostasis model assessment estimate of insulin resistance (HOMA-IR)²⁰⁷, quantitative insulin sensitivity check index (QUICKI)²⁰⁸. Basing on HOMA index, the subjects were classified in insulin/ non-insulin resistance. Further on, the obese subjects were classified in normal glucose tolerance (NGT) or impaired glucose tolerance (IGT), on the base of OGTT.

Moreover, whole body insulin sensitivity index (WBISI), areas under the curve of glucose (AUCG) and insulin (AUCI) were calculated from a five-point OGTT. The data are shown in Table 11.

Table 13. Biochemical data, and fasting indices of insulin-resistance and calculated from the OGTT

Parameter	Obese (mean± SEM)	Controls (mean± SEM)
Insulin	15,53 ± 2,02	13,03± 1,29
Glucose	81,97 ± 1,07	81,63± 0,82
FGIR	7,42 ± 0,67*	16,34±3,36
HOMA-IR	3,16 ± 0,4 *	2,04±0,26
QUICKI	0,34 ± 0,01	//
Insulinogenic Index	0,19 ± 0,03	0,12±0,01
WBISI	3,57 ± 0,28	//
AUCG	238,98 ± 5,39	//
AUCI	228,44 ± 18,58	//

The metabolic syndrome diagnosis was performed on the base of the Global international diabetes federation criteria²⁰⁹.

Urine concentrations of DEHP metabolites, MEHP, 6-OH-MEHP, 5-OH-MEHP, 5-oxo-MEHP, 5-cx-MEHP, were measured in triplicate using the RP-HPLC-ESI-MS method described above. In urine from obese children we found detectable levels of MEHP, 5-OH-MEHP, 6-OH-MEHP, 5-oxo-MEHP and 5-cx-MEHP in 77%, 85%, 90%, 99%, and 85% of patients respectively. In urine from healthy controls we found detectable levels of MEHP, 5-OH-MEHP, 6-OH-MEHP, 5-oxo-MEHP and 5-cx-MEHP in 90%, 74%, 64%, 63%, and 51% respectively. Significant concentrations of

5-OH-MEHP and 5-oxo-MEHP were detected in obese patients, compared with healthy controls (Table 12).

Table 14. Concentrations of DEHP metabolites in non-insulin resistant and insulin-resistant obese patients compared to healthy controls ($\mu\text{g/ml}$)

Metabolites	Non insulin-resistant	insulin-resistant	Controls
MEHP	0.08[0.00-0.23]	0.14[0.00-0.36]	0.06[0.13-0.16]
5-cx-MEHP	0.55[0.07-1.15]	0.45[0.25-1.11]	-
5-OH-MEHP	0.38[0.17-2.05]	0.73[0.00-1.52]	0.18[0.03-0.69]*
5-oxo-MEHP	0.32[0.15-0.72]	0.24[0.05-0.55]	0.18[0.26-0.51]*
6-OH-MEHP	0.67[0.40-1.36]	0.82[0.27-0.88]	0.36[0.00-0.81]

. * $p < 0.05$ versus all obese subjects

The data were analyzed applying an innovative statistical methods based on Artificial Neural Networks (ANNs) and principal component analysis and connectivity map^{210,211}. This new mapping method, aimed to understand the natural processes and recreate those processes using automatic models, is particularly useful to understand the relationships between variables, especially in non-linear relationships.

The method is based on an artificial adaptive system able to define the strength of the associations of each variable with all the others in any dataset, the Auto Contractive Map (AutoCM). After the training phase, the weights matrix of the AutoCM represents the warped landscape of the dataset. We apply a simple filter to the weights matrix of AutoCM system to show the map of the main connections between the variables. Applying AutoCM we are able to obtain a subsequent semantic map of actual relationship between variables.

3.8 Results

A negative correlation of MEHP with the age at onset of obesity was shown ($r: -0,4$; $p: 0,03$; Figure 50A). A negative correlation was also found between MEHP and AUCI ($r: -0,35$; $p: 0,04$; Figure 50B), and between MEHP and AUCG ($r: -0,33$; $p: 0,05$; Figure 50C). On the contrary a positive correlation was observed between MEHP and WBISI ($r: 0,33$; $p: 0,05$; Figure 50D). 5-oxo-MEHP instead was significantly correlated with the age at onset of obesity ($R: +0.51$).

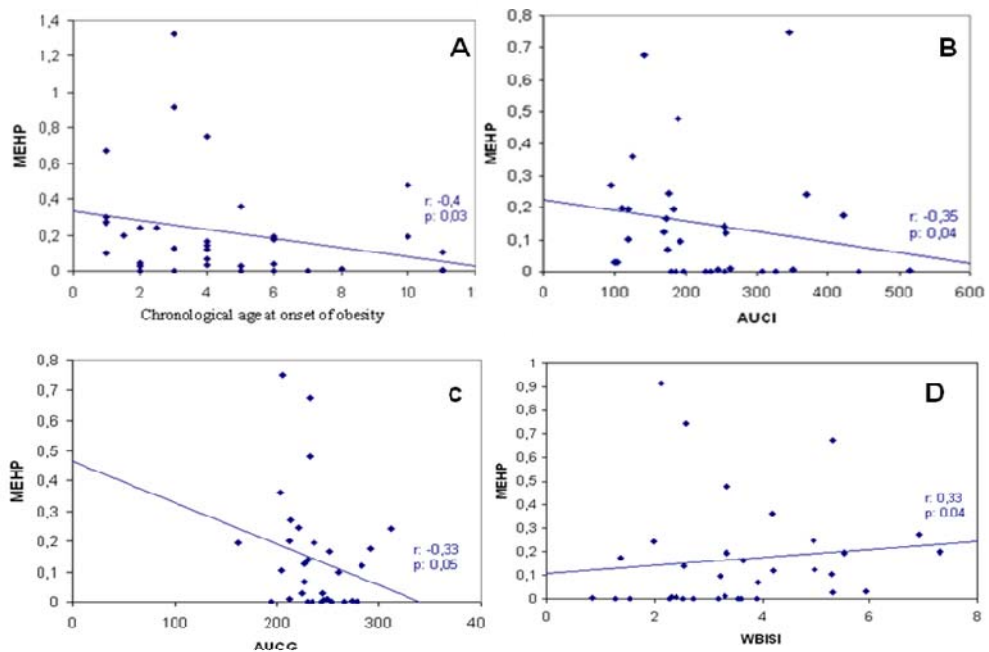


Figure 50. **A:** Relationship between MEHP and Chronological age at onset of obesity; **B:** Relationship between MEHP and AUCI; **C:** Relationship between MEHP and AUCC; **D:** Relationship between MEHP and WBISI

The connectivity map showed a direct relationship of 5-oxo-MEHP with BMI SDS (Figure 51). MEHP showed a direct relationship with the insulinogenic index, and normal insulin sensitivity. The sum of the metabolites showed a direct relationship with the height SDS (Figure 51) suggesting that height may be related with the ability to metabolize phthalates. This latter was directly related with 5-oxo-MEHP. Interestingly, 5-OH-MEHP was directly connected with the HOMA index and abnormal insulin sensitivity.

In conclusion, the results supported the hypothesis that the higher metabolites in urine, the earlier the onset of obesity, and suggested that some DEHP metabolites are capable of influencing insulin sensitivity. However, the less phthalates were metabolized (higher MEHP urine concentrations) the later was the onset of obesity. It remains, thus, to be elucidated whether exposure to phthalates *per se* is actually the risk factor or if the ability of the body to metabolize phthalates is actually the key point. This could explain also the positive relationship of MEHP with WBISI.

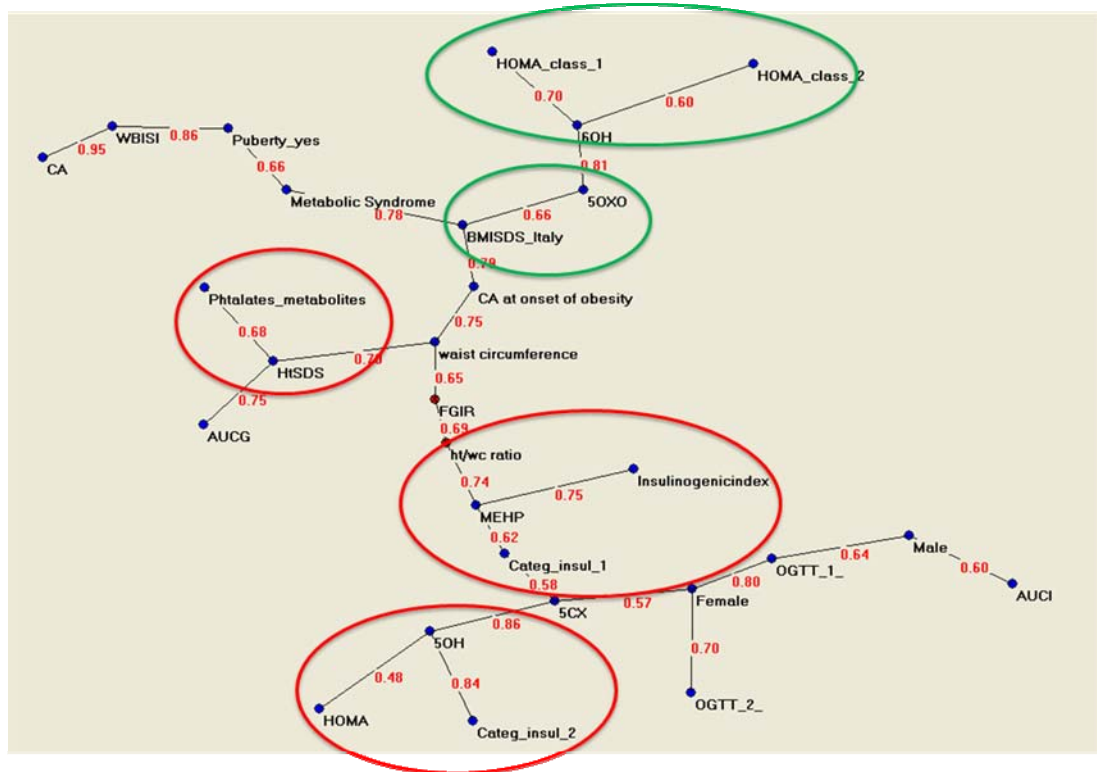


Figure 51. Connectivity map

3.9 Association between urinary excretion of di(2-ethylhexyl)phthalate secondary metabolites and autism spectrum disorders in children

3.9.1 Autism spectrum disorders

Autism spectrum disorders (ASDs), also known as pervasive developmental disorders (PDDs), are a group of complex neurodevelopment disorders, characterized by social impairments, communication difficulties, and restricted, repetitive, and stereotyped patterns of behavior. ASD is a severe neurodevelopmental disorder, with a great cost for society as well as for patients and their families. ASDs refer to five disorders characterized by delay in the development of multiple basic functions:

- **Classic autism** affects information processing in the brain by altering how nerve cells and their synapses connect and organize. Classic autism is characterized by widespread abnormalities of social interactions and communication, and severely restricted interests and highly repetitive behavior.
- The hyper functional form known as **Asperger syndrome**, that is characterized by significant difficulties in social interaction, alongside restricted and repetitive patterns of behavior and interests. Unlike with autism, people with Asperger syndrome have no substantial delay in language development.
- The rare genetic condition known as **Rett syndrome**²¹². Rett syndrome is a neurodevelopmental disorder of the grey matter of the brain that almost exclusively affects females. It is caused by mutations in the gene MECP2 located on the X chromosome.
- **The childhood disintegrative disorder**, that is a rare (1.7 cases per 100,000) condition characterized by late onset (>3 years of age) of developmental delays in language, social function, and motor skills.
- The **pervasive developmental disorder not otherwise specified (PDD-NOS)**. PDD-NOS is often referred to as atypical autism.

The manifestations of ASDs cover a wide spectrum, ranging from individuals with severe impairments, who may be silent, mentally disabled, and locked into hand flapping and rocking, to high functioning individuals who may have active but distinctly odd social approaches, narrowly focused interests, and verbose, pedantic communication. The most widely used diagnostic criteria for ASDs are those

described in the text of diagnostic and statistical manual of mental disorders (DSM-IV-TR) of the American Psychiatric Association²¹³. Those criteria involve qualitative impairment of reciprocal social interaction, marked impairment in the development of communication and severely restricted stereotyped and repetitive patterns of behaviors. Most individuals with ASDs have significant lifelong impairments in social and language functioning, and only a small percentage of individuals with ASDs are able to live and work independently as adults.

3.9.2 Etiology of ASDs

ASDs etiology is unknown, but it is believed to result from disruption of normal neurobiological mechanisms primarily in the prenatal period²¹⁴. Moreover, it is widely recognized that ASD might have a genetic component²¹⁵. Nevertheless no more than 5% of all autism cases appear to be due primarily to a genetic disorder. In particular, on a total of about 2,000 autism cases in the last 10 years, about 1% can be attributed to X-fragile syndrome, about 2% to gene microdeletions, about 1% to tuberous sclerosis, 1.5/1000 (0.15%) to phenylketonuria (PKU) or other genetic-metabolic inborn errors of metabolism, about 3/1000 (0.3%) to Down syndrome with autistic features, that all summed up is about a 4.45% fraction of all autism cases observed in a relatively large series. On the other hand, it is difficult to truly ascertain the sub-prevalence of Rett syndrome among the ASDs. However it is well known that the world frequency is of one Rett syndrome case in 8,000 to 10,000 females, that is about 1 case in 16,000 to 20,000 in the general population.

A dramatic increase in frequency of children with ASDs has been reported during the last 10 years. Nevertheless, it is difficult to determine how much of this increase may be due to actual increase in the incidence or to increased awareness and diagnosis.

This data suggest that environmental causes, such as exposure to chemicals such as heavy metals, pesticides, phthalates or childhood vaccines, etc., could play a significant role in the etiology of ASDs.

Consequently, the focus of autism research is shifting from purely genetic influences to multifactorial diseases in which complex set of genes should be associated to relevant environmental factors^{216,217}. Moreover, recent studies describe a number of gene-environment interactions in which, exposure to a pre- or post-natal

environmental pathogen, causes a behavioral disorder only if an exposed individual carries a specific genetic predisposition²¹⁸.

Prenatal exposure to stressful events was found to have significant effects on postnatal behavior and was also associated with increased risk of ASD.

In fact, prenatal stress can reduce uterine and placental circulation, inducing fetal hypoxia. This could stimulate the release of maternal stress hormones that can cross the placenta and alter the development of the HPA axis. Stress can also disrupt the normal patterns of prenatal exposure to sex hormones that program typical sex differences in brain structure and function, which tend to be atypical in children with ASDs. ASDs are devastating and there is, with rare exception, no established method for its prevention. Consequently it is urgently needed to identify potential environmental factors that can contribute to ASDs. Identification of environmental factors that can be avoided, prevented, or ameliorated by programs of primary prevention is therefore especially important.

As concerns arise about exposure to phthalates during critical periods of human development, assessing phthalate exposure using biological matrix may become desirable to investigate the exposure of potentially vulnerable population such as children.

3.9.3 Subjects' population

A total of 48 children with ASDs [M: 36, F: 12; age at examination: 11.0 ± 5 years] were recruited from the staff of Children Neuropsychiatric Department, Siena, Italy. All the 48 patients with ASDs, diagnosed by DSM IV (Diagnostic and Statistical Manual of mental disorders) and evaluated using ADOS (Autism Diagnostic Observation Schedule), ABC (Autism Behaviour Checklist), and CARS (Childhood Autism Rating Scalescores) entered the study. Patients with Rett syndrome, X-fragile syndrome, inborn errors of metabolism, 21 trisomy, tuberous sclerosis, and gene microdeletions were excluded from the present study. Informed consent from the parents or tutors was obtained as well as institutional review board approval for the study. Mean age at diagnosis was between 30-36 months. However, the diagnosis for the examined ASDs population go back to procedures employed several years ago (today, mean age at the diagnosis for infantile autism is about 18-24 month). 45

gender and age-matched healthy controls (HC) [M: 25, F: 20; age at examination: 12 ± 5] were randomly chosen from outpatients who had no pathological symptoms.

Urines from children with ASDs and HCs were collected in polypropylene specimen cups, shared in aliquots (1.0 mL) and frozen at -20 °C until analysis. Field blanks consisted in purified water collected in polypropylene tubes and frozen at -20 °C.

The concentration of DEHP metabolites in urine from ASDs children and HCs were determinate by the RP-HPLC-ESI-MS method described above.

First morning urine specimens were collected. All specimens displayed urinary creatinine in the children reference value range, dependent on age and lean body mass (0.5-4.0 mg/Kg/24 h).

3.9.4 Statistical analysis

All variables were tested for normal distribution (D'Agostino-Pearson test) and data were presented as means with 95% confidence intervals (95% C.I.) for normally distributed variables or medians means and with 95% C.I. for non-normally distributed data. Differences between groups were evaluated using independent-sample t test (continuous normally distributed data), Mann-Whitney rank sum test (continuous non-normally distributed data), chi-square statistics (categorical variables with minimum number of cases per cell ≥ 5) of Fisher's exact test (categorical variables with minimum number of cases per cell < 5). Associations between variables were tested by unvaried regression analysis. The efficiency of urinary phthalates metabolites in discriminating ASDs patients from healthy controls were evaluated using Receiver Operating Characteristic (ROC) curve analyses. All analyses were considered to be statistically significant for p -values < 0.05 . Correction for multiple comparisons was made (Bonferroni's correction). The MedCalc version 9.5.2.0 statistical software package (MedCalc Software, Mariakerke, Belgium) was used.

3.9.5 Results

Among the four metabolites of DEHP measured in urines of ASDs, we detected urinary concentration with geometric mean for MEHP (55 $\mu\text{g/L}$), 5-OH-MEHP (180 $\mu\text{g/L}$), 6-OHMEHP (17 $\mu\text{g/L}$), 5-oxo-MEHP (96 $\mu\text{g/L}$). On the contrary, in urine

from healthy controls we found the following values for MEHP (28 µg/L), 5-OH-MEHP (4 µg/L), 6-OH-MEHP (19 µg/L), 5-oxo-MEHP (4 µg/L).

We found detectable levels of MEHP, 5-OH-MEHP, and 5-oxo-MEHP in 79.2%, 52.1%, and 46.0% of ASDs patients, respectively (Table 13).

Table 15. ROC curve for di(2-ethylhexyl)phthalate secondary metabolites urinary excretion and infantile autism.

Urinary phthalates	Cut-off	AUC±SE	95% CI	P-value	Sens (%)	Spec. (%)	+PV (%)	-PV (%)
5-OH-MEHP	>.177	.638±.057	.531-.735	.0154	52.1	75.6	69.4	59.6
5-oxo-MEHP	>.142	.666±.055	.561-.759	.0028	46.0	91.1	85.2	60.3
MEHP	>.01	.631±.058	.524-.730	.0233	79.2	44.2	61.3	65.5
ALL	>.724	.671±.055	.568-.764	.0021	39.2	97.8	95.2	58.7

AUC: Area under the Curve; SE: Standard error; 95% CI: 95% confidence intervals for the Area under the Curve; Sens.: sensitivity; spec.: specificity; +PV: positive predictive value; -PV: negative predictive value; ALL: total sum of all the examined di(2-ethylhexyl)phthalate secondary metabolites (5-OH-MEHP + 5-oxo-MEHP + 6-OH-MEHP+ MEHP).

Interestingly, 5-OH-MEHP was the major metabolite in terms of urine concentrations, followed by 5-oxo-MEHP and MEHP. Urinary excretion of 5-oxo-MEHP ($p = 0.005$), 5-OH-MEHP ($p=0.0224$), and MEHP ($p=0.0312$) was significantly higher in autistic patients compared to gender- and age-matched healthy controls (Table 14).

Table 16. Comparisons of urinary excretion of secondary metabolites for di(2-ethylhexyl)phthalate in autistic patients (N = 48) vs. healthy controls (N = 45) in (µg/mL).

	ASDs	Healthy Controls	P-value*
5-OH-MEHP	0.18 (0.037-0.399)	0.04 (0-0.124)	0.0224
5-oxo-MEHP	0.096 (0.04-0.17)	0.04 (0.015-0.079)	0.005
6-OH-MEHP	0.017 (0.01-0.034)	0.019 (0-0.043)	0.9305
MEHP	0.055 (0-0.11)	0.028 (0-0.059)	0.0312

Values are medians (95% confidence intervals of the median); * Mann-Whitney test for independent samples; statistically significant differences are highlighted in bold.

On the contrary, 6-OH-MEHP ($p = 0.9305$) was not able to discriminate ASDs. High levels of 5-OH-MEHP were detected in 26.6% of healthy controls. A significant positive correlation between 5-OH-MEHP and 5-oxo-MEHP could be observed only in autistic children ($r_s = 0.668$, $p < 0.0001$), but not in the control population ($r_s =$

0.125, $p = 0.5565$). The oxidised form of the metabolites pathway, corresponding to 5-oxo-MEHP had a specificity of 91.1% in identifying autistic children (Figure 52).

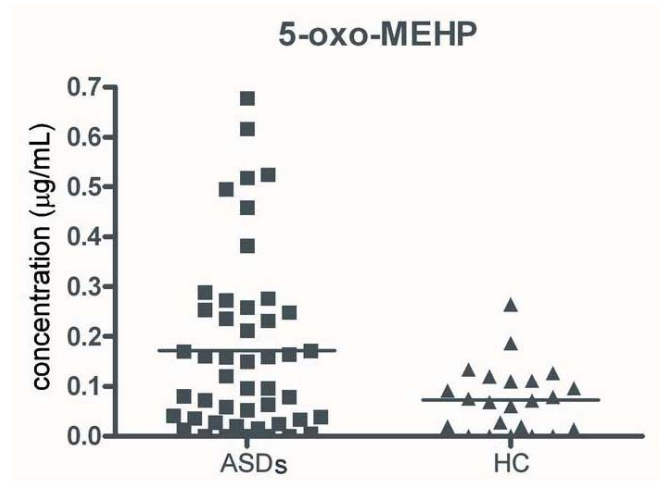


Figure 52. Column scattergrams for 5-oxo-MEHP values in ASDs' urine samples (ASDs, $n = 48$, and Healthy Controls (HC, $n = 23$))

The horizontal lines indicate the selected cut-off values (at mean \pm 3SD of the control healthy group) and is graphically represented as a horizontal line.

The efficiency of urinary secondary metabolites in discriminating ASDs patients from healthy controls was evaluated using ROC curve analyses (Table 13, Table 15).

Finally, we analyzed the correlations between total Childhood Autism Rating Scale (CARS) score and levels of the different metabolites. Total CARS scores were (means \pm SD) 44 ± 7.4 (range: 31- 60).

A positive correlation between CARS scores and urinary MEHP levels was observed ($\rho = 0.429$, $p = 0.0033$), whereas no significant relationships with the levels of the other examined metabolites were found (total CARS vs. 5-OH-MEHP: $\rho=0.120$, $p=0.4298$; total CARS vs. 5-oxo-MEHP: $\rho=0.127$, $p=0.3931$; total CARS vs. 6-OH-MEHP: $\rho=0.0085$, $p=0.9529$).

Moreover, comparing ASDs with $n=10$ patients with Rett syndrome (a genetic form of autism due in up to 95% of cases to mutation of a gene. i.e., MeCP2), urinary phthalate metabolites appear to be, once again, significantly elevated in ASDs patients (Table 15).

Table 17. Comparisons of urinary excretion of secondary oxidative metabolites of DEHP in ASDs with n=10 patients with Rett syndrome in ($\mu\text{g}/\text{mL}$).

Urinary Phthalate Metabolite	ASDs	Rett syndrome	p-value
5-oxo-MEHP	0.0997 (0.0397-0.1708)	0 (0 -0.0755)	0.0344
5-OH-MEHP	0.1740 (0.0311-0.35)	0 (0 -0.0091)	0.0601
6-OH-MEHP	0.0107 (0-0.0261)	0 (0 -0.0832)	0.2246
MEHP	0.0287 (0.0159-0.0847)	0 (0 -0.1344)	0.7098

(data are expressed as medians and 95% confidence intervals; phthalate metabolite concentrations are adjusted to creatinine and are calculated per 100 mg of urinary creatinine)

Therefore, 5-oxo-MEHP urinary excretion appears to be lower in Rett syndrome ($p=0.0344$), whereas 5-OH-MEHP ($p=0.0601$), 6-OH-MEHP ($p=0.2246$), and MEHP ($p=0.7098$) excretion is comparable to that observed in healthy controls, despite the heavy medications needed in this multi-system genetic disease. These results indicate that medications are likely not the main cause for the increased urinary phthalate excretion evidenced in ASDs, while suggesting the likely intervention of environmental factors in the pathogenesis of this pervasive development disorder.

As ASDs are disorders of brain development, any factors which regulate brain development and are known to be altered in autism should be considered as possibly contributing to the phenotype.

It is interesting to note that in 87% of the ASDs urine samples we detected MEHP and 5-oxo-MEHP levels higher than the levels recently published, by Cho et al.¹⁸⁸. In that study Cho et al. report a possible relationship between environmental phthalate exposure (external contamination) and the intelligence level of 667 School-Age children randomly recruited from nine elementary schools in five South Korean cities. The reported geometric mean was 21.3 $\mu\text{g}/\text{L}$ for MEHP, and 18.0 $\mu\text{g}/\text{L}$ for 5-oxo-MEHP, while in our study we found 55 $\mu\text{g}/\text{L}$ and 96 $\mu\text{g}/\text{L}$, respectively. Likewise in ASDs, MEHP was found to be the minor urinary metabolite compared to the corresponding oxidized metabolites as in some adult metabolic diseases^{219,220}. It is possible to hypothesize that, in the case of ASDs, a high MEHP urinary excretion does not correspond to external contamination, but rather MEHP could likely act as an endocrine disrupter.

From our data it is possible to speculate that phthalates metabolites as endocrine disrupters may play an important and previously not recognized role either in the neurotransmitter system and/or in neurodevelopment possibly increasing the risk of ASDs. In any case, our findings indicate for the first time that specific DEHP metabolites are statistically significantly increased in ASDs. It is intriguing that urinary levels of the oxidized form of the DEHP metabolites (5-oxo-MEHP) are able to efficiently discriminate ASDs from Healthy Controls. Nevertheless, it has already been reported that the most oxidized DEHP metabolites have longer half-life of excretion in urine¹⁶⁴. Therefore, it is possible that environmental factors and oxidative stress unbalance may interact in leading to increased ASDs risk, although further investigation is needed in dissecting this interaction in vivo. A link between oxidative brain damage and ASDs has been previously reported by several authors^{221,222,223}.

Over the last years, De Felice *et al.* has demonstrated that the biological “duo” hypoxia-oxidative stress (OS) is a key player in modulating genotype-phenotype expression in Rett syndrome, a well established genetic form of ASD²²⁴.

Moreover, in previous reports, a correlation between OS and ASDs has been widely explored by measuring different molecules, possibly coming from oxidative pathway as metabolic biomarkers of OS, in biological fluids²²⁵. We could speculate that in susceptible subjects, DEHP exposure, when finding OS conditions, can lead to in vivo accumulation of toxic metabolites (i.e., the oxidized phthalates metabolites), possibly acting as EDs.

Considering that urinary 5-oxo-MEHP reported in this study as increased in ASDs compared to healthy controls, we can state that our findings are in agreement with an increased OS environment. Moreover, phthalates are known as EDs but it is unclear how they could be involved in etiology of neurodevelopment disorders. As described before, phthalate metabolites activate α -PPAR that may alter lipid metabolism in the brain. Recently signal transduction pathway of α -PPAR was correlated to progression of neurodegenerative and psychiatric diseases. Phthalates also interfere with the thyroid hormone system by inducing hypothyroidism. Recent studies correlated utero hypothyroxinemia to decreased intellectual capacity, mental retardation, and ASDs²²⁶. Transient intrauterine deficits of thyroid hormones have been shown to result in permanent alterations of cerebral cortex similar to those

found in brains of children with autism²²⁶. As a consequence, the current surge of this disease could be related to transient maternal hypothyroxinemia resulting from exposure to antithyroid environmental contaminants.

In conclusion, our findings generate the idea that prenatal plus postnatal phthalate exposure may have synergistic and cumulative actions affecting brain development, thus possibly contributing to the ASDs phenotype. While continued exploration of the potential causes for neurodevelopmental disorders is important for the health of the population as well as in reducing the economical burden associated with these devastating conditions, our data suggest the importance of a prenatal / postnatal screening for urinary DEHP metabolites in the population at high risk for ASDs.

References

-
- ¹⁵⁷ Latini G., Wittassek M., Del Vecchio A., Presta G., De Felice C., Angerer J., *Environ Int*, **2009**, *35*, 236–239.
- ¹⁵⁸ Wormuth M., Scheringer M., Vollenweider M., Hungerbuhler K., *Risk Anal*, **2006**, *26*, 803–824.
- ¹⁵⁹ Schettler T., *Int J Androl*, **2006**, *29*, 134–139.
- ¹⁶⁰ Albro P.W., Corbett J.T., Schroeder J.L., Jordan S., *et al.*, *Environ. Health Perspect.* **1982**, *45*, 19-25.
- ¹⁶¹ Calafat A.M., Ye X., Silva M.J., Kuklennyik K., *et al.*, *Int. J. Androl.* **2006**, *29*, 166-171.
- ¹⁶² Rusyn I., Peters J.M., Cunningham M.L., *Crit. Rev. Toxicol*, **2006**, *36*, 459-479.
- ¹⁶³ Heindel J.J., Powell C.J., *Toxicol. Appl. Pharmacol*, **1992**, *115*, 116-123.
- ¹⁶⁴ Koch H.M., Preuss R., Angerer J., *Int J Androl*, **2006**, *29*, 155–165.
- ¹⁶⁵ Albro P.M., *Environ Health Perspect*, **1986**, *65*, 293–298.
- ¹⁶⁶ Dirven H.A., van den Broek P.H., Jongeneelen F.J., *Int Arch Occup Environ Health*, **1993**, *64*, 555–60.
- ¹⁶⁷ Clark K., Cousins I., MacKay D., Yamada K., In: Staples CA, editors, *The Handbook of Environmental Chemistry*, 3Q: Phthalate Esters New York:Springer; **2003**.
- ¹⁶⁸ Crisp T.M., Clegg E.D., Cooper R.L., Wood W.P., Anderson D.G., Baetcke K.P., Hoffmann J.L., Morrow M.S., Rodier D.J., Schaeffer J.E., Touart L.W., Zeeman M.G., Patel Y.M., *Environ. Health Perspect*, **1998**, *106* (1), 11–56.
- ¹⁶⁹ Borch J., Ladefoged O., Hass U., Vinggaard A.M., *Reprod Toxicol*, **2004**, *18*, 53-61.
- ¹⁷⁰ Backer K., Seiwert M., Angerer J., Heger W., Koch H.M., Nagorka R., Rpbkamp E., Schuler C., Seifert B., Ullrich D., *Int J. Environ. Health*, **2004**, *207*, 409-417.
- ¹⁷¹ Fisher J.S., Macpherson S., Marchetti N., Sharpe R.M., *Hum. Reprod.*, **2003**, *18*, 1383-1394.
- ¹⁷² Skakkebaek N., Jorgensen N., Main K.M., Rajpert-De Meyts *et al*, *Int. J. Androl.*, **2006**, *29*, 2-11.
- ¹⁷³ ECB- *European Chemicals Bureau, Risk Assesment report for Bis(2-ethylhexyl)phthalate*, **2004**.
- ¹⁷⁴ Grande S.W., Andrade A.J., Taslerness C.E., Grote K., *et al.*, *Toxicol. Sci.* **2006**, *91*, 247-254.
- ¹⁷⁵ Ward J.M., Perella C.M., Gonzalez F.J., *Toxicol. Pathol*, **1998**, *26*, 240-246.
- ¹⁷⁶ Stahlhut R.W., van Wijngaarden E., Dye T.D., Cook S., Swan S.H., *Environ. Health Perspect*, **2007**, *115* (6), 876–882.

-
- ¹⁷⁷ Clark-Taylor T., Clark-Taylor B.E., *Med Hypotheses*, **2004**, *62*, 970–975.
- ¹⁷⁸ A) De Felice C., Ciccoli L., Leoncini S., Signorini C., Rossi M., Vannuccini L., *et al.*, *Free Radic Biol Med*, **2009**, *47*, 440–448. B) Pecorelli A., Ciccoli L., Signorini C., Leoncini S., Giardini A., D'Esposito M., *et al.*, *Clin Biochem*, **2011**, *44*, 368–371.
- ¹⁷⁹ Villagonzalo K. A., Dodd S., Dean O., Gray K., Tonge B., Berk M., *Expert Opin Ther Targets*, **2010**, *14*, 1301–1310.
- ¹⁸⁰ Cho B.N.K., Kim Y., Shin M.S., Yoo H.J., Kim J.W., Yang Y.H., Kim H.W., Bhang S.Y., Hong Y.C., *Biol Psychiatry*, **2009**, *66*, 958–963.
- ¹⁸¹ Cunningham F.G., Leveno K.J., Bloom S.L., Hauth J.C., Gilstrap L.C., Wenstrom K.D. *William Obstetrics*, 22nd ed. New York, NY: McGraw-Hill, **2006**.
- ¹⁸² Wolff J., *Pharmacol Rev*, **1998**, *50*, 89–105.
- ¹⁸³ Poppe K., Glinoe D., *Hum Reprod Update*, **2003**, *9*, 149–161.
- ¹⁸⁴ Pop V.J., Kuijpers J.L., van Baar A.L., Verkerk G., van Son M.M., de Vijlder J.J., Vulsma T., Wiersinga W.M., Drexhage H.A., Vader H.L., *Clin Endocrinol*, **1999**, *50*, 149–155.
- ¹⁸⁵ Meeker J.D., Calafat A.M., Hauser R., *Environ Health Perspect*, **2007**, *115*, 1029–1034.
- ¹⁸⁶ Roman G.C., *Journal of the Neurological Sciences*, **2007**, *262*, 15–26.
- ¹⁸⁷ Heindel J.J., *Reprod Toxicol*, **2007**, *23*, 257–259.
- ¹⁸⁸ Cho S.C., Bhang S.Y., Hong Y.C., Shin M.S., Kim B.N., Kim J.W., *et al.*, *Environ Health Perspect*, **2010**, *118*, 1027–1032.
- ¹⁸⁹ Latini G., De Felice C., Presta G., Del Vecchio A., Paris I., Ruggieri F., *et al.*, *Environ Health Perspect*, **2003**, *111*, 1783–1785.
- ¹⁹⁰ Latini G., Verzotti A., De Felice C., *Curr Drug Targets Immune Endocr Metabol Disord*, **2004**, *4*, 37–40.
- ¹⁹¹ Hines E.P., Calafat A.M., Silva M.J., Mendola P., Fenton S.E., *Environ Health Perspect*, **2009**, *117*, 86–92.
- ¹⁹² Latini G., Wittassek M., Del Vecchio A., Presta G., De Felice C., Angerer J., *Environ Int* **2009**, *35*, 236–239.
- ¹⁹³ Bern B., *The Fragile Fetus*. Princeton Scientific Pub. Co., **1992**, Princeton, N.J. (USA).
- ¹⁹⁴ Nuti F., Hildenbrabd S., Chelli M., Wodarz R., Papini A.M., *Bioorg Med Chem*, **2005**, *13*, 3461–3465.
- ¹⁹⁵ Kato K., Silva M.J., Reidy J.A., Hurtz D. III, Malek N.A., Needham L.L., *et al.*, *Environ Health Perspect*, **2004**, *112*(3), 327–330.
- ¹⁹⁶ Blount B.C., Milgram K.E., Silva M.J., Malek N.A., Reidy J.A., Needham L.L., *et al.* *Anal Chem*, **2000**, *72*, 4127–4134.

-
- ¹⁹⁷ ICH 2001. International Conference of Harmonization. Guidance for Bioanalytical Method Validation. Center for Drug Evaluation and Research (CDER).
- ¹⁹⁸ Kato K., Silva M.J., Needham L.L., Calafat A.M., *Anal Chem*, **2005**, 77, 2985–2991.
- ¹⁹⁹ Koch H.M., Rossbach B., Drexler H., Angerer J., *Environ Res*, **2003**, 93, 177–185.
- ²⁰⁰ Caballero B., *Epidemiol Rev*, **2007**, 29, 1-5.
- ²⁰¹ <http://www.cdc.gov/nccdphp/dnpa/obesity>. In: Centers for Disease Control and Prevention.
- ²⁰² Vasiliu O., Cameron L., Gardiner J., Deguire P., Karmaus W., *Epidemiology*, **2006**, 17, 352-359.
- ²⁰³ Heindel J.J., Levin E., *Birth Defects Res A Clin Mol Teratol*, **2005**, 73, 469.
- ²⁰⁴ Anway M.D., Skinner M.K., *Reprod Biomed Online*, **2008**, 16, 23-25.
- ²⁰⁵ Shinomiya N., Shinomiya M., *Toxicol Lett*, **2003**, 137, 175-183.
- ²⁰⁶ Silfen M.E., Manibo M., McMahon D.J., Levine L.S., Murphy A.R., Oberfield S.E., *J Clin Endocrinol Metab*, **2001**, 88(6), 2863-2868.
- ²⁰⁷ Matthews D.R., Hosker J.P., Rudenski A.S., Naylor B.A., Treacher D.F., Turner R.C., *Diabetologia*, **1985**, 28(7), 412-419.
- ²⁰⁸ Cutfield W.S., Jefferies C.A., Lackson W.E., Robinson E.M., Hofman P.L., *Pediatr Diabetes*, **2003**, 4(3), 119-125.
- ²⁰⁹ Zimmet P., Alberti G., Kaufman F. *et al.*, *Lancet*, **2007**, 369, 2059-61.
- ²¹⁰ Street M.E., Grossi E., Volta C., Faleschini E., Bernasconi S., *BMC Pediatr*, (2008), 17, 8-24.
- ²¹¹ Buscema M., Grossi E.. In Proceedings IEEE Interational Conference on Systems, Man and Cybernetics (SCM 2007), Montreal. IEEE, **2007**, 3457-3463.
- ²¹² Kim Y.S., Leventhal B.L., Koh Y.J., Fombonne E., Laska E., Lim E.C., *et al.*, *Am J Psychiatry*, **2011**, 168, 904-912.
- ²¹³ American Psychiatric Association. Diagnostic and Statistical Manual of Mental Disorders, (4th Ed. text revision) Washington, DC: Authors; **2000**.
- ²¹⁴ Nelson K.B., *Pediatrics*, **1991**, 87, 761–766.
- ²¹⁵ Risch N., Spiker D., Lotspeich L., Nouri N., Hinds D., Hallmayer J., *et al.*, *Am J Hum Genet*, **1999**, 65, 493–507.
- ²¹⁶ Larsson M., Weiss B., Janson S., Sundell J., Bornhag C.G., *Neurotoxicology*, **2009**, 30, 822–831.
- ²¹⁷ Herbert M., *Curr Opin Neurol*, **2010**, 23, 103–110.
- ²¹⁸ Caspi A., Moffit T.E., *Nature reviews. Neuroscience*, **2006**, 7(7), 583-590.
- ²¹⁹ Wittassek M., Angerer J., *Int J Androl*, **2008**, 31, 131–138.

-
- ²²⁰ Silva M.J., Barr D.B., Reidy J.A., Kato K., Malek N.A., Hodge C.C., *et al.* *Arch Toxicol*, **2003**, *77*, 561–567.
- ²²¹ Villagonzalo K. A., Dodd S., Dean O., Gray K., Tonge B., Berk M., *Expert Opin Ther Targets*, **2010**, *14*, 1301–1310.
- ²²² Sajdel-Sulkowska E.M., Xu M., McGinnis W., Koibuchi N., *Cerebellum*, **2011**, *10*, 43–48.
- ²²³ James S.J., Cutler P., Melnyk S., Jernigan S., Janak L., Gaylor D.W., *et al.*, *Am J Clin Nutr*, **2004**, *80*, 1611–1617.
- ²²⁴ A) De Felice C., Ciccoli L., Leoncini S., Signorini C., Rossi M., Vannuccini L., *et al.*, *Free Radic Biol Med*, **2009**, *47*, 440–448. B) Pecorelli A., Ciccoli L., Signorini C., Leoncini S., Giardini A., D'Esposito M., *et al.*, *Clin Biochem*, **2011**, *44*, 368–371.
- ²²⁵ Chauhan V., Chauhan A., Cohen I.L., Brown W.T., Sheikh A., *Life Sci*, **2004**, *74*, 1635–1643.
- ²²⁶ Roman G.C., *J Neurol Sci*, **2007**, *262*, 15–26.

4 EXPERIMENTAL PART

4.1 Materials and methods

The chemicals were purchased from Sigma-Aldrich and were used without further purification. The ω -alkynyl-alcohols, were purchased from Alfa Aesar; protected amino acids and Rink-amide NovaSyn® TGR resin were purchased from Novabiochem (Laufelfingen, Switzerland). The following amino acid side-chain-protecting groups were used: OtBu (Asp, Glu), tBu (Ser, Thr), Pbf (Arg), Trt (Gln, His) and Boc (Lys). HOBt and TBTU were purchased from Iris Biotech GmbH (Marktredwitz, Germany); Fmoc-L-Arg(Pbf)-OH and Fmoc-L-His(Trt)-OH amino acids were purchased from CBL (Patras, Greece); Fmoc-L-Nleu was purchased from NeoMPS (Strasburgo, France). β -Glucuronidase (*Escherichia coli* K12) was purchased from Roche Biochemical (Mannheim, Germany).

Peptide-synthesis grade N,N-dimethylformamide (DMF), and N-methylpyrrolidone (NMP) for peptide synthesis were purchased from Scharlau (Barcellona, Spain); acetonitrile (ACN) from Carlo Erba; dichloromethane (DCM), trifluoroacetic acid (TFA), piperidine, acetic anhydride (Ac₂O), N,N-diisopropylethylamine (DIEA), diethyl ether, and N-methylmorpholine (NMM) were purchased from Sigma Aldrich; TIS was purchased from Fluka/Aldrich. The scavengers for cleavage of peptides from resin, 1,2-ethanedithiol (EDT), thioanisole and phenol (PheOH), were purchased from Acros Organics, Jansenn Chimica and Carlo Erba. TLC were carried out precoated on silica gel plates (Merck; 60 Å F254) and spots located with: (a) UV light (254 and 366 nm), (b) ninhydrine (solution in acetone), (c) Cl₂/toluidine, (d) fluorescamine, (e) I₂, (f) a basic solution of permanganate [KMnO₄ (3 g), K₂CO₃ (20 g), and NaOH (0.25 g) in water (300 ml)], (g) 10% H₂SO₄ in EtOH. Flash Column Chromatography (FCC) was performed on Merck silica gel 60 (230-400 mesh) according to Still et al.¹. Solutions for Kaiser test were prepared as follows: ninhydrine (5 g) in EtOH (100 ml), Phenol (80 g) in EtOH (20 ml), KCN 1 mM (2 ml) in pyridine (98 ml).

[¹] Still, W. C.; Kahn, M.; Mitra, A. *J. Org. Chem.* **1978**, *43*, 2923–2925.

The products were characterized by nuclear magnetic resonance (NMR), infrared spectra (IR), liquid chromatography-electrospray ionization/ mass spectrometry (LC-ESI-MS), and Ultra Performance Liquid Chromatography (UPLC).

^1H and ^{13}C NMR spectra were recorded at 400 and 100 MHz, and 200 and 50 MHz respectively, on a Varian spectrometer in deuterated solutions and are reported in parts per million (ppm), with solvent resonance used as reference.

Infrared spectra were recorded on a Perkin Elmer mod. BX II FT-IR spectrometer. Products were analyzed and characterized by ACQUITY UPLC (Waters Alliance 2695 Waters Corporation, Milford, Massachusetts) coupled to UV diode array Waters 2996 and to a single quadrupole ESCI-MS (Micromass ZQ) using a C18 Phenomenex Kinetex (100x3mm, 2.6 μm , C18, 100Å) at 30 °C, with a flow rate of 0.6 mL/min. The solvent systems used were A (0.1% TFA in H_2O) and B (0.1% TFA in CH_3CN). Peptides were analyzed by analytical RP-HPLC (Alliance, model 2695 equipped with a diode array detector, Waters) using a Jupiter C18 (5 μm , 250 \times 4.6 mm) column (Phenomenex) at 1 mL/min. The solvent systems used were A (0.1% TFA in H_2O) and B (0.1% TFA in CH_3CN). Peptides were purified by semipreparative RP-HPLC on a Supelco C18 180 Å (250 \times 10 mm, 5 μm) column (Sigma Aldrich, St. Louis, MO, USA), using methods and solvent system as reported. Fractions were analyzed by ACQUITY UPLC (Waters Corporation, Milford, Massachusetts) coupled to a single quadrupole ESI-MS (Micromass ZQ) using a 2.1 x 50 mm 1.7 μm ACQUITY BEH C18

Purification of Nickel complex [Gly-Ni-BPB], of azido and alkynyl amino acids and of DEHP metabolites were performed as reported by flash chromatography.

Cartridge for urine pretreatment (SPE) were purchased from Waters (Oasis HBL 3mL/60 mg). For creatinine measurement, a Beckman Synchron AS/ASTRA clinical analyzer (Beckman Instruments, Inc., Brea, CA) was used. We used value (micrograms per liter)/creatinine (grams per liter) for dilution correction in the analyses. The HPLC quantitative analyses were carried out using an high-performance liquid chromatography tandem mass spectrometry RP-HPLC -ESI-MS (Waters, Alliance 2695, Waters, Micromass ZQ) equipped with phenyl column (Betasil, 5 μm , 50 mm x 3 mm, Keystone Scientific, Bellefonte, PA) and with a Waters 2996 Photodiode Array Detector.

5 Solid Phase Peptide Synthesis (SPPS).

5.1 General procedure for in batch SPPS on a manual synthesizer

Peptides were synthesized on a manual batch synthesizer (PLS 4×4, Advanced ChemTech) using a Teflon reactor (10 mL), following the Fmoc/tBu SPPS procedure. The syntheses were performed on Rink-amide NovaSyn TGR resin (0.14 mmol/g, 300 mg). The resin was swelled with DMF (1 mL/100 mg of resin) for 20 min before use.

Stepwise peptide assembly was performed by repeating for each added amino acid the following deprotection-coupling cycle:

- Swelling: DMF (1 mL/100 mg of resin) for 5 min;
- Fmoc-deprotection: resin is washed twice with 20% piperidine in DMF (1 mL/100 mg of resin), one wash for 5 min followed by another wash for 20 min);
- Resin-washings: DMF (3×5 min);
- Coupling: scale employing TBTU/HOBt/NMM (2 eq./2 eq./3 eq.) as the coupling system and 2 eq. of the Fmoc protected amino acids, except for N^α-Fmoc-Xaa(ω-N₃)-OH and N^α-Fmoc-Yaa(ω-yl)-OH for which 1.5 eq. were used. The coupling was carried out in DMF (1mL/100 mg of resin) for 50 min.
- Resin-washings: DMF (3×5 min) and DCM (1×5 min).
- Each coupling was checked by Kaiser Test ¹⁴⁸: In our case all tests were negative therefore it was not necessary to repeat the coupling reaction.

Kaiser test procedure: to a small amount of peptide-resin placed in a test tube, three drops for each of the following solutions were added: ninhydrine (5 g) in ethanol (100 mL); phenol (80 g) in ethanol (20 mL); KCN (2 mL of 1 mM aqueous solution) in pyridine (98 mL). The tube is heated at 100 °C for 5 min. A positive test (resin beads and solution appears strongly blue-violet) states the presence of at least 5% free amino groups.

5.1.1 Conventional and MW-assisted synthesis of PTHrP(1–34)NH₂

Room temperature and MW-assisted SPPS of PTHrP(1-34)NH₂ were performed using Liberty™ microwave peptide synthesizer (CEM) on Rink-amide NovaSyn® TGR resin (0.2 mmol/g, 500 mg), which was suspended in a solution of DMF/DCM (1 : 1 v/v) and swelled for 30 min. The reactions were performed in a Teflon vessel and mixed by nitrogen bubbling. Reaction temperatures were measured by an internal fiber optic sensor. The protocol for RT and for MW-assisted SPPS is shown in Table 16. The ongoing of synthesis was monitored by UPLC-ESI-MS of MW-assisted mini-cleavages of intermediate fragments. During the general coupling cycle, the N-terminal Fmoc-protecting group was removed with a solution of 20% piperidine in DMF. Fresh stock solutions of the Fmoc-protected amino acids (5 equiv., 0.2 M) and TBTU (5 equiv. 0.5 M) in DMF, and DIEA (10 equiv. 2M) in NMP were prepared in separated bottles and used as reagents during the SPPS. In particular, the coupling cycles were performed using 2.5 ml of Fmoc-protected amino acids, 1 ml of TBTU and 0.5 ml of DIEA in NMP of stock solutions. Washing steps are performed with DMF and DCM.

RT-SPPS protocol: consisted of two consecutive deprotection steps of 5 and 10 min, respectively, and a 20 min coupling step.

MW-SPPS protocol: consisted of two deprotection steps performed at 75 °C using 35W for 0.5 min for the first one and 60W for 3 min for the second one, whereas the coupling steps were performed at 75 °C, using 30W for 5 min for all amino acids except for Arg and His residues that required specific coupling parameters performed in two steps.

Table 18. RT and MW-assisted SPPS deprotection and coupling protocols used for the PTHrP(1-34)NH₂ synthesis.

Step	MW-assisted Synthesis			RT-Synthesis		
	Temp(°C)	MW Power (W)	Time(min)	Temp(°C)	MW Power (W)	Time(min)
1st deprotection	75°	35 W	0,5	20		5
2nd deprotection	75°	60 W	3	20		10
Coupling	75°	30 W	5	20		20

5.2 Amino terminal acetylation. General procedure

The free *N*-terminal α -amino of the resin-bound peptides was acetylated by two consecutive steps using $\text{Ac}_2\text{O}/\text{NMM}$ in DCM (20 equiv. 1.6 mL of DCM). The first step of 30 min is followed by an additional step with fresh acetylation mixture of 90 min. The reaction was monitored by Kaiser test.

5.3 Deprotection, cleavage and purification of free peptide. General procedure

Peptides cleavage from the resin and simultaneous deprotection of the amino-acids side chains were carried out with the cleavage mixture (1 mL/100 mg of resin-bound peptide). For PTHrP(1-34) NH_2 , it was used TFA/TIS/water solution (95:2.5:2.5 v/v/v) as cleavage mixture. For MTII analogues (I'-X'), it was used TFA/thioanisole/1,2-ethanedithiol/phenol/ H_2O solution (94:2:2:2:2 v/v/v/v/v). The cleavage was maintained for 3 h with vigorous stirring at RT. Resins were filtrated and washed with TFA. After partial evaporation under nitrogen flux, filtrates were precipitated with cold diethyl ether, separated by centrifugation, dissolved in H_2O and lyophilized with an Edwards apparatus, model Modulyo.

Lyophilized crude peptides were purified by semipreparative RP-HPLC using methods and solvent system as reported. Fractions were analyzed by ACQUITY UPLC (Waters Corporation, Milford, Massachusetts) coupled to a single quadrupole ESI-MS (Micromass ZQ) using a 2.1 x 50 mm 1.7 μm ACQUITY BEH C18.

5.4 General procedure for solid-phase extraction SPE

- SPE were performed on RP-C18 LiChrorep columns, with CH₃CN in H₂O as eluents. Main steps are reported here:
- Column washings with MeOH (3 column volumes) and CH₃CN (3 column volumes)
- Column conditioning with H₂O (3 column volumes)
- Dissolving the peptide in H₂O (1 column volume), checking the pH that should be neutral.
- Adsorbing peptide solution on silica for 3 times
- Eluting with H₂O (3 column volumes).
- Eluting with 5%, 10%, 15%, 20% of H₂O/CH₃CN (column volume for each concentration), and 100% of CH₃CN.
- Fractions were checked by analytical UPLC-ESIMS, and then lyophilized.

5.5 MW-assisted mini-cleavage. General procedure

MW-assisted mini-cleavages were performed using DiscoverTMS-Class single-mode MW reactor equipped with Explorer-48 autosampler (CEM). The mixing of the cleavage reaction was accomplished by magnetic stirring and the reaction temperature was monitored at the bottom of the reactor vessels by an IR sensor. A small sample of beads carrying Fmoc-protected resin-bound peptide (10 mg) was weighted into a fritted polypropylene tube and treated twice with a 20% solution of piperidine in DMF (1 ml) each time for 5 min. The beads were then washed with DMF (2 × 1ml) and DCM(3 × 1 ml), dried under vacuum and transferred into a 10 ml glass tube containing the cleavage mixture that was placed into the MW cavity. The minicleavages were carried out with 2 ml of TFA/TIS/water solution (95:2.5:2.5 v/v/v) at 45 °C, using 15W for 15 min with external cooling of the reactor vessel. The reaction mixture was then filtered and the crude peptide was precipitated from the cleavage mixture by addition of ice-cold diethyl ether followed by cooling for 5 min at -20 °C. The product was collected by centrifugation and directly subjected to UPLC ESI- MS analysis.

5.6 HPLC analysis of PTHrP(1–34)NH₂

Crude PTHrP(1–34)NH₂ obtained from both the RT and MWassisted SPPSs were analyzed by analytical RP-HPLC (Alliance 2695 HPLC system equipped with a 2996 photodiode array detector, Waters (Milford, MA, USA)) using a JupiterC18 (5 μ m, 250 \times 4.6 mm) column (Phenomenex, Torrance, CA, USA) at 1 ml/min. The solvents used were A (0.1% TFA in H₂O) and B (0.1% TFA in ACN).

5.7 UPLC-ESI-MS analysis of intermediate fragments of PTHrP(1–34)NH₂

UPLC-ESI-MS system consisted of an ACQUITYTM UPLC system (Waters) coupled with a Micromass[®] Q-ToF MICROTM mass spectrometer (Waters) equipped with an ESI source. The chromatographic separation was achieved on a Symmetry 300 C18 column (100 mm \times 2.1 mm, ID 3.5 μ m, Waters) with the column temperature set at 30 °C. The flow rate was 0.15 ml/min with a linear gradient running from 0 to 30% of B (solvent A: 2% ACN, 0.1% formic acid in H₂O; solvent B: 2% H₂O, 0.1% formic acid in ACN) in 7 min, followed by 30–60% B in the next 3 min, then by 95% B for 2 min, and returned to initial condition for 3 min for re-equilibration. The total run time per sample was 15 min. The ESI-MS analysis was carried out in the positive ESI mode, the optimal MS parameters were as follows: capillary voltage 3.2 kV, cone voltage 30 kV, source temperature 120 °C and desolvation temperature 320 °C. Nitrogen was used as desolvation and cone gas with a flow rate of 450 and 40 l/h, respectively. For MS/MS analyses, argon was used as collision gas, and the collision energy was set to 40 eV. Data were acquired and processed using MassLynxTM software (Waters).

6 Synthesis of N^α-Fmoc-ω-azido-α-amino acids and N^α-Fmoc-ω-alkynyl-α-amino acids

6.1 Deprotection of Boc-protecting group. General procedure

Cleavage of Boc protecting group of N^α-Boc-ω-azido-α-amino acid (3.96 mmol), or N^α-Fmoc-N^ω-Boc-α-amino acid (2.2 mmol), was achieved by treatment with an excess of HCl 2 M (10 ml) at RT for 2 h. The solution was diluted in water and lyophilized.

6.2 Fmoc protection of the free amino acid. General procedure

A solution of (2,4-dioxo-1-pyrrolidinyloxy)(9H-fluoren-9-ylmethoxy) carbonate (Fmoc-O-Su 4.36 mmol) in dioxane (20 mL) was added dropwise to a stirred solution of the deprotected amino acid (1.85 mmol, 1 eq.) in dioxane (30 mL). A solution of 1M NaOH was subsequently slowly added until pH 8-9 and the reaction mixture was stirred at RT for 2 h and 30 min. The reaction was checked by TLC (CH₂Cl₂/MeOH, 9:2, detected by (a) and (b)). Water (12 mL) was added and the solution was acidified with 2M HCl until pH 3. The product was extracted with DCM (3 x 30 ml), dried with anhydrous Na₂SO₄, filtered and the solvent removed under vacuum.

The crude material was purified by FCC on silica gel (employing a step-gradient of MeOH in DCM, 2-20%) to obtain the corresponding pure N^α-Fmoc-ω-azido-α-amino acids or N^α-Fmoc-ω-alkynyl-α-amino acids.

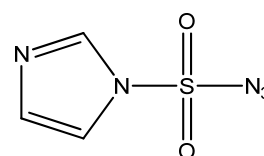
6.3 Diazotransfer on ω-aminic group of N^α-Boc or N^α-Fmoc-amino acids with triflic anhydride. General procedure

A solution of TfN₃ in CH₂Cl₂ was obtained as follows: Tf₂O (1.35 ml, 8.13 mmol, 2 eq.) was added dropwise to a vigorously stirred mixture of NaN₃ (2.635 g, 40.5 mmol, 10 eq) in H₂O (6.5 mL) and CH₂Cl₂ (11 mL) at 0 °C. The resulting mixture was allowed to warm to RT and stirring was continued for 2 h. The water layer was extracted with CH₂Cl₂ (2 × 4 mL) and the combined organic layers were washed with saturated aqueous Na₂CO₃ (12.5 mL). The resulting solution of TfN₃ in CH₂Cl₂ was then added dropwise to a solution amino acid (4.06 mmol, 1 eq.), K₂CO₃ (0.84 g, 6.08 mmol, 1.5 eq.) e CuSO₄·5H₂O (0.01 g, 0.04 mmol) in H₂O (13 ml) and MeOH (27 ml). The mixture was stirred overnight and the reaction was checked by TLC

(iPrOH/AcOEt/H₂O 6:1:3, detected by (a) and (b), *R_f* 0.81). The organic solvents were evaporated under vacuum. The water layer was acidified to pH 6 with concd. HCl, diluted with 0.25 M of phosphate buffer at pH 6.2 (25 mL), and extracted with CH₂Cl₂ (4 × 50 mL). The organic layers were washed with brine (25 mL), dried over Na₂SO₄, and concentrated under vacuum. The crude colorless oil was purified by flash chromatography using column of RP-18 LiChroprep by solutions of different concentrations of H₂O/CH₃CN to afford the desired product.

6.4 Synthesis of imidazole-1-sulfonyl azide hydrochloride as diazotransfer reagent

Sulfuryl chloride (16.1 ml, 200 mmol) was added drop-wise to an ice-cooled suspension of NaN₃ (13.0 g, 200 mmol) in MeCN (200 ml) and the mixture stirred overnight at room temperature. Imidazole (25.9 g, 380 mmol) was added to the



ice-cooled mixture and the resulting slurry stirred for 3 h. at room temperature. The mixture was diluted with EtOAc (400 mL), washed with H₂O (2 × 400 mL) then with saturated aqueous NaHCO₃ (2 × 400 mL), dried over MgSO₄ and filtered. A solution of HCl in EtOH [obtained by the drop-wise addition of AcCl (21.3 mL, 300 mmol) to ice-cooled dry ethanol (75 mL)] was added drop-wise to the filtrate with stirring, the mixture chilled in an ice-bath, filtered and the filter cake washed with EtOAc (3 × 100 mL) to give imidazole-1-sulfonyl azide hydrochloride as colourless needles. Yield 63%. IR(KBr) 2100 cm⁻¹ (N₃). ¹H-NMR (600 MHz, D₂O) δ = 7.68 (dd, 1, H, J = 1.3, 2.2 Hz, H-4), 8.09 (dd, 1 H, J = 1.6, 2.2 Hz, H-5), 9.53 (dd, 1 H, J = 1.3, 1.6 Hz, H-2); ¹³C-NMR (150.9 MHz, D₂O) δ = 120.8, 123.4, 138.3.

6.5 Diazotransfert on ω-aminic group of N^α-Fmoc- amino acids with Imidazole-1-sulfonyl azide hydrochloride. General procedure

Imidazole-1-sulfonyl azide hydrochloride (1.32 mmol, 1.5 eq) was added to a solution of N^α-Fmoc-amino acid (0.88 mmol, 1 eq.), K₂CO₃ (n+0.5 mmol)² and CuSO₄ × 5H₂O (8.8 μmol, 0.01 eq.) in MeOH (30 ml). The mixture is stirred at RT for 10 min. The reaction is checked by TLC (DCM/MeOH 10:1, detected by (a) and

² Where 'n' is the number of mols of acid in the system

(b)). The solution is diluted with H₂O (30 ml), acidified until pH 2 with HCl 0.1 M, and extracted with DCM (3x50 ml). The combined organic layers were dried with anhydrous Na₂SO₄, filtered and the solvent removed under vacuum. The crude product is purified by Flash Column Chromatography (FCC) on silica gel (employing a step-gradient of MeOH in DCM, 2-20%) to obtain the corresponding pure N^α-Fmoc-ω-azido-α-amino acids as yellow oils.

6.5.1 6-Azido-2S-[(9H-fluoren-9-ylmethoxy)carbonyl] amino]hexanoic acid (6-Azido-Fmoc-L-norleucine) (m=4)

Yield 70%. RP-UPLC: *R*_t 4.28 min (50-100% B in 5

min.). IR (KBr): 2100 cm⁻¹ (N₃). ESI-MS: *m/z* calcd for C₂₁H₂₂N₄NaO₄ [M + Na]⁺: 417.15; found 417.2. [α]_D –

2.5 (*c* 1.0, MeOH). ¹H NMR (CDCl₃, 400 MHz): δ 7.74

(d, 2H, *J*_{3,4} = *J*_{5,6} = 7.4 Hz, fluorenyl 4-H e 5-H), 7.54 (d,

2H, *J*_{1,2} = *J*_{7,8} = 7.4 Hz, fluorenyl 1-H e 8-H), 7.37

(*pseudo t*, 2H, fluorenyl 3-H e 6-H), 7.28 (*pseudo t*, 2H,

fluorenyl 2-H e 7-H), 6.19 (s broad, COOH), 5.46 (m, 1H, NH), 4.49–4.33 (m, 3H,

CH₂-O and α-H), 4.18 (t, 1H, *J* = 6.4 Hz, fluorenyl 9-H), 3.24–3.21 (m, 2H, ε-H₂),

1.70–1.42 (m, 6H, 3 × CH₂). ¹³C NMR (CDCl₃, 100 MHz): δ 176.97 (COOH),

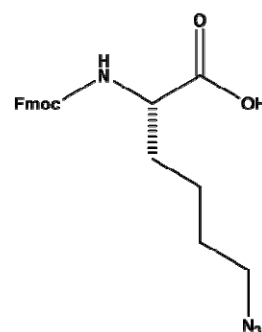
156.35 (CONH), 143.75, 143.60, e 141.28 (fluorenyl C-4a, C-4b, C-8a, e C-9a),

127.74, 127.06, e 125.01 (fluorenyl C-2- C-7), 120.00 (fluorenyl C-1 and C-8), 67.14

(CH₂-O), 53.90 (C-α), 51.02 (C-ε), 47.07 (fluorenyl C-9), 31.68 (CH₂), 28.31 (CH₂),

22.55 (CH₂). Anal. Calcd for C₂₁H₂₂N₄O₄: C, 63.95; H, 5.62; N, 14.20. Found: C,

64.01; H, 5.58; N, 14.23.



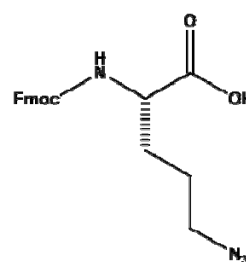
6.5.2 5-Azido-2S-[(9H-fluoren-9-ylmethoxy)carbonyl]amino] pentanoic acid (5-azido-Fmoc-L-Norvaline) (m=3)

Yield 83%. RP-UPLC: *R*_t 3.81 min (50-100% di B in 5

min). IR (KBr): 2100 (N₃) cm⁻¹. [α]_D –2.3 (*c* 1.0,

MeOH). ESI-MS: *m/z* calcd. for C₂₀H₂₀N₄NaO₄ [M +

Na]⁺ 403.14; found 403.3. ¹H NMR (CDCl₃, 400 MHz):

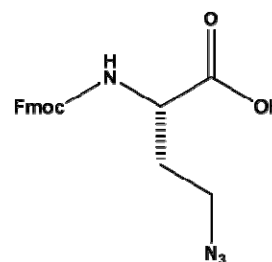


δ 7.76 (d, 2H, $J_{3,4} = J_{5,6} = 7.6$ Hz, fluorenyl 4-H e 5-H), 7.61 (*pseudo* d, 2H, $J_{1,2} = J_{7,8} = 7.6$ Hz, fluorenyl 1-H e 8-H), 7.40 (*pseudo* t, 2H, fluorenyl 3-H e 6-H), 7.31 (*pseudo* t, 2H, fluorenyl 2-H e 7-H), 6.16 (s broad, COOH), 5.34 (m, 1H, NH), 4.45–4.40 (m, 3H, CH₂-O e α -H), 4.22 (t, 1H, $J = 6.6$ Hz, fluorenyl 9-H), 3.37–3.30 (m, 2H, δ -H₂), 2.01–1.46 (m, 4H, 2 \times CH₂). ¹³C NMR (CDCl₃, 100 MHz): δ 175.72 (COOH), 156.72 (CONH), 143.75, 143.57, e 141.33 (fluorenyl C-4a, C-4b, C-8a, e C-9a), 127.76, 127.08, e 125.00 (da fluorenyl C-2 a C-7), 120.02 (fluorenyl C-1 e C-8), 67.12 (CH₂-O), 53.16 (C- α), 50.76 (C- δ), 47.15 (fluorenyl C-9), 29.62 (CH₂), 24.81 (CH₂). Anal. Calcd for C₂₀H₂₀N₄O₄: C, 63.15; H, 5.30; N, 14.73. Found: C, 63.09; H, 5.25; N, 14.80.

6.5.3 4-Azido-2S-[[**(9H-fluoren-9-ylmethoxy) carbonyl**]amino] butanoic acid (Fmoc-Abu(γ -N₃)-OH) (m=2)

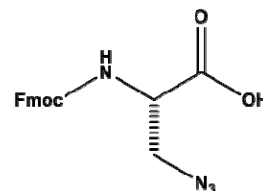
Yield 89%. RP-UPLC: R_t 3.34 min (50- 100% B in 5 mini). IR: 2100 cm⁻¹ (N₃). ESI-MS: m/z calcd for C₁₉H₁₈N₄NaO₄ [M + Na]⁺ 389.12; found 389.4. $[\alpha]_D - 11.5$ (c 1.0, MeOH).

¹H NMR (CDCl₃, 400 MHz): δ 7.75 (*pseudo* d, 2H, $J = 7.6$ Hz, fluorenyl 4-H e 5-H), 7.54 (*pseudo* d, 2H, $J = 7.4$ Hz, fluorenyl 1-H e 8-H), 7.39 (*pseudo* t, 2H, fluorenyl 3-H e 6-H), 7.31 (*pseudo* t, 2H, fluorenyl 2-H e 7-H), 6.14 (s broad, COOH), 5.63 (m, 1H, NH), 4.53–4.41 (m, 3H, CH₂-O and α -H), 4.21 (t, 1H, $J = 6.8$ Hz, fluorenyl 9-H), 3.42–3.39 (m, 2H, γ -H₂), 2.19–1.96 (m, 6H, 3 \times CH₂). ¹³C NMR (CDCl₃, 100 MHz): δ 172.71 (COOH), 156.26 (CONH), 143.53 e 141.29 (fluorenyl C-4a, C-4b, C-8a, e C-9a), 127.76, 127.08, 125.04, 124.99 (fluorenyl C-2, C-7), 120.00 (fluorenyl C-1, C-8), 67.17 (CH₂-O), 51.70 (C- α), 47.68 (C- γ), 47.09 (fluorenyl C-9), 31.21 (CH₂). Anal. Calcd for C₁₉H₁₈N₄O₄: C, 62.29; H, 4.95; N, 15.29. Found: C, 62.36; H, 4.99; N, 15.24.



6.5.4 3-Azido-2S-[[**(9H-fluoren-9-ylmethoxy)carbonyl**]amino] propanoic acid (**3-Azido-Fmoc-L-Alanine**) (**m=1**)

Yield 75 %. RP-UPLC: R_t 4.02 min (50-100% B in 5 min). IR: 2100 cm^{-1} (N_3). ESI-MS: m/z calcd. for $\text{C}_{18}\text{H}_{16}\text{N}_4\text{NaO}_{44}$ $[\text{M} + \text{Na}]^+$ 375.12; found 375.4. ^1H NMR (CDCl_3 , 400 MHz): d 7.70 (pseudo d, 2H, $J = 7.4$ Hz, fluorenyl 4-H e 5-H), 7.48 (pseudo d, 2H, $J = 7.6$ Hz, fluorenyl 1-H and 8-H), 7.40 (pseudo t, 2H, fluorenyl 3-H and 6-H), 7.28 (pseudo t, 2H, fluorenyl 2-H e 7-H), 6.3 (s broad, COOH), 5.78 (m, 1H, NH), 4.57–4.45 (m, 3H, $\text{CH}_2\text{-O}$ and $\alpha\text{-H}$), 4.32 (t, 1H, $J = 6.8$ Hz, fluorenyl 9-H), 3.52–3.35 (m, 2H, $\gamma\text{-H}_2$).



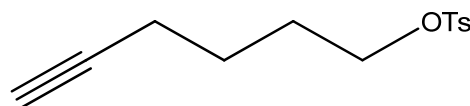
Anal. Calcd for $\text{C}_{18}\text{H}_{16}\text{N}_4\text{O}_4$: C, 61.36; H, 4.58; N, 15.90. Found: C, 61.46; H, 4.98; N, 15.68.

6.6 General procedure for the synthesis of *p*-toluenesulfonate derivatives

p-Toluenesulfonyl chloride (61.49 mmol, 1.5 eq.) in pyridine (10 mL) was added to a stirred solution of the ω -alkynyl-alcohol (40.75 mmol, 1 eq.) in pyridine (15 mL), at 0 °C. The reaction was stirred overnight at room temperature and checked by TLC [AcOEt —*n*-hexane 1:3, detected by (a)]. The reaction mixture was neutralized with 2 M HCl (10 mL/1 mL pyridine), the *p*-toluenesulfonate derivative extracted with CHCl_3 , and the organic layer evaporated under vacuum to afford the product as a pale yellow oil.

6.6.1 5-Hexyn-1-ol 1-(4-methylbenzene sulfonate)

Yield 69%. TLC: (AcOEt / *n*-hexane 1:3, detected with (a), R_f 0.6). ^1H -NMR (CDCl_3 , 200 MHz): δ 7.78 e 7.34 (syst. AA'BB', 4H,



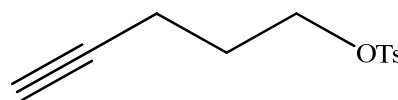
$J = 8.4$ Hz, MeC_6H_4), 3.57 (t, 2H, $J = 6.2$ Hz, 1- H_2), 2.45 (s, 3H, MeC_6H_4), 2.13–2.09 (m, 2H, 4- H_2), 1.90 (t, 1H, 6-H), 1.93–1.72 (m, 4H, 2- H_2 and 3- H_2).

6.6.2 4-Pentyn-1-ol 1-(4-methylbenzene sulfonate)

Yield 82%. TLC: (AcOEt/ *n*-hexane 1:3, detected with (a), *R_f* 0.62). ¹H-NMR (CDCl₃, 200MHz): δ

7.77 e 7.35 (syst. AA'BB', 4H, *J* = 8.4 Hz,

MeC₆H₄), 4.12 (t, 2H, *J* = 5.8 Hz, 1-H₂), 2.43 (s, 3H, MeC₆H₄), 2.32–2.15 (m, 2H, 3-H₂), 1.93 (t, 1H, 5-H), 1.91–1.82 (m, 2H, 2-H₂).

**6.7 Synthesis of ω-alkynyl bromo derivatives. General procedure**

Lithium bromide (17.95 mmol, 1.5 eq.) was added in portions to a stirred solution of the *p*-toluenesulfonate derivative (11.97 mmol, 1 eq.) in acetone (15 mL) at room temperature. The reaction mixture was heated at 40 °C and stirred for 1 h. The reaction was checked by TLC (AcOEt-hexane 1:3; revealed with KMnO₄ and by UV 254 nm). The solvent was evaporated by flushing with N₂. The residue was treated with *n*-hexane, filtration of the residue and evaporation of DCM under nitrogen flux, afforded the bromo derivative as a yellow oil.

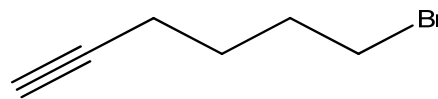
6.7.1 6-Bromohex-1-yne

Yield 65%. ¹H NMR (CDCl₃, 200 MHz): δ

3.41 (t, 2H, *J* = 7.2 Hz, 6-H₂), 2.21 (dt, 2H,

J = 3.0 Hz, 7.4 Hz, 4-H₂), 2.02–1.91 (m, 2H,

3-H₂), 1.96 (t, 1H, *J* = 3.8 Hz, 1-H), 1.71-1.60 (m, 2H, 5-H₂).

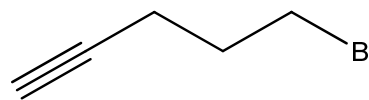
**6.7.2 5-Bromopent-1-yne**

Yield 82%. ¹H NMR (CDCl₃, 200 MHz): δ 3.44 (t,

2H, *J* = 6.4 Hz, 5-H₂), 2.75 (dt, 2H, *J* = 2.6 Hz, 7.0

Hz, 3-H₂), 2.02-1.95 (m, 2H, 4-H₂), 1.86 (t, 1H, *J* =

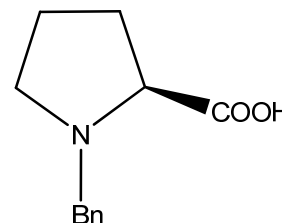
3.6 Hz, 1-H).



6.8 Synthesis of chiral inducer

6.8.1 Synthesis of (S)-N-benzylproline (BP)

A solution of 10 g of (S)-proline (86.8 mmol, 1 eq.) and 18,5 g of KOH (330 mmol, 3.8 eq.) in 70 mL of iPrOH was prepared with stirring at 40°C. As soon as the solution became transparent, slow addition of freshly distilled BnCl (18.3 g, 130 mmol, 1.5 eq.) was added under stirring at the

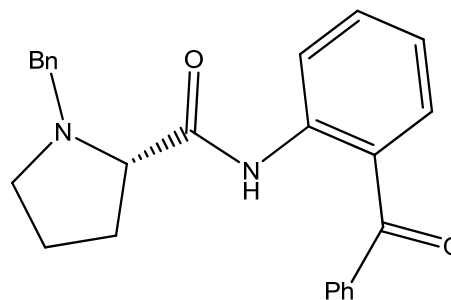


same temperature for 6h. The reaction mixture was neutralized with concentrated aqueous HCl until pH 5-6 (indicator paper), then was added to the reaction mixture CHCl_3 (30 mL) with stirring. The mixture was left overnight, then filtered and the precipitate was washed with CHCl_3 . The CHCl_3 solutions were combined and evaporated, the residue was treated with cold acetone and the precipitate of crude BP filtered and additionally washed with acetone. Some BP was also recovered from the acetone washings. The crude material was dried in air and then over P_2O_5 .

Yield 23.3%. RP-UPLC: R_t 1.57 min (10–60% of B in 5 min). ESI-MS: m/z calcd for $\text{C}_{12}\text{H}_{15}\text{NO}_2$ $[\text{M}-\text{H}]^-$. 204.11; 204.15. ^1H NMR (CDCl_3 , 400 MHz): δ 7.44-7,34 (m, 5H, Bn), 6.99 (br s, OH), $\delta_{\text{A}}=4.33$, $\delta_{\text{B}}=4.14$ (syst AB, 2H, $J_{\text{AB}}=15.3$ Hz, CH_2Bn), 3.78 (dd, 1H, $J_{\alpha,\beta}=16$ Hz, $J_{\alpha,\beta}=7.0$ Hz, H_α), 3.64 (ddd, 1H, $J_{\delta,\delta}=9.0$ Hz, $J_{\delta,\gamma}=19$ Hz, $J_{\delta,\gamma}=27$ Hz, Hz, H_δ), 2.88-2.81 (m, 1H, H_δ'), 2.33-2.23 (m, 2H, H_β , H_β'), 2.00-1.88 (m, 2H, H_γ , H_γ'). ^{13}C NMR (CDCl_3 , 100 MHz): δ 171.17 (COOH), 131.21, 130.39, 129.41, 129.15 (Bn), 67.64 (C_α), 58.04 (CH_2Bn), 53.45 (C_δ), 29.04 (C_β), 23.09 (C_γ).

6.8.2 Synthesis of (S)-2-(N-benzylprolyl)aminobenzophenone (BPB)

N-Benzyl-L-proline (4.37 g, 21.4 mmol, 1 eq.) was added at RT under N_2 to a stirred freshly prepared solution of PCl_5 (8.91 g, 42.8 mmol, 2 eq.) in anhydrous CH_2Cl_2 (150 mL). After 30 min, cold petroleum ether was added and the acyl chloride precipitated as a yellow oil. The oil was dissolved in anhydrous CH_2Cl_2



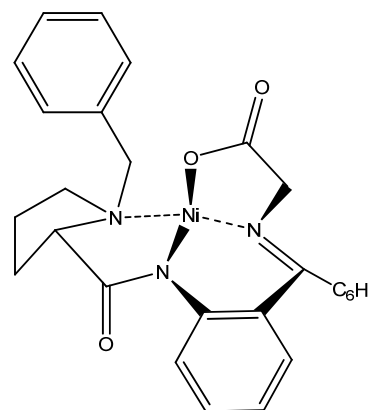
(80 mL) under N_2 and 2-aminobenzophenone (4.64 g, 23.54 mmol, 1.1 eq) was added in one portion, followed by Et_3N until pH 8. The mixture was stirred for 2 h at

room temperature, then washed with a saturated solution of Na_2CO_3 and twice with H_2O . The organic layer was evaporated under reduced pressure. The crude BPB was recrystallized from dried EtOH. Some product was also recovered from the EtOH washings. The material was dried under vacuum over P_2O_5 to give the chiral inductor BPB.

Yield 48.5%. RP-UPLC: R_t 3.44 min (30–90% di B in 5 min). ESI-MS: m/z calcd for $\text{C}_{25}\text{H}_{24}\text{N}_2\text{O}_2$ $[\text{M} + \text{H}]^+$: 385,18; found 385,2. ^1H NMR (CDCl_3 , 400 MHz): δ 11.52 (s, 1H, NH), 8.56 (d, 1H, $J = 8.4$ Hz, Bn), 7.79–7.36 (m, 9H, Bn), 7.15 (m, 4H, Bn), $\delta_{\text{A}} = 3.92$, $\delta_{\text{B}} = 3.59$ (syst AB, 2H, $J_{\text{AB}} = 12.8$ Hz, CH_2Bn), 3.32 (dd, 1H, $J_{\alpha,\beta} = 4.4$ Hz, $J_{\alpha,\beta} = 10.0$ Hz, H_{α}), 3.22 (dd, 1H, $J_{\delta,\delta} = J_{\delta,\gamma} = 6.4$ Hz, H_{δ}), 2.41 (dd, 1H, $J_{\beta,\beta} = 8.8$ Hz, $J_{\beta,\gamma} = 16$ Hz, $\text{H}_{\beta'}$), 2.26 (ddd, 1H, $J_{\delta\delta} = 6.4$ Hz, $J_{\delta\gamma} = 12.8$ Hz, $J_{\delta\gamma} = 22$ Hz, $\text{H}_{\delta'}$), 1.96 (ddd, 1H, $J_{\beta,\beta} = 8.8$ Hz, $J_{\beta,\gamma} = 4.4$ Hz, $J_{\beta,\gamma} = 16.4$ Hz, H_{β}), 1.85–1.76 (m, 2H, $\text{H}_{\gamma}, \text{H}_{\gamma'}$). ^{13}C NMR (CDCl_3 , 100 MHz): δ 198.03 (Ph-CO-Ph), 174.64 (COOH), 139.16, 138.54, 138.12, 133.37, 132.55, 132.48, 130.11, 129.12, 128.30, 128.15, 127.05, 125.32, 122.19, 121.52 (18 Ar), 68.25 (C_{α}), 59.82 (CH_2Bn), 53.85 (C_{δ}), 30.98 (C_{β}), 24.14 (C_{γ}).

6.8.3 Synthesis of [Gly-Ni-BPB]

A solution of BPB 3 g (7.79 mmol, 1 eq), glycine 1.17 g (15.58 mmol, 2 eq.), and $\text{Ni}(\text{NO}_3)_2 \cdot 6\text{H}_2\text{O}$ 4.53 g di (15.58 mmol, 2 eq.) in dry MeOH (25 ml) was prepared under N_2 . Then, a freshly prepared solution of 2.5 M MeONa/MeOH (8 mL, 20 mmol) was added. The resulting mixture was stirred at 55–65°C for 1h (a prolonged heating of the reaction mixture might result to a partial racemization of the BPB moiety), and then neutralized with 10% aqueous citric acid (500 mL). The product was extracted with CH_2Cl_2 (4×40 mL), dried over Na_2SO_4 , and the solvent removed under vacuum.



The product was extracted with CH_2Cl_2 (4×40 mL), dried over Na_2SO_4 , and the solvent removed under vacuum.

Yield 95%. TLC: R_f 0.31 (DCM/Aceton 2:1, detected with UV 254 nm). ESI-MS: m/z calcd for $\text{C}_{27}\text{H}_{25}\text{N}_3\text{NiO}_3$ $[\text{M} + \text{H}]^+$: 498,20 ; found 498,3. ^1H -NMR (CDCl_3 , 200MHz): δ 8.27 (d, 1H, $J = 8.8$ Hz, Bn), 8.07 (d, 1H, $J = 7.2$ Hz, Bn), 7.51–7.30 (m, 6H, Bn), 7.24–6.69 (m, 6H, Bn), $\delta_{\text{A}} = 4.48$, $\delta_{\text{B}} = 3.69$ (syst AB, 2H, $J_{\text{AB}} = 6.2$ Hz,

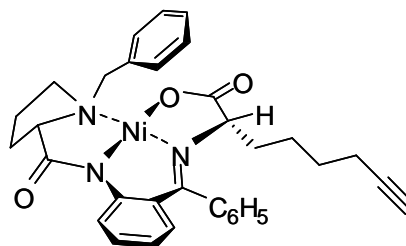
CH₂Bn), 3.51-3.31 (m, 2H, H_{αPro}), 2.63-2.41 (m, 3H, H_{δPro}, H_{αα'Gly}), 2.13-1.91 (m, 4H, H_{β'Pro}, H_{δ'Pro}, H_{βPro}, H_{γ'Pro}, H_{γ'Pro}). ¹³C-NMR (CDCl₃, 50MHz): δ 181.19 (CO_{Gly}), 177.18 (CO-N-Ph), 171.49 (C=N), 134.53, 133.11, 132.16, 131.66, 129.67, 129.53, 129.28, 129.06, 128.87, 126.19, 125.60, 125.12, 124.21, 120.82 (18 Ar), 69.96 (C_{αPro}), 63.23 (CH₂Bn), 61.38 (C_{αGly}), 57.60 (C_{δPro}), 30.90 (C_{βPro}), 23.89 (C_{γPro}).

6.9 Alkylation of the Gly-Ni-BPB complex with bromoalkynes. General procedure

To a stirred mixture of Gly-Ni-BPB (1.56 g, 3.14mmol, 1 eq.) in anhydrous DMF (4 ml) were added, under N₂, finely powdered NaOH (753 mg, 18.84 mmol, 6 eq., pH 12) and bromoalkyne (4.71 mmol, 1.5 eq.). The reaction was checked by TLC (DCM/acetone 2:1, detected by UV 254 nm). After 20 min., the reaction mixture was treated with 0.1 M HCl (100 ml) and the red product extracted with CH₂Cl₂ (4 × 40 mL), dried over MgSO₄, and the solvent removed under vacuum. The crude was purified by flash chromatography on silica gel (CH₂Cl₂—Me₂CO 2/1) affording the product as a red amorphous solid.

6.9.1 Alkylation of the Gly-Ni-BPB complex with 6-bromohex-1-yne (n=4)

Yield 59%. TLC: *R_f* 0.63 (DCM/ Me₂CO 2:1; detected by UV 254 nm). ESI-MS: *m/z* calcd for C₃₃H₃₄N₃NiO₃ [M + H]⁺: 578.2; found 578.4. ¹H NMR (CDCl₃, 400 MHz): δ 8.12 (d, 1H, *J* = 8.4 Hz, ArH), 8.04 (d, 2H, *J* = 7.6 Hz, ArH), 7.50–7.44 (m, 3H, ArH), 7.33 (t, 2H, *J* = 7.6 Hz, ArH),

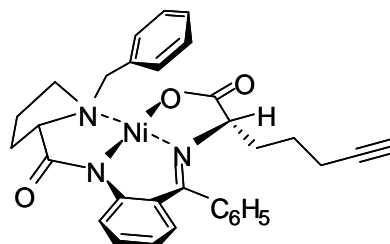


7.26–7.10 (m, 3H, ArH), 6.92 (d, 1H, *J* = 7.6 Hz, ArH), 6.66–6.60 (m, 2H, ArH), 4.42 (d, 1H, *J* = 12.8 Hz, PhCH₂), 3.91 (dd, 1H, *J*₁ = 3.4 Hz; *J*₂ = 7.8 Hz, Pro α-H), 3.57 (d, 1H, *J* = 12.8 Hz, PhCH₂), 3.52–3.43 (m, 3H), 2.79–2.73 (m, 1H), 2.56–2.46 (m, 1H), 2.36–2.30 (m, 1H), 2.16–2.02 (m, 4H), 1.97–1.88 (m, 1H), 1.91 (t, 1H, *J* = 2.4 Hz, C≡CH), 1.76–1.61 (m, 2H), 1.44–1.32 (m, 2H). ¹³C NMR (CDCl₃, 50 MHz): δ 180.32 (O–C=O), 179.30 (N–C=O), 170.46 (C=N), 142.27, 133.81, 133.21, 132.12, 131.54, 129.73, 128.94, 128.89, 128.85, 127.55, 127.14, 126.47, 123.66,

120.69 (18 × Ar), 83.86 (HC≡C), 70.28 (HC≡C), 70,10 (Pro C-α), 68.83 (Bn CH₂), 63.13 (C-COO), 56.99 (Pro C-δ), 34.53 (Pro C-β), 30.76 (C≡C-CH₂-C), 27.93 [C≡C-(CH₂)₃-C], 24.30 (Pro C-γ), 23.67 (C≡C-(CH₂)₂-C), 18.14 (C≡C-C).

6.9.2 Alkylation of the Gly-Ni-BPB complex with 5-bromopent-1-yne (n=3)

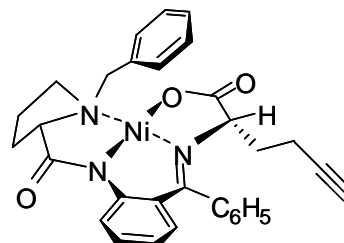
Yield 56%. TLC: *R_f* 0.58 (DCM/ Me₂CO 2:1; detected by UV 254 nm). RP-UPLC: *R_t* 3.59 min. (50–100% of B in 5 min). ESI-MS: *m/z* calcd for C₃₂H₃₂N₃NiO₃ [M + H]⁺: 564.2; found 564.5. ¹H NMR (CDCl₃, 400 MHz): δ 8.12 (d, 1H, *J* = 8.4 Hz, ArH), 8.04 (d, 2H, *J* = 7.6 Hz, ArH), 7.50–7.41 (m, 3H, ArH), 7.33 (t, 2H,



J = 7.6 Hz, ArH), 7.25–7.10 (m, 3H, ArH), 6.95 (d, 1H, *J* = 7.6 Hz, ArH), 6.64–6.60 (m, 2H, ArH), 4.43 (d, 1H, *J* = 12.6 Hz, PhCH₂), 3.86 (dd, 1H, *J*₁ = 3.4 Hz; *J*₂ = 8.8 Hz, Pro α-H), 3.56 (d, 1H, *J* = 12.6 Hz, PhCH₂), 3.52–3.43 (m, 3H), 2.79–2.72 (m, 1H), 2.54–2.48 (m, 1H), 2.35–2.20 (m, 1H), 2.20–2.05 (m, 3H), 2.05–1.95 (m, 2H), 1.93 (t, 1H, *J* = 2.6 Hz, C≡CH), 1.78–1.70 (m, 2H). ¹³C NMR (CDCl₃, 100 MHz): δ 180.37 (O-C=O), 179.15 (N-C=O), 170.54 (C=N), 142.27, 133.67, 133.24, 132.16, 131.54, 129.71, 129.01, 128.89, 128.86, 127.63, 127.07, 126.38, 123.71, 120.71 (18 × Ar C), 83.47 (HC≡C), 70.27 (HC≡C), 69.99 (Pro C-α), 69.06 (Bn CH₂), 63.11 (C-COO), 57.05 (Pro C-δ), 34.53 (Pro C-β), 30.75 (C≡C-CH₂-C), 24.36 [C≡C-(CH₂)₂-C], 23.73 (Pro C-γ), 18.15 (C≡C-C).

6.9.3 Alkylation of the Gly-Ni-BPB complex with 4-bromo-1-butyne (n=2)

Yield 32%. TLC: *R_f* 0.62 (DCM/Me₂CO 2:1; detected by UV 254 nm). RP-UPLC: *R_t* 2.56 min. (50–100% of B in 5 min). ESI-MS: *m/z* calcd for C₃₁H₃₀N₃NiO₃ [M + H]⁺: 550.2; found 550.19. ¹H NMR (CDCl₃, 400 MHz): δ 8.04-7.94 (m, 3H, *J* = 8.4 , ArH), 7.48–7.35 (m, 3H, ArH), 7.3-7.27 (m,



2H, ArH), 7.25–7.10 (m, 3H, ArH), 6.89 (d, 1H, *J* = 7.2 Hz, ArH), 6.60–5.50 (m, 2H, ArH), 4.39 (d, 1H, *J* = 12.4 Hz, PhCH₂), 3.79 (dd, 1H, *J*₁ = 3.6 Hz; *J*₂ = 8.4 Hz, Pro

α -H), 3.52 (d, 1H, $J = 12.4$ Hz, PhCH₂), 3.50–3.42 (m, 3H), 2.8–2.7 (m, 1H), 2.48–2.23 (m, 2H), 2.20–2.0 (m, 1H), 2.00–1.95 (m, 2H), 1.89 (t, 1H, $J = 2.2$ Hz, C \equiv CH), 1.75–1.67 (m, 2H).

6.10 Hydrolysis of the alkylated complexes. General procedure

A solution of the alkylated complex (1.85 mmol) in MeOH (31 ml) was added to warm 2 M HCl (21.8 mL) and the mixture refluxed for 30 min. The solution changes color from deep red to yellow and was detected by TLC (DCM/Me₂CO 2:1, detected by UV 254 nm). After cooling to RT, 1 M NaOH was added until pH 6 and the solvent removed under vacuum. The yellow solid residue was washed with DCM and dried under vacuum. BPB was quantitatively recovered by extraction with CH₂Cl₂. The dried solid product was dissolved in H₂O/MeOH 4:3 (23 ml) and then gently swirled overnight with Chelex 100 H⁺ resin (7.7 g), converted from its Na⁺ form by treatment with HNO₃ 2.5 M (46 ml) by washing with H₂O. The mixture was filtered and the resin washed with water, the layers of combined filtrates were evaporated under vacuum, and the residue lyophilized. The crude was purified by FCC (CH₂Cl₂ to CH₂Cl₂—MeOH 10/1) to obtain the pure amino acid as a yellow oil.

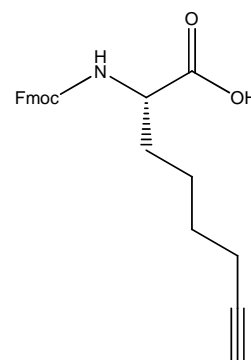
6.10.1 2S-[[[(9H-Fluoren-9-ylmethoxy) carbonyl]amino]-7-octynoic acid (n=4)

Yield 38%. TLC: R_f 0.5 (DCM/MeOH 10:1). RP-UPLC: R_t 4.12 min (50–100% di B in 5 minuti). ESI-MS: m/z calcd for

C₂₃H₂₃NNaO₄ [M + Na]⁺ 400.15; found 400.3. [α]_D –3.1 (c 1.0,

MeOH). ¹H NMR (CDCl₃, 400 MHz): δ 7.75 (*pseudo* d, 2H, $J = 7.6$ Hz, fluorenyl 4-H and 5-H), 7.59 (*pseudo* d, 2H, $J = 7.6$ Hz, fluorenyl 1-H and 8-H), 7.37 (*pseudo* t, 2H, fluorenyl 3-H and 6-H), 7.28 (*pseudo* t, 2H, fluorenyl 3-H and 6-H), 5.79

(broad s, COOH), 5.48(m, 1H, NH), 4.44–4.38 (m, 3H, CH₂–O and α -H), 4.21 (t, 1H, $J = 6.8$ Hz, fluorenyl 9-H), 2.08–1.99 (m, 3H), 1.94 (t, 1H, $J = 2.4$ Hz, HC \equiv C), 1.80–1.75 (m, 1H), 1.58–1.42 (m, 4H, 2 \times CH₂). ¹³C NMR (CDCl₃, 100 MHz): δ 176.63 (COOH), 156.17 (CONH), 143.83, 143.67 and 141.29 (fluorenyl C-4a, C-4b, C-8a, and C-9a), 127.71, 127.06, 125.04 (fluorenyl C-2 to C-7), 119.98 (fluorenyl C-



1 and C-8), 83.97 (HC≡C), 68.69 (CH₂-O), 67.06 (HC≡C), 53.83 (C-α), 47.15 (fluorenyl C-9), 31.73 and 27.81 (C-β and δ), 24.31 (C-γ), 18.15 (C-ε).

6.10.2 2S-[[*(9H*-Fluoren-9-ylmethoxy)carbonyl] amino]-6-heptynoic acid (n=3)

Yield 28%. TLC: R_f 0.47 (DCM/MeOH 9:1). RP-UPLC: R_t

3.54 min. (50–100% B in 5 min). ESI-MS: *m/z* calcd for

C₂₂H₂₁NNaO₄ [M + Na]⁺ 386.14; found 386.2. [α]_D -3.0 (*c*

1.0, MeOH). ¹H NMR (CDCl₃, 400 MHz): δ 7.73 (d, 2H, *J* =

7.2 Hz, fluorenyl 4-H and 5-H), 7.57 (d, 2H, *J* = 7.4 Hz,

fluorenyl 1-H and 8-H), 7.39 (*pseudo t*, 2H, fluorenyl 3-H and

6-H), 7.30 (*pseudo t*, 2H, fluorenyl 2-H and 7-H), 6.60 (broad s, COOH), 5.51 (m,

1H, NH), 4.43–4.35 (m, 3H, CH₂-O and α-H), 4.18 (t, 1H, *J* = 6.6 Hz, fluorenyl 9-

H), 2.08–1.99 (m, 3H), 1.94 (t, 1H, *J* = 2.4 Hz, HC≡C), 1.80–1.75 (m, 1H), 1.58–

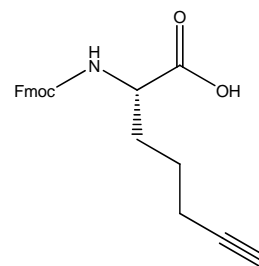
1.42 (m, 2H, CH₂). ¹³C NMR (CDCl₃, 100 MHz): δ 177.06 (COOH), 156.26

(CONH), 143.81, 143.62 and 141.27 (fluorenyl C-4a, C-4b, C-8a, and C-9a), 127.70,

127.06 and 125.05 (fluorenyl C-2 to C-7), 119.96 (fluorenyl C-1 and C-8), 83.49

(HC≡C), 69.11 (CH₂-O), 67.06 (HC≡C), 53.77 (C-α), 47.11 (fluorenyl C-9), 31.33

(C-β), 24.28 (C-γ), 18.01 (C-δ).



6.10.3 2S-[[*(9H*-Fluoren-9-thoxy) carbonyl] amino]-5-hexynoic acid (n=2)

Yield 32%. RP-UPLC: R_t 3.37 min. (50–100% B in 5

min.). ESI-MS: *m/z* calcd for C₂₁H₁₉NNaO₄ [M + Na]⁺

372.14; found 372. ¹H NMR (CDCl₃, 400 MHz): d 7.73

(d, 2H, *J* = 7.2 Hz, fluorenyl 4-H e 5-H), 7.56 (d, 2H, *J*

= 7.3 Hz, fluorenyl 1-H e 8-H), 7.37 (*pseudo t*, 2H,

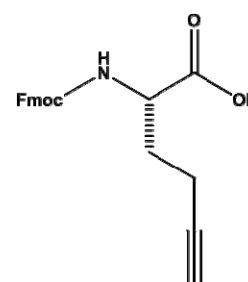
fluorenyl 3-H e 6-H), 7.30 (*pseudo t*, 2H, fluorenyl 2-H

e 7-H), 6.71 (s broad, COOH), 5.8 (m, 1H, NH), 4.48–

4.30 (m, 3H, CH₂-O e α-H), 4.21 (t, 1H, *J* = 6.7 Hz,

fluorenyl 9-H), 2.45–2.31 (m, 3H), 2.22–2.10 (m, 1H), 2.00 (t, 1H, *J* = 2.1 Hz,

HC≡C).



6.11 General procedure for click chemistry

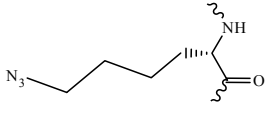
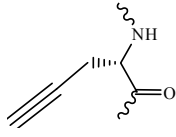
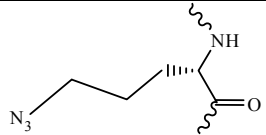
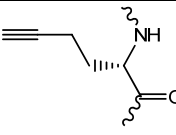
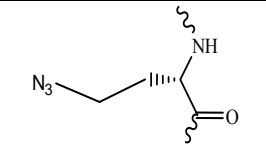
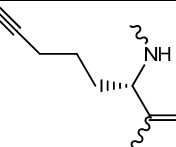
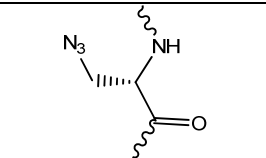
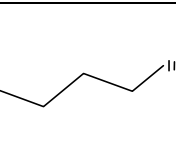
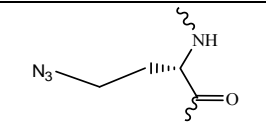
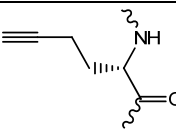
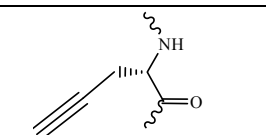
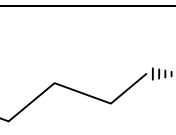
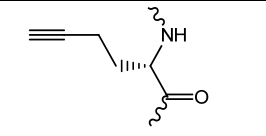
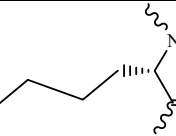
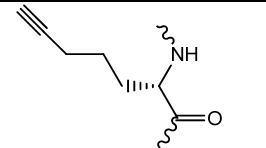
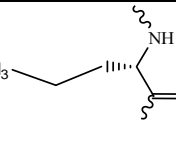
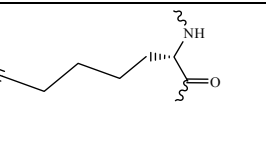
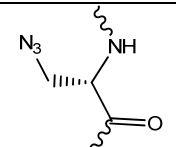
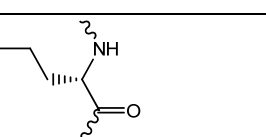
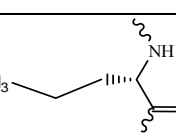
Purified linear peptide precursors I'-X' (>95% purity), were subjected to solution-phase intra chain Cu^I-catalyzed side chain-to-side-chain azide-alkyne 1,3-dipolar Huisgen cycloaddition (CuAAC). Linear pure peptides 5 mg (4.77 μmol) were added to a solution of CuSO₄·5H₂O (10 mg, 40 μmol), ascorbic acid (10 mg, 56 μmol) in 5 mL of H₂O/tBuOH :2/1 v/v.

Mixture was stirred at RT overnight and the solution was concentrated and lyophilized. Complete and clean conversion of all linear precursors into the desired 1,2,3-triazolyl-containing cyclopeptides I-X was observed. The reaction of cyclization was monitored by ACQUITY UPLC (Waters Corporation, Milford, Massachusetts) coupled to a single quadrupole ESI-MS (Micromass ZQ) using a 2.1 x 50 mm 1.7 μm ACQUITY BEH C18 at 30 °C, with a flow rate of 0.6 mL/min employing a linear gradient of 10% to 60% of B in A in 5 min (A 0.1% TFA in H₂O; B 0.1% TFA in ACN).

6.12 Lactam bridge formation. General procedure

The fully protected resin-bound peptide was synthesized on a manual batch synthesizer, as described in general procedure. The formation of the lactam bridges between side chain groups of Lys¹⁰ and Asp⁵ was performed in solid phase, following an orthogonal protocol of deprotection. In particular Lys¹⁰ was protected in side chain with 1-[(4,4 - dimethyl - 2,6 - dioxocyclohex -1-ylidene)ethyl] group (Dde), stable in the condition of elongation of the peptide. After acetylation of the *N*-terminal, Dde was removed by two consecutive steps, using hydrazine 20% in DMF (1mL), first for 5 min, followed by an additional step with freshly prepared deprotection mixture for 15 min. After deprotection of Lys¹⁰, the formation of intramolecular lactam bond was performed using TBTU/HOBt/NMM (2.5:2.5:3.5 equiv.) as coupling system in DMF for 40 min.

The reaction of cyclization was monitored by UPLC-ESI-MS analysis of MW-assisted mini-cleavage resin bond fragment. Mini-cleavages were performed using DiscoverTMS-Class single-mode MW reactor as described before.

Linear peptide	Yaa(& ¹) ⁵	Xaa(& ²) ¹⁰
V'		
VI'		
VII'		
VIII'		
X'		
I'		
II'		
III'		
IV'		
X'		

6.13 cAMP based functional bioassay

HEK-293 cells stably expressing the mouse melanocortin receptors were transiently transfected with 4 μg CRE/ β -galactosidase reporter gene as described in the literature^{149, 150}. Briefly, 5,000 to 15,000 post transfection cells were plated into collagen treated 96 well plates (Nunc) and incubated overnight. Forty-eight hours post-transfection the cells were stimulated with 100 μL peptide (10^{-6} - 10^{-12} M) or forskolin (10^{-4} M) control in assay medium (DMEM containing 0.1 mg/mL BSA and 0.1 mM isobutylmethylxanthine) for 6 hrs. The assay media was aspirated and 50 μL of lysis buffer (250 mM Tris-HCl pH=8.0 and 0.1% Triton X-100) was added. The plates were stored at -80°C overnight. The plates containing the cell lysates were thawed the following day. Aliquots of 10 μL were taken from each well and transferred to another 96-well plate for relative protein determination. To the cell lysate plates 40 μL phosphate-buffered saline with 0.5% BSA was added to each well. Subsequently, 150 μL substrate buffer (60 mM sodium phosphate, 1 mM MgCl_2 , 10 mM KCl, 5 mM β -mercaptoethanol, 2 mg/mL ONPG) was added to each well and the plates were incubated at 37°C . The sample absorbance, OD_{405} , was measured using a 96 well plate reader (Molecular Devices). The relative protein was determined by adding 200 μL 1:5 dilution Bio Rad G250 protein dye:water to the 10 μL cell lysate sample taken previously, and the OD_{595} was measured on a 96 well plate reader (Molecular Devices). Data points were normalized to the relative protein content. EC_{50} values represent the mean of three or more independent experiments. EC_{50} estimates, and their associated standard errors of the mean, were determined by fitting the data to a nonlinear least-squares analysis using the PRISM program (v4.0, GraphPad Inc.).

6.14 NMR conformational analysis

Sample for NMR were prepared by dissolving 1.2 mg of the lactam- and heterodetic [1,2,3]triazolyl-containing cyclo-heptapeptides in 0.5 mL of aqueous phosphate buffer (pH 6.6, 100 mM). Samples were lyophilized and dissolved in a mixture of DMSO/water (0.5 mL, 80:20, v/v). NMR spectra were recorded on a Bruker DRX-600 spectrometer. One-dimensional (1D) NMR spectra were recorded in the Fourier mode with quadrature detection. The water signal was suppressed by a low-power selective irradiation in the homogated mode. DQF-COSY, TOCSY, and NOESY experiments were run in the phase-sensitive mode using quadrature detection in ω_1 by time-proportional phase incrementation of the initial pulse. Data block sizes comprised of 2048 addresses in t_2 and 512 equidistant t_1 values. Before Fourier transformation, the time domain data matrices were multiplied by shifted \sin^2 functions in both dimensions. A mixing time of 70 ms was used for the TOCSY experiments. NOESY experiments were run at 300 K with mixing times in the range of 100-250 ms. The qualitative and quantitative analyses of DQF-COSY, TOCSY and NOESY spectra were obtained using the SPARKY interactive program package. Complete proton resonance assignments were achieved following Wüthrich's procedure. Sequential and medium range Nuclear Overhauser Effects (NOEs)-derived distances were used to generate 3D models of the heterodetic [1,2,3]triazolyl-containing cyclo-heptapeptides. The final *pdb* files were analyzed and validated using PROMOTIF software.

6.14.1 NMR structure calculation

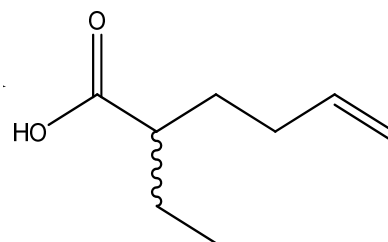
On the basis of sequential and medium range NOE derived distances, 3D models of lactam- and [1,2,3]triazolyl-peptides were generated with a simulated annealing procedure using the DYANA software package²²⁷. All structures were energy minimized with the SANDER module of the AMBER 5 program^{228,229} using for 1000 steps the steepest descent method and for 4000 steps the conjugate gradient method. A non-bonded cut-off of 12 Å and a distance-dependent dielectric term ($\epsilon = 4 * r$) were used. The minimization protocol included three steps in which NOE derived distances were used as constraints with a force constant, respectively, of 1000, 100, and 10 kcal/molÅ. The final *pdb* files were analyzed and validated using PROCHECK software²³⁰.

7 EXPERIMENTAL PART B

7.1 Synthesis of 1-hydroxy-2-ethylhex-5-ene

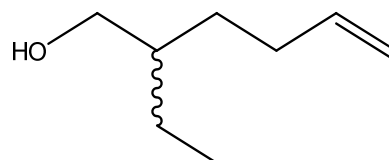
7.1.1 2-ethylhex-5-enoic acid

To a cooled solution (0 °C) of lithium diisopropylamide (31.0 mL of a 2 M solution in THF–n-heptane, 62 mM) was added, under nitrogen, hex-5-enoic acid (2.8 g, 24 mM) in anhydrous THF (28 mL). After stirring at room temperature for 30 min and subsequent cooling to 0 °C, iodoethane (5.7 g, 36 mM) was added. The mixture was stirred for 3 h at room temperature and the reaction was then quenched with 3 M HCl (100 mL). After removal of THF, the reaction mixture was extracted with Et₂O and the combined organic phases were washed with 1 M NaOH. The aqueous basic layer was acidified to pH ~ 1 with conc. HCl and then extracted with Et₂O. The crude acid isolated after drying over Na₂SO₄ and removal of the solvent, was used without further purification in the next step. Yield 96%; TLC: (Et₂O–n-hexane 1:1, detected by (e), *R_f* = 0.47); ¹H NMR (CDCl₃) 0.94 (3H, t, J 7.4 Hz, CH₃), 1.55–1.81 (4H, m, CH₂), 2.12 (2H, m, CH₂–CH=CH₂), 2.38 (H, m, CH), 5.02 (2H, m, =CH₂), 5.80 (H, ddt, J 16.9, 10.1, 6.9 Hz, CH=).



7.1.2 2-ethylhex-5-en-1-ol

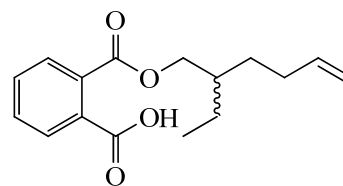
To a solution of 2-ethylhex-5-enoic acid (3.25 g, 23 mM) in dry Et₂O (65 mL) at 0 °C was slowly added LiAlH₄ (2.15 g, 57 mM). After stirring at room temperature for 2 h, the mixture was quenched with H₂O (200 mL) and concd. HCl was added until the solution became clear. The resulting mixture was extracted with Et₂O. The combined organic phases were washed with brine and dried over Na₂SO₄, followed by column chromatography on silica gel with Et₂O–petroleum ether 1 :5, then Et₂O–petroleum ether 1 :2 as eluent to give 1 (1.8 g, 64%); TLC: (Et₂O–petroleum ether



1:5, detected by (g), $R_f = 0.20$); IR(KBr): $\nu_{\text{max}}(\text{film})/\text{cm}^{-1}$ 3340 (OH), 1640 (C=C), 1040 (C–O); ^1H NMR (CDCl_3) 0.91 (3H, t, J 7.4 Hz, CH_3), 1.26–1.60 (6H, m, CH_2 , CH, OH), 2.09 (2H, m, $\text{CH}_2\text{-CH=CH}_2$), 3.57 (2H, d, J 4.4 Hz, OCH_2), 4.96 (H, dm, J 10, 2 Hz, $=\text{CH}_2$), 5.03 (H, dm, J 17 Hz, $=\text{CH}_2$), 5.38 (H, ddt, J 17, 10.2, 6.6 Hz, CH=); ^{13}C NMR (CDCl_3) 11.03 (CH_3), 23.25, 29.66, 30.86 (CH_2), 39.12 (CH), 67.35 (OCH_2), 114.0 ($\text{CH}_2=$), 139.0 (CH=).

7.1.3 Mono(2-ethylhexenyl) 1,2-benzenedicarboxylate (MEHP)

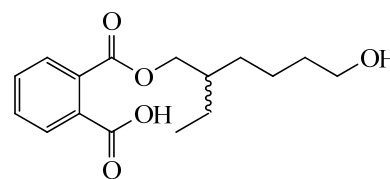
2-Ethyl-5-hexen-1-ol (2.2 g, 17.2 mmol), phthalic anhydride (2.54 g, 17.2 mmol) and pyridine (1.6 mL) were refluxed under nitrogen for 3 h. The mixture was quenched with cold water and extracted with Et_2O . The organic phase was washed



twice with a solution of 10% HCl to remove pyridine. Finally, the mixture was extracted with 0.4 M K_2CO_3 . The aqueous basic layer was acidified to pH 1 with 1 M HCl and then extracted with Et_2O . After drying with Na_2SO_4 and evaporation of the solvent under vacuum, MEHP was obtained as a colourless oil and used without further purification in the next step. Yield 94%. TLC: (Et_2O /hexane 1:1, detected by (a), $R_f = 0.15$). ESI-MS: calcd for $[\text{M}+\text{H}]^+$ 277.3. Found 277.9. ^1H NMR d 0.90 (3H, t, $J = 8$ Hz, CH_3), 1.24–2.14 [7H, m, $\text{CH}_2 = \text{CH}(\text{CH}_2)_2\text{CHCH}_2\text{CH}_3$], 4.25 (2H, d, $J = 6$ Hz, COOCH_2), 4.96 (2H, dd, $J = 10$, $J = 1.8$ Hz, $\text{CH}_2=$), 5.02 (1H, br, OH), 5.76 (1H, m, CH=), 7.61 and 7.81 (4H, 2 m, aromatic CH). ^{13}C NMR d 10.9 (CH_3), 23.6 (CH_3CH_2), 29.9 ($\text{CH}_2\text{CH=CH}_2$), 30.9 ($\text{CH}_2\text{CH}_2\text{CH=CH}_2$), 38.1 ($\text{CH}_3\text{CH}_2\text{CH}$), 68.0 (COOCH_2), 114.5 (CH=CH₂), 128.6–133.4 (aromatic C), 138.5 (CH=CH₂), 168.2 (COOCH_2), 172.3 (COOH).

7.1.4 Mono(2-ethyl-6-hydroxyhexyl) 1,2-benzenedicarboxylate (6-OH-MEHP)

B_2H_6 (1 M) in THF (5.5 mL) was added, drop by drop at 0 °C under nitrogen, to a solution of MEHP (1.52 g, 5.5 mmol) in anhydrous THF (50 mL). After stirring at room temperature for 1 h, excess of hydride was destroyed with H_2O (0.1 mL). After 5 min, 3 N



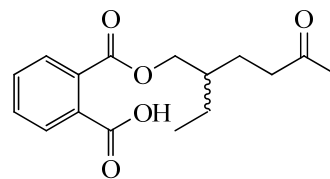
NaOH (0.5 mL) and 30% H_2O_2 (0.5 mL) were added and the reaction mixture was

stirred for 1 h at 50 °C. The mixture was extracted with Et₂O, washed with brine and dried over Na₂SO₄ and FeSO₄. The crude alcohol was isolated after evaporation of the solvent under vacuum, and purified by FCC (CHCl₃/MeOH/AcOH 90:2:2) to obtain the product as a yellow oil.

Yield 89%. TLC: (AcOEt/petroleum ether 1:1, detected by (a) and (f), *R_f* = 0.3). ESI-MS: calcd for [M+H]⁺ 295.3. Found 295.4; calcd for [M+Na]⁺ 317.3. Found 317.3. ¹H NMR d 0.90 (3H, t, CH₃), 1.44 [9H, m, CH₃CH₂CH(CH₂)₃CH₂OH], 2.92 (1H, br, OH), 3.84 (2H, m, CH₂OH), 4.23 (2H, m, COOCH₂), 7.56 and 7.74 (4H, 2 m, aromatic CH). ¹³C NMR d 11.1(CH₃), 22.0 (CH₃CH₂), 24.0 [CH₂(CH₂)₂OH], 29.9 [CH₂(CH₂)₃OH], 31.9 (CH₂CH₂OH), 38.9 (CHCH₂CH₃), 61.9 (CH₂OH), 67.4 (COOCH₂), 128.5–132.9 (aromatic C), 168.6 (COOCH₂), 170.1 (COOH).

7.1.5 Mono(2-ethyl-5-oxohexyl) 1,2-benzenedicarboxylate (5-oxo-MEHP)

MEHP (2.46 g, 8.9 mmol) was added, drop by drop in 5 min, to a solution of PdCl₂ (16 mg, 0.089 mmol) and p-benzoquinone (1.06 g, 9.8 mmol) in DMF/H₂O (7:1, 24 mL). After stirring overnight at room

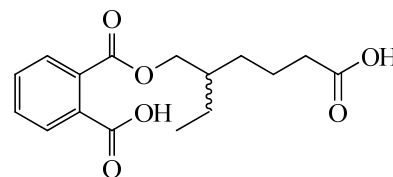


temperature, the reaction mixture was quenched with 3 N HCl (60 mL) and extracted with ether. The organic phase was washed with 10% NaOH and brine. The aqueous basic layer was acidified to pH 1 with 3 N HCl and then re-extracted with Et₂O. The crude product was purified by FCC (CHCl₃/MeOH/AcOH 90:2:2), and obtained as yellow oil.

Yield 41%. TLC: (AcOEt/petroleum ether 2:1, detected by (a), *R_f* = 0.2). ESI-MS: calcd for [M+H]⁺ 291.3. Found 291.1. IR (KBr) cm⁻¹: 3500–2500 (OH), 2964.5 (CH), 1714.2 (C=O). ¹H NMR d 0.92 (3H, t, CH₃), 1.3 (2H, m, CH₂CH₃), 1.69 (3H, m, CHCH₂CH₂CO), 2.19 (3H, s, COCH₃), 2.52 (2H, m, CH₂CO), 4.2 (2H, m, OCH₂), 7.64 and 7.8 (4H, m, aromatic CH). ¹³C NMR d 11.1 (CH₃CH₂), 23.7 (CH₃CH₂), 24.7 (CH₂CH₂CO), 30.0 (aliphatic CH), 38.2 (CH₃CO), 40.6 (CH₂CO), 63.5 (OCH₂), 128.7–131.5 (aromatic C),

7.1.6 Mono(5-carboxy-2-ethylpentyl) 1,2-benzenedicarboxylate (5-cx-MEHP)

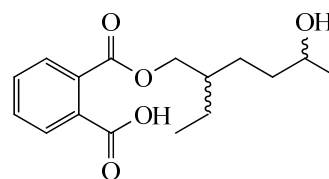
Jones' reagent (1 M, 2 mL), prepared from CrO₃ (6.7 g) in 96% H₂SO₄ (6 mL) and H₂O (50 mL), was added, drop by drop at 15–20 °C, to 6-OH-MEHP (553 mg, 1.88 mmol) in anhydrous acetone (6 mL). The precipitated reduced



chromium salt was centrifuged off. The solution was quenched by addition of H₂O and extracted with Et₂O that was dried over Na₂SO₄. Methanol or NaHSO₃ was added to the brown solution to eliminate residue Cr(VI) salts. The crude acid was extracted with 0.4 M K₂CO₃. The aqueous layer, acidified to pH 1 with 1 M HCl, was extracted with CHCl₃ and dried over Na₂SO₄. The product was purified by FCC (CHCl₃/MeOH/AcOH 90:2:2). 5-cx-MEHP was obtained as a colourless oil. Yield 94%. TLC: (AcOEt/hexane 1:1, detected by (a), *R_f* = 0.5). ESI-MS: calcd for [M+H]⁺ 309.3. Found 309.0. ¹H NMR δ 0.90 (3H, t, CH₃), 1.42 (4H, m, (CH₂)₂CH₂COOH), 1.65 (3H, m, CHCH₂CH₃), 2.38 (2H, m, CH₂COOH), 4.22 (2H, m, OCH₂), 6.25 (2 COOH), 7.8–7.5 (4H, m, aromatic CH). ¹³C NMR δ 10.9 (CH₃), 23.6 (CH₂CH₂COOH), 30.0 (CH₂CH₂CH₂COOH), 34.2 (CHCH₂CH₃), 38.5 (CH₂COOH), 67.7 (OCH₂), 132.9–128.7 (aromatic C), 168.1 (COOCH₂), 172.1 (CH₂COOH), 179.8 (aromatic C).

7.1.7 Mono(2-ethyl-5-hydroxyhexyl) 1,2-benzenedicarboxylate (5-OH-MEHP)

A solution of NaBH₄ (117 mg, 3.16 mmol) in ethanol (2 mL) was slowly added to compound 5-oxo-MEHP (231 mg, 0.79 mmol). After stirring at room temperature for 2 h, the mixture was



quenched with H₂O (1 mL). The aqueous basic layer was acidified to pH 1 with concd HCl and then extracted with n-hexane. The crude alcohol, isolated after concentration under vacuum, was purified by FCC (CHCl₃/MeOH/AcOH 90:2:2) affording 5-OH-MEHP as an oil. Yield 48%. TLC: (EtOAc/petroleum ether 2:1, detected by (a) and (f), *R_f* = 0.3). ESI-MS: calcd for [M+H]⁺ 294.3. Found 294.8. ¹H NMR δ 0.90 (3H, t, CH₃), 1.25 (3H, d, *J* = 6.2, CH₃CHOH), 1.45 (6H, m, CH₂CH₂CHOH and CH₃CH₂), 1.75 (1H, m, HCH₂CH₃), 4.07 (2H, m, OCH₂), 4.36 (1H, m, CHOH), 6.25 (1H, br, OH), 7.41 and 7.74 (4H, m, aromatic CH). ¹³C NMR

d 11.1 (CH₃CH₂), 23.9 (CH₃CHOH), 24.7 (CH₃CH₂), 27.2 (CH₂CH₂CHOH), 35.7 (CHCH₂CH₃), 39.3 (CH₂CHOH), 66.7 (CHOH), 69.5 (OCH₂), 128.8–131.8 (aromatic C), 168.4 (COOCH₂), 170.6 (COOH).

8 Detection of DEHP metabolites in urines

8.1.1 Calibration curves

The quantitative analysis was carried out using an high-performance liquid chromatography tandem mass spectrometry RP-HPLC -ESI-MS (Waters, Alliance 2695, Waters, Micromass ZQ) equipped with phenyl column (Betasil, 5 µm, 50 mm x 3 mm, Keystone Scientific, Bellefonte, PA) and with a Waters 2996 Photodiode Array Detector. An aliquot of each sample (20 µL) was injected into the apparatus. All reagents were of at least analytical reagent grade. Calibration curves for the quantitative urine analysis were calculated for all the DEHP metabolites plotting peak area average (y) against concentration of standards (x). Stock solutions (100 µg/mL in ACN) of all the metabolites were prepared and stored at -20 °C in Teflon-capped glass bottle until use. Five working solutions (2.5µg/mL; 1.5µg/mL; 1.0µg/mL; 0.25 µg/mL, 0.025µg/mL) for calibration curve plotting, were prepared for all the metabolites by dilution of the stocks in water. These solutions spanned the desired analytical range for each analyte (2.5 to 2500 ng/mL) without exceeding the linear range of the method. Standard solutions were stable 6 months once stored at 4 °C. The chromatographic separations of metabolites were resolved using a linear gradient from 3% to 60 % B in 10 min (solvent system A: 0.1% acetic acid in water; B: 0.1% acetic acid in ACN). The flow rate was 0.6 mL/min. The column temperature was 32 °C. A guard column (XBridgeTm Phenyl 3.5µm, 3.0x20 mm) was used to prevent column degradation. Column eluates were monitored at 215, 230 and 254 nm. The mass specific detection was achieved using a Waters, Micromass ZQ Electrospray ionization (ESI) in positive ion mode. The product ion with higher signal intensity was selected for the quantitative analysis for each of the four phthalates. The optimal MS parameters were as follows: the source and desolvation temperature were 120 °C and 400 °C respectively; the capillary voltage was 3.24 kV; cone voltage 30 kV, nitrogen gas was used as desolvation gas and as cone gas as well; the cone gas and the desolvation flow was 60 L/h and 800 L/h respectively;

The collision gas was argon with a flow of 0.60 ml/min. Data were acquired and processed using MassLynx™ software (Waters). All standards were injected three times in the same day. Curves with correlation coefficients (R^2) greater than 0.998 were generated (MEHP, 5-OH-MEHP, 5-oxo-MEHP 0.999; 6-OH-MEHP 0.998). Instrument software Empower Software built 1154 generated a result spreadsheet.

8.2 Samples pre-treatment

For urines pre-treatment the following buffers were prepared: buffer ammonium acetate 1 M pH 6.5; acid buffer pH 2.0 by preparing a solution of NaH_2PO_4 (0.14 M) and 1% of 85% H_3PO_4 ; basic buffer was prepared by adding concentrated ammonium hydroxide (1 mL 30% NH_3 solution) to a 50:50 acetonitrile/water (200 mL). All buffers were stored in sealed bottles at room temperature: basic buffer was discarded after one week, acid buffer after one month.

8.2.1 Sample preparation: solid-phase extraction (SPE)

Human urine (1.00 mL) defrosted, sonicated, mixed, and dispensed in glass tubes. Samples were subsequently buffered with ammonium acetate (250 μL , pH 6.5). Incubation with β -glucuronidase (5 μL , 200 units/mL) was performed at 37 °C for 90 min, resulting in quantitative glucuronide hydrolysis of phthalates metabolites. First, an SPE cartridge was equilibrated with 1.0 mL of acetonitrile followed by 2.0 mL of basic buffer. This SPE cartridge was used to retain compounds that are hydrophobic at basic pH while allowing the more acidic analytes to elute. Next, the deconjugated urine samples were diluted with 1.0 mL of basic buffer solution and vortex mixed for 5 s. These samples were then added to an equilibrated SPE cartridge (3 mL/60 mg of Oasis HLB, Waters). The eluate was collected in borosilicate glass tubes. Residual analyte on the first cartridge was eluted by adding a second 1.0 mL of basic buffer to the cartridge. The combined basic buffer eluates were acidified by adding 3.0 mL of acidic buffer and mixed thoroughly. SPE solvent flows were monitored while samples were on the cartridges to maximize sorbent-analyte interaction (<2 mL/min). A second SPE cartridge (3 mL/60 mg of Oasis HLB, Waters) was equilibrated by washing with acetonitrile (1.0 mL) followed by water (1.0 mL) and acidic buffer (2.0 mL). We further purified the acidified sample by adding it to the second SPE cartridge and washing this cartridge with acidic buffer

(3.0 mL, Figure 2). We removed residual salts by washing the second cartridge with water (9 mL). The analytes were eluted with acetonitrile (2 mL) followed by ethyl acetate (2 mL). This pooled eluate was evaporated to dryness under a stream of dry nitrogen. The residue was resuspended in water (200 μ L), transferred to a glass autosampler vial insert, and analyzed by RP-HPLC-ESI-MS. Prepared samples could be stored at 4 °C for up to two weeks before analysis without degradation; no significant loss of analyte signal was observed until after 10 days of room-temperature storage. Long-term storage of unextracted urine specimen at -40 °C for six months showed no decrease in phthalate monoester levels.

8.2.2 Daily protocol

In typical sample set were included water samples as blank, processed through the entire process along with unknown urine samples to monitor contamination, and one quality control (QC) sample. The QC sample was spiked with pooled urine and DEHP metabolites standards in known concentration (200 ng/mL). When urine analysis resulted in values of metabolites concentration exceeding from linear range of the analytical method, we subjected a new aliquot of the same sample to the entire process (deconjugation and SPE) and we analysed again. To verify the absence of DEHP metabolites contamination, all materials used during the analysis and SPE, were prescreened by RP-HPLC-ESI-MS. Before analysis, known concentration samples were treated by SPE and analysed by HPLC-ESI-MS to test SPE efficiency.

References

- ²²⁷ Guntert P., Mumenthaler C., Wuthrich K., *J. Mol. Biol.*, **1997**, 273(1), 283-298.
- ²²⁸ Case D.A., Pearlman D.A., Caldwell J.W., Cheatham I.T.E., Ross W.S., Simmerling C.L., Darden T.A., Merz K.M., Stanton R.V., Cheng A.L., Vincent J.J., Crowley M., Ferguson D.M., Radmer R.J., Seibel G.L., Singh U.C., Weiner P.K., Kollman P.A. Amber 5. *University of California, San Francisco* **1997**.
- ²²⁹ Pearlman D.A., Case D.A., Caldwell J.W., Ross W.S., Cheatham I.T.E., DeBolt S., Ferguson D., Seibel G., Kollman P.A. *Comput. Phys. Commun.* **1995**, 91, 1-41.
- ²³⁰ Laskowski R.A., Rullmann J.A., MacArthur M.W., Kaptein R., Thornton J.M., *J. Biomol. NMR* **1996**, 8 (4), 477-486.

9 Abbreviations

ABC: Autism Behaviour Checklist

AC: Adenilato cyclise

ACN: Acetonitrile

ACTH: Adrenocorticotropic Hormone

ADHD: attention-deficit/hyperactivity disorder

ADOS: Autism Diagnostic Observation Schedule

AgRP: Agouti-related protein

AK: actinic keratosis

AIFA: Agenzia Italiana del Farmaco

ANN: Artificial Neural Networks

ASD: Autism Spectrum Disorder

ATP: Adenosina trifosfato

AUCG: Areas Under the Curve of glucose

AUCI: Areas Under the Curve of insulin

AutoCM: Auto Contractive Map

BMI: Body mass index

cAMP: cyclic Adenosine MonoPhosphate

CARS: Childhood Autism Rating Scalescores

CDC: Center for Disease Control

CPE: carboxypeptidase E

CSI: chemical shift index

BMI: Body mass index

Boc: tert-butoxycarbonyl

BP: *N*-benzyl-(*S*)-proline

BPB: (*S*)-2-(*N*-benzylprolyl)aminobenzophenone

BSA: phosphate-buffered saline

β -LPH: β lipotropina

5-cx-MEHP: mono(2-ethyl-5-carboxypentyl) 1,2-benzenedicarboxylate

CD: Circular Dichroism

CDC: Center for Disease Control

CNS: central nervous system

CPE: carboxypeptidase E
CREB: cAMP response element binding protein
CuAAC: Copper catalysed azide alkyne cycloaddition
DAG: Diacilglicerolo
DBP: Dibutyl phthalate
DCM: dichloromethane
Dde: 1-[(4,4 - dimethyl - 2,6 - dioxocyclohex -1-ylidene)ethyl]
DEHP: di-2-ethyl hexyl phthalate
DIEA: N,N-Diisopropylethylamine,
DMF: *N,N*-dimethylformamide
DMSO: Dimetilsolfossido
DNA: Acido desossiribonucleico
DOTA: tetraazacyclododecane tetraacetic acid
DSM-IV-TR: Diagnostic and Statistical Manual of Mental Disorders
DTPA: diethylene triamine pentaacetic acid
ED: Endocrine Disruptors
EDT: 1,2-ethanedithiole
EMA: European Medicines Agency
EPP: erythropoietic protoporphyria
ESI-MS: Electrospray Ionization Mass Spectrometry
FDA: US Food and drug administration
FGIR: fasting glucose/ insulin ratio
Fmoc: 9-H-fluoren-9-yl-methoxycarbonyl
Fmoc-OSu: N-(9-fluoren-9-yl-methoxycarbonyloxy)-succinimide
FSD: Female Sexual Dysfunction
GABA: γ aminobutyric aci
GH: growth hormone
GPCRs: G protein-coupled receptors
GTP: Guanosintrifosfato
HDL: High-density lipoprotein
HOBt: 1-hydroxybenzotriazole
HOMA-IR: homeostasis model assessment estimate of insulin resistance
HPA/HTPA: Hypothalamic-Pituitary-Testicular Axis

HPLC: high performance liquid chromatography
IARC: International Agency for Cancer Research
IGT: impaired glucose tolerance
IP3: inositol 1,4,5-trisphosphate
IR: infrared
LC-ESI-MS: liquid chromatography-electrospray ionization/ mass spectrometry
LH: luteinizing hormone
LLOD: lower limit of detection
LLOQ: lower limit of quantification
LPH: lipotropin
MCRs: Melanocortin Receptors
MEHP: mono(2-ethylhexenyl) 1,2-benzenedicarboxylate
mRNA: Acido ribonucleico messaggero
MSH: Melanocyte stimulating hormon
MT-I: Melanotan I
MT-II: Melanotan II
MW: microwave
N-AT: N-acetyltrasferase
NDP-MSH: [Nle⁴, D-Phe⁷]- α -MSH
NGT: normal glucose tolerance
NMM: N-methylmorpholine
NMP: N-methylpyrrolidone
NMR: nuclear magnetic resonance
NOE: Nuclear Overhauser Effects
5-OH-MEHP: mono(2-ethyl-5-hydroxyhexyl) 1,2-benzenedicarboxylate
6-OH-MEHP: : mono(2-ethyl-6-hydroxyhexyl) 1,2-benzenedicarboxylate
5-oxo-MEHP: mono(2-ethyl-5-oxohexyl) 1,2-benzenedicarboxylate
OGTT: oral glucose tolerance test
ON: overnight
PAM: peptidyl α -amidating monooxygenase
Pbf: 2,2,4,6,7-pentametildiidrobenzofurano-5-sulfonile
PC1: Proormone convertasi 1
PCBs: polychlorinated biphenyls

PDD: Pervasive Developmental Disorders
PDD-NOS: pervasive developmental disorder non otherwise specified
PK A: protein kinase A
PKU: phenylketonuria
PMLE: polymorphous light eruption
POMC: Proopiomelanocortina
PPAR: peroxisome-proliferator activated receptor
PRCP: prolylcarboxypeptidase
Pro-ACTH: proormone adrenocorticotropo
PTH: Parathyroid hormone
PTH-Rc: PTH-Receptor
PTHrP: PTH-related protein
PVC: Polyvinylchloride
QC: quality-control
QUICKI: Quantitative Insulin Sensitivity Check Index
RCM: Ring Closing Metathesis
RNA: Ribonucleic Acid
ROC: Receiver Operating Characteristic
RP-HPLC: reverse phase-high performance liquid chromatography
RSD: relative standard deviation
RT: room temperature
Rt: retention time
RuAAC: Ruthenium catalysed azide alkyne cycloaddition
SAR: Structure Activity Relationship
SD: standard deviation
SEM: Standard Error of Mean
SNN: Sistema Sanitario Nazionale
SPE: Solid Phase Extraction
SPPS: Solid Phase Peptide Synthesis
SRIF: somatotropin release-inhibiting factor
SST: somatostatin receptors
SU: solar urticaria
T3: triiodothyronine

T4: thyroxine

TBTU: 2-(1H-benzotriazole-1-yl)-1,1,3,3-tetramethyluronium tetrafluoroborate

tBu: tert-butyl

TFA: trifluoroacetic acid

TFE: 2,2,2-trifluoroethanol

TLC: thin layer chromatography

TGA: Australian Therapeutic Good Administration

Trt: triphenylmethyl

TSH: Thyroid Stimulating Hormone

UGT: UDP-glucuronyltransferase

UPLC: Ultra Performance Liquid Chromatography

UV: Ultraviolet

WBISI: whole body insulin sensitivity index

**Conventional and Microwave-assisted SPPS approach: a comparative study of
PTHrP(1-34) synthesis**

**Fabio Rizzolo,^{1,3} Chiara Testa,^{1,2,3} Michael Chorev,^{4,5} Paolo Rovero,^{1,6} Anna Maria
Papini,^{1,2,3}**

¹ *Laboratory of Peptide & Protein Chemistry & Biology, Polo Scientifico e Tecnologico, University of Florence, I-50019 Sesto Fiorentino (FI), Italy,* ² *Laboratoire SOSCO – EA4505 Université de Cergy-Pontoise Neuville-sur-Oise, 95031 Cergy-Pontoise, France,* ³ *Department of Chemistry “Ugo Schiff”, University of Florence, I-50019 Sesto Fiorentino (Fi), Italy,* ⁴ *Laboratory for Translational Research, Harvard Medical School, One Kendall Square, Building 600, Cambridge, MA 02139, USA,* ⁵ *Department of Medicine, Brigham and Women’s Hospital, 75 Francis Street, Boston, MA 02115, USA,* ⁶ *Department of Pharmaceutical Science, Polo Scientifico e Tecnologico, University of Florence, Via Ugo Schiff 3, I-50019 Sesto Fiorentino (Fi), Italy*

Parathyroid hormone (PTH) is an 84-amino acid polypeptide playing a significant role in calcium homeostasis. Parathyroid hormone-related peptide is a distant homologue of PTH and is not a true hormone. It is synthesized in cartilage and in many more tissues than parathyroid hormone, and its secretion is not regulated by serum calcium. It mimics the actions of PTH as a result of its structural homology and its ability to bind and signal via the PTH/PTHrP receptor in bone and kidney [1].

Based on the amino acid sequence, it was deduced that the first 34 amino-terminal amino acids should be sufficient for biological activity. Availability of highly purified parathyroid polypeptide and active synthetic fragments made it possible to develop radioimmunoassay.

Considering the presence of sterically hindered amino acid residues in the sequences, such as Arginine and Phenylalanine between position 19-23, and the length of the peptide, we optimised the synthesis of PTHrP(1–34), comparing conventional Solid-Phase Peptide Synthesis (SPPS) protocol with a Microwave-assisted one.

References

T.J. Gardella, M.D. Luck, A.K. Wilson, H.T. Keutmann, S.R. Nussbaum, J.T. Potts, Jr. and H.M. Kronenberg, *J. Biol. Chem.* **1995**, *270*, 6584-6588.

Click chemistry reaction: a challenge for peptide engineering to play with bioactive secondary structure

Chiara Testa^{1,2,3}, Stefano Carganico^{1,2,3}, Alexandra Le Chevalier Isaad^{1,2}, Mario Scrima⁴, Anna Maria D'Ursi⁴, Paolo Rovero^{1,5}, Sonia Cantel⁶, Michael Chorev⁶, and Anna Maria Papini^{1,2,3}.

¹Laboratory of Peptide & Protein Chemistry & Biology, Polo Scientifico e Tecnologico, University of Firenze, 50019 Sesto Fiorentino, Italy; ²Dipartimento di Chimica "Ugo Schiff", Polo Scientifico e Tecnologico, University of Firenze, via della Lastruccia 13, 50019 Sesto Fiorentino, Italy; ³Laboratoire de Synthèse Organique Sélective et Chimie bioOrganique EA4505, University of Cergy-Pontoise ⁴Dipartimento di Scienze Farmaceutiche, via Ponte Don Melillo 11C, 84084 Salerno, Italy; ⁵Dipartimento di Scienze Farmaceutiche, University of Firenze, via Ugo Schiff 3, Polo Scientifico e Tecnologico, 50019 Sesto Fiorentino, Italy ⁶Laboratory for Translational Research, Harvard Medical School, One Kendall Square, Building 600, Cambridge, Massachusetts 02139, USA.

Peptide engineering relies on synthetic procedures to fold peptides into bioactive structures. Side chain-to-side chain cyclization is used to stabilize a bioactive conformation and to reduce proteolytic degradation. Among the numerous modes of cyclization, bioisosteric modifications and cyclizations that do not require orthogonal protection schemes, are of great interest. The recently introduced Cu(I)-catalyzed azide-alkyne 1,3-dipolar Huisgen's cycloaddition [1-3] as click chemistry reaction [4] presents a promising opportunity to develop a new paradigm for intramolecular cyclization. In fact, the proteolytic stable 1,4-disubstituted [1,2,3]triazolyl bridge surrogates the isosteric peptide bond for a new structural constraint. We report the preparation of N α -Fmoc- ω -azido- α -amino acids by diazo-transfer of the N α -protected ω -amino- α -amino acid or a multistep strategy from the N α -protected ω -hydroxy- α -amino acid. The N α -Fmoc- ω -ynoic- α -amino acids were prepared by alkylation of Ni(II) complexes of the Schiff bases derived from glycine and a chiral inducer with alk- ω -ynyl bromides [5]. These building blocks were used in solid phase synthesis of series of 8 linear nonapeptides derived from the sequence of PTHrP(11-19) where ω -azido- and ω -ethynyl- α -amino acids replaced Lys¹³ and Asp¹⁷. Cleavage from the resin and side chain deprotection, followed by intramolecular Cu(I)-catalyzed click reaction, generated a series of i-to-i+4 1,4-disubstituted [1,2,3]triazole-bridged cyclopeptides.[6] The CD and NMR conformational analysis allowed to identify the permutations that mimic at the best the cyclo[Lys13,Asp14]PTH(11-19) [7]. This study lays the ground work to design novel bioactive cyclopeptidomimetics using this novel intramolecular rigidification mode. Further applications of this strategy [8] will be shown on octreotide analogs conjugated to tetraazamacrocycles to be used in tumour pretargeting as well as on MTH analogs.

SUPPLEMENTARY MATERIAL

References

- [1] Huisgen, R. in 1,3-Dipolar Cycloaddition Chemistry, Wiley, New York, 1984, pp 1-176.
- [2] Rostovtsev, V. V. et al. *Angew. Chem. Int. Ed. Engl.* 2002, 41, 2596.
- [3] Tornøe, C. W. et al. *J. Org. Chem.* 2002, 67, 3057.
- [4] Kolb, H. C. et al. *Angew. Chem. Int. Ed. Engl.* 2001, 40, 2004.
- [5] Le Chevalier Isaad, A. et al. *Eur. J. Org. Chem.* 2008, 5308.
- [6] Cantel, S. et al. *J. Org. Chem.* 2008, 73, 5663.
- [7] Scrima M. et al. *Eur. J. Org. Chem* 2010, 3, 446.
- [8] Le Chevalier-Isaad, A. et al. *Peptide Protocol Paper. J. Pept. Sci.* 2009, 15, 451.

Relationships between urinary concentrations of PHTALOX, obesity and insulin sensitivity in obese children: a pilot study.

Street ME¹, Papini AM^{2,3}, Testa C^{2,3}, Nuti F^{2,3}, Grossi E.⁴, Bernasconi S

¹University Hospital of Parma, Italy, ²Laboratory of Peptide & Protein Chemistry & Biology, University of Florence, Italy and Laboratoire SOSCO – EA4505 Université de Cergy-Pontoise, France; ³Department of Chemistry “Ugo Schiff”, University of Florence, Italy, ⁴Bracco Foundation, Milan, Italy

Data suggest that endocrine-disrupting chemicals, as phthalates, found in a variety of household products, may influence mechanisms related to obesity. In vitro studies have shown that these chemicals may interact with PPARs and play a key role in the differentiation of adipocytes and deposition of triglycerides in adipose tissue.

The aim was to evaluate possible associations among urinary phthalate secondary metabolites and age, gender, pubertal development, age at onset of obesity, BMI, waist circumference, indexes of insulin sensitivity and metabolic syndrome in obese children.

We studied 39 subjects (20 M, 19 F, age: 12,23 ± 0,45 yr, BMI SDS: 3,34 ± 0,06).

Whole body insulin sensitivity index (WBISI), Areas Under the Curve of glucose (AUCG) and insulin (AUCI) were calculated from a five-point OGTT. HOMA-IR and QUICKI, were calculated. Urine concentrations of secondary metabolites derived from di(2-ethylhexyl)phthalate (PHTALOX) were measured in triplicate using an RP-HPLC method, using as synthetic standards the corresponding univocally characterised MEHP, mono(2-ethyl-6-hydroxyhexyl) and the oxidised forms 6-OH-MEHP, 5-OH-MEHP, and 5-oxo-MEHP.

Results were analyzed by standard statistical methods and using a special kind of artificial neural network (Auto-CM) obtaining a subsequent semantic map of actual relationship between variables.

A negative correlation of MEHP with the age at onset of obesity was shown (R: -0,36). MEHP was correlated also with AUCG (R: -0,33), AUCI (R: -0,35) and WBISI (R: +0,33). 5-Oxo-MEHP instead was significantly correlated with the age at onset of obesity (R: +0,51).

The connectivity map showed a direct relationship of 5-oxo-MEHP with BMISDS. The sum of the metabolites showed a direct relationship with the height SDS suggesting that height may be related with the ability to metabolise phthalates. MEHP showed a direct relationship with the insulinogenic index, and normal insulin sensitivity. This latter was directly related with 5-oxo-MEHP. Interestingly, 5-OH-MEHP was directly connected with the HOMA index and abnormal insulin sensitivity.

SUPPLEMENTARY MATERIAL

In conclusion, the results supported the hypothesis that the higher metabolites in urine, the earlier the onset of obesity, and suggested that some PHTALOX metabolites are capable of influencing insulin sensitivity. However, the less phthalates were metabolised (higher MEHP urine concentrations) the later was the onset of obesity. It remains, thus, to be elucidated whether exposure to phthalates *per se* is actually the risk factor or if the ability of the body to metabolise phthalates is actually the key point. This could explain also the positive relationship of MEHP with WBISI.

**Probing the Bioactive Conformation of melanocortin like peptide by
Click Reaction**

**Chiara Testa,^[a,b,c] Francesca Nuti,^[a,b] Mario Scrima,^[d] Anna Maria D'Ursi,^[d] Nadeje
Lubin Germain^[c], Michael Chorev,^[e,f] Paolo Rovero,^[a,g] Anna Maria Papini,^[a,b,c]**

^[a] Laboratory of Peptide & Protein Chemistry & Biology, Polo Scientifico e Tecnologico, Università di Firenze, I-50019 Sesto Fiorentino (FI), Italy, ^[b] Department of Chemistry, Università di Firenze, I-50019 Sesto Fiorentino (Fi), Italy, ^[c] Laboratoire SOSCO - UMR 8123 Université de Cergy-Pontoise Neuville-sur-Oise, 95031 Cergy-Pontoise, France, ^[d] Department of Pharmaceutical Science, Via Ponte Don Melillo 11C, Salerno, I-84084, Italy, ^[e] Laboratory for Translational Research, Harvard Medical School, One Kendall Square, Building 600, Cambridge, MA 02139, USA, ^[f] Department of Medicine, Brigham and Women's Hospital, 75 Francis Street, Boston, MA 02115, USA, ^[g] Department of Pharmaceutical Science, Polo Scientifico e Tecnologico, University of Firenze, Via Ugo Schiff 3, 50019 Sesto Fiorentino (Fi), Italy

MT-II is a potent super-agonist of melanocortin receptors, characterized by lactam bridge between residues i and i+5 stabilizing a type-II β -turn structure fundamental for the bioactivity.^[1] The minimal active sequence is identified by the following tetrapeptide: His⁶-D-Phe⁷-Arg⁸-Trp⁹^[2].

Side chain-to-side chain cyclizations are of great interest because they are bioisosterics to the lactam bridge and do not require orthogonal protection schemes.

Intramolecular side chain-to-side chain cyclization is an established approach to achieve stabilization of specific conformations and represents a recognized strategy to avoid proteolytic degradation.

In our previous work^[3] we designed and studied a new intramolecular side chain-to-side chain [1,2,3]triazolyl modification, based on the well studied i-to-i+4 side-chain to side-chain structure present in parathyroid hormone-related protein (PTHrP).

Therefore we applied this strategy on MT-II sequence, stabilizing the β -turn conformation by the introduction of i-to-i+5 side chain-to-side chain cyclization *via* formation of a 1,4-disubstituted 1,2,3-triazolyl bridge.

In this context we performed the synthesis of different azido and alkynyl amino acids^[4,5], to introduce them as building blocks in the sequence of MT-II. By click reaction we obtained 1,4-disubstituted 1,2,3-triazolyl-bridge corresponding to the ring size of MT-II, characterized by 5 methylenes. Our goal is to explore all the different permutations in terms of location and orientation of the 1,2,3-triazolyl bridge. Conformational studies are in progress to evaluate the best type-II β -turn behavior required for biological activity.

SUPPLEMENTARY MATERIAL

References

- [¹] F. Al-Obeidi, A.M. de Lauro Castrucci, V.J. Hadley, *J. Med Chem.*, **1989**, *32*, 2555-2561.
- [²] J. Ying, K.E. Kövér, X.Gu, G. Han, D.B. Trivedi, M.J. Kavarana, V.J. Hruby, *Biopolymers*, **2003**, *71*, 696-716.
- [³] S.Cantel, A. Le Chavelier Isaad, M. Scrima, J.J. Levy, R. D. DiMarchi, P.Rovero, J.A. Halperin, A.M. D'Ursi, A.M. Papini, M. Chorev, *J.Org.Chem*, **2008**, *73*, 5663-5674.
- [⁴] A. Le Chevalier Isaad, A. M. Papini, M. Chorev and P. Rovero, *J. Pept. Sci.*, **2009**, *15*, 451-454.
- [⁵] A. Le Chevalier Isaad, F. Barbetti, P. Rovero, A. M. D'Ursi, M. Chelli, M.Chorev, A.M. Papini, *Eur.J. Org. Chem*, **2008**, *31*, 5308-5314.

Conventional and microwave-assisted SPPS approach: a comparative synthesis of PTHrP(1-34)NH₂

Fabio Rizzolo,¹ Chiara Testa,^{1,2} Duccio Lambardi,³ Michael Chorev,^{4,5} Mario Chelli,¹ Paolo Rovero,³ and Anna Maria Papini^{1,2}

¹Laboratory of Peptide & Protein Chemistry & Biology, c/o Department of Chemistry "Ugo Schiff", Via della Lastruccia 3/13, Polo Scientifico e Tecnologico, University of Florence, I-50019 Sesto Fiorentino, Italy. ²Laboratoire PeptLab-SOSCO - EA4505 Université de Cergy-Pontoise, 5 mail Gay-Lussac, Neuville-sur-Oise, Cergy-Pontoise 95031, France. ³Laboratory of Peptide & Protein Chemistry & Biology, c/o Department of Pharmaceutical Science, Via Ugo Schiff 6, Polo Scientifico e Tecnologico, University of Florence, I-50019 Sesto Fiorentino, Italy. ⁴Laboratory for Translational Research, Harvard Medical School, Cambridge, MA 02139, USA. ⁵Department of Medicine, Brigham and Women's Hospital, Boston, MA 02115, USA.

The application of microwave irradiation in peptide chemistry has been reported in several publications, most of which describe case studies of successful syntheses of difficult peptides [1,2,3]. Our herein reported study compares the RT with MW-assisted SPPS of the 1-34 N-terminal fragment of parathyroid hormone-related peptide (PTHrP) using the same instrument (Liberty™, CEM), and monitors the synthesis by UPLC-ESI-MS of microwave-assisted mini-cleaved fragments of the growing peptide chain (Figure 1). Identification of some deletion sequences was helpful to recognize critical couplings and helped to guide the introduction of microwave irradiations to these stages.

PTHrP is an autocrine, paracrine and intracrine regulator of processes such as endochondrial bone formation and epithelial-mesenchymal interactions during the development of mammary glands. In the past, this sequence was the subject of numerous structure-activity-conformation relationship studies [4,5]. Importantly, the proximity of clusters of arginines, sterically hindered, and hydrophobic amino acids sequences represent a synthetic challenge that was the subject of our comparative study reported herein.

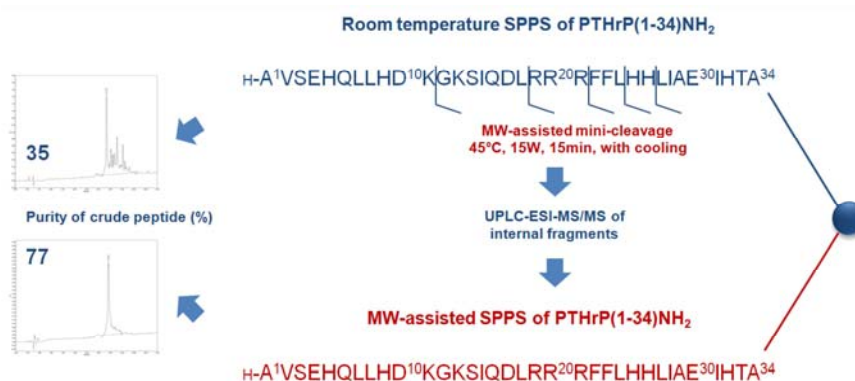


Figure 1. General SPPS scheme.

SUPPLEMENTARY MATERIAL

[1] Rizzolo F, Sabatino G, Chelli M, Rovero P, Papini AM, *Int. J. Pept. Res. Ther.* 2007; **13**: 203-208.

[2] Bacsa B, Bosze S, Kappe CO. Direct solid-phase synthesis of the beta-amyloid (1-42) peptide using controlled microwave heating. *J. Org. Chem.* 2010; **75**: 2103-2106.

[3] Friligou I, Papadimitriou E, Gatos D, Matsoukas J, Tselios T. Microwave-assisted solid-phase peptide synthesis of the 60-110 domain of human pleiotrophin on 2-chlorotrityl resin. *Amino Acids* 2010 (published on line 26 September), pp. 1-10.

[4] Stewart AF. Hypercalcemia associated with cancer. *N. Engl. J. Med.* 2005; **352**: 373-379.

[5] Mannstadt M, Jüppner H, Gardella TJ. Receptors for PTH and PTHrP: their biological importance and functional properties. *Am. J. Physiol.* 1999; **277**: 665-675.



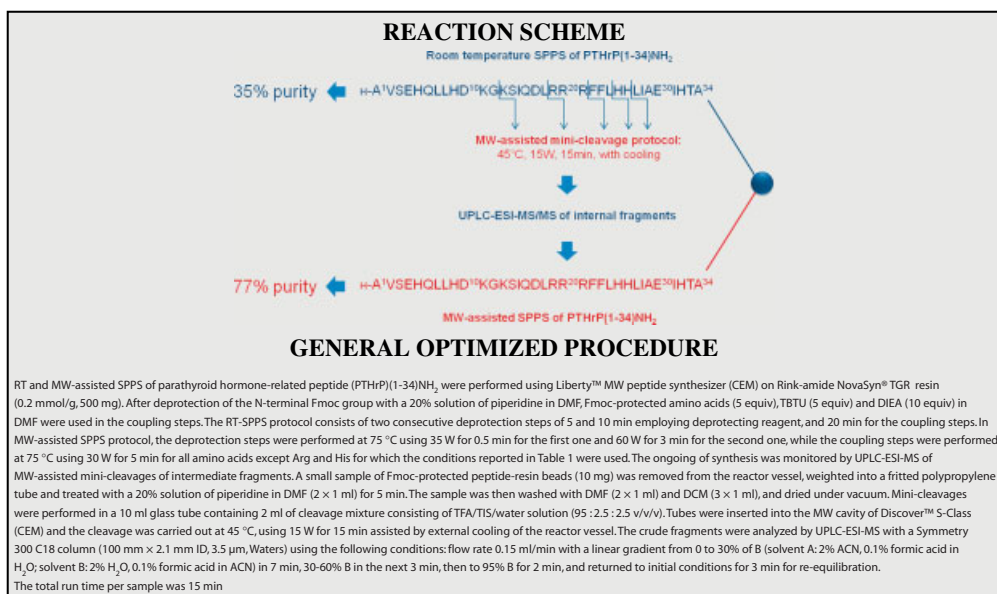
Conventional and microwave-assisted SPPS approach: a comparative synthesis of PTHrP(1–34)NH₂

Fabio Rizzolo,^a Chiara Testa,^{a,b} Duccio Lambardi,^c Michael Chorev,^{d,e} Mario Chelli,^a Paolo Rovero^c and Anna Maria Papini^{a,b*}

Attracted by the possibility to optimize time and yield of the synthesis of difficult peptide sequences by MW irradiation, we compared Fmoc/tBu MW-assisted SPPS of 1–34 N-terminal fragment of parathyroid hormone-related peptide (PTHrP) with its conventional SPPS carried out at RT. MWs were applied in both coupling and deprotection steps of SPPS protocol. During the stepwise elongation of the resin-bound peptide, monitoring was conducted by performing MW-assisted mini-cleavages and analyzing them by UPLC-ESI-MS. Identification of some deletion sequences was helpful to recognize critical couplings and as such helped to guide the introduction of MW irradiations to these stages. Copyright © 2011 European Peptide Society and John Wiley & Sons, Ltd.

Supporting information may be found in the online version of this article

Keywords: microwave irradiation; solid-phase peptide synthesis; microwave-assisted mini-cleavages; difficult peptide sequences; parathyroid hormone-related peptide; UPLC-ESI-MS analysis



Scope and Comments

The introduction in 1992 of MW irradiation in peptide chemistry stimulated a host of interest followed by numerous efforts to use it to overcome synthetic difficulties resulting in sluggish reactions, low yields and complex reaction crude products that were hard to purify [1]. During the last decade the growing interest in MW field has been marked by the progress in developing scientific MW equipment to embrace specific research needs [2–5]. In general, introduction of MW technology led to the shortening of reaction time that resulted in higher purity of crudes and increased yields of the pure final product.

* Correspondence to: Anna Maria Papini, Department of Chemistry "Ugo Schiff", Laboratory of Peptide & Protein Chemistry & Biology, Via della Lastruccia 3/13, Polo Scientifico e Tecnologico, University of Florence, I-50019 Sesto Fiorentino, Italy. E-mail: annamaria.papini@unifi.it

- a Department of Chemistry "Ugo Schiff", Laboratory of Peptide & Protein Chemistry & Biology, Via della Lastruccia 3/13, Polo Scientifico e Tecnologico, University of Florence, I-50019 Sesto Fiorentino, Italy
- b Laboratoire PeptLab-SOSCO – EA4505 Université de Cergy-Pontoise, 5 mail Gay-Lussac, Neuville-sur-Oise, Cergy-Pontoise 95031, France
- c Department of Pharmaceutical Sciences, Laboratory of Peptide & Protein Chemistry & Biology, Via Ugo Schiff 6, Polo Scientifico e Tecnologico, University of Florence, I-50019 Sesto Fiorentino, Italy
- d Laboratory for Translational Research, Harvard Medical School, Cambridge, MA 02139, USA
- e Department of Medicine, Brigham and Women's Hospital, Boston, MA 02115, USA

Abbreviations used: ACN, acetonitrile; MW, microwave; NMP, N-methyl-2-pyrrolidone; RT, room temperature; TIS, triisopropylsilane.

The application of MW irradiation in peptide chemistry has been reported in several publications, most of which describe case studies of successful syntheses of difficult peptide sequences [6–8]. However, a definitive comparison of conventional RT and MW-assisted-SPPS protocols must be performed on identical instruments. In fact, comparing conventional RT and MW-assisted SPPS carried out on different instruments that apply protocols that differ in the equivalent excess of reagents and their molar ratios, stirring techniques and the nature and number of washing steps, may be misleading. Moreover, the automated synthesizers are generally developed to produce peptides without monitoring of the progress of the synthesis. Therefore by-products caused by side reactions such as aspartimide and diketopiperazine formation, incomplete couplings and deprotections may be detected only after the final cleavage of the deprotected peptide from the resin.

In this study we compared the Fmoc/tBu RT-SPPS with the MW-assisted synthesis of the 1–34 *N*-terminal fragment of PTHrP using the same instrument (Liberty™, CEM, Matthews, NC, USA), and monitoring the progress of the synthesis by UPLC-ESI-MS of MW-assisted mini-cleaved fragments of the growing peptide chain.

PTHrP is an autocrine, paracrine and intracrine regulator of processes such as endochondrial bone formation and epithelial–mesenchymal interactions during the development of mammary glands. In analogy to PTH, most of the known biological functions are exerted by the *N*-terminal PTHrP(1–34) fragment that has 60% sequence similarity to PTH(1–34). The sequence of PTHrP(1–34)NH₂ is shown in Figure 1. In the past, this sequence was the subject of numerous structure–activity–conformation relationship studies [9,10]. Importantly, the presence of clusters of arginine, of sterically hindered and hydrophobic amino acid residues in the sequence represents a synthetic challenge that was the subject of our comparative study reported herein.

The synthesis was initially carried out following the conventional RT protocol using the Liberty™ automated peptide synthesizer excluding MW irradiations. As modern automated SPPS protocols allow the assembly of larger and increasingly complex peptides, a precise control of the coupling reactions is a crucial prerequisite in peptide synthesis. In fact monitoring the progress of synthesis allows the detection of undesirable products caused by side reactions, incomplete couplings or deprotections. Although different methods have been developed for monitoring of SPPS, we observed that the use of colorimetric monitoring or continuous-flow UV absorbance of the reaction column effluent was not informative enough to identify difficult steps in the synthesis. Therefore, we decided to monitor the progress of PTHrP(1–34)NH₂ synthesis by UPLC-ESI-MS analyses of small aliquots of cleaved peptide fragments obtained by MW-assisted mini-cleavages. The application of MW-assisted mini-cleavages of resin-bound peptides has been proposed as a fast, reliable method to monitor SPPS [11]. After specific coupling cycles, suspected to be difficult, we stopped the synthesizer and withdrew a small aliquot for analysis by UPLC-ESI-MS. In particular, we focused our attention on the PTHrP fragments related to the 19–28 sequence, characterized by clusters of Arg residues and highly hydrophobic residues (see Reaction Scheme and Figure 1).

By UPLC-ESI-MS analyses of intermediate fragments of the PTHrP(1–34)NH₂ included in the 19–34 sequence we noticed the presence of the desired peptide as well as of some by-products (Table 1 and Figure 2). The fragmentation patterns of these by-products in ESI-MS/MS allowed us to confirm the formation of deletion sequences as reported in Supporting Information (Figure S1).

As the length of the resin-bound peptide increases, the related UPLC-ESI-MS analyses become much more complex. We report as an example the characterization of the 12–34 fragment of PTHrP(1–34)NH₂. The deconvoluted spectrum obtained for the cleaved mixture of this sample resulted in several deletion sequences (Figure 3). The fragments desLys¹³/Gln¹⁶-f(12–34) and desLys¹³/Gln¹⁶,Leu²⁷-f(12–34) were identified as two isobaric peptide sequences lacking either Lys¹³ or Gln¹⁶ residues.

The UPLC-ESI-MS/MS analyses of the intermediate resin-bound fragments obtained from the RT-SPPS of PTHrP(1–34)NH₂ confirm that it is a difficult sequence for SPPS. The desired peptide was usually present as the major component in the cleavage mixture, but it was accompanied by some deletion peptides mainly lacking Arg, Leu and His residues. It is well known that Arg-containing peptides are difficult to synthesize due to the sterically hindered Pbf group as side-chain protection and the tendency to form γ -lactam leading to low yield couplings [12].

With the above information in hand we sought to improve the synthesis of this difficult sequence of PTHrP(1–34)NH₂ by employing MW-assisted SPPS using Liberty™ automated peptide synthesizer with MW irradiations. To address the difficulties observed during the incorporation of Arg and His residues we applied the protocols reported in Table 2. Specifically, we have decreased the power of MW irradiation and lowered the temperature in order to avoid side reactions such as γ -lactam formation for Arg and racemization for His [13].

Indeed, after semi-preparative purification the MW-assisted SPPS of PTHrP(1–34)NH₂ yielded 27 mg of >95% pure peptide, whereas RT-SPPS gave only 18 mg of >95% of pure peptide. This improvement is attributed to the higher purity of the crude cleaved peptide mixture (Table 3 and Figure 4).

On the basis of the results of the analytical RP-HPLC of the crude PTHrP(1–34)NH₂, we conclude that the use of MW irradiations in SPPS has enhanced the efficiency of crucial coupling cycles improving the final yield and purity of crude peptide and speeding up the remaining coupling cycles. This improvement can be attributed to the prevention of peptide backbone aggregation and acceleration of deprotection and coupling steps.

In summary, although the application of MW-assisted SPPS to the synthesis of PTHrP(1–34)NH₂ led only to a moderate improvement in final yield (6.3% vs 4.4%), it allowed us to obtain a crude product of higher quality (77% vs 35%) and in a shorter time (20 h vs 34 h used for the RT and MW-assisted SPPS strategies). Moreover, we demonstrated the usefulness of the combination of an MW-assisted mini-cleavage protocol and the UPLC-ESI-MS analysis for monitoring the quality of the reaction step (see Supporting Information). Compared to the ninhydrin colorimetric monitoring, our strategy is faster and the UPLC-ESI-MS/MS analysis is more accurate and more informative. We think that application of the strategy presented in this report will help to improve many syntheses of difficult sequences.

Experimental Procedures

RT and MW-assisted SPPS of PTHrP(1–34)NH₂

All Fmoc-protected amino acids and TBTU were purchased from Iris Biotech. (Marktdrewitz, Germany). The following amino acid side-chain-protecting groups were used: OtBu (Asp, Glu), tBu (Ser, Thr), Pbf (Arg), Trt (Gln, His) and Boc (Lys). Rink-amide NovaSyn® TGR resin was purchased from Novabiochem (Laufelfingen, Switzerland). ACN, DCM and diethyl ether from Sigma-Aldrich

H-Ala¹-Val-Ser-Glu-His-Gln-Leu-Leu-His-Asp¹⁰-Lys-Gly-Lys-Ser-Ile-Gln-Asp-Leu-Arg-Arg²⁰-Arg-Phe-Phe-Leu-His-His-Leu-Ile-Ala-Glu³⁰-Ile-His-Thr-Ala³⁴-NH₂

— Hydrophobic amino acid residues
— Sterically hindered amino acid residues

Figure 1. Characteristics of the PTHrP(1–34)NH₂ sequence are a cluster of arginine residues in the positions 19–21, sterically hindered and hydrophobic amino acid sequences.

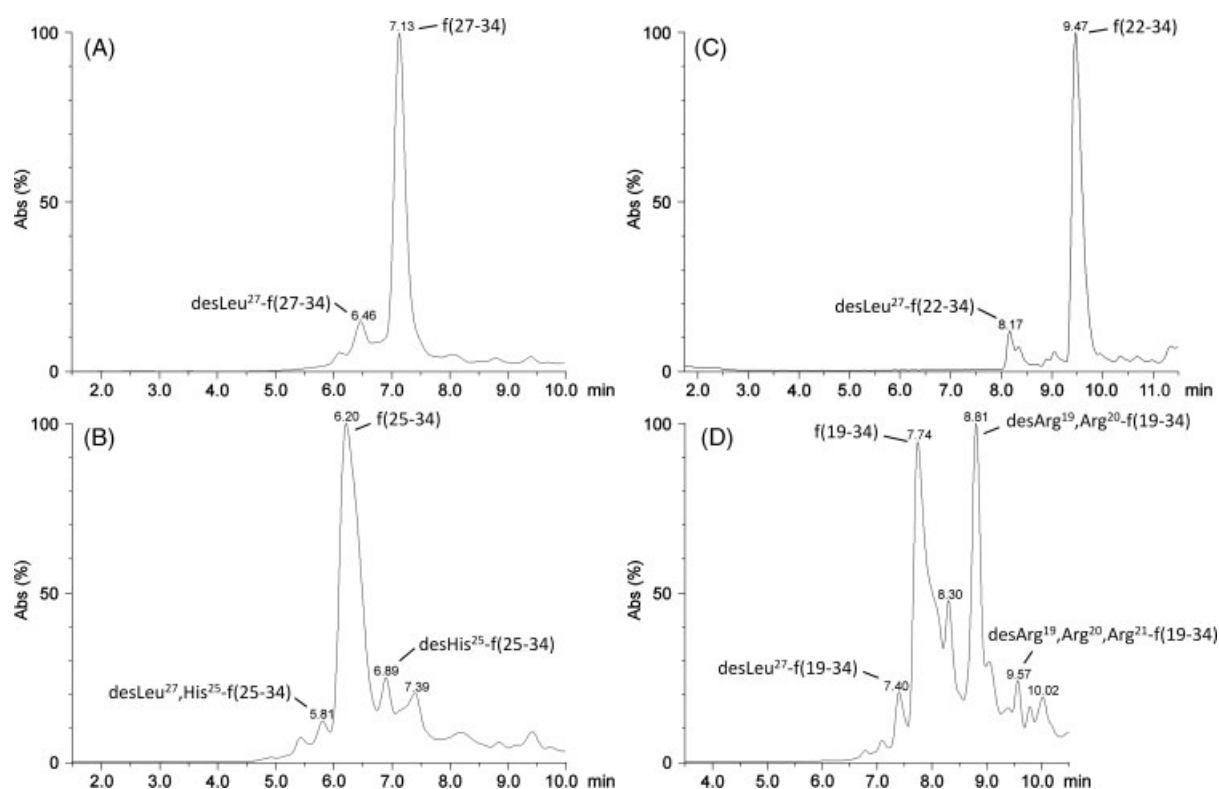


Figure 2. (A–D) TIC chromatogram of selected crude mixtures of intermediate resin-bound sequences obtained during the synthesis of PTHrP(1–34)NH₂ (Fmoc/tBu RT-SPPS) generated by the MW-assisted mini-cleavages. The related MS/MS spectra are shown in Supporting Information (Figure S1).

(St. Louis, MO, USA), DMF and NMP from Scharlau (Barcelona, Spain), DIEA and TFA from Acros Organics (Geel, Belgium) and TIS from Fluka/Aldrich (St. Louis, MO, USA). The synthesis of PTHrP(1–34)NH₂ was carried out using Fmoc/tBu SPPS strategy on a LibertyTM automated peptide synthesizer with a single-mode MW reactor (CEM), by RT and MW-assisted strategies. The reactions were performed in a Teflon vessel and mixed by nitrogen bubbling. Reaction temperatures were measured by an internal fiberoptic sensor. The RT-SPPS protocol consisted of two consecutive deprotection steps of 5 and 10 min, respectively, and a 20 min coupling step. In MW-SPPS protocol, the two deprotection steps were performed at 75 °C using 35 W for 0.5 min for the first one and 60 W for 3 min for the second one, whereas the coupling steps were performed at 75 °C, using 30 W for 5 min for all amino acids except for Arg and His residues that required specific coupling parameters performed in two steps (RT followed by MW irradiation, Table 1).

The syntheses were performed on Rink-amide NovaSyn[®] TGR resin (0.2 mmol/g, 500 mg), which was suspended in a solution of DMF/DCM (1:1 v/v) and swelled for 30 min. During the general coupling cycle, the *N*-terminal Fmoc-protecting group was removed with a solution of 20% piperidine in DMF. Fresh stock solutions of the Fmoc-protected amino acids (0.2 M) and TBTU (0.5 M) in DMF, and of DIEA (2 M) in NMP were prepared

in separated bottles and used as reagents during the SPPS. In particular, the coupling cycles were performed using 2.5 ml of Fmoc-protected amino acids, 1 ml of TBTU and 0.5 ml of DIEA in NMP of stock solutions. The fully assembled peptide was cleaved from the resin by treatment with 7 ml of a TFA/TIS/water solution (95:2.5:2.5 v/v/v) for 3 h at RT. The resin was filtered and the combined filtrates were concentrated under a stream of nitrogen. The crude peptide was precipitated from the cleavage mixture by addition of ice-cold diethyl ether and stored for 30 min at –20 °C. The precipitated product was collected by centrifugation, washed with diethyl ether (3 × 7 ml) and centrifuged. The remaining solid was dried under a stream of nitrogen and lyophilized.

MW-assisted Mini-cleavage of PTHrP(1–34)NH₂ Fragments

Both RT and MW-assisted SPPSs were monitored by UPLC-ESI-MS analysis of MW-assisted mini-cleavages of intermediate resin-bound fragments using DiscoverTM S-Class single-mode MW reactor equipped with Explorer-48 autosampler (CEM). The mixing of the cleavage reaction was accomplished by magnetic stirring and the reaction temperature was monitored at the bottom of the reactor vessels by an IR sensor. A small sample of beads carrying

Table 1. Fmoc/tBu RT-SPSS of PTHrP(1–34)NH₂: list of fragments produced by MW-assisted mini-cleavages of intermediate resin-bound peptides

Analyzed resin-bound sequences	Sequence	Calculated monoisotopic mass	Intact sequences Qtof MS (ESI+) (<i>m/z</i>) found	Deletion sequences Qtof MS (ESI+) (<i>m/z</i>) found	Missing amino acid residues from deletion sequences	Amount of deletion sequences (%)
27–34	H-Leu-Ile-Ala-Glu-Ile-His-Thr-Ala-NH ₂	865.51	866.39 [M + H] ⁺	753.41 [M + H] ⁺	Leu ²⁷	7
25–34	H-His-His-Leu-Ile-Ala-Glu-Ile-His-Thr-Ala-NH ₂	1139.62	1140.90 [M + H] ⁺	1003.95 [M + H] ⁺ 890.93 [M + H] ⁺	His ²⁵ Leu ²⁷ His ²⁵	2 5
22–34	H-Phe-Phe-Leu-His-His-Leu-Ile-Ala-Glu-Ile-His-Thr-Ala-NH ₂	1546.84	1547.41 [M + H] ⁺	1434.44 [M + H] ⁺	Leu ²⁷	8
19–34	H-Arg-Arg-Arg-Phe-Phe-Phe-Leu-His-His-Leu-Ile-Ala-Glu-Ile-His-Thr-Ala-NH ₂	2015.15	1008.69 [M + 2H] ²⁺	952.19 [M + 2H] ²⁺ 852.72 [M + 2H] ²⁺	Leu ²⁷	6
12–34	H-Gly-Lys-Ser-Ile-Gln-Asp-Leu-Arg-Arg-Arg-Phe-Phe-Leu-His-His-Leu-Ile-Ala-Glu-Ile-His-Thr-Ala-NH ₂	2756.55	1379.24 [M + 2H] ²⁺	774.73 [M + 2H] ²⁺ 1322.29 [M + 2H] ²⁺	Arg ¹⁹ Arg ²⁰ Arg ¹⁹ Arg ²⁰ Arg ²¹ Leu ²⁷	39 51 5
				1315.26 [M + 2H] ²⁺ 1258.81 [M + 2H] ²⁺ 1065.43 [M + 2H] ²⁺	Gln ¹⁶ /Lys ¹³ Leu ²⁷ Gln ¹⁶ /Lys ¹³ Gly ¹² -Lys-Ser-Ile-Gln-Asp ¹⁷	55 3 12

The relative amounts of the deletion sequences are calculated in percentage of area under the peak from the total area under the curve obtained from the TIC chromatogram.

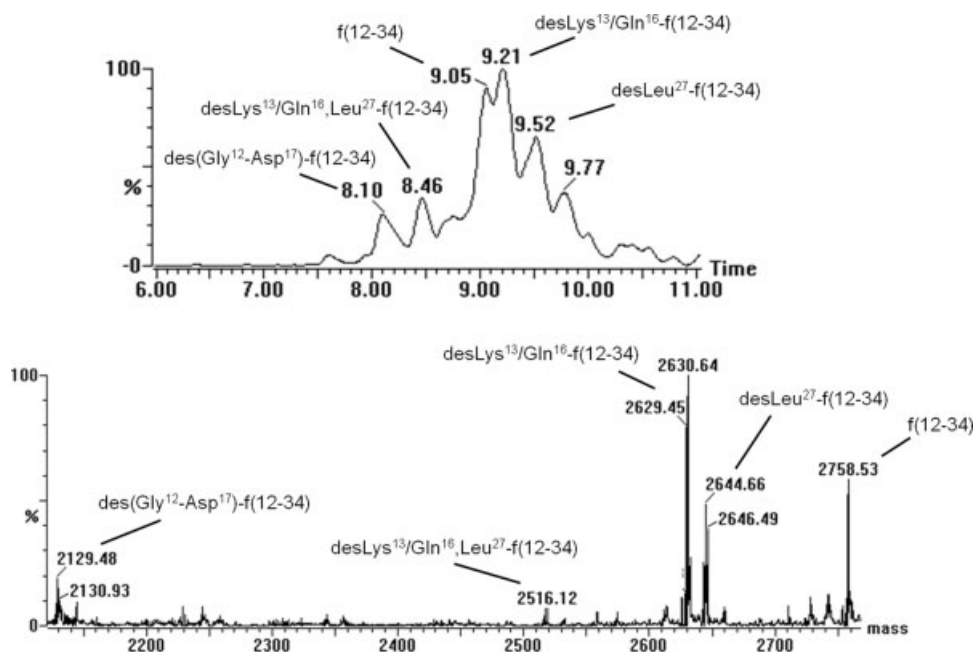


Figure 3. TIC chromatogram and deconvoluted spectrum of the cleaved mixture of the intermediate resin-bound sequence PTHrP(12–34)NH₂ (Fmoc/tBu RT-SPPS) generated by the MW-assisted minicleavages.

Table 2. Fmoc/tBu RT and MW-assisted SPPS deprotection and coupling protocols used for the synthesis of PTHrP(1–34)NH₂

Protocol	First deprotection			Second deprotection			Coupling		
	Time (min)	Power (W)	Temperature (°C)	Time (min)	Power (W)	Temperature (°C)	Time (min)	Power (W)	Temperature (°C)
RT-SPPS	5	–	20	10	–	20	20	–	20
MW-assisted SPPS	0.5	35	75	3	60	75	5	30	75
Arg ^a	Step 1			–			25	–	20
	Step 2			–			5	25	75
His	Step 1			–			2	–	20
	Step 2			–			4	30	50

^a The Arg cycle (step 1 and 2) was performed twice refreshing the coupling solution.

Table 3. Yield of PTHrP(1–34)NH₂ obtained from the RT versus MW-assisted SPPS

SPPS strategy	Purity of crude peptide (%)	Yield of >95% pure peptide
RT	35	4.4% (18 mg)
MW-assisted	77	6.3% (27 mg)

Fmoc-protected resin-bound peptide (10 mg) was weighted into a fritted polypropylene tube and treated twice with a 20% solution of piperidine in DMF (1 ml) each time for 5 min. The beads were then washed with DMF (2 × 1 ml) and DCM (3 × 1 ml), dried under vacuum and transferred into a 10 ml glass tube containing the cleavage mixture that was placed into the MW cavity. The minicleavages were carried out with 2 ml of TFA/TIS/water solution (95:2.5:2.5 v/v/v) at 45 °C, using 15 W for 15 min with external cooling of the reactor vessel at the positions shown in the Reaction Scheme. All the parameters, i.e. pressure, temperature

and power, involved in the MW-assisted mini-cleavage reactions were monitored as reported in Supporting Information (Figure S2). The reaction mixture was then filtered and the crude peptide was precipitated from the cleavage mixture by addition of ice-cold diethyl ether followed by cooling for 5 min at –20 °C. The product was collected by centrifugation and directly subjected to UPLC-ESI-MS analysis (see Supporting Information).

HPLC Analysis of PTHrP(1–34)NH₂

Crude PTHrP(1–34)NH₂ obtained from both the RT and MW-assisted SPPSs were analyzed by analytical RP-HPLC (Alliance 2695 HPLC system equipped with a 2996 photodiode array detector, Waters (Milford, MA, USA)) using a Jupiter C18 (5 μm, 250 × 4.6 mm) column (Phenomenex, Torrance, CA, USA) at 1 ml/min. The solvents used were A (0.1% TFA in H₂O) and B (0.1% TFA in ACN).

RP-HPLC Semi-preparative of PTHrP(1–34)NH₂

Lyophilized crude peptide was prepurified by solid-phase extraction with an RP-18 LiChrorep silica column from Merck

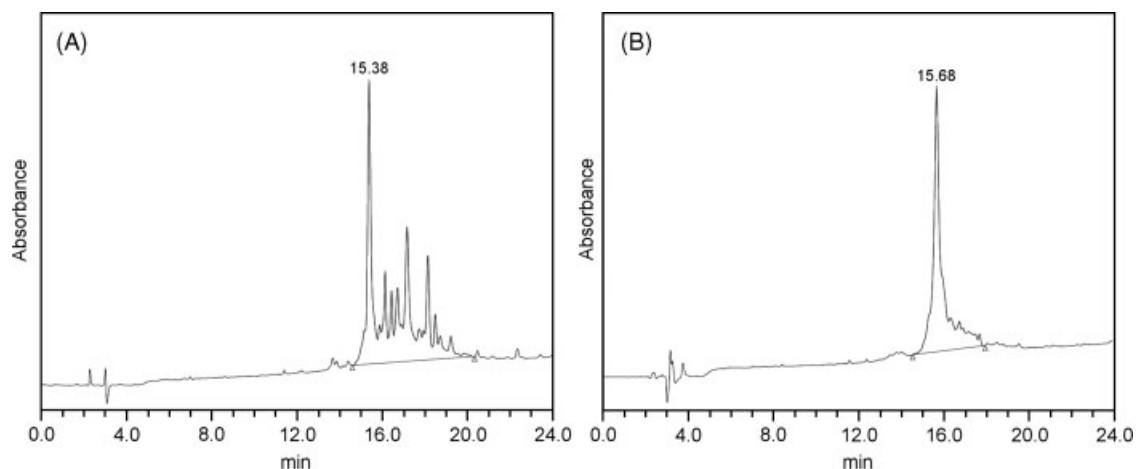


Figure 4. Analytical RP-HPLC of crude PTHrP(1–34)NH₂. Fmoc/tBu RT-SPPS (A) and Fmoc/tBu MW-assisted SPPS (B). HPLC: 10–60% B (0.1% TFA in ACN) in A (0.1% TFA in H₂O) over 20 min.

(Darmstadt, Germany) using H₂O/ACN as eluents. The purification of the peptide was performed by semi-preparative RP-HPLC on a Supelco C18 180 Å (250 × 10 mm, 5 μm) column (Sigma Aldrich, St. Louis, MO, USA); eluents: A 0.1% TFA in H₂O; B 0.1% TFA in ACN; flow 4 ml/min; gradient 30–60% of B in 30 min.

UPLC-ESI-MS Analysis of PTHrP(1–34)NH₂ Fragments

UPLC-ESI-MS system consisted of an ACQUITY™ UPLC system (Waters) coupled with a Micromass® Q-ToF MICRO™ mass spectrometer (Waters) equipped with an ESI source. The chromatographic separation was achieved on a Symmetry 300 C18 column (100 mm × 2.1 mm, ID 3.5 μm, Waters) with the column temperature set at 30 °C. The flow rate was 0.15 ml/min with a linear gradient running from 0 to 30% of B (solvent A: 2% ACN, 0.1% formic acid in H₂O; solvent B: 2% H₂O, 0.1% formic acid in ACN) in 7 min, followed by 30–60% B in the next 3 min, then by 95% B for 2 min, and returned to initial condition for 3 min for re-equilibration. The total run time per sample was 15 min. The ESI-MS analysis was carried out in the positive ESI mode, the optimal MS parameters were as follows: capillary voltage 3.2 kV, cone voltage 30 kV, source temperature 120 °C and desolvation temperature 320 °C. Nitrogen was used as desolvation and cone gas with a flow rate of 450 and 40 l/h, respectively. For MS/MS analyses, argon was used as collision gas, and the collision energy was set to 40 eV. Data were acquired and processed using MassLynx™ software (Waters).

Highlights and Limitations

This protocol describes two advantages of MW radiation in SPPS. The first one is monitoring of traditional RT-SPPS by MW-assisted mini-cleavages combined with fast, efficient and sensitive UPLC-ESI-MS analysis (15 min/analysis vs 30–45 min/analysis for traditional mini-cleavage). We use this procedure to confirm the presence of difficult coupling steps that result in truncated and deletion sequences. The second advantage is the specifically tuned MW-assisted SPPS that uses modified cycles targeting difficult couplings. In these couplings the first step is carried out at RT (without applying MW power, 20 °C) and for variable duration (25 or 2 min) and the second step is carried out in the presence of MW power (75 or 50 °C) for shorter time intervals (5 or 4 min). In the reported

synthesis we applied such type of couplings for the three arginine residues (R¹⁹-R²¹) and for the two histidine residues (H²⁵-H²⁶). Evidently, carrying out the RT and MW-assisted SPPSs on the same instrument allowed unbiased side-by-side comparison and the conclusion that the latter procedure is superior to the RT-SPPS.

Although the modification of the coupling steps for Arg and His in the MW-assisted SPPS seems to be empirical in nature, it was guided by strong rational that took into account the distinct capacity of this methodology to overcome putative hydrophobic interactions and aggregation. The impact of these phenomena increases with the progression of the coupling reactions. We therefore decided to take advantage of the MW radiation only for a short duration after the bulk of the reaction has been already taken place. In this manner, the completion of the coupling reaction was facilitated without causing undesired side reactions. We propose this MW-based protocol as a general strategy for overcoming difficult coupling reactions. Admittedly, applying this strategy to different peptides will require fine tuning that will include the adjustment of parameters such as duration of coupling and recoupling steps as well as the level of MW energy employed in the recoupling step. We are confident that adapting the strategy outlined in this protocol will be advantageous over the 'one generic MW-assisted coupling cycle fits all'.

Acknowledgements

Chaire d'Excellence ANR 2009-2013 and Fondazione Ente Cassa di Risparmio di Firenze are gratefully acknowledged.

Supporting information

Supporting information may be found in the online version of this article.

References

- 1 Yu H-M, Chen S-T, Wang K-T. Enhanced coupling efficiency in solid-phase peptide synthesis by microwave irradiation. *J. Org. Chem.* 1992; **57**: 4781–4784.
- 2 Collins JM, Leadbeater NE. Microwave energy: a versatile tool for the biosciences. *Org. Biomol. Chem.* 2007; **5**: 1141–1150.
- 3 Malik L, Tofteng AP, Pedersen SL, Sørensen KK, Jensen KJ. Automated 'X-Y' robot for peptide synthesis with microwave heating: application

- to difficult peptide sequences and protein domains. *J. Pept. Sci.* 2010; **16**: 506–512.
- 4 Sabatino G, Papini AM. Advances in automatic, manual and microwave-assisted solid-phase peptide synthesis. *Curr. Opin. Drug. Discov. Devel.* 2008; **11**: 762–770.
 - 5 Katritzky AR, Haase DN, Johnson JV, Chung A. Benzotriazole-assisted solid-phase assembly of Leu-enkephalin, amyloid beta segment 34–42, and other “difficult” peptide sequence. *J. Org. Chem.* 2009; **74**: 2028–2032.
 - 6 Rizzolo F, Sabatino G, Chelli M, Rovero P, Papini AM. A convenient microwave-enhanced solid-phase synthesis of difficult peptide sequences: case study of Gramicidin A and CSF114(Glc). *Int. J. Pept. Res. Ther.* 2007; **13**: 203–208.
 - 7 Bacsa B, Bosze S, Kappe CO. Direct solid-phase synthesis of the beta-amyloid (1–42) peptide using controlled microwave heating. *J. Org. Chem.* 2010; **75**: 2103–2106.
 - 8 Friligou I, Papadimitriou E, Gatos D, Matsoukas J, Tselios T. Microwave-assisted solid-phase peptide synthesis of the 60–110 domain of human pleiotrophin on 2-chlorotrityl resin. *Amino Acids* 2011; **40**: 1431–1440.
 - 9 Stewart AF. Hypercalcemia associated with cancer. *N. Engl. J. Med.* 2005; **352**: 373–379.
 - 10 Mannstadt M, Jüppner H, Gardella TJ. Receptors for PTH and PTHrP: their biological importance and functional properties. *Am. J. Physiol.* 1999; **277**: 665–675.
 - 11 Kluczyk A, Rudowska M, Stefanowicz P, Szewczuk Z. Microwave-assisted TFA cleavage of peptides from Merrifield resin. *J. Pept. Sci.* 2010; **16**: 31–39.
 - 12 White P, Collins J, Cox Z. *Comparative study of conventional and microwave assisted synthesis.* In Poster Presentation at the 19th American Peptide Symposium, San Diego, CA, 2005.
 - 13 Loffredo C, Assuncao NA, Gerhardt J, Miranda MTM. Microwave-assisted solid-phase peptide synthesis at 60 °C: alternative conditions with low enantiomerization. *J. Pept. Sci.* 2009; **15**: 808–817.

Stabilization of β Turn Conformation in Melanocortin-Like Peptide by Click Side Chain-To-Side Chain Cyclization

Chiara Testa^{1,2,3}, Stefano Carganico^{1,2,3}, Francesca Nuti^{2,3},
Mario Scrima⁴, Anna Maria D'Ursi⁴, Marvin L. Dirain⁵,
Nadeje Lubin Germain¹, Carrie Haskell-Luevano⁵, Michael Chorev^{6,7},
Paolo Rovero^{2,8}, and Anna Maria Papini^{1,2,3}

¹Laboratoire SOSCO – EA4505 Université de Cergy-Pontoise Neuville-sur-Oise, 95031, Cergy-Pontoise, France; ²Laboratory of Peptide & Protein Chemistry & Biology, Polo Scientifico e Tecnologico, University of Florence, I-50019, Sesto Fiorentino (FI), Italy; ³Department of Chemistry “Ugo Schiff”, University of Florence, I-50019, Sesto Fiorentino (Fi), Italy; ⁴Department of Pharmaceutical Science, Via Ponte Don Melillo 11C, Salerno, I-84084, Italy; ⁵Department of Pharmacodynamics, University of Florida, Gainesville, FL, 32610, U.S.A.; ⁶Laboratory for Translational Research, Harvard Medical School, One Kendall Square, Building 600, Cambridge, MA, 02139, U.S.A.; ⁷Department of Medicine, Brigham and Women's Hospital, 75 Francis Street, Boston, MA, 02115, U.S.A.; ⁸Department of Pharmaceutical Science, Polo Scientifico e Tecnologico, University of Florence, Via Ugo Schiff 3, I-50019, Sesto Fiorentino (Fi), Italy

Introduction

Interaction of linear and flexible peptides with their macromolecular target, such as GPCRs, involves a limited number of closely related conformations that are recognized by, bind to and either activate or block the biological activity of these targets. Hence, the so called bioactive conformation represents only a small subset of the larger ensemble of accessible conformations which are in a dynamic equilibrium. A growing arsenal of structural rigidifications offers means to capture and stabilize the biological conformation of linear peptides in an effort to enhance target specificity, biological potency, binding affinity and metabolic stability [1,2]. Herein we report on the extension of an innovative strategy for stabilization peptide β -turn conformation by side chain-to-side chain cyclization employing a bridge containing a [1,2,3]triazole [5-8].

Results and Discussion

Melanocortin GPCR receptors (MCRs) are involved in many biological pathways, including sexual function, feeding behaviour, energy homeostasis and pigmentation, making them potential targets for drugs to treat diseases such as obesity and sexual dysfunction. Therefore, understanding the bioactive conformation of the ligand and the structure of the receptor–ligand complex is crucial to design more potent and MCR-subtype selective ligands. MT-II is a potent long acting non-selective super-agonist of MCRs, characterized by lactam bridge between residues Asp⁵ and Lys¹⁰ stabilizing a type-II β turn structure that is critical for its bioactivity [3]. The minimal active sequence is identified by the tetrapeptide His⁶-D-Phe⁷-Arg⁸-Trp⁹ [4], which is included in the cyclic portion formed by lactam ring. In previous work [5] we designed and studied a new intramolecular side chain-to-side chain [1,2,3]triazolyl-bridged modification. This 1,4-disubstituted [1,2,3]triazolyl moiety is bioisosteric to the peptide bond and was recently introduced by us as an α -helix stabilizing rigidification replacing the *i*-to-*i*+4 side chain-to-side chain bridging lactam in peptides derived from parathyroid hormone-related protein (PTHrP). In the current study, we applied the [1,2,3]triazolyl-bridging strategy to stabilize a β -turn conformation in MT-II by replacing the lactam bridge with a *i*-to-*i*+5 side chain-to-side chain cyclization via

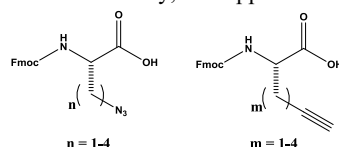


Fig. 1. Azido and Alkynyl Amino acid building blocks for Fmoc-tBu SPPS.

Cu^I-catalyzed azido-to-alkyne 1,3-dipolar cycloaddition (CuAAC) generating 1,4-disubstituted [1,2,3]triazolyl-containing ring structures. In this context, we have developed synthesis of N^α-Fmoc- ω -azido- α -amino- and N^α-Fmoc- ω -ynolic- α -amino acids (Figure 1) by diazo-transfer of the N^α-protected ω -amino- α -amino acids [6,7] and by alkylation of a Ni(II) complex of the Schiff base derived from glycine

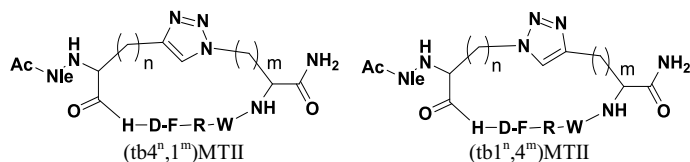


Fig. 2. Schematic representation of all the possible MTII peptide analogs cyclized by [1,2,3]triazolyl-containing bridges that vary in the size of the bridge and the position and direction of the triazolyl moiety within the ring. In the notation *tb* stands for [1,2,3]triazolyl-bridged, the superscripts *m* and *n* define the number of methylenes connecting the triazole moiety to the N- and C-proximal bridge heads and the numbers in the bracket identify the orientation of the triazolyl within the bridge.

and a chiral inducer with alk- ω -ynyl bromides respectively [8]. Clicked MT-II analogs I-IV presenting different permutations of bridges containing 5 methylenes and a triazolyl moiety were synthesized by a combination of solid phase assembly of the linear peptide precursor I'-IV' and were followed by solution phase CuAAC. The adenylate cyclase activity (EC_{50}) of the linear precursor I'-IV' and cyclic MTII peptide analogs I-IV was evaluated in the murine melanocortin receptors mMC1R, mMC3R, mMC4R and mMC5R (Table 1). Indeed the cyclic peptides are more potent than their linear precursors confirming that conformational stabilization in the form of side chain-to-side chain cyclization enhances *in vitro* potency. Moreover, the clicked cyclic peptides have similar potency compared to the parent lactam-containing MTII analog. There are indications of emerging selectivity toward receptor subtypes but these need to be further optimized.

Table 1. Biological activity (EC_{50}) of the MTII peptide analogs towards the principal murine melanocortin receptors. *Lin stands for linear precursor.

Peptide	mMC1R	mMC3R	mMC4R	mMC5R
	EC_{50} (nM)	EC_{50} (nM)	EC_{50} (nM)	EC_{50} (nM)
MTII	-	0.33	0.04	0.27
I (tb4 ¹ , 1 ⁴)MTII	-	3.14	1.62	1.93
II (tb1 ⁴ , 4 ¹)MTII	-	3.70	0.58	1.76
III (tb4 ² , 1 ³)MTII	0.11	0.59	0.15	0.47
IV (tb1 ³ , 4 ²)MTII	0.51	2.95	0.36	2.30
I' Lin[Nle ³ (δ -N ₃),Pra ¹⁰]MTII*	1.04	3.67	0.71	6.62
II' Lin[Pra ³ ,Nle ¹⁰ (δ -N ₃)]MTII	0.58	4.13	0.43	3.91
III' Lin[hAla ⁵ (γ -N ₃),Nva ¹⁰ (δ -yl)]MTII	1.25	8.57	1.48	12.4
IV' Lin[Nva ⁵ (δ -yl),hAla ¹⁰ (γ -N ₃)]MTII	2.11	9.90	1.35	11.8

In summary, our studies support our contention that the [1,2,3]triazolyl-bridged peptides achieve conformational stabilization that enhances their *in vitro* potency. In the future we will continue to fine-tune this modification to improve receptor-subtype selectivity.

Acknowledgments

The present work has been supported by the Agence Nationale de la Recherche chaire d'Excellence 2009-2013 (France).

References

- 1 Henchey, L.K., Jochim, A.L., Arora, P.S. *Current Opinion in Chemical Biology* **12**, 692 (2008).
- 2 Kim, Y.W., Verdine, G.L. *Bioorganic and Medicinal Chemistry Letters* **19**, 2533 (2009).
- 3 Al-Obeidi, F., de Lauro Castrucci, A.M., Hadley, V.J. *J. Med. Chem.* **32**, 2555-2561 (1989).
- 4 Ying, J., et al. *Biopolymers* **71**, 696-716 (2003).
- 5 Cantel, S., et al. *J. Org. Chem.* **73**, 5663-5674 (2008).
- 6 Le Chevalier Isaad, A., Papini, A.M., Chorev, M., Rovero, P. *J. Pept. Sci.* **15**, 451-454 (2009).
- 7 Le Chevalier Isaad, et al. *Eur. J. Org. Chem.* **31**, 5308-5314 (2008).
- 8 Scrima, M., et al. *Eur. J. Org. Chem.* 446-457 (2010).

Conventional and Microwave-Assisted SPPS Approach: A Comparative Study of PTHrP(1-34)NH₂ Synthesis

Fabio Rizzolo^{1,2}, Chiara Testa^{1,2,3}, Michael Chorev^{4,5}, Mario Chelli^{1,2},
Paolo Rovero^{1,6}, and Anna Maria Papini^{1,2,3}

¹Laboratory of Peptide & Protein Chemistry & Biology, University of Florence, Polo Scientifico e Tecnologico, Sesto Fiorentino (Fi) I-50019, Italy; ²Department of Chemistry "Ugo Schiff", Via della Lastruccia 3/13, University of Florence, Polo Scientifico e Tecnologico, Sesto Fiorentino (Fi) I-50019, Italy; ³Laboratoire SOSCO – EA4505 Université de Cergy-Pontoise, 5 mail Gay-Lussac, Neuville-sur-Oise, Cergy-Pontoise 95031, France; ⁴Laboratory for Translational Research, Harvard Medical School, Cambridge, MA, 02139, U.S.A.; ⁵Department of Medicine, Brigham and Women's Hospital, Boston, MA, 02115, U.S.A.; ⁶Department of Pharmaceutical Science, Via Ugo Schiff 6, University of Florence, Polo Scientifico e Tecnologico, Sesto Fiorentino (Fi), I-50019, Italy

Introduction

Parathyroid hormone-related peptide (PTHrP) is an autocrine/paracrine regulator of endochondral bone development and involved in excessive osteoclastic bone resorption associated with humoral hypercalcaemia of malignancy (HHM) [1]. PTHrP is a 139 to 173-amino acid protein having the first thirteen N-terminal amino acids in common with parathyroid hormone (PTH). Like PTH, PTHrP releases calcium from bone and increases secretion of calcium and phosphate in the distal tubule [2].

Similar to PTH the calcium metabolism-related activities are located in the first 34 N-terminal residues. Consequently, our synthetic efforts focused on this bioactive sequence that was the subject of numerous structure-activity-conformation relationship studies [3].

Considering the presence of clusters of arginines, sterically hindered and hydrophobic amino acid residues in the 19-28 sequence of PTHrP and the considerable length of the peptide, the synthesis of PTHrP(1-34)NH₂ is quite challenging. We therefore undertook the synthesis comparing the conventional (room temperature) Solid-Phase Peptide Synthesis (SPPS) vs. the MicroWave-assisted SPPS [4].

Results and Discussion

PTHrP(1-34)NH₂ sequence is: H-Ala¹-Val-Ser-Glu-His-Gln-Leu-Leu-His-Asp¹⁰-Lys-Gly-Lys-Ser-Ile-Gln-Asp-Leu-Arg-Arg²⁰-Arg-Phe-Phe-Leu-His-His-Leu-Ile-Ala-Glu³⁰-Ile-His-Thr-Ala-NH₂. The peptide was synthesized by SPPS, following Fmoc/tBu strategy, at room temperature and by microwave irradiation, using in both cases Liberty peptide synthesizer (CEM) and the same reagents concentration. The synthesis was monitored by LC-MS using MW-assisted mini-cleavages of the intermediate fragments using Discover single mode microwave system (CEM).

The SPPS was performed using the NovaSyn TGR (500 mg, 0.2 mmol/g), 0.2 M solution of amino acids in DMF (5 equiv.), 0.5 M solution of TBTU in DMF (5 equiv.), 2 M solution of DIPEA in NMP (10 equiv.). Final cleavage of the peptide from the resin and side-chain deprotections were performed with *ad hoc* cleavage cocktail TFA/water/TIS solution (95:2.5:2.5 v/v/v) for 3 hours at room temperature.

The room temperature-SPPS cycle (Liberty, CEM) consisted of two deprotection steps (5 and 10 min respectively) and 20 min for the coupling steps. The MW-SPPS cycle (Liberty, CEM), the deprotection steps were performed at 75 °C using 35 W for 30 sec for the first one and 60 W for 180 sec for the second one, while the coupling steps were performed at 75 °C, using 30 W for 300 sec.

MW-assisted mini-cleavage cycles (Discover, CEM) were carried out at 45 °C, using 15 W for 15 min with external cooling of the reaction vessel.

In this comparative study of PTHrP(1-34)NH₂ SPPS, using the same instrumentation and the same reagents concentration, MW-assisted strategy gave an increased purity of the crude peptide as compared with the conventional approach. RP-HPLC purification of the crude peptide was evaluated by LC-MS (ACQUITY UPLC™ System coupled with Micromass® Quattro micro API Mass Spectrometer, Waters) yielded 27 mg and 18 mg of >95% pure PTHrP(1-34)NH₂ from the MW-assisted synthesis and SPPS at room temperature, respectively (Table 1).

Table 1. Room temperature- vs MW-assisted synthetic approach

SPPS strategy	Purity of crude peptide (%)	% Yield of pure >95% peptide (mg)
Room temperature	35	4.4 (18 mg)
MW-assisted	77	6.3 (27 mg)

In conclusion, microwave technology has improved SPPS of particularly difficult sequences as compared with the conventional room temperature method. This improvement is attributed to prevention of peptide backbone aggregation and acceleration of deprotection and coupling steps.

In general, MW-assisted SPPS is proposed as a reliable strategy to overcome some limitations encountered in conventional SPPS. In our case, although the application of microwaves in SPPS led only to moderate improvement in final yield it allowed us to obtain a crude PTHrP(1-34)NH₂ of higher quality and enabled the development of a fast micro-cleavages as an alternative method for monitoring SPPS.

Therefore, based on our experience, the advantages of MW-assisted SPPS vs RT-SPPS can be summarized as follow: 1) shortening reaction time, 2) shortening micro-cleavage time, 3) crude peptides of higher quality facilitating the subsequent purification steps.

Acknowledgments

Ente Cassa Risparmio di Firenze and ANR Chaire d'Excellence 2009-2013 PepKit (France) are gratefully acknowledged.

February 2012

References

1. Stewart, A.F. *N. Engl. J. Med.* **352**, 373-379 (2005).
2. Wysolmerski, J.J., Stewart, A.F. *Annu. Rev. Physiol.* **60**, 431-460 (1998).
3. Horiuchi, N., et al. *Science* **238**, 1566-1568 (1987).
4. Sabatino, G., Papini, A.M. *Curr. Opin. Drug Discov. Devel.* **11**, 762-770 (2008).

Di-(2-ethylhexyl) phthalate and autism spectrum disorders

Chiara Testa^{*,†,‡}, Francesca Nuti^{†,‡}, Joussef Hayek[§], Claudio De Felice[¶], Mario Chelli[†], Paolo Rovero^{†,||}, Giuseppe Latini^{**††} and Anna Maria Papini^{*,†,‡1}

^{*}Laboratoire PeptLab-SOSCO-Université de Cergy-Pontoise Neuville-sur-Oise, Cergy-Pontoise, France

[†]Laboratory of Peptide and Protein Chemistry and Biology, Polo Scientifico e Tecnologico, University of Florence, Sesto Fiorentino (FI), Italy

[‡]Department of Chemistry 'Ugo Schiff', University of Florence, Sesto Fiorentino (FI), Italy

[§]Child Neuropsychiatry Unit, University Hospital AOUS of Siena, Siena, Italy

[¶]Neonatal Intensive Care Unit, University Hospital AOUS of Siena, Siena, Italy

^{||}Department of Pharmaceutical Sciences, Polo Scientifico e Tecnologico, University of Florence, Sesto Fiorentino (FI), Italy

^{**}Division of Neonatology, Perrino Hospital, Brindisi, Italy

^{††}Clinical Physiology Institute (IFC-CNR), National Research Council of Italy, Lecce Section, Lecce, Italy

Cite this article as: Testa C, Nuti F, Hayek J, De Felice C, Chelli M, Rovero P, Latini G and Papini AM (2012) Di-(2-ethylhexyl) phthalate and autism spectrum disorders. ASN NEURO 4(4):art:e00089.doi:10.1042/AN20120015

ABSTRACT

ASDs (autism spectrum disorders) are a complex group of neurodevelopment disorders, still poorly understood, steadily rising in frequency and treatment refractory. Extensive research has been so far unable to explain the aetiology of this condition, whereas a growing body of evidence suggests the involvement of environmental factors. Phthalates, given their extensive use and their persistence, are ubiquitous environmental contaminants. They are EDs (endocrine disruptors) suspected to interfere with neurodevelopment. Therefore they represent interesting candidate risk factors for ASD pathogenesis. The aim of this study was to evaluate the levels of the primary and secondary metabolites of DEHP [di-(2-ethylhexyl) phthalate] in children with ASD. A total of 48 children with ASD (male: 36, female: 12; mean age: 11 ± 5 years) and age- and sex-comparable 45 HCs (healthy controls; male: 25, female: 20; mean age: 12 ± 5 years) were enrolled. A diagnostic methodology, based on the determination of urinary concentrations of DEHP metabolites by HPLC-ESI-MS (HPLC electrospray ionization MS), was applied to urine spot samples. MEHP [mono-(2-ethylhexenyl) 1,2-benzenedicarboxylate], 6-OH-MEHP [mono-(2-ethyl-6-hydroxyhexyl) 1,2-benzenedicarboxylate], 5-OH-MEHP [mono-(2-ethyl-5-hydroxyhexyl) 1,2-benzenedicarboxylate] and 5-oxo-MEHP [mono-(2-ethyl-5-oxohexyl) 1,2-benzenedicarboxylate] were measured and compared with unequivocally characterized, pure synthetic compounds (>98%) taken as standard. In ASD patients, significant increase in 5-OH-MEHP (52.1%, median 0.18) and 5-oxo-MEHP (46.0%,

median 0.096) urinary concentrations were detected, with a significant positive correlation between 5-OH-MEHP and 5-oxo-MEHP ($r_s=0.668$, $P<0.0001$). The fully oxidized form 5-oxo-MEHP showed 91.1% specificity in identifying patients with ASDs. Our findings demonstrate for the first time an association between phthalates exposure and ASDs, thus suggesting a previously unrecognized role for these ubiquitous environmental contaminants in the pathogenesis of autism.

Key words: autism, di-(2-ethylhexyl) phthalate, endocrine disruptors, HPLC-ESI-MS urine analysis, secondary metabolites.

INTRODUCTION

ASDs (autism spectrum disorders), also known as PDDs (pervasive developmental disorders), are a group of complex neurodevelopment disorders, characterized by social impairments, communication difficulties, and restricted, repetitive and stereotyped patterns of behaviour.

A dramatic increase in frequency of ASDs has been reported over the last 20 years (Weintraub, 2011; Kim et al., 2011). Nevertheless, it is difficult to determine how much of this increase may be due to actual increase in the incidence or to increased awareness and diagnosis. The aetiology is unknown, but it is believed to result from disruption of normal neurobiological mechanisms primarily in the prenatal period (Nelson, 1991). Although it is widely recognized that ASDs may

¹To whom correspondence should be addressed (email annamaria.papini@unifi.it).

Abbreviations: ASD, autism spectrum disorder; CARS, childhood autism rating scale; CI, confidence interval; DEHP, di-(2-ethylhexyl) phthalate; ED, endocrine disruptor; HC, healthy control; HPLC-ESI-MS, HPLC electrospray ionization MS; MEHP, mono-(2-ethylhexenyl) 1,2-benzenedicarboxylate; 5-OH-MEHP, mono-(2-ethyl-5-hydroxyhexyl) 1,2-benzenedicarboxylate; 6-OH-MEHP, mono-(2-ethyl-6-hydroxyhexyl) 1,2-benzenedicarboxylate; OS, oxidative stress; 5-oxo-MEHP, mono-(2-ethyl-5-oxohexyl) 1,2-benzenedicarboxylate; QC, quality control; RP-HPLC-ESI-MS, reverse-phase HPLC-ESI-MS; ROC, receiver operating characteristic; SPE, solid phase extraction; PPAR α , peroxisome-proliferator-activated receptor α ; TH, thyroid hormone.

© 2012 The Author(s) This is an Open Access article distributed under the terms of the Creative Commons Attribution Non-Commercial Licence (<http://creativecommons.org/licenses/by-nc/2.5/>) which permits unrestricted non-commercial use, distribution and reproduction in any medium, provided the original work is properly cited.

have a strong genetic component (Risch et al., 1999; Anney et al., 2011). To the best of our clinical experience, not more than 5% of all autism cases appear to be due primarily to single gene mutations. In particular, syndromic ASD accounts for 15–20% of ASDs, and other complex genetic factors appear to play a major role in non-syndromic forms of autism. World literature evidence seems to indicate that autism has a strong genetic component (10–20%, Geschwind, 2011) which, by itself, does not fully explain the prevalence of the disorder exponentially increasing over the last two decades. It is quite likely that exposure to potential environmental factors has differential effects depending on genetic background.

According to our observation, the focus of autism research is shifting from purely genetic influences to multifactorial diseases in which complex set of genes should be associated with relevant environmental factors (Larsson et al., 2009; Herbert, 2010). To date, no information is available on the potential role in the pathogenesis of autism for phthalates, ubiquitous contaminants (Griffiths et al., 1985; Bauer and Herrmann, 1997) used as plasticizers, solvents and additives in many consumer products, i.e. vinyl flooring, wall coverings, food containers and cosmetics (Schettler, 2006; Wormuth et al., 2006). In particular, DEHP [di-(2-ethylhexyl) phthalate] represents one of the most commonly used plasticizer in pharmaceutical and medical devices (U.S. FDA 2011). DEHP is primarily metabolized to monoester, further oxidized in ω and $\omega-1$ positions leading to a pool of secondary metabolites (Albro, 1986; Koch et al., 2003, 2006), and it can be hypothesized that all DEHP metabolites, derived from a hydrolytic/oxidative pathway could, after glucuronidation, be excreted in urine (Figure 1).

Children are known to be exposed to DEHP levels twice as high as those for adults (Hellerstedt et al., 2008; Wittassek et al., 2009). Foetuses and neonates are highly sensitive to physiologically active agents because they are exposed during critical periods of human development (Latini et al., 2003; Kim et al., 2009; Cho et al., 2010; Suzuki et al., 2010). Furthermore, in the case of intensive therapy procedures, neonates can have higher exposure to phthalates and to their toxic monoesters supposed to be EDs (endocrine disruptors) (Silva et al., 2003a, 2003b; Latini et al., 2004). EDs may also be transferred from the mother to the developing foetus across the placenta or to the newborn through breast-feeding (Hines et al., 2009; Latini et al., 2009). For these reasons, the French National Assembly has required the ban of phthalates and parabens (Bill of Law adopted by French National Assembly on 3 May 2011). Moreover, very recently, prenatal phthalate exposure has been reported to decrease child mental/motor development, and increase internalizing behaviour during the preschool years (Whyatt et al., 2011), thus consolidating the concept of an adverse effect of these contaminants on function of the CNS (central nervous system).

The aim of the present study was to evaluate the levels of the primary and secondary metabolites of DEHP in autistic children by using innovative chemical reverse approach (Alcaro et al., 2009; Papini, 2009).

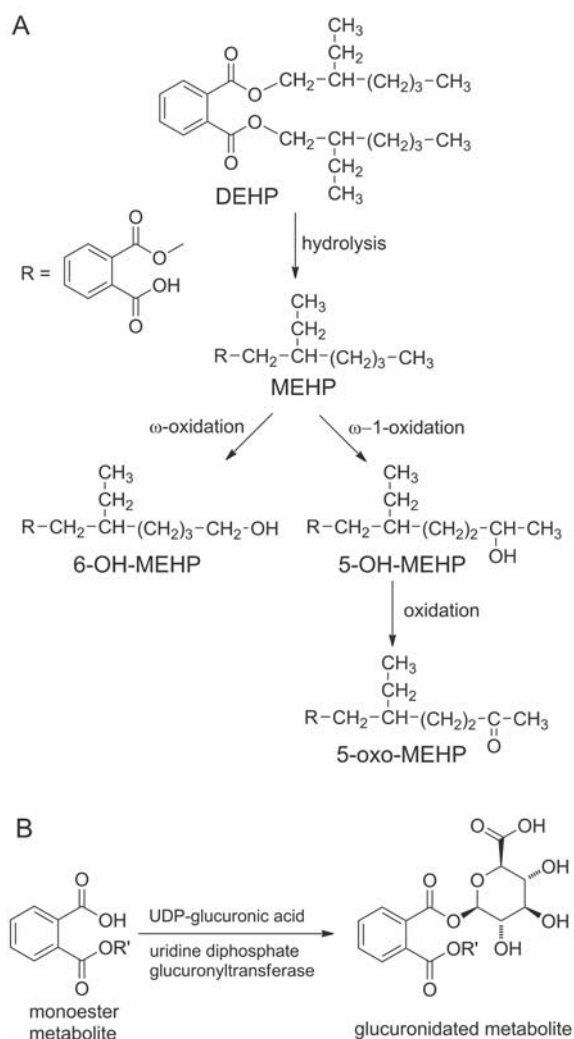


Figure 1 Metabolism of DEHP

(A) Hydrolytic/oxidative pathway leading to MEHP and secondary metabolite formation. (B) Formation of glucuronic conjugates of DEHP metabolites.

MATERIALS AND METHODS

Subject population

A total of 48 children with ASD (male: 36, female: 12; age at examination: 11.0 ± 5 years) were recruited from the staff of Children Neuropsychiatric Department, Siena, Italy. All the 48 patients with ASD, diagnosed by DSM IV (Diagnostic and Statistical Manual of mental disorders) and evaluated using ADOS (autism diagnostic observation schedule), ABC (autism behaviour checklist) and CARS (childhood autism rating scale) scores entered the study. Patients with Rett syndrome, X-fragile syndrome, inborn errors of metabolism, 21 trisomy, tuberous sclerosis and gene microdeletions were excluded from the present study. Informed consent from the parents or

tutors was obtained, and institutional review board approval was obtained for the study. Mean age at diagnosis was between 30 and 36 months. However, the diagnosis for the examined ASDs population go back to procedures employed several years ago (today, mean age at the diagnosis for infantile autism is about 18–24 months). Forty-five gender- and age-comparable HCs (healthy controls) [male: 25, female: 20; age at examination: 12 ± 5 years] were randomly chosen from outpatients who had no pathological symptoms.

Urine from children with ASD and HCs were collected in polypropylene specimen cups, divided into aliquots (1.0 ml) and frozen at -20°C until analysis. Field blanks consisted in purified water collected in polypropylene tubes and frozen at -20°C .

Determining secondary metabolites in urine

The metabolites measured in this study included: MEHP [mono-(2-ethylhexenyl) 1,2-benzenedicarboxylate] and 6-OH-MEHP [mono-(2-ethyl-6-hydroxyhexyl) 1,2-benzenedicarboxylate], 5-oxo-MEHP [mono-(2-ethyl-5-oxohexyl) 1,2-benzenedicarboxylate] and 5-OH-MEHP [mono-(2-ethyl-5-hydroxyhexyl) 1,2-benzenedicarboxylate]. All these metabolites were synthesized in the Laboratory of Peptide and Protein Chemistry and Biology (PeptLab) following their previously described procedure (Nutti et al., 2005). The unequivocally characterized synthetic metabolites were used as pure analytical standards (>98% purity) for quantitative determination in urine from ASD children and HCs.

All the solvents (acetonitrile, water, buffers, etc.), labware (polypropylene vials containing urine, solvent bottles, SPE (solid phase extraction) cartridge, Teflon capped-glass bottles, pipettes) and instrumentation used during SPE procedure and the HPLC-ESI-MS (HPLC electrospray ionization MS) analytical process, to detect MEHP and/or secondary metabolites in ASD patients and HCs, were verified to be MEHP- and secondary oxidative metabolites-free. The internal standards were prepared in acetonitrile and were used as reported in the literature (Blount et al., 2000; Kato et al., 2004).

First morning urine specimens were collected. All specimens displayed urinary creatinine in the children reference value range, dependent on age and lean body mass (0.5–4.0 mg/kg per 24 h). For creatinine measurement, we used a Synchron AS/ASTRA clinical analyser (Beckman Instruments). We used values ($\mu\text{g/l}$) for creatinine and (g/l) for dilution correction in the analyses.

For SPE treatment of urine, we prepared the following buffers: ammonium acetate buffer 1 M, pH 6.5; acid buffer, pH 2.0 by preparing a solution of NaH_2PO_4 (0.14 M) and 1% of 85% H_3PO_4 ; basic buffer was prepared by adding concentrated ammonium hydroxide (1 ml of 30% NH_3 solution) to a 50:50 acetonitrile/water (200 ml). All buffers were stored in sealed bottles at room temperature (20°C): basic buffer was discarded after 1 week, acid buffer after 1 month.

Human urines (1 ml) were defrosted, sonicated, mixed and dispensed in glass tubes. Then ammonium acetate buffer (250 μl , pH 6.5) was added. Incubation with β -glucuronidase (5 μl ,

200 units/ml, Roche Biochemical) was performed at 37°C for 90 min, resulting in quantitative glucuronide hydrolysis of phthalates and metabolites. *Escherichia coli* K12 β -glucuronidase has excellent glucuronidase activity and no measurable lipase activity on phthalate diesters (Blount et al., 2000; Kato et al., 2004). After deconjugation, samples were treated with two steps of SPE, using SPE cartridge (3 ml/60 mg of Oasis HBL, Waters) to remove any contamination of biological matrix, following the procedure described by Blount et al. (2000). The first cartridge was used to retain hydrophobic compounds while the phthalate metabolites were eluted. The second cartridge was helpful in removing residual salts. Analytes were finally eluted with acetonitrile and ethyl acetate, concentrated, re-suspended in water and transferred into vials. All the samples were analysed by RP-HPLC-ESI-MS (reverse-phase HPLC-ESI-MS). One blank and one QC (quality control) sample were included in each batch of samples. The QC sample was spiked with pooled urine and MEHP and secondary oxidative metabolite standards in known concentration (200 ng/ml). When urine analysis resulted in values for metabolite concentrations exceeding the linear range of the analytical method, we subjected a new aliquot of the same sample to the entire process (deconjugation and SPE) and we analysed again. Before analysis, known concentration samples were treated by SPE and analysed by RP-HPLC-ESI-MS to test SPE efficiency. In our study the efficiency of SPE procedure is in accordance with the literature (Mazzeo et al., 2007). Treated urine samples could be stored at 4°C without degradation. Storage of untreated urines at -40°C for 6 months showed no decrease in phthalate monoester levels.

The analytical methodology adapted for measuring MEHP and secondary oxidative metabolites in urine had already been described in the literature (Blount et al., 2000; Silva et al., 2003a, 2003b; Kato et al., 2005).

In particular, we used an HPLC tandem MS, RP-HPLC-ESI-MS (Waters, Alliance 2695, Waters, Micromass ZQ) equipped with phenyl column (Betasil, 5 μm , 50 mm \times 3 mm, Keystone Scientific) and with a Waters 2996 Photodiode Array Detector. All reagents were of at least analytical reagent grade. The lower LOQs (limits of quantification) were 0.042 $\mu\text{g/l}$ MEHP, 0.048 $\mu\text{g/l}$ 5-OH-MEHP, 0.049 $\mu\text{g/l}$ 5-oxo-MEHP and 0.008 $\mu\text{g/l}$ 6-OH-MEHP. In urine, the LODs (limits of detection) were 0.014 $\mu\text{g/l}$ MEHP, 0.016 $\mu\text{g/l}$ 5-OH-MEHP, 0.016 $\mu\text{g/l}$ 5-oxo-MEHP and 0.002 $\mu\text{g/l}$ 6-OH-MEHP. The chromatographic separations of metabolites were resolved using a linear gradient from 3 to 60% B in 10 min (solvent system A: 0.1% acetic acid in water; B: 0.1% acetic acid in acetonitrile). The flow rate was 0.6 ml/min. The column temperature was 32°C . A guard column (XBridgeTm Phenyl 3.5 μm , 3.0 \times 20 mm) was used to prevent column degradation. Column eluates were monitored at 215, 230 and 254 nm. The mass-specific detection was achieved using a Waters, Micromass ZQ ESI in positive ion mode. The product ion with higher signal intensity was selected for the quantitative analysis for each of the four phthalates. The

Table 1 ROC for DHEP secondary metabolite urinary excretion and infantile autism

AUC, area under curve; 95% CI, 95% confidence intervals for the AUC; Sens., sensitivity; spec., specificity; +PV, positive value; -PV, negative value; ALL, total sum of all the examined di(2-ethylhexyl)phthalate secondary metabolites (5-OH-MEHP+5-oxo-MEHP+6-OH-MEHP+MEHP).

Urinary phthalate	Cut-off	AUC \pm S.E.M.	95% CI	P-value	Sens (%)	Spec. (%)	+PV (%)	-PV (%)
5-OH-MEHP	>0.177	0.638 \pm 0.057	0.531–0.735	0.0154	52.1	75.6	69.4	59.6
5-Oxo-MEHP	>0.142	0.666 \pm 0.055	0.561–0.759	0.0028	46.0	91.1	85.2	60.3
MEHP	>0.01	0.631 \pm 0.058	0.524–0.730	0.0233	79.2	44.2	61.3	65.5
ALL	>0.724	0.671 \pm 0.055	0.568–0.764	0.0021	39.2	97.8	95.2	58.7

optimal MS parameters were as follows: the source and desolvation temperature were 120 and 400 °C respectively; the capillary voltage was 3.24 kV; cone voltage 30 kV, nitrogen gas was used as desolvation gas and as cone gas as well; the cone gas and the desolvation flow was 60 and 800 l/h respectively; the collision gas was argon with a flow of 0.60 ml/min. Data were acquired and processed using MassLynx™ software (Waters).

Calibration curves for the quantitative urine analysis were calculated for all analytes plotting peak area average (*y*) against concentration of standards (*x*). Five standard solutions (linear range: 2.5–2500 ng/ml) for calibration curve plotting, were prepared for all the metabolites. Curves with correlation coefficients (*r*²) greater than 0.998 were generated (MEHP, 5-OH-MEHP, 5-oxo-MEHP 0.999 and 6-OH-MEHP 0.998).

Statistical analysis

All variables were tested for normal distribution (D'Agostino-Pearson test) and data were presented as means with 95% CI (confidence interval) for normally distributed variables or medians means and with 95% CI for non-normally distributed data. Differences between groups were evaluated using independent-sample *t* test (continuous normally distributed data), Mann-Whitney rank sum test (continuous non-normally distributed data), χ^2 statistics (categorical variables with minimum number of cases per cell ≥ 5) of Fisher's exact test (categorical variables with minimum number of cases per cell < 5). Associations between variables were tested by unvaried regression analysis. The efficiency of urinary phthalates metabolites in discriminating ASD patients from HCs were evaluated using ROC (receiver operating characteristic) curve analyses. All analyses were considered to be statistically significant for *P*-values < 0.05 . Correction for multiple comparisons was made (Bonferroni's correction). The MedCalc version 9.5.2.0 statistical software package (MedCalc Software) was used.

RESULTS

Among the four metabolites (MEHP and secondary oxidative metabolites) measured in urines of ASDs, we could detect urinary concentration with median values for MEHP (0.055 μ g/ml), 5-OH-MEHP (0.18 μ g/ml), 6-OH-MEHP (0.017 μ g/ml) and 5-oxo-MEHP (0.096 μ g/ml). By contrast, in urine from HCs we found the following values for MEHP (0.028 μ g/ml), 5-OH-MEHP (0.04 μ g/ml), 6-OH-MEHP (0.019 μ g/ml) and 5-oxo-MEHP (0.04 μ g/ml). However, the data illustrated in Table 2 are without urinary creatinine correction. Differences between groups by using creatinine-adjusted data were comparable with those employing raw data (data not shown). The statistical significance of variables was independent of effects of urinary creatinine concentration. In fact, it is well known that urine concentration/dilution can affect the results of measurements of urinary metabolites.

We found detectable levels of MEHP, 5-OH-MEHP and 5-oxo-MEHP in 79.2, 52.1 and 46.0% of ASD patients respectively (Table 1). Interestingly, 5-OH-MEHP was the major metabolite in terms of urine concentrations, followed by 5-oxo-MEHP and MEHP. Urinary excretion of 5-oxo-MEHP (*P*=0.005), 5-OH-MEHP (*P*=0.0224) and MEHP (*P*=0.0312) was significantly higher in autistic patients compared with gender- and age-comparable HCs (Table 2). By contrast, 6-OH-MEHP (*P*=0.9305) was not able to discriminate ASDs. High levels of 5-OH-MEHP were detected in 26.6% of HCs. A significant positive correlation between 5-OH-MEHP and 5-oxo-MEHP could be observed only in autistic children (*r*_s=0.668, *P*<0.0001), but not in the control population (*r*_s=0.125, *P*=0.5565) (data not shown). The completely oxidized form of the metabolite pathway, corresponding to 5-oxo-MEHP, had a specificity of 91.1% in identifying autistic children (Figure 2).

The efficiency of urinary secondary metabolites in discriminating ASD patients from HCs was evaluated using ROC curve analyses (Figure 3, Tables 1 and 2).

Table 2 Comparisons of urinary excretion of secondary metabolites for DEHP in autistic patients (*n*=48) versus HCs (*n*=45) in μ g/ml. Values are medians (95% confidence intervals of the median).

	ASD healthy	Controls	<i>P</i> -value*
5-OH-MEHP	0.18 (0.037–0.399)	0.04 (0–0.124)	0.0224
5-Oxo-MEHP	0.096 (0.04–0.17)	0.04 (0.015–0.079)	0.005
6-OH-MEHP	0.017 (0.01–0.034)	0.019 (0–0.043)	0.9305
MEHP	0.055 (0–0.11)	0.028 (0–0.059)	0.0312

* Mann-Whitney test for independent samples; statistically significant differences are highlighted in bold.

Finally, we analysed the correlations between total CARS (childhood autism rating scale) score and levels of the different metabolites. Total CARS scores were (means \pm S.D.) 44 ± 7.4 (range: 31–60). A positive correlation between CARS scores and urinary MEHP levels was observed ($\rho=0.429$, $P=0.0033$), whereas no significant relationships with the levels of the other examined metabolites were found (total CARS versus 5-OH-MEHP: $\rho=0.120$, $P=0.4298$; total CARS versus 5-oxo-MEHP: $\rho=0.127$, $P=0.3931$; total CARS versus 6-OH-MEHP: $\rho=0.0085$, $P=0.9529$).

Moreover, we compared ASDs with $n=10$ patients with Rett syndrome (a genetic form of autism due in up to 95% of cases to mutation of a gene, i.e. MeCP2), urinary phthalate metabolites appear to be, once again, significantly elevated in ASD patients (Table 3). Actual behaviour for most patients with Rett syndrome is not autistic even if all of them do show autistic traits during stage 2 of the disease. Therefore 5-oxo-MEHP urinary excretion appears to be lower in Rett syndrome ($P=0.0344$), whereas 5-OH-MEHP ($P=0.0601$), 6-OH-MEHP ($P=0.2246$) and MEHP ($P=0.7098$) excretion is comparable with that observed in HCs, despite the heavy medication needed in this multi-system genetic disease. These results indicate that medications are likely not the main cause for the increased urinary phthalate excretion evidenced in ASDs, while suggesting the likely intervention of environmental factors in the pathogenesis of this pervasive development disorder.

DISCUSSION

As ASDs are disorders of brain development, any factors that regulate brain development and are known to be altered in autism should be considered as possibly contributing to the phenotype.

Our findings, for the first time, demonstrate an association between phthalates and ASDs. It is interesting to note that, in 87% of the ASD urine samples, we detected MEHP and

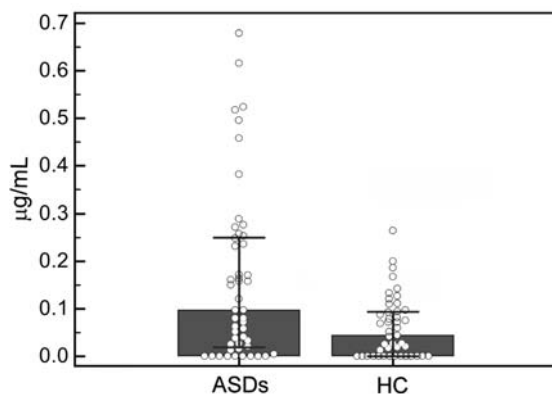


Figure 2 Differences between groups: scatterplots for 5-oxo-MEHP values in ASDs urine samples (ASDs, $n=48$; HC, $n=45$) Data are medians and inter-quartile range.

5-oxo-MEHP levels higher than the levels recently reported, by Cho et al. (2010). In that study Cho et al. reported a possible relationship between environmental phthalate exposure (external contamination) and the intelligence level of 667 school-age children randomly recruited from nine elementary schools in five South Korean cities. The reported median values were for MEHP (0.055 $\mu\text{g/ml}$), 5-OH-MEHP (0.18 $\mu\text{g/ml}$) and 5-oxo-MEHP (0.096 $\mu\text{g/ml}$) respectively. As spot urines are among the most commonly used samples in clinical toxicology, we showed the data unadjusted for creatinine. In fact, in epidemiological studies it is not practical to collect 24 h urine samples or, when young children are involved, even first morning voids. In particular, spot urines have also been used in a widely promoted paper relating maternal urinary-phthalate metabolite excretion in mothers to psychomotor development in their children at age 3, recently published (Whyatt et al., 2011). Likewise in ASDs, MEHP was found to be the minor urinary metabolite compared with the corresponding oxidized metabolites as in some adult metabolic diseases (Wittassek and Angerer, 2008). It is possible to hypothesize that, in the case of ASDs, a high MEHP urinary excretion does not correspond to external contamination, but rather MEHP could likely act as an ED.

From our data it is possible to speculate that phthalate metabolites as EDs may play an important and previously not recognized role either in the neurotransmitter system and/or in neurodevelopment, possibly increasing the risk of ASDs. In any case, our findings indicate for the first time that specific DEHP metabolites are statistically significantly increased in ASDs. It is intriguing that urinary levels of the most oxidized form of the DEHP metabolites (5-oxo-MEHP) is able to efficiently discriminate ASDs from HCs (Figure 2). Nevertheless, it has already

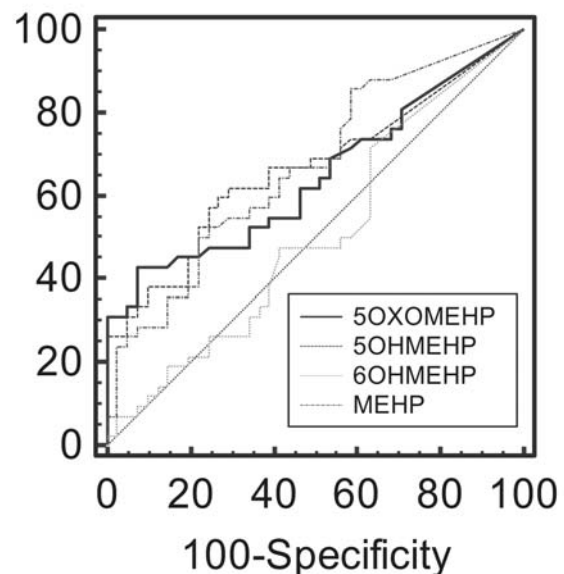


Figure 3 ROC curve analysis (ASD patients versus HC) for DEHP metabolites

Table 3 Comparisons of urinary excretion of secondary oxidative metabolites of DEHP in ASDs with $n=10$ patients with Rett syndrome in $\mu\text{g/ml}$. Data are expressed as medians and 95% CI; phthalate metabolite concentrations are adjusted to creatinine and are calculated per 100 mg of urinary creatinine. Statistically significant differences are highlighted in bold.

Urinary phthalate metabolite	ASD Rett	Syndrome	P-value
5-Oxo-MEHP	0.0997 (0.0397–0.1708)	0 (0–0.0755)	0.0344
5-OH-MEHP	0.1740 (0.0311–0.35)	0 (0–0.0091)	0.0601
6-OH-MEHP	0.0107 (0–0.0261)	0 (0–0.0832)	0.2246
MEHP	0.0287 (0.0159–0.0847)	0 (0–0.1344)	0.7098

been reported that the most oxidized DEHP metabolites have longer half-life of excretion in urine (Koch et al., 2006). Therefore it is possible that environmental factors and OS (oxidative stress) imbalance may interact in leading to increased ASD risk, although further investigation is needed in dissecting this interaction *in vivo*.

A link between oxidative brain damage and ASD has been previously reported by several authors (James et al., 2004; Villagonzalo et al., 2010; Sajdel-Sulkowska et al., 2011). Over the last few years, our team has demonstrated that the biological 'duo' hypoxia–OS is a key player in modulating genotype–phenotype expression in Rett syndrome, a well-established genetic form of ASD (De Felice et al., 2009; Pecorelli et al., 2011; Signorini et al., 2011).

Moreover, in previous reports, a correlation between OS and ASD has been widely explored by measuring different molecules, possibly coming from oxidative pathway as metabolic biomarkers of OS, in biological fluids (Chauhan et al., 2004; James et al., 2004).

To the best of our knowledge, a strict relationship between OS entity and the *in vivo* presence of oxidized forms of DEHP has not been reported before. Therefore we could speculate that, in susceptible subjects, DEHP exposure, when finding OS conditions, can lead to *in vivo* accumulation of toxic metabolites (i.e. the oxidized phthalate metabolites), possibly acting as EDs. Considering that urinary 5-oxo-MEHP reported in our study as increased in ASDs compared with HCs, we can state that our findings are in agreement with an increased OS environment.

Moreover, phthalates are known as EDs, but it is unclear how they could be involved in aetiology of neurodevelopment disorders. Phthalate metabolites activate α -PPAR α (peroxisome proliferator-activated receptor α), interfering with cellular proliferation and lipid metabolism. Activation of PPAR α by phthalates may alter lipid metabolism in the brain (Clark-Taylor and Clark-Taylor, 2004). Recently the signal transduction pathway of PPAR α was correlated with progression of neurodegenerative and psychiatric diseases.

Phthalates also interfere with the TH (thyroid hormone) system by inducing hypothyroidism. Recent studies correlated *in utero* hypothyroxinaemia to decreased intellectual capacity, mental retardation and ASD (Roman, 2007), thus reinforcing our speculation. Moreover, exposure to DBP (di-*n*-butyl phthalate) seems to affect thyroid activity in pregnant women, thus leading to adverse effects on the foetus (Huang et al., 2007).

On the other hand, transient intra-uterine deficits of THs have been shown to result in permanent alterations of

cerebral cortex similar to those found in brains of children with autism (Roman, 2007). As a consequence, the current surge of this disease could be related to transient maternal hypothyroxinemia resulting from exposure to anti-thyroid environmental contaminants.

For the first time in this study we correlated different levels of the primary and secondary metabolites with ASDs compared with HC children. These data generate the idea that either current exposure is higher in children with ASD, or alternatively, and more likely, ASD children may differ in their ability to metabolize phthalates.

In conclusion, our findings generate the idea that prenatal plus postnatal phthalate exposure may have synergistic and cumulative actions affecting brain development, thus possibly contributing to the ASD phenotype, according to the general concept generated by Herbert (2010) of 'environmentally vulnerable physiology'. Therefore a prenatal/postnatal screening for urinary DEHP metabolites in the population at high risk for ASDs could have an important social impact.

ACKNOWLEDGEMENT

We gratefully acknowledge Dr R. Zannolli (Dipartimento Materno-Infantile, University of Siena, Siena, Italy) for collecting HC urine samples.

FUNDING

This work was partly funded by ANR Chaire d'Excellence 2009–2013 (France) and Ente Cassa Risparmio di Firenze. Région Ile-de-France supported the 'Cotutelle internationale de thèse de doctorat' of C. Testa (Ecole doctorale University of Cergy-Pontoise, France and Dottorato in Scienze Chimiche of University of Florence, Italy).

REFERENCES

- Albro PM (1986) Absorption, metabolism, and excretion of di(2-ethylhexyl) phthalate by rats and mice. *Environ Health Perspect* 65:293–298.
- Alcaro MC, Paolini I, Lolli F, Migliorini P, Rovero P, Papini AM (2009) Peptide contribution to the diagnosis of autoimmune diseases. *Chemistry Today* 27:11–14.
- Anney RJL, Kenny EM, O'Dushlaine C, Yaspan BL, Parkhomenka E, Buxbaum JD, Sutcliffe J, Gill M, Gallagher (2011) Gene-ontology enrichment analysis in two independent family-based samples highlights biologically plausible processes for autism spectrum disorders. *Eur J Hum Genet* 19:1082–1089.

- Bauer ML, Herrmann R (1997) Estimation of the environmental contamination by phthalic acid esters leaching from household wastes. *Sci Total Environ* 208:49–57.
- Blount BC, Milgram KE, Silva MJ, Malek NA, Reidy JA, Needham LL, Brock JW (2000) Quantitative detection of eight phthalate metabolites in human urine using HPLC-APCIMS/MS. *Anal Chem* 72:4127–4134.
- Chauhan V, Chauhan A, Cohen IL, Brown WT, Sheikh A (2004) Alteration in amino-glycerophospholipids levels in the plasma of children with autism: a potential biochemical diagnostic marker. *Life Sci* 74:1635–1643.
- Cho SC, Bhang SY, Hong YC, Shin MS, Kim BN, Kim JW, Yoo HJ, Cho IH, Kim HW (2010) Relationship between environmental phthalate exposure and the intelligence of school-age children. *Environ Health Perspect* 118:1027–1032.
- Clark-Taylor T, Clark-Taylor BE (2004) Is autism a disorder of fatty acid metabolism? Possible dysfunction of mitochondrial beta-oxidation by long chain acyl-CoA dehydrogenase. *Med Hypotheses* 62:970–975.
- De Felice C, Ciccoli L, Leoncini S, Signorini C, Rossi M, Vannuccini L, Guazzi G, Latini G, Comporti M, Valacchi G, Hayek J (2009) Systemic oxidative stress in classic Rett syndrome. *Free Radical Biol Med* 47:440–448.
- Geschwind DH (2011) Genetics of autism spectrum disorders. *Trends Cogn Sci* 15:409–16.
- Griffiths WC, Camara P, Lerner KS (1985) Bis-(2-ethylhexyl)phthalate, an ubiquitous environmental contaminant. *Ann Clin Lab Sci* 15:140–151.
- Hellerstedt WL, McGovern PM, Fontaine P, Oberg CN, Cordes JE (2008) Prenatal environmental exposures and child health: Minnesota's role in the National Children's Study. *Minn Med* 91:40–43.
- Herbert M (2010) Contributions of the environment and environmentally vulnerable physiology to autism spectrum disorders. *Curr Opin Neurol* 23:103–110.
- Hines EP, Calafat AM, Silva MJ, Mendola P, Fenton SE (2009) Concentrations of phthalate metabolites in milk, urine, saliva, and serum of lactating North Carolina women. *Environ Health Perspect* 117:86–92.
- Huang PC, Kuo PL, Guo YL, Liao PC, Lee CC (2007) Associations between urinary phthalate monoesters and thyroid hormones in pregnant women. *Hum Reprod* 22:2715–2722.
- James SJ, Cutler P, Melnyk S, Jernigan S, Janak L, Gaylor DW, Neubrandt JA (2004) Metabolic biomarkers of increased oxidative stress and impaired methylation capacity in children with autism. *Am J Clin Nutr* 80:1611–1617.
- Kato K, Silva MJ, Needham LL, Calafat AM (2005) Determination of 16 phthalate metabolites in urine using automated sample preparation and on-line preconcentration/high-performance liquid chromatography/tandem mass spectrometry. *Anal Chem* 77:2985–2991.
- Kato K, Silva MJ, Reidy JA, Hutz D III, Malek NA, Needham LL, Nakazawa H, Barr DB, Calafat AM (2004) Mono(2-ethyl-5-hydroxyhexyl) phthalate and mono-(2-ethyl-5-oxohexyl) phthalate as biomarkers for human exposure assessment to di-(2-ethylhexyl) phthalate. *Environ Health Perspect* 112:327–330.
- Kim BN, Cho SC, Kim Y, Shin MS, Yoo HJ, Kim JW, Yang YH, Kim HW, Bhang SY, Hong YC (2009) Phthalates exposure and attention-deficit/hyperactivity disorder in school-age children. *Biol Psychiatry* 66:958–963.
- Kim YS, Leventhal BL, Koh YJ, Fombonne E, Laska E, Lim EC, Cheon KA, Kim SJ, Kim YK, Lee HK, Song DH, Grinker RR (2011) Prevalence of autism spectrum disorders in a total population sample. *Am J Psychiatry* 168:904–912.
- Koch HM, Preuss R, Angerer J (2006) Di(2-ethylhexyl)phthalate (DEHP): human metabolism and internal exposure – an update and latest results. *Int J Androl* 29:155–165.
- Koch HM, Rossbach B, Drexler H, Angerer J (2003) Internal exposure of the general population to DEHP and other phthalates-determination of secondary and primary phthalate monoester metabolites in urine. *Environ Res* 93:177–185.
- Larsson M, Weiss B, Janson S, Sundell J, Bornhag CG (2009) Associations between indoor environmental factors and parental-reported autistic spectrum disorders in children 6–8 years of age. *Neurotoxicology* 30:822–831.
- Latini G, De Felice C, Presta G, Del Vecchio A, Paris I, Ruggieri F, Mazzeo P (2003). In utero exposure to di-(2-ethylhexyl)phthalate and duration of human pregnancy. *Environ Health Perspect* 111:1783–1785.
- Latini G, Verzotti A, De Felice C (2004) Di-2-ethylhexylphthalate and endocrine disruption: a review. *Curr Drug Targets Immune Endocr Metabol Disord* 4:37–40.
- Latini G, Wittassek M, Del Vecchio A, Presta G, De Felice C, Angerer J (2009) Lactational exposure to phthalates in Southern Italy. *Environ Int* 35:236–239.
- Mazzeo P, Di Pasquale D, Ruggieri F, Fanelli M, D'Archivio AA, Carlucci G (2007) HPLC with diode-array detection for the simultaneous determination of di(2-ethylhexyl)phthalate and mono(2-ethylhexyl)phthalate in seminal plasma. *Biomed Chromatogr* 21:1166–1171.
- Nelson KB (1991) Prenatal and perinatal factors in the etiology of autism. *Pediatrics* 87:761–766.
- Nuti F, Hildenbrabd S, Chelli M, Wodarz R, Papini AM (2005) Synthesis of DEHP metabolites as biomarkers for GC-MS evaluation of phthalates as endocrine disrupters. *Bioorg Med Chem* 13:3461–3465.
- Papini AM (2009) The use of post-translationally modified peptides for detection of biomarkers of immune-mediated diseases. *J Pept Sci* 15:621–628.
- Pecorelli A, Ciccoli L, Signorini C, Leoncini S, Giardini A, D'Esposito M, Filosa S, Pecorelli A, Valacchi G, Hayek J (2011) Increased levels of 4HNE-protein plasma adducts in Rett syndrome. *Clin Biochem* 44:368–371.
- Risch N, Spiker D, Lotspeich L, Nouri N, Hinds D, Hallmayer J, Kalaydjieva L, McCague P, Dimiceli S, Pitts T, Nguyen L, Yang J, Harper C, Thorpe D, Vermeer S, Young H, Hebert J, Lin A, Ferguson J, Chiotti C, Wiese-Slater S, Rogers T, Salmon B, Nicholas P, Petersen PB, Pingree C, McMahon W, Wong DL, Cavalli-Sforza LL, Kraemer HC, Myers RM (1999) A genomic screen of autism: evidence for a multilocus etiology. *Am J Hum Genet* 65:493–507.
- Roman GC (2007) Autism: transient *in utero* hypothyroxinemia related to maternal flavonoid ingestion during pregnancy and to other environmental antithyroid agents. *J Neurol Sci* 262:15–26.
- Sajdel-Sulkowska EM, Xu M, McGinnis W, Koibuchi N (2011) Brain region-specific changes in oxidative stress and neurotrophin levels in autism spectrum disorders (ASD). *Cerebellum* 10:43–48.
- Schettler T (2006) Human exposure to phthalates via consumer products. *Int J Androl* 29:134–139.
- Signorini C, De Felice C, Leoncini S, Giardini A, D'Esposito M, Filosa S, Della Ragione F, Rossi M, Pecorelli A, Valacchi G, Ciccoli L, Hayek J (2011) F(4)-neuroprostanes mediate neurological severity in Rett syndrome. *Clin Chim Acta* 412:1399–1406.
- Silva MJ, Barr DB, Reidy JA, Kato K, Malek NA, Hodge CC, Hutz D, Calafat AM, Needham LL, Brock JW (2003a) Glucuronidation patterns of common urinary and serum monoester phthalate metabolites. *Arch Toxicol* 77:561–567.
- Silva MJ, Malek NA, Hodge CC, Reidy JA, Kato K, Barr DB, Needham LL, Brock JW (2003b) Improved quantitative detection of 11 urinary phthalate metabolites in humans using liquid chromatography-atmospheric pressure chemical ionization tandem mass spectrometry. *J Chromatogr* 789:393–404.
- Suzuki Y, Niwa M, Yoshinaga J, Mizumoto Y, Serizawa S, Shiraishi H (2010) Prenatal exposure to phthalate esters and PAHs and birth outcomes. *Environ Int* 36:699–704.
- U.S. FDA (Food and Drug Administration) (2011) Safety assessment of di(2-ethylhexyl)phthalate (DEHP) released from PVC medical devices. Available online at <http://www.fda.gov/downloads/MedicalDevices/Device-RegulationandGuidance/GuidanceDocuments/UCM080457.pdf> (accessed 22 September 2011).
- Villagonzalo KA, Dodd S, Dean O, Gray K, Tonge B, Berk M (2010) Oxidative pathways as a drug target for the treatment of autism. *Expert Opin Ther Targets* 14:1301–1310.
- Weintraub K (2011) The prevalence puzzle: autism counts. *Nature* 479:22–24.
- Whyatt RM, Liu X, Rauh VA, Calafat AM, Just AC, Hoepner L, Diaz D, Quinn J, Adibi J, Perera FP, Factor-Litvak P (2011) Maternal prenatal urinary phthalate metabolite concentrations and child mental, psychomotor and behavioral development at age three years. *Environ Health Perspect* 120: 290–295.
- Wittassek M, Angerer J (2008) Phthalates: metabolism and exposure. *Int J Androl* 31:131–138.
- Wittassek M, Angerer J, Gehring J, Schäfer SD, Klockenbusch W, Dobler L, Günzel AK, Müller A, Wiesmüller GA (2009) Fetal exposure to phthalates – a pilot study. *Int J Hyg Environ Health* 212:492–498.
- Wormuth M, Scherlinger M, Vollenweider M, Hungerbühler K (2006) What are the sources of exposure to eight frequently used phthalic acid esters in Europeans? *Risk Anal* 26:803–824.

Received 2 March 2012/22 March 2012; accepted 29 March 2012

Published as Immediate Publication 27 April 2012, doi 10.1042/AN20120015